SOME STUDIES OF HYDROGEN BONDING IN ORGANIC AND ORGANOMETALLIC CRYSTALS: APPLICATIONS TO CRYSTAL ENGINEERING

A Thesis
Submitted for the Degree of
DOCTOR OF PHILOSOPHY

by

Kumar Biradha

School of Chemistry
University of Hyderabad
Hyderabad 500 046
INDIA

September 1996

Contents

Statement

I hereby declare that the matter embodied in this thesis is the result of the investigations carried out by me in the School of Chemistry, University of Hyderabad under the supervision of Prof. Gautam R. Desiraju.

In keeping with the general practice of reporting scientific observations due acknowledgements have been made wherever the work described is based on the findings of other investigators.

Hyderabad
September 1996

Kumar Biradha

Certificate

Certified that the work "**Some Studies of Hydrogen Bonding in Organic and Organometallic Crystals: Applications to Crystal Engineering**" has been carried out by **Kumar Biradha** under my supervision and that the same has not been submitted else where for a degree.

Dean
School of Chemistry

Gautam R. Desiraju

Prof. Gautam R. Desiraju
Thesis Supervisor

Acknowledgements

I express my deep sense of gratitude, respect and profound thanks to Professor Gautam R. Desiraju for his inspiring guidance and constant encouragement throughout the course of this work. My stay with him is memorable in my life.

It is a pleasure to thank Professor Dario Braga, University of Bologna, Italy for suggesting some excellent problems and for supervising some of the work presented in this thesis. Thanks to internet which made it possible to have many elegant and thought provoking discussions.

I thank Prof. P.S. Zacharias, Dean, School of Chemistry and all the faculty members of the School for their cooperation on various occasions. I thank Dr. A. Nangia of this School, under whose supervision some of the work described in this thesis was carried out. I would also like to thank Dr. J.A.R.P. Sarma, P & I C Division, I.I.C.T, Hyderabad for many helpful discussions during the thesis writing.

I wish to express my regards to my friendly and cooperative labmates Dr. V.R. Pedireddi, Dr. C.V.K. Sharma, Dr. B. Satish Goud, Dr. D. Shekhar Reddy, Venkat R. Thalladi, T. Ram, K.S. Srinivasan, Dr. P. Sivaswaroop and Dr. K. Panneerselvam. Also it is a pleasure to thank my friends Kiran, Prasad, Rajashekar, Sridhar, Vittal, Sharma, Sindhu, Murali, Nagu, Lakshmi Narayana, Ravi, Ramana, Sirish, Prasanna, Rama Reddy, Rajender, Vishwanath, Srinivas, Giribabu, Ravi Krishna, Anthony, Pankaz

Chapter 1:

Introduction

Hydrogen bonding is the master-key to molecular recognition and a thorough understanding of this phenomenon is indispensable to the field of crystal engineering. Crystal engineering has been defined as "the understanding of intermolecular interactions in the context of crystal packing and in the utilisation of such understanding in the design of new solids with desired physical and chemical properties". CSD studies on various aspects of intermolecular interactions help in understanding their nature and robustness. Once the nature and robustness of an intermolecular interaction is known, one can use this knowledge to understand the packing of a molecular crystal of interest and extract some qualitative information on its crystal engineering.

In this chapter a brief discussion on various studies of hydrogen bonding interactions X-H···A (X=O, N, C; A=O, N, π, Tr) in organic and organometallic chemistry will be presented and the role of CSD in these studies will be given particular attention.

Chapter 2:

N-H···O Hydrogen Bonds in Transition Metal Complexes Containing Amido Groups.

In spite of the large number of studies devoted to hydrogen bonding in organic compounds, little has been done in this context with regard to organometallics and metal complexes. The differences between organic systems and organometallic systems arise from the interaction of the organic molecules (the ligands) with the metal centres. The metal-ligand bonding influences the patterns of hydrogen bonds that can be established. A lack of knowledge of N-H···O hydrogen bonds in transition metal amido complexes has led to a gap in our ability to design new crystals of these substances.

This chapter discusses the distribution and geometry of N-H···O hydrogen bonds in crystals of transition metal complexes containing primary and secondary amido groups as obtained from the CSD. The distributions of hydrogen bonds in these complexes have been compared with those observed in organic crystals. To compare the robustness of inter-amide bonding in organometallic amides with that in organic amides, the study is divided into the following four categories according to changes in the acceptor moiety.

A. O=C-N-H···O

B. O=C-N-H···O=C

C. O=C-N-H···O=C-N-H

D. 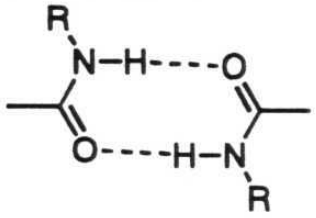

The analysis shows that the inter-amide bond is more robust in organic amides than in organometallic amides. These differences in robustness are due to the presence of other competing acceptors, such as H_2O and NO_3^- and also due to the existence of cases in which the O-amide atom is engaged in coordination to the metal centre via one of its lone pairs. Further, the distribution and average values of H···O distances suggests that on average, organometallic amides form longer hydrogen bonds than organic amides. These differences in H···O distances are due to the existence of a greater number of bifurcated interactions in organomeatallic amides when compared to organic amides. Analysis of C=O···H angle distributions reveals that hydrogen bonds in organic primary amides show more directionality when compared to organic secondary and organometallic amides. It is also found that the amide N-H is generally not involved in N-H···O hydrogen bonds with the CO-ligand. Some selected crystal structures are examined in detail in order to

understand the differences in packing of organic and organometallic amides.

Chapter 3:

C-H···O Hydrogen Bonds in Organometallic Ist row Metal Carbonyl Compounds

It is remarkable that, in spite of the interest that the C-H···O hydrogen bond has attracted, little has been done in this context with regard to organometallic solids. A further reason of interest arises from the presence in organometallic molecules of an additional and different type of potential hydrogen bonding acceptor, namely the CO-ligand.

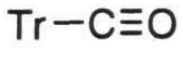

CO-t

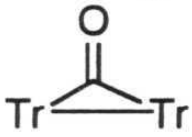

CO-b

In this chapter, C-H···O hydrogen bonding interactions in crystalline organometallic complexes and clusters have been investigated. The analysis takes the form of retrieval from the CSD of all intra and intermolecular H···O distances in organometallic crystal structures of the first row transition elements containing terminal and bridging CO-ligands represented as CO-t and CO-b respectively. The average values and distributions of C···O distances suggests that the CO-b forms shorter and

more linear hydrogen bonds than do the CO-t, reflective of their higher basicity. This effect is especially pronounced for intermolecular hydrogen bonds. C-H···O hydrogen bonds formed by both CO-t and CO-b are also directional. In both cases, there is a tendency for the CO···H angle to be around 140^{o}. This suggests the presence of the two extreme valence bond structures for CO-t ligand as shown in Scheme-1.

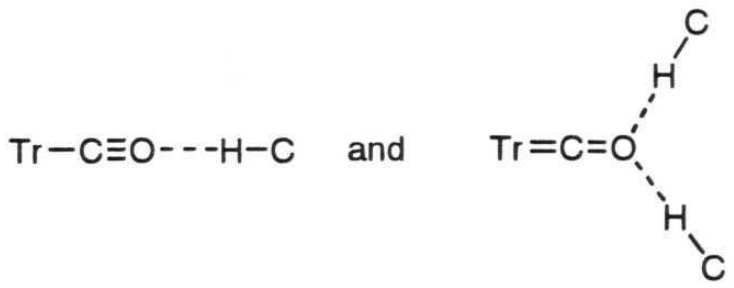

Scheme-1: Two valence bond structures for CO-t

Individual crystal structures have also been examined to evaluate the role of C-H···O hydrogen bonds in the packing of organometallic compounds. There is a definite manifestation of C-H···O hydrogen bonding in this group of crystalline substances. Analysis of anisotropic displacement parameters (ADP) of atoms in the neutron derived crystal structure of $(\mu_3\text{-H})FeCo_3(CO)_9(POMe_3)_3$ shows that ADP's of oxygen atoms of CO-ligands which are involved in C-H···O hydrogen bonding are smaller than those of other oxygen atoms of CO-ligands. Formation of C-H···O hydrogen bonds between C-H groups and CO-ligands suggests that the C-H···O hydrogen bond is an example of a soft intermolecular

dependence on O-atom basicity, directionality and reduction of ADP's indicates that the C-H···O hydrogen bond shows many of the properties of stronger hydrogen bonds.

Chapter 4:

M-H···O Hydrogen bonds in Organometallics

In the previous chapter it has been shown that the C-H group can interact with the CO-ligand to form C-H···O hydrogen bonds. Both the M-H and C-H group are of low polarity and can react as H^+, $H\cdot$, or H^- donors. Therefore M-H···O hydrogen bonds that are similar to C-H···O hydrogen bonds might be anticipated.

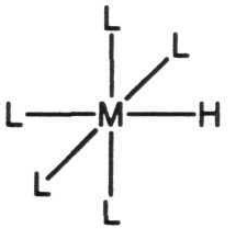

I

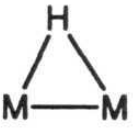

II

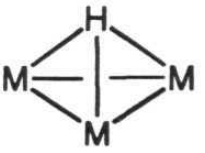

III

This chapter describes M-H···O hydrogen bonding interactions in crystalline organometallic complexes and clusters of transition metals. Molecular and crystal structures determined by neutron and/or X-ray diffraction data have been retrieved from the CSD. In a number of cases there is a clear manifestation of M-H···O bonds involving metal bound H ("hydride") atom(s) and oxygen atoms [illegible]

The hydrogen atom can bind to mono and polynuclear metal complexes in terminal (I) or bridging fashions. Bridging hydrogen atoms can span a metal-metal bond (μ_2 bridging mode, II) or cap a triangulated metal face of a higher nuclearity cluster (μ_3 bridging mode, III). In majority of the cases, configuration II is involved in the formation of M-H···O hydrogen bonds as shown in Scheme 2. The absence of M-H···O interactions is most often due to the steric congestion around the coordination sites of the H ligands. Individual crystal structures have been examined in detail. The geometrical properties of M-H···O hydrogen bonds suggests that, the M-H···O hydrogen bond is comparable in strength to that of the C-H···O hydrogen bond.

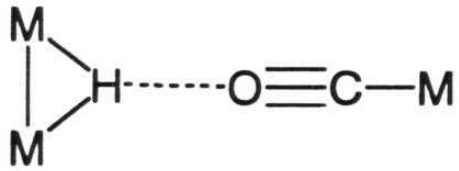

Scheme-2: M-H···O hydrogen bonds formed between the μ_2 bridged H atom and CO ligand.

Chapter 5:

Agostic Interactions in Transition Metal Complexes

Agostic interactions of C-H bonds with electron-deficient metals have been well-studied using crystallographic and spectroscopic techniques. The strengths of these interactions are estimated to be in the

order of 30-60 kJ mol^{-1} and are of comparable strength to those of conventional hydrogen bonds (10-65 kJ mol^{-1}). Agostic interactions are 3-centre 2-electron interactions (3c-2e).

In this chapter, agostic interaction geometries, C-H···M (M = Li, IVB, VB group transition metals and others) and the similarity in behaviour of Li to the heavier transition metals have been described with data retrieved from the CSD. A bonafide agostic interaction was considered to be one where the H···Tr distance is between 1.80-2.50Å. For C-H···Li interactions, the interaction was considered only when the H···Li distance is between 1.80 and 2.20Å. The analysis was carried out by examining both neutron and X-ray derived structures. The results shows that in both these cases, the strengthening of the H···M agostic bond is accompanied by a corresponding weakening of the C-H bond (Scheme-3). It is also found that dibridged (V) and tribridged (VI) C-H···Li geometries with alkyl groups exist both in intra and intermolecular cases.

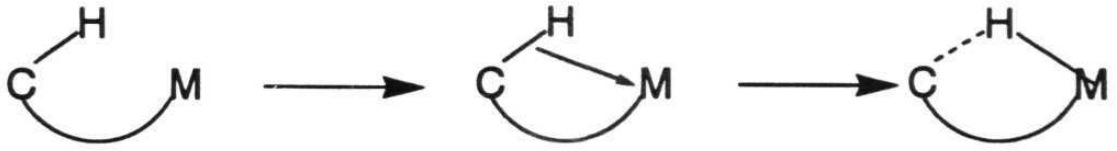

Scheme-3: Weakening of C-H bond as H-M bond strengthens.

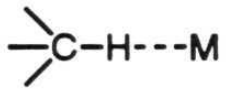

IV

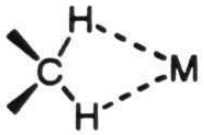

V

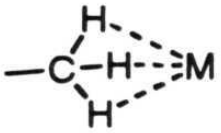

VI

Chapter 6:

Multi-point Supramolecular Synthons that Contain C-H···O Hydrogen Bonds.

A crystal has been termed a supermolecule *par excellence* and the recognition patterns that are formed in crystals may be termed as supramolecular synthons keeping in mind that a crystal may be viewed as a retrosynthetic target. Crystal engineering with conventional (or strong) O-H···O and N-H···O hydrogen bonds may appear simple and reliable, but it is incomplete if weak intermolecular interactions are not considered. Among weak intermolecular interactions, C-H···O hydrogen bonds have attracted considerable attention because the C-H group is a common functional group. Owing to the inherent weakness of these interactions, one should generally use multi-point recognition rather than single-point recognition for synthon robustness.

This chapter describes the design of the three-point C-H···O hydrogen bonded supramolecular synthon VII, which is a mimic of the strong hydrogen bonded synthon VIII. Synthon I is found in the crystal structures of complexes **3a**, **3b**, **3c**, **3d** and **3e** whilst it is not found in

complexes **3f** and **3g.** Analysis of C-H···O hydrogen bonds formed in complexes **3a, 3b** and **3c** indicates that the C-H···O hydrogen bonds involved in I are stronger than the other C-H···O hydrogen bonds formed in those complexes. Further, the CSD is used to characterise all the C-H···O hydrogen bonded patterns that are observed in this study.

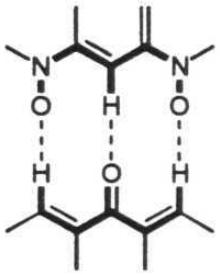

VII

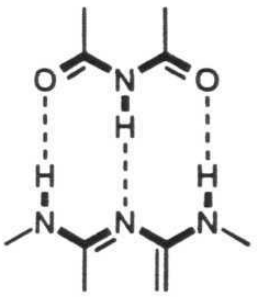

VIII

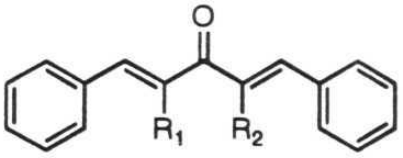

1

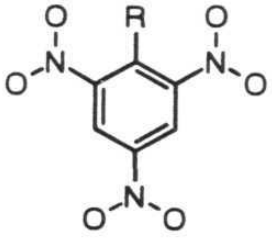

2

1a. $R_1 = R_2 = H$

1b. R_1-R_2 = -CH_2-CH_2-

1c. R_1-R_2 = -CH_2-CH_2-CH_2

1d. R_1-R_2 = -CH=CH-

2a. R = H

2b R = Cl

2c. R = OH

3a. 1a:2a (1:2)

3b. 1b:2a (1:2)

3c. 1c:2a (1:2)

3e. 1d:2b (1:2)

3f. 1b:2c (1:1)

3g. 1a:2c (1:1)

Chapter 1

Introduction

1.1 Crystal Engineering

The ever-increasing requirements of solid state materials for a number of practical applications such as SHG materials, organic ferromagnets, organic conductors superconductors and so on, has led to the emergence of the field of crystal engineering. Crystal engineering has been defined as *the understanding of intermolecular interactions in the context of crystal packing and in the utilisation of such understanding in the design of new solids with desired physical and chemical properties.*[1] The understanding of intermolecular interactions is therefore as vital to crystal engineering as the understanding of the covalent bond is to molecular chemistry. A crystal has been termed a *supermolecule par excellence.*[2] If a crystal is the supramolecular equivalent of a molecule, crystal engineering is the supramolecular equivalent of organic synthesis. Accordingly, a supramolecular synthon in the context of crystal engineering has been defined as *a structural unit within a supermolecule which can be formed and/or assembled by known or conceivable synthetic operations involving intermolecular interactions.*[3]

In organic synthesis, targets are defined in terms of covalent bonds whereas in crystal engineering targets are defined in terms of intermolecular interactions. All crystal structures of organic molecules may be formally depicted as networks with the molecules being nodes and intermolecular interactions being node connections.[4] Therefore the

predictable self-organisation of molecules into one-, two- or thr dimensional networks is of utmost importance in crystal engineering.

While crystal engineering studies of organic molecular syst progressed smoothly to the point of effectively designing these solids, s a study in inorganic systems has only just started as till now they have b viewed as spherically symmetrical atoms packed with very l electrostatic interactions lacking directional features.[5] A similar studies organometallic systems (which can be an intersectional area of both systems, consisting of metal complexes and clusters), so far been ma concerned with the molecular structure; the crystal packing characteris have just begun to be viewed. The great structural variability and flexib of organometallic molecules reflects in the patterns of intermolec interactions established by mononuclear and polynuclear coordina complexes.[6] Recently, it has been shown that in contrast to org compounds metal complexes are subject to observable distortions in b lengths and angles as well as torsional angles due to the crystal f effects.[7] Efforts have been made to apply the crystal engineering strate to organic, inorganic and organometallic chemistry.[8]

1.1.1 CSD as methodology in crystal engineering

If crystal engineering be likened to supramolecular synthesis, t the study of intermolecular interactions with the Cambridge Struct

Database (CSD)[9] may be likened to synthetic methodology. CSD studies on various aspects of intermolecular interactions help in understanding their nature and robustness. Once the nature and robustness of an intermolecular interaction is known, one can use this knowledge to understand the packing of a molecular crystal of interest and extract some qualitative information on its crystal engineering.

The use of the CSD in crystal engineering allows one to take advantage of one of the oldest methods available to the synthetic chemist, namely the reterosynthetic analogy. This process involves the identification of a supramolecular target structure or synthon and the subsequent examination of the CSD for all known structures that display this desired characteristic. The results of this examination leads to the identification of the starting materials and conditions that will produce the target structure.

The CSD at present contains information on over 152,000 crystal structures of organic and organometallic compounds. This is categorised as 1D, 2D and 3D information. 1D information refers to the compound name, journal reference, molecular formula, unit-cell parameters, R-factor etc., while 2D information contains atomic coordinates and bond properties. The atom properties consists of atom sequence number, element symbol, number of connected non-H atoms, number of terminal H-atoms and net charge. Bond property is the chemical bond type between a pair of atoms. These bond types are represented as 1, 2, 3, 4, 5, 7 and 9

(single, double, triple, quadruple, aromatic, delocalised double and π-bond respectively). While the positive bond types are acyclic, the negative ones are cyclic. 3D information contains the details on space-group, symmetry operators and it establishes the crystallographic connectivity using covalent radii.

A 3D-search allows a search for a non bonded interaction by defining the distance between specified atoms as well as the geometrical attributes of the desired synthon. The geometries obtained for these searches can be directly viewed and analysed by using the VISTA (Visual Statistical Analysis) program.

The use of the CSD is not only limited to nonbonded interactions, but one can use crystallographic information to also establish reaction pathways by the principle of structure correlation.[10] The structure correlation hypothesis assumes that gradual changes that the molecular fragment of interest undergoes along a given reaction coordinate is manifested collectively over a large variety of crystalline frameworks. According to this *the various crystal or molecular structures are considered to constitute a series of 'frozen-in' points, or snapshots, taken along reaction pathway, which, when viewed in the correct order, yield a cinematic film of the reaction.*[11] One can also use this method of structure correlation to predict biologically active conformations of various ligands that are involved in ligand-protein complexes. This is

possible by analysing the conformations of ligands in a number of small molecule crystal structures that contains these ligands. Accordingly, the conformations of β-lactam skeletons have been studied to correlate the structure-activity relationship.

1.1.2 Intermolecular interactions in crystal engineering

As defined earlier, crystal engineering deals with the understanding of intermolecular interactions and as such a number of interactions like hydrogen bonding, halogen-halogen, halogen-oxygen, halogen-nitrogen, sulphur-sulphur, sulphur-oxygen, sulphur-nitrogen, π-π interactions have been recognised as important interactions from the studies of CSD. Among these interactions, hydrogen bonding, the master-key to molecular recognition,[12] is the most reliable directional interaction in supramolecular construction[13] and its significance in crystal engineering cannot be underestimated.[3] The understanding of the important geometrical properties of hydrogen bonds such as lengths, angles and planes and also network features by which molecules may be linked in one, two or three dimensions is not possible from the rationalisation of isolated crystal structures. Such an understanding is only possible by the rationalisation of crystal structures of groups of molecules. Thus more emphasis has been given to studies of the hydrogen bond.

1.2 What is a hydrogen bond?

Pauling's definition of a hydrogen bond is that 'a hydrogen bond is largely ionic in character and is formed only between the most electronegative atoms.[14] According to Pauling's idea, the strength of the hydrogen bond depends upon the relative electronegativity of the donor and acceptor atoms. This classical definition of a hydrogen bond, which requires that the relevant proton be shared between two typically electronegative atoms must be revised, in view of the strong evidence for the existence of hydrogen bonds such as C-H···O, C-H···N, X-H···π where X = O, N and C. A more general definition that does not consider the nature of donor and acceptor atoms was given by Pimentel and McClellan, in terms of existence of such a bond which sterically involves a hydrogen atom that is already bonded to another atom.[15]

The geometries and relative energies of hydrogen bonding interactions has been analysed by several experimental techniques, including X-ray and neutron diffraction studies of crystal structures, NMR and IR spectroscopic measurements in the solid state and in solution, *ab initio* and semi-empirical calculations. In NMR studies, deshielding of X-H proton will occur in proportion to the extent of association, which can be evaluated by titrating one component against the other and plotting concentration versus $\Delta\delta$. In IR studies, the X-H stretching band moves to lower wave numbers with an accompanying increase in breadth and

intensity.[16] Likewise, the degree of H-bonding can be estimated by the magnitude of these effects.

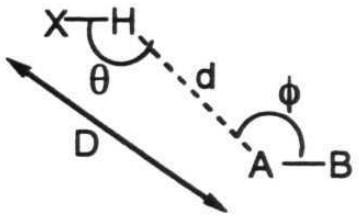

One of the main impediments to the crystallographic studies of the hydrogen bond is the location of the H atom. X-ray diffraction studies cannot locate hydrogen atom accurately. In general hydrogen bonding is characterised by four parameters namely d, D, θ and ϕ as shown above. D and d are the X···A and H···A distances respectively and θ and ϕ are X-H···A and B-A···H angles respectively. While θ represents the linearity of a hydrogen bond, ϕ represents the directionality of the B-A bond. If D and d are generally less than the sum of the van der Waals radii, then that interaction can be termed a hydrogen bond. However, Jeffrey and Saenger have stated that the use of the van der Waals sum of the heavy atoms should be discouraged because the X···A distance is a function of the covalent bond length X-H, the hydrogen bond length d and the angle θ.[17]

The O-H and N-H groups are the most general proton donor groups that form strong hydrogen bonds. Similarly, the most conventional proton acceptors are the O-atom and the N-atom. There is well-accumulated evidence for the C-H group to act as a proton donor even though the polarity of C-H group is supposedly less than that of O-H and

N-H groups. Recently, the capacity of π electronic clouds of -C≡C- bonds and aromatic rings to act as hydrogen bond acceptors has been recognised. Thus an array of different types of hydrogen bonds are given in Table 1. Apart from the variations in the donor and acceptor strengths, in general the strength of the hydrogen bond decreases while moving from left to right and top to bottom in the Table 1. For example whilst the first element in Table 1, namely O-H···O represents very strong directional hydrogen bonding interactions, C-H···π interactions can also be classified as much weaker herringbone interactions.

Table 1: Various types of hydrogen bonds.

X-H\A	O	N	π	M
O-H	O-H···O	O-H···N	O-H···π	O-H···M
N-H	N-H···O	N-H···N	N-H···π	N-H···M
C-H	C-H···O	C-H···N	C-H···π	C-H···M

The last column in Table 1 represents a new type of hydrogen bonds in organometallic complexes where the electron rich transition metals act as acceptors to form X-H···M hydrogen bonds. In the following sections, the nature of some of these X-H···A (X = O, N, C and A = O, N, π, M) hydrogen bonding interactions that are found in organic compounds are reviewed in the context of organometallic structural chemistry.

1.2.1 X-H···O Hydrogen bonds

The common O-acceptors that are found in molecular crystals are carbonyl (carboxylic, ester, amide and acyl halides), hydroxyl, ethers, sulphonyl, phosphonyl and nitro groups.

1.2.1.1 O-H···O Hydrogen bonds

These O-H···O hydrogen bonds can be formed by functional groups such as -COOH and -OH. Carboxylic acids exist either in synplanar or in antiplanar conformations. The antiplanar conformation **1** is very rare and the synplanar conformation usually forms centrosymmetric dimers, **2** and less often catemers, **3**. Alcohols forms chains, trimers, and tetramers such as **4**, **5**, and **6** respectively. These patterns can be regarded as synthons in supramolecular synthesis.

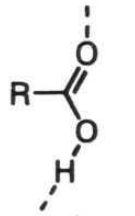

1

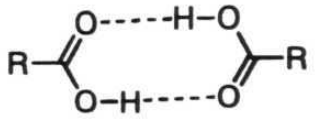

2

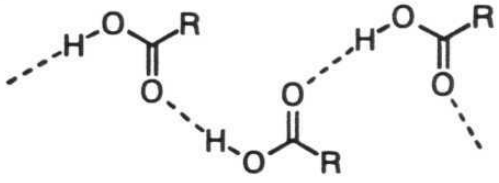

3

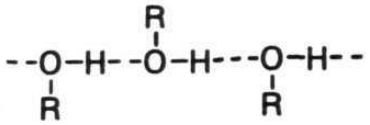

4

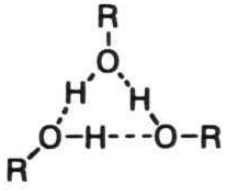

5

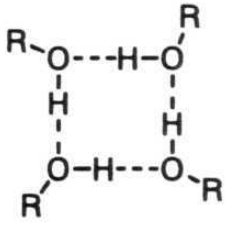

6

The carboxylic acid dimer, synthon **2** has been widely used in crystal engineering. For example, terphthalic acid forms a one dimensional ribbon structure,[18] trimesic acid forms a two dimensional hydrogen bonded sheet[19] and adamantane-1,3,5,7-tetracarboxylic acid[20] forms a three dimensional diamondoid network.

1.2.1.2 N-H···O Hydrogen bonds

The importance of N-H···O hydrogen bonds in nucleic acids is well recognised as the two sets of base pairs are held by these interactions. Amides generally adopt N-H···O hydrogen bonded synthons **7** and **8**.

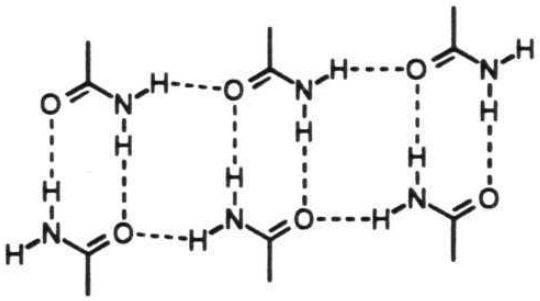

7

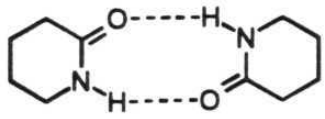

8

1.2.1.3 C-H···O Hydrogen bonds

Among the weaker intermolecular interactions, C-H···O hydrogen bonds have attracted considerable attention.[21] For a study of a weak hydrogen bond such as C-H···O, a statistical approach like CSD analysis is necessary to evaluate a standard H···O distances for a particular type of C-H group. CSD studies on a large variety of carbon acids show that the mean C···O values for chemically distinct C-H groups correlate well with

mean pK_a values in DMSO for representative compounds within each of the functional groups considered.[22] Interestingly, this correlation extends to C···O distances up to 4.00 Å and such an observation follows from the electrostatic nature of the C-H···O hydrogen bond. Further, studies on terminal alkynes, show that the anisotropic displacement parameter of C-atom decreases as the C···O distance of C-H···O hydrogen bond decreases.[23]

Recently, attempts have been made to utilise these C-H···O hydrogen bonds in crystal engineering.[24] For example, the crystal structures of the complex of 4-N,N-dimethylamino benzoic acid and 4-nitrobenzoic acid forms a linear chain **9** with C-H···O and O-H···O hydrogen bonded dimers.[24b] It is known that the benzene clathrate of 1,3-cyclohexanedione is stabilised by O-H···O hydrogen bonds as shown in **10**.[25] An analogous 1:4 organometallic molecular complex formed by the cation $(C_6H_6)_2Cr^+$ and a tetramolecular anion consisting of three molecules of 1,3-cyclohexanedione and one molecular anion of 1,3-cyclohexanedione is shown in **11**.[26] The similarities in O-H···O hydrogen bonds between **10** and **11** can be easily noticed.

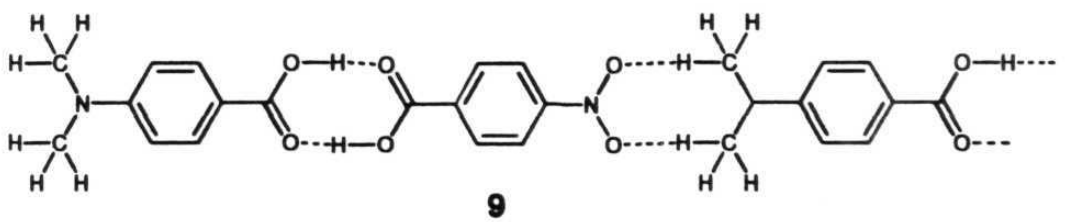

9

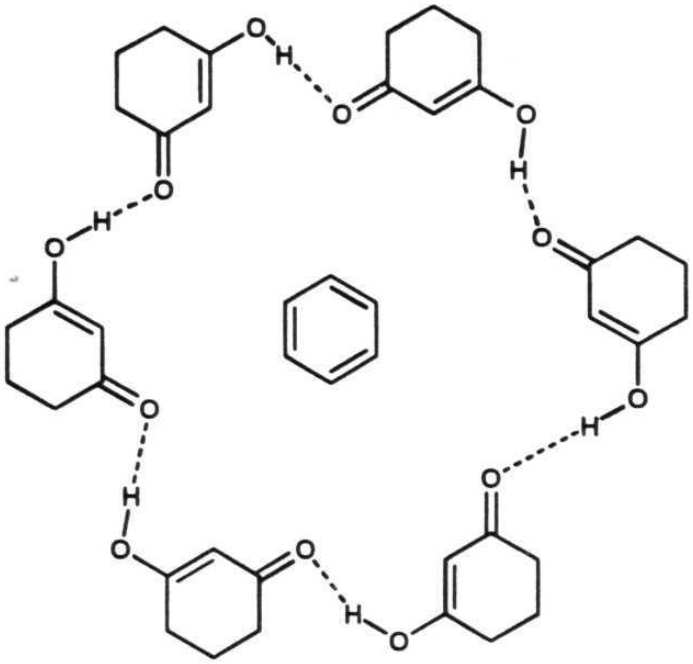

10

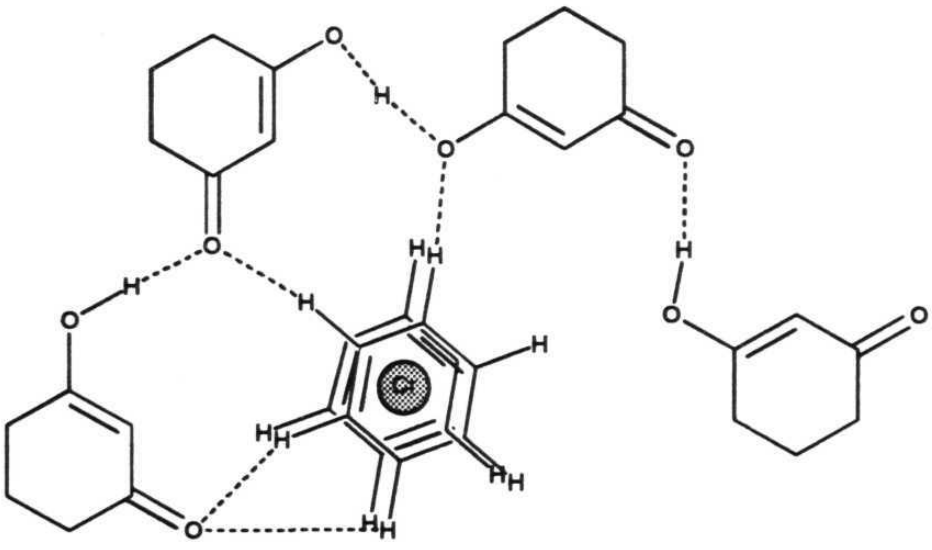

11

1.2.2 X-H···N Hydrogen bonds

To act as a better acceptor, the nitrogen should usually be in sp and sp^2 states. Thus the common N-acceptors found in molecular crystals are nitriles, pyridinium salts, pyridines, quinolines and enamines.

1.2.2.1 O-H···N Hydrogen bonds

These O-H···N Interactions have also been used in crystal engineering studies. For example 2,3-dichloro-5,6-dicyanohydroquinone and 4'-cyano-2,6-dimethyl-4-hydroxyazo-benzene adopts the O-H···N hydrogen bonded patterns **12** and **13** respectively.[27]

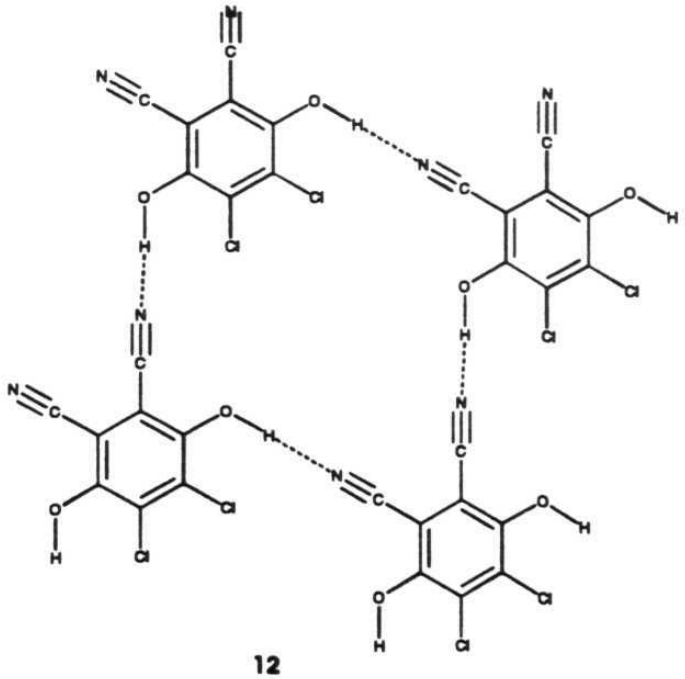

12

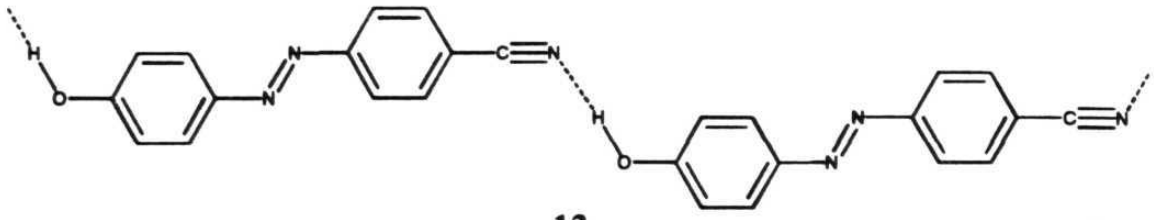

13

1.2.2.2 N-H···N Hydrogen bonds

It is known that 2-aminopyrimidine forms the hydrogen bonded network **14** in its crystal via N-H···N hydrogen bonds.[28] N-H···N hydrogen bonds are one of the constituent element of the three centre hydrogen bonded synthon **15**. For example, the crystal structures of the complexes of 2,4,6-triaminopyridines and barbituric acid derivatives form a variety of patterns through synthon **15**.[29] The formation of **15** has also been noted in metal complexes. The crystal structure of Ni(dithiobiureto)$_2$ and 1,8-napthalimide complex **16** has been built with synthon **15**.[30]

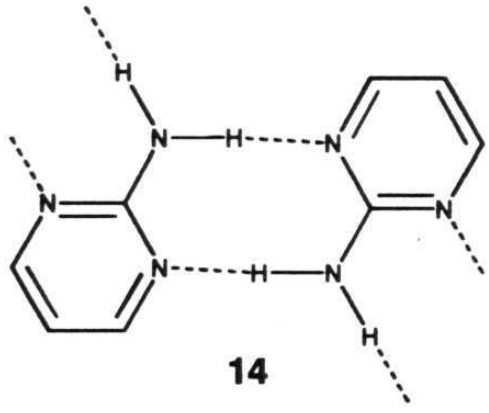

14

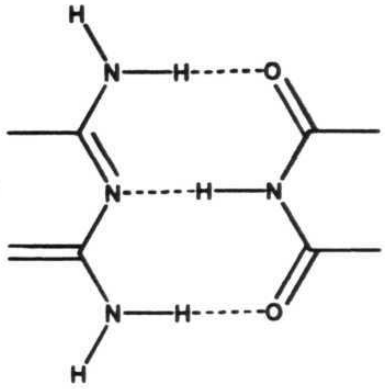

15

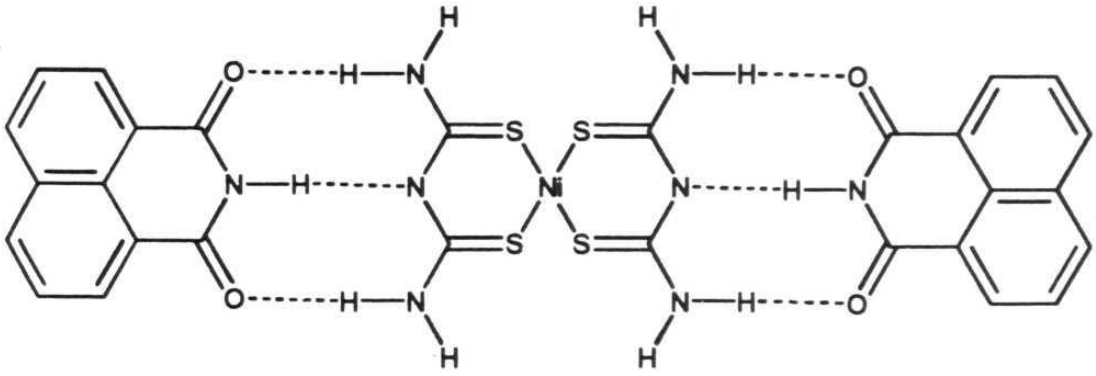

16

1.2.2.3 C-H···N Hydrogen bonds

C-H···N interactions are also of importance in governing crystal packing. These interactions are generally observed in nitriles. For example, if a nitrile group is trans to a C-H group a chain like structures such as **17** are formed. If it is cis to C-H group it forms a dimeric motif **18**. Recently, it was reported that in the complex of 1,3,5-tricyanobenzene and hexamethylbenzene, 1,3,5-tricyanobenzene forms a hexagonal structure **19**.[31]

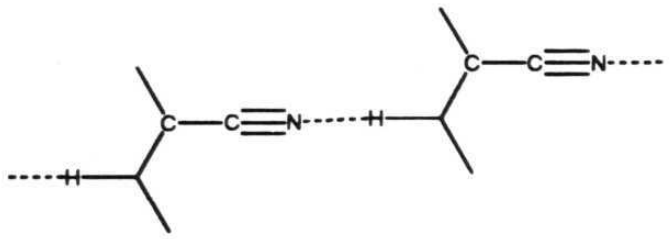

17

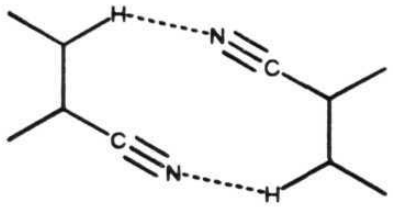

18

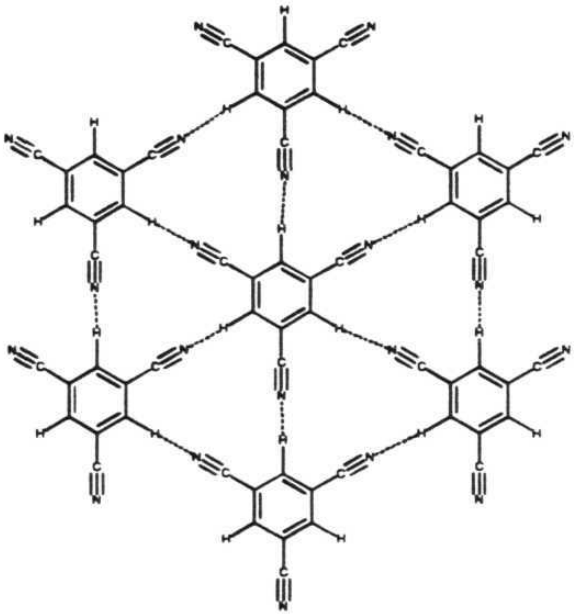

19

1.2.3 X-H···π Hydrogen bonds

In these interactions, the hydrogen bond acceptor is the π cloud of an aromatic ring or a triple bond.

1.2.3.1 O-H···π Hydrogen bonds

Ab initio calculations on model systems like methylacetylene-methanol show that the O-H···π interaction is attractive in nature and the interaction energy is around -1.8 kcal/mol.[32] These calculations also show

that the H···C≡C angle lies ideally between 60 and 120^0, presumably due to steric hindrance in other alternative positions. Recently, neutron diffraction studies on 2-ethynyladamantan-2-ol provided a direct evidence for the O-H···π interaction.[33] In this compound the O-H···π hydrogen bond is short and the O-H group is clearly directed towards the midpoint of the triple bond rather than towards either of the two alkyne carbon atoms as shown in **20.**

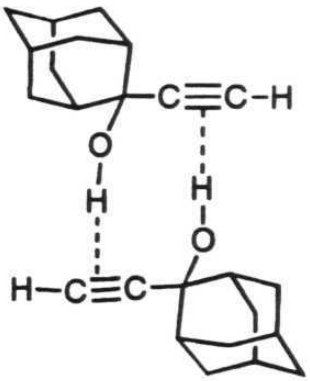

20

X-ray diffraction study of Na_4[calix[4]arene sulphonate].$13.5H_2O$ structure indicates that the water molecule is embedded within the cavity of four aromatic rings.[34] The hydrogen atoms are directed towards the nearest centroids, which are opposite to one another as shown in **21**. The oxygen atoms of the embedded water molecules completes its tetrahedral coordination with hydrogen bonds to two water molecules outside the cavity.

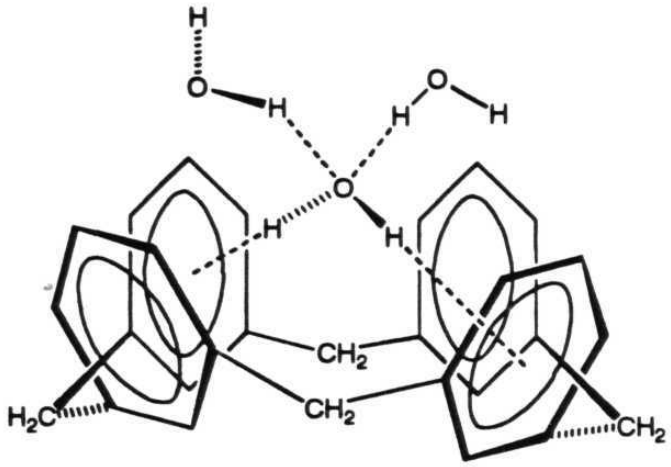

21

1.2.3.2 N-H···π Hydrogen bonds

High-resolution optical and microwave spectral studies on benzene and ammonia dimer in gas phase, show that the ammonia molecule resides above the benzene plane and undergoes free or nearly free internal rotation.[35] In the vibrational averaged structure, the C_3 symmetry axis of NH_3 structure is tilted by about 58^0 relative to benzene C_6 axis, such that ammonia protons interact with benzene π-cloud. This evidence show the existence of N-H···π interactions in the gas phase.

1.2.3.3 C-H···π (C) Hydrogen bonds

Ab initio calculations on binary systems consisting of chloroform, hydrogen cyanide, acetylene, etc., as the acidic C-H component and of the benzene and C≡C as the π components showed that the T-shaped geometries **22** are most stable.[36] These calculations also suggest that the

dispersive or attractive van der Waals forces contribute most predominantly to these interactions. However, the substituent effects on several seemingly CH/π interacted systems reveal that the electron-rich π system is more favourable than the electron deficient systems to form these interactions. In fact, these interactions have been regarded as being identical to herringbone interactions in a number of aromatic structures. Even though the relative energy of these interactions is low, their contribution is significant to the crystal packing forces due to the presence of a large number of carbon and hydrogen atoms in any given organic molecule.

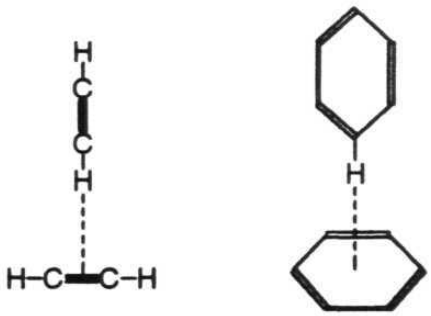

22

A number of recent papers have addressed C-H···π interactions by X-ray structure determinations.[37] For example, it has been shown that in the crystal structure of DL-prop-2-ynylglycine, the alkyne groups form a zigzag pattern, **23** which is suggestive of cooperative hydrogen bonding.[37b] A particularly short C-H···phenyl contact is found in (±)-3-phenylbut-1yn-3-ol, with an H···midpoint separation of only 2.51 Å. The

alkynyl groups of this molecule forms short intermolecular contacts as shown in **24**.

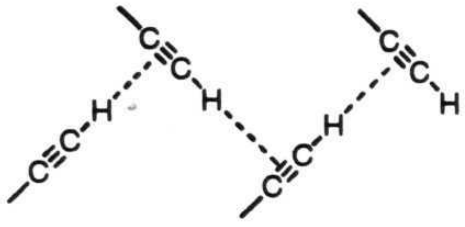

23

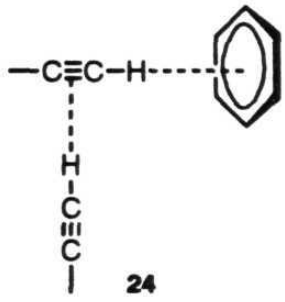

24

Recently, another structural evidence for the existence of C-H···π interaction has been provided with the X-ray crystallographic characterisation of the chloroform solvated complexes of $NpPh_2Au$-C≡C-$AuPh_2Np$ (**25**) and Np_2PhAu-C≡C-$AuPhNp_2$ (**26**).[38] In both cases the C-H bond of the chloroform molecules directs perpendicularly to the C≡C axis in a T-shaped arrangement. Further, *ab initio* calculations on the ethyne and $CHCl_3$ system reveal that the replacement of two hydrogen atoms in ethyne with more electron donating atoms like Na substantially increases the hydrogen bond strength due to the increase of electron density in the C-C π bond.[39]

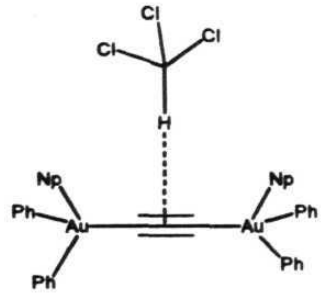

25

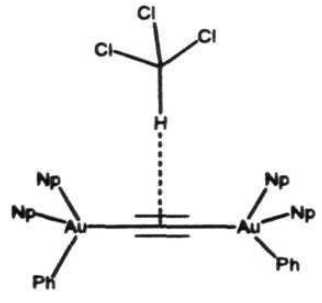

26

1.2.4 X-H···M Hydrogen bonds

Hydrogen bonds to transition metal centres have attracted attention due to the well known agostic interactions where the activation of C-H bond takes place by transition metal complexes.[40] It was also found that the electron rich transition metals can interact with X-H groups to form three-centre-four-electron (3c-4e) interactions which can be distinguished from well known three-centre-two-electron (3c-2e) interactions i.e. agostic interactions. These X-H···M hydrogen bonds, i.e. 3c-4e interactions, were recently reviewed by Brammer.[41] For d^8 square-planar complexes in which the X-H ligand is positioned above the plane and directed approximately towards the central metal atom, there are two orbitals along the z direction, Pt $5d_z^2$ and Pt $6p_z$. In the absence of suitably empty orbitals, the interaction is therefore not of the 3c-2e agostic type **27**, but a 3c-4e interaction **28** instead. 3c-4e X-H···M interactions are of importance in understanding intermolecular interactions between organometallic molecules and are particularly relevant to understanding proton transfer reactions that directly involve transition metal centres.

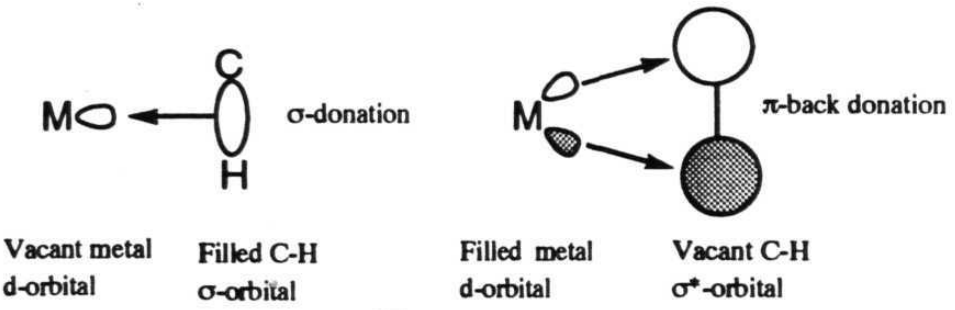

27

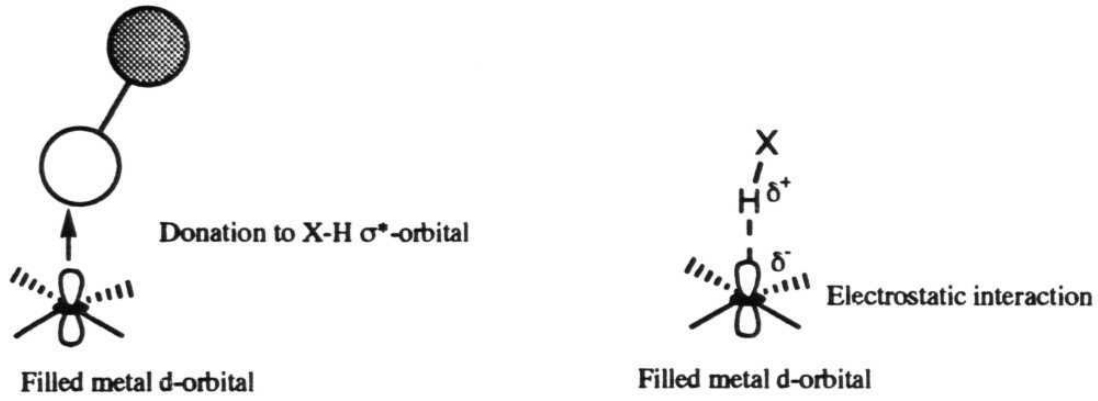

28

1.2.4.1 O-H···M Hydrogen bonds

IR studies on perfluoro alcohols and an extensive series of 18-electron complexes of η^5-$(C_5R_5)ML_2$ (R = H, Me; M = Co, Rh, Ir; L = CO, C_2H_4, N_2, PMe_3) shows a reduction of O-H stretching frequencies indicating the formation of O-H···M hydrogen bonds.[42] The perfluro alcohols were used because of the high acidity of the O-H group. For example, addition of CF_3CH_2OH (pK_a = 12.3) to $Cp^*Ir(CO)_2$ (**29**) causes a shift of 4.9 cm^{-1} in the ν(C-O) band whereas the addition of $(CF_3)_3COH$ (pK_a = 5.4) causes a shift of 12.4 cm^{-1}. This indicates the dependence of the O-H···Ir interaction on the acidity of the O-H group. It

was also shown that the strength of this interaction increases with the basicity of the metal centre.

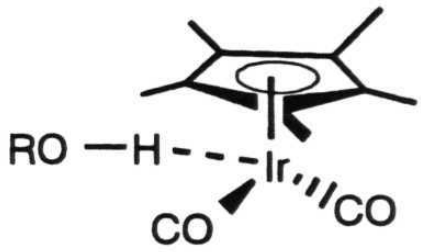

29

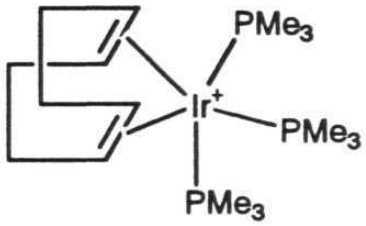

30

Further, the 18-electron Ir species $[Ir(cod)(PMe_3)_3]^+$ (**30**) can undergo oxidative addition to O-H groups of carboxylic acid and alcohol, this process proceeding via initial protonation of the metal centre followed by nucleophilic attack of the carboxylate oxygen.[43] These reactions indicates the initial formation of O-H···M hydrogen bond, which weakens O-H bond and more readily facilitates the protonation step.

1.2.4.2 N-H···M Hydrogen bonds

X-ray determination of compounds **31** and **32** reveals the formation of N-H···M hydrogen bonds.[44] Brammer and co-workers studied the salts $R_3NH^+Co(CO)_3L^-$, where L = CO, $P(OR)_3$ or PR_3 and showed that an increase of the basicity of the hydrogen bond acceptor by changing L leads to a strengthening of the N-H···Co hydrogen bond.[45] These studies also reveal that when there is a competition between N-H···N and N-H···Co interactions, N-H···N interactions are formed preferentially, inferring that the hydrogen bonds to the metal centres are

weaker. However, if there is a possibility to form both N-H···N and N-H···Co interactions simultaneously, one can observe the N-H···Co interactions also. For example **33** is composed of N-H···N and N-H···Co hydrogen bonds.

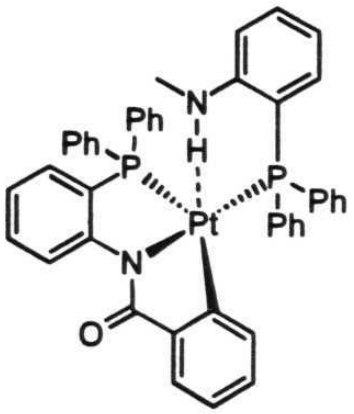

31

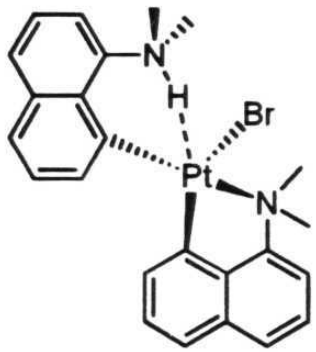

32

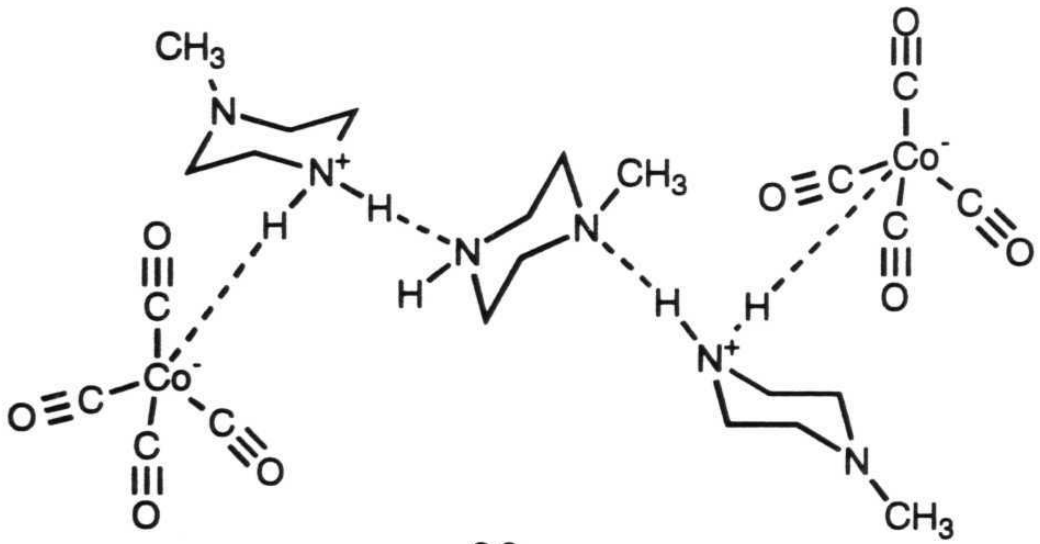

33

1.2.4.3 C-H···M hydrogen bonds

The C-H bond is well-known to interact with electron deficient metals to form 3c-2e bonds i.e. agostic interactions.[40] However, the X-ray determination of compounds **34** and **35** reveal that the C-H group can also interact with electron rich metals to form C-H···M hydrogen bonds i.e. 3c-4e interactions.[45]

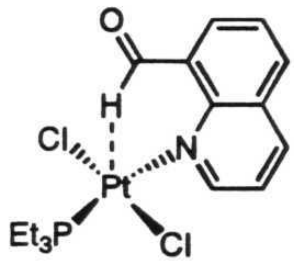

34

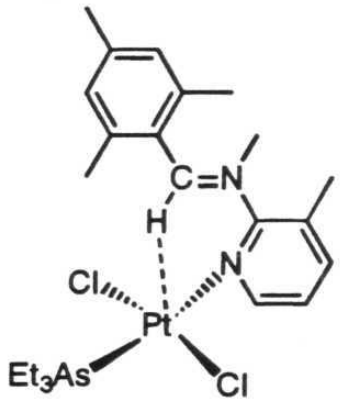

35

1.3 Aim of the present study

A lack of a fuller understanding of hydrogen bonding interactions in transition metal complexes has led to a gap in our ability to design new crystals of these substances. Hence, the present work is aimed at an understanding of hydrogen bonding in organometallic complexes in order to address the differences between the nature and patterns of hydrogen bonding in organic and organometallic compounds. Such an understanding is in turn expected to lead to organometallic compounds with new

properties. This work also aims to explore the utility of weak hydrogen bonding interactions such as C-H···O hydrogen bonds in the design of organic multi-point synthons. Finally, a practical utility of a CSD analysis on β-lactams reveals the importance of structure-activity relationship and paves the way for the better design of newer and higher active drug molecules.

1.4 References

1. G.R. Desiraju, *'Crystal Engineering: The Design of Organic Solids'*, Elsevier, Amsterdam 1989.
2. (a) J. D. Dunitz, *Perspectives in Supramolecular Chemistry: The Crystal as a Supramolecular Entity*, Vol. 2, Ed. G.R. Desiraju, Wiley, Chichester, 1996, 1
3. (a) G.R. Desiraju, *Angew. Chem., Int. Ed. Engl.*, 1995, **34**, 2311.
4. D.S. Reddy, D.C. Craig and G.R. Desiraju, *J. Chem. Soc., Chem. Commun.*, 1995, 339.
5. A. Müller, H. Reuter and S. Dillinger, *Angew. Chem., Int. Ed. Engl.*, 1995, **34**, 2328.
6. D. Braga and F. Grepioni, *Chem. Commun.*, 1996, 571.
7. A. Martin and A.G. Orpen, *J. Am. Chem. Soc.*, 1996, **118**, 1464.
8. G.R. Desiraju, *J.Mol.Str.*, 1996, **374**, 191.
9. F.H. Allen, J.E. Davies, J.J. Galloy, O. Johnson, O. Kennard, C.F. Macrae and D.G.Watson, *J. Chem. Inf. Comput. Sci.*, 1991, **31**, 204.
10. H.B. Bürgi and J.D. Dunitz, *Structure Correlation, Volume* . Eds. H.-B. Bürgi and J.D. Dunitz , VCH, Weinheim, 1994, pp 163-204.
11. T.P.E. Auf der Heyde and H.B. Bürgi, *Inorg. Chem.*, 1989, **28**, 3960.

12. (a) G.R. Desiraju and C.V.K. Sharma, *Perspectives in Supramolecular Chemistry: The Crystal as a Supramolecular Entity*, Vol. 2, Ed. G.R. Desiraju, Wiley, Chichester, 1996, 31.

13. J.-M. Lehn, *Supramolecular Chemistry*, VCH, Weinheim, 1995.

14. L.Pauling, '*The Nature of Chemical Bond and the Structure of Molecules and Crystals - An Introduction to Modern Structural Chemistry*', Oxford University Press, London, 1940.

15. G.C. Pimentel and A.L. McClellan, '*The Hydrogen Bond*', Freeman, San Francisco, 1960.

16. H. Frohlich, *J. Chem. Educ.*, 1993, **70**, A3.

17. G.A. Jeffrey and W. Saenger, *Hydrogen Bonding in Biological Structures*, Springer-Verlag, Berlin, 1991, pp. 24.

18. M. Bailey and C.J. Brown, *Acta. Crystallogr.*, 1967, **22**, 387.

19. F.H. Herbstein in '*Topics of Current Chemistry*', ed. E. Weber, Springer, Berlin, 1987, pp 107-140.

20. O. Ermer, *J. Am. Chem. Soc.*, 1988, **110**, 3747.

21. (a) J.A.R.P. Sarma and G.R. Desiraju, *Acc. Chem. Res.*, 1986, **19**, 222. (b) G.R. Desiraju, *Acc. Chem. Res.*, 1991, **24**, 290. (c) G.R. Desiraju, *Acc. Chem. Res.*, 1996, **29**, 000(in press).

22. V.R. Pedireddi and G.R. Desiraju, *J.Chem.Soc.,Chem., Commun.*, 1992, 988.

23. T. Steiner, *J. Chem. Soc., Chem. Commun.*, 1994, 101.

24. (a) V.R. Thalladi, K. Panneerselvam, C.J. Carrell, H.L. Carrell and G.R. Desiraju, *J. Chem. Soc., Chem. Commun.*, 1995, 341. (b) C.V.K. Sharma and G.R. Desiraju, *J. Chem. Soc., Perkin Trans., 2*, 1994, 2345. (c) T. Suzuki, H. Fujii and T. Miyashi, *J.Org.Chem.*, 1992, **57**, 6744.

25. M.C. Etter, Z. Urbanczyk-Lipkowska, D.A. Jahn and J.S. Frye, *J. Am. Chem. Soc.*, 1986, **108**, 5871.

26. D. Braga, F. Grepioni, J.J. Byrne and A. Wolf, *J. Chem. Soc., Chem. Commun.*, 1995, 1023.

27. (a) D.S. Reddy, Y.E. Ovchinnikov, O.V. Shishkin, Y.T. Struchkov and G.R. Desiraju, *J. Am. Chem. Soc.*, 1996, **118**, 4085. (b). J.A.R.P. Sarma, M.S.K. Dhurjati, K. Bhanuprakash and K. Ravikumar, *J. Chem. Soc., Chem. Commun.*, 1993, 440.

28. M.C. Etter and D.A. Adsmond, *J. Chem. Soc., Chem. Commun.*, 1990, 589.

29. J.A. Zerkowski, C.T. Seto and G.M. Whitesides, *J. Am. Chem. Soc.*, 1992, **114**, 5473.

30. A. Houlton, D.M.P. Mingos and D.J. Williams, *Transition Met. Chem.*, 1994, **19**, 653.

31. D.S. Reddy, B.S. Goud, K. Panneerselvam and G.R. Desiraju, *J. Chem. Soc., Chem. Commun.*, 1993, 663.

32. M.A. Viswamitra, R. Radhakrishnan, J. Bandekar and G.R. Desiraju, *J. Am. Chem. Soc.,* 1993, **115**, 4868.

33. F.H. Allen, J.A.K. Howard, V.J. Hoy, G.R. Desiraju, D.S. Reddy and C.C. Wilson, *J. Am. Chem. Soc.,* 1996, **118**, 4081.

34. J.L. Atwood, F. Hamada, K.D. Robinson, G.W. Orr and R.L. Vincent, *Nature*, 1991, **349**, 683.

35. D.A. Rodham, S. Suzuki, R.D. Suenram, F.J. Lovas, S. Dasgupta, W.A. Goddard III and G.A. Blake, *Science*, 1993, **362**, 735.

36. M. Nishio and M. Hirota, *Tetrahedron,* 1989, **45**, 7201 and references cited therein.

37. (a) T. Steiner, *J. Chem. Soc., Chem. Commun.,* 1995, 95. (b) T. Steiner, E.B. Starikov, A.M. Amado and J.J.C. Teixeira-Dias, *J. Chem. Soc., Perkin Trans. 2*, 1995, 1321. (c) T. Steiner and W. Saenger, *J. Chem. Soc., Chem. Commun.,* 1995, 2087. (d) T. Steiner, M. Tamm, B. Lutz and J. van der Mass, *Chem. Commun.,* 1996, 1127.

38. (a) T.E. Muller, D.M.P. Mingos and D.J. Williams, *J. Chem. Soc., Chem. Commun.,* 1994, 1787. (b) T.E. Muller, W.K. Choi, D.M.P. Mingos, D. Murphy, D.J. Williams and W.W. Yam, *J. Organomet. Chem.,* 1994, **484**, 209.

39. M.-F. Fan, Z. Lin, J.E. McGrady and D.M.P. Mingos, *J. Chem. Soc., Perkin Trans. 2.* 1996, 563.

40. (a) M. Brookhart, M.L.H. Green and L.-L. Wong, *Prog. Inorg. Chem.*, 1988, **36**, 1; R.H. Crabtree, *Chem. Rev.*, 1985, **85**, 245. (b) R.H. Crabtree, *Angew. Chem. Int. Ed. Engl.*, 1993, **32**, 789.

41. L. Brammer, D. Zhao, F.T. Ladipo and J.B. Wilking, *Acta. Crystallogr.*, 1995, **B51**, 632.

42. S.G. Kazarian, P.A. hamley and M. Poliakoff, *J. Am. Chem. Soc.*, 1993, **115**, 9069.

43. F.T. Ladipo, M. Kooti and J.S. Merrola, *Inorg. Chem.*, 1993, **32**, 1681.

44. (a) D. Hedden, D.M. Roundhill, W.C. Flutz and A.L. Rheingold, *Organometallics,* 1986, **5**, 336. (b) I.C.M. Wehman-Ooyevaar, D.M. Grove, H. Kooijman, P. van der Sluis, A.L. Spek and G. van Koten, *J. Am. Chem. Soc.*, 1992, **114**, 9916.

45. (a) A. Albinati, C.G. Anklin, F. Ganazzoli, H. Ruegg and P.S. Pregosin, *Inorg. Chem.*, 1987, **26**, 503. (b) A. Albinati, C. Arz and P.S. Pregosin, *Inorg. Chem.*, 1987, **26**, 508.

Chapter 2

N-H···O Hydrogen Bonds in Transition Metal Complexes Containing Amido Groups

2.1 Introduction

Like organic crystals, the assembly of mononuclear and polynuclear organometallic complexes in the solid state is governed,[1,2] by a balance between non-directional close-packing forces[3] and directional interactions between metal atoms[4] or charged groups.[5] However, because of the greater flexibility of organometallic molecules, the crystal packing and molecular shape influence each other in a manner which is much more complex than what is observed in the majority of organic crystals.[6] Flexible shapes and the availability of different bonding modes which differ little in energy for the same type of ligands result in structural non-rigidity for most organometallic molecules. This, in turn is responsible for the many fluxional processes of organometallic molecules in solution and for the existence of polymorphism in the solid state.[7]

The importance of hydrogen bonding interactions in the crystal engineering studies of organic compounds has been described in the Chapter 1. Hydrogen bonding is a major cohesive force in many molecular crystals of the organic, organometallic and inorganic type.[8] In spite of a large number of studies devoted to hydrogen bonding in organic compounds, little has been done with organometallics and metal complexes. Along these lines the role played by 'strong' or conventional hydrogen bonds in organometallic crystals containing hydrogen bond

donor and acceptor groups such as -COOH, -OH, -COOR as well as CO-ligands has been investigated recently.[11]

Differences between organic and organometallic systems arise from the interaction of the organic molecules (the ligands) with the metal centres in the later. The metal-ligand bond influences the patterns of hydrogen bonds, although the variability is high. The effect of the coordination to the metal(s) is essentially twofold. On the one hand, one must consider the electronic effects of donation/backdonation in bonding of ligands (arenes, cyclopentadienyl ligands, alkynes, alkenes, etc.) as well as in the direct M-X σ-bonding (X = C, N, O, etc.) which affects the polarity of C-H, N-H, and O-H bonds and therefore the acidity of the hydrogen atoms. On the other hand, there is a definite possibility that hydrogen-bond acceptors can bind alternatively *via* lone-pair donation to empty orbitals on the metal atoms.

In this chapter an analysis on the hydrogen bonding patterns in transition metal amido-complexes will be presented, hereinafter referred to as OM-complexes. This group includes complexes in which primary and secondary amido groups are either directly linked to the transitional metal centre(s) or belong to a larger metal-coordinated ligand system (see Scheme 1).

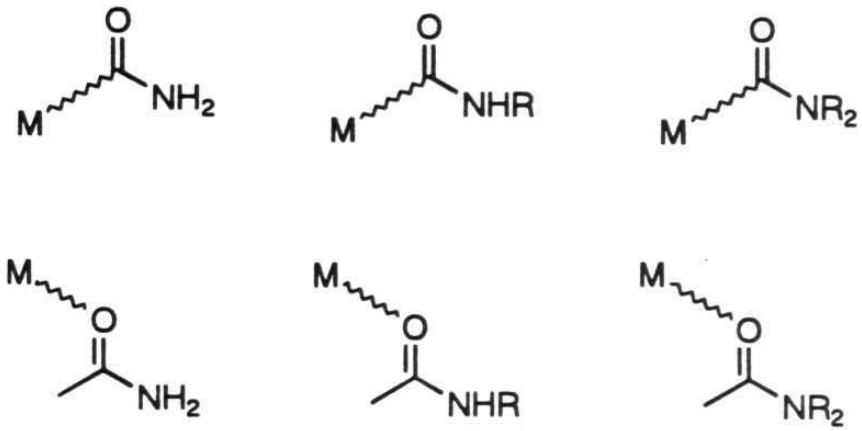

Scheme 1: Metal binding modes with primary, secondary and tertiary amides

At this point, it is important to discuss some of the other key aspects of hydrogen bonding in organic amides that have not been covered in Chapter 1.[12] In primary amides the CO-NH_2 group is planar and the maximum electrostatic strength of the intermolecular hydrogen bond is achieved when the N-H vector is collinear with the lone pairs of the oxygen atoms. In general, the O-atom of a C=O fragment optimises the C=O···H angle (ϕ in **1**) to a value around 120-140°, even though deviation form this range is not uncommon tending the N-H···O angle (θ in **1**) to linearity.

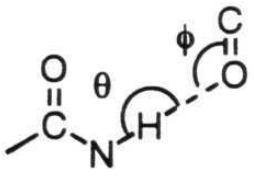

1

As discussed in Chapter 1, organic amides form hydrogen bonded dimers of the type shown in **2** similar to those observed for carboxylic acids, although donor-acceptor N···O distances in amides span a much

wider range than O···O hydrogen bonded distances in acids. Relevant exceptions are the tetragonal and rhombohedral forms of acetamide as well as adipamide, chloroacetamide, azodicarbonamide, and nicotinamide in which hydrogen-bonded dimers of type **2** are not formed.[12a] It is relevant to note here that hydrogen bonding in amides has also been approached theoretically.[13] These studies revealed that average geometrical parameters have no appreciable difference in primary and secondary amide crystals, although the average N···O distance is slightly longer in the former [2.95(6) versus 2.90(7) Å].

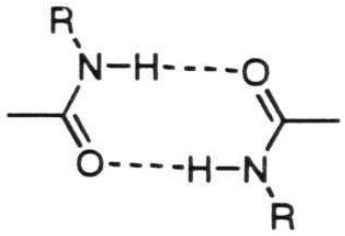

2

Organometallic amides are of interest in the studies of hydrogen bonding interactions not only because they have potential donors and acceptors, but also because of the definite possibility for the amide to act as a ligand by coordinating to metal centres *via* the O-atom lone pairs. This type of coordination, brings one of the amide hydrogen atoms close to the metal centre, thus preventing the participation of this H atom in hydrogen bond formation. A second aspect of some importance is the competition of other acceptor groups with the amide O-atom.

In this chapter, the following questions will be discussed:

i) Do amide groups behave in the same way in organic and organometallic crystals with regard to their hydrogen bond formation ability?

ii) Is there any difference in H-bonding patterns formed by primary and secondary amides?

iii) What is the effect of the coordination of amide oxygen to the metal centre on the hydrogen bonding patterns?

iv) Is the CO ligand (when present) capable of competing with the amide oxygen in terms of hydrogen bonding acceptor capacity ?

In order to address these questions, the Cambridge Structural Database (CSD)[14] has been searched for amide groups in organic and organometallic compounds. The nature and the patterns of the hydrogen bonding interactions in organometallic amides has been examined by comparing with that of the organic amides. Some selected crystal structures will be discussed with particular attention to very short N-H···O contacts.

2.2 Results and Discussion

For the sake of a consistent description and comparison between organic and OM systems, N-H···O hydrogen bonds are classified into four categories according to changes in the acceptor moiety. In this way, one

can also look in to the robustness of interamide hydrogen bonds. The first set (A) contains all N-H···O hydrogen bonds formed by amide protons with all possible acceptor O-atoms (carbonyl O, ether O, water, *etc.*); the second set (B) contains hydrogen bonds formed by only keto-, amide and ester carbonyl groups; the third group (C) contains bonds formed by only amide carbonyl groups. Thus the third group is a sub-set of the second which is a sub-set of the first. The fourth group (D) is likewise a sub-set of the third and contains cyclic bonds of the type described in **2**. These four categories are shown below. The results are summarised in Table 1.

A. O=C-N-H···O

B. O=C-N-H···O=C

C. O=C-N-H···O=C-N-H

D. 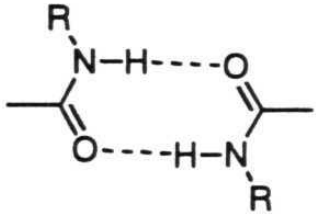

With respect to the data collected in Table 1 one can observe that only 52% of the OM primary amides (49 out of 95) form the inter-amide N-H···O hydrogen bonds in category C, whereas such bonds are present in as many as 71% of the organic primary amides (308 out of 432). Similarly, only 30% of the OM secondary amides (69 out of 220) form the N-H···O bonds of category C, while as many as 65% of the pure organic secondary

Table 1. Mean geometrical parameters for N-H···O hydrogen bonds in organometallic and organic amides.

PRIMARY AMIDES - OM Complexes					
Set type	H···O (Å)	N···O (Å)	No. of contacts	Unique Refcodes	N-H···O (°)
A	2.21 (1)	3.09(1)	369	95	149(1)
B	2.14(2)	3.03(1)	120	66	153(2)
C	2.15(3)	3.04 (2)	77	49	151(2)
D	2.07(3)	2.99(1)	38	35	157(3)
	2.07(3)	3.00(2)			158(3)
SECONDARY AMIDES - OM Complexes					
A	2.10(1)	3.02(1)	1014	432	156(1)
B	2.04(1)	2.98 (1)	709	375	159(1)
C	2.03(1)	2.97(1)	513	308	160(1)
D	1.97(1)	2.95(1)	192	181	167(1)
	1.97(1)	2.95(1)			167(1)
PRIMARY AMIDES - Organics					
A	2.10(2)	3.00(1)	451	220	153(1)
B	2.03(2)	2.96(2)	151	96	151(1)
C	2.02(2)	2.96(2)	112	69	159(1)
D	1.89(2)	2.89(2)	56	45	168(1)
	1.90(2)	2.89(2)			168(1)
SECONDARY AMIDES - Organics					
A	2.01(1)	2.95(1)	3974	2659	159.6(3)
B	1.99(1)	2.94(1)	3026	2125	159.6(4)
C	1.98(1)	2.93(1)	2422	1724	160.5(4)
D	1.90(1)	2.87(1)	664	593	166.3(6)
	1.91(1)	2.88(1)			166.5(6)

amides (1724 out of 2659) form this type of hydrogen bond. The participation of water (either as solvent or as ligand in the OM complex) in intermolecular hydrogen bonds does not affect the inter-amide hydrogen bonding. Water is found in 27 primary and 34 secondary OM amides, respectively.

For both organic and OM structures, category C hydrogen bonding is more frequent for primary rather than for secondary amides, a factor which may be attributed to the greater number of amide H-atoms in the former group. Another fact worth noting is that the proportion of OM primary and secondary amides in category C (that is O=C-N-H···O=C-N-H) is significantly less than for the organic amides. This difference is not only a consequence of the presence of other competing donors and acceptors, such as H_2O, NO_3^-, etc., with respect to organic amides, but also reflects the existence of cases in which the O-amide atom is engaged in coordination to the metal centre *via* one of its lone-pairs. The behaviour of primary and secondary amides as O-bound ligands has a two-fold effect, since it decreases the number of acceptor sites available for hydrogen bonding and increases the steric hindrance around the oxygen atoms, which, in some cases, can altogether prevent inter-amide hydrogen bonding formation.

This aspect has been analysed with respect to the data grouped in the more general category A. Of the 95 primary and 220 secondary OM

amido complexes in this category, 67 and 90 compounds respectively correspond to cases where the amide O-atom is bound to a transition metal. Of these, in a further subset of 33 and 23 cases respectively, the O-atom is additionally bonded to an amide N-H group. The remainder, that is 34 and 67 may also be bonded but not to amide N-H groups. These hydrogen bonds are no different from the rest and suggests that ligation to a metal atom does not prevent an amide O-atom from accepting a hydrogen bond.

Of the 95 and 220 OM compounds containing primary and secondary amido groups, respectively, referred to above, 1 primary amide and 15 secondary amides contain the CO-ligand and, of these, 7 of the latter category form N-H···O hydrogen bonds to this CO-ligand. Although these statistics are sparse, they are in general agreement with the concept of hard and soft hydrogen bonds according to which the hard donor N-H prefers hard acceptors like amido-CO groups, water and so on, rather than the soft CO-ligand acceptor.

2.2.1 Hydrogen bond (N-H···O) distances

Histograms of the N-H···O distances present in both organic and OM-crystals are given for primary (Figure 1a) and secondary amides (Figure 1b). Both histograms show that the N-H···O distribution for organic compounds is tighter than that for the OM compounds for which

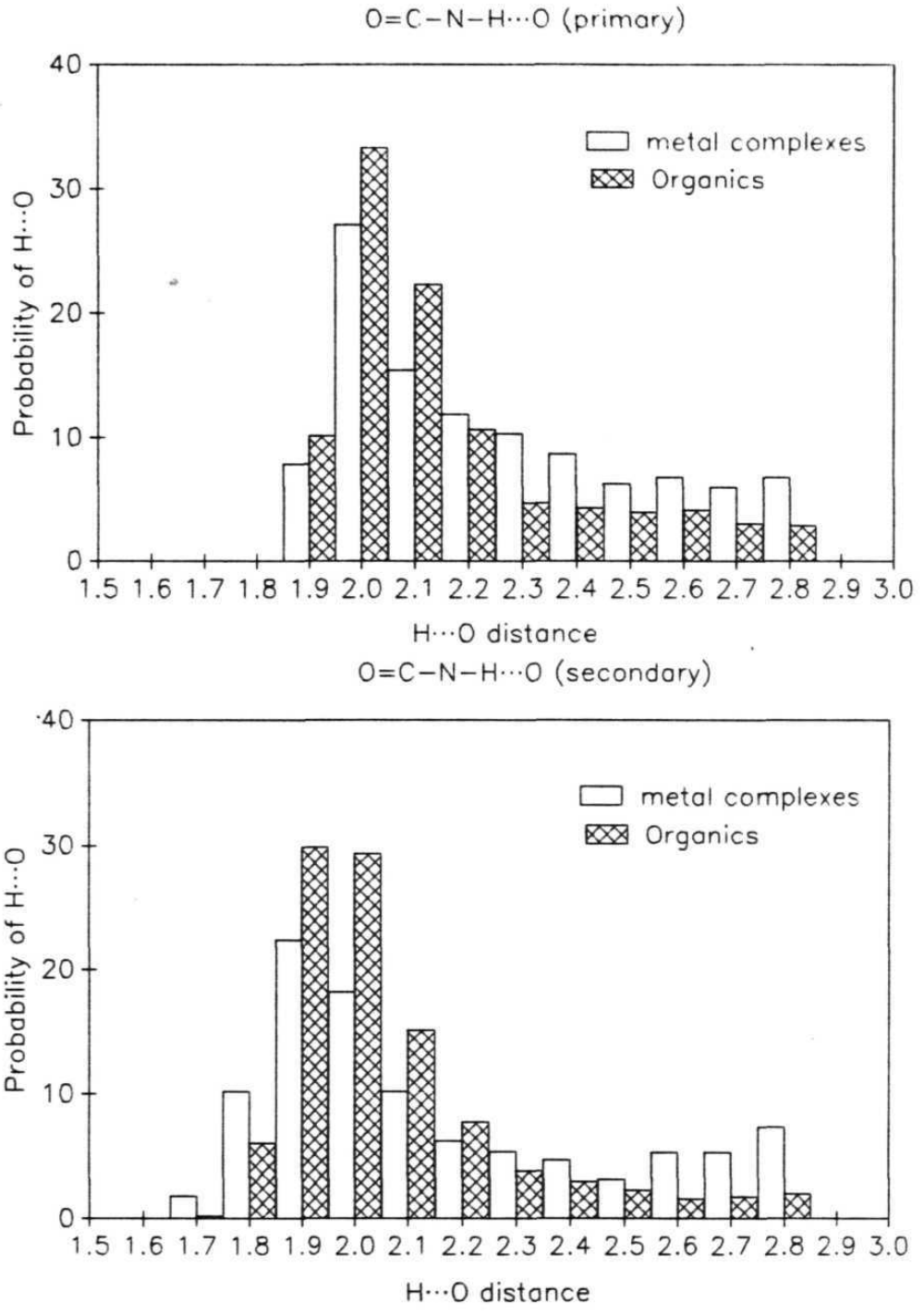

Figure 1. Distribution of the N-H···O distances in organic (shaded columns) and OM-crystals as observed for (a) primary and (b) secondary amido groups.

there is a higher proportion of longer hydrogen bonds. For instance, while 33% and 27% of organic and OM hydrogen bonds occur in the peak range of 1.90-2.00 Å, this order is reversed at longer separations: in the N-H···O range 2.70-2.80 Å, one obtains 3% and 6% in the two respective categories. Again, by comparing Figures 1a and 1b, it can be noted that the lower limit of N-H···O distances in secondary amides are somewhat shorter than for primary amides.

A steric factor may explain the presence of longer hydrogen bonds for OM compounds. However, this appears to be compensated by a larger number of bifurcated hydrogen bonds with respect to pure organic amides. This is borne out by the statistics on bifurcated hydrogen bonds: 39% of the hydrogen bonds in the primary amide OM compounds (144 out of 369) correspond to bifurcated interactions. The percentage of bifurcated hydrogen bonds is only 25% in organic primary amides (252 out of 1014).[15] A similar situation prevails for the secondary amides also. In general, these donor-bifurcated (or three-centre) interactions are formed when the number of acceptors is greater than the number of donors. In OM compounds the acceptor-donor imbalance is certainly accentuated by the presence of other acceptors such as water of crystallisation.

Contrary to organic systems, many OM complexes are ionic. These ionic complexes may be analysed to explore the effect of the ionic charge on the N-H···O hydrogen bond lengths. There are total of 206 and 216 N-

H···O bonds in the primary and secondary amides respectively. The distributions of H···O distances for ionic and nonionic amides are shown in Figure 2. From these distributions it is clear that the ionic charge does not cause any major change in the hydrogen bond lengths. It can be noted that in majority of the cases positive charge is on the metal atom not on the amide N-H group.

The distributions of H···O distances in type C interactions has been examined, inorder to understand the effect of metal coordination to amide O-atom on N-H···O hydrogen bonds (Scheme 2).

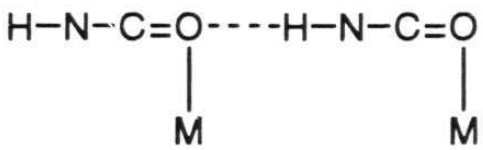

Scheme 2: N-H···O Hydrogen bonds between metal coordinated amide O-atom and amide proton

There are 33 and 23 compounds for the above fragment in the primary and secondary OM amido complexes respectively. Although the sample is not large enough to justify subtle comparisons one can note the differences between primary and secondary OM amides may be noted. The lower limit of N-H···O distance in primary amides is 2.1 Å, while it is 2.0 Å in secondary amides. The M-O distances in primary amides are shorter than those of secondary amides (2.1 versus 2.2 Å). This difference in M-O distances arises from the greater steric hindrance of secondary amides with

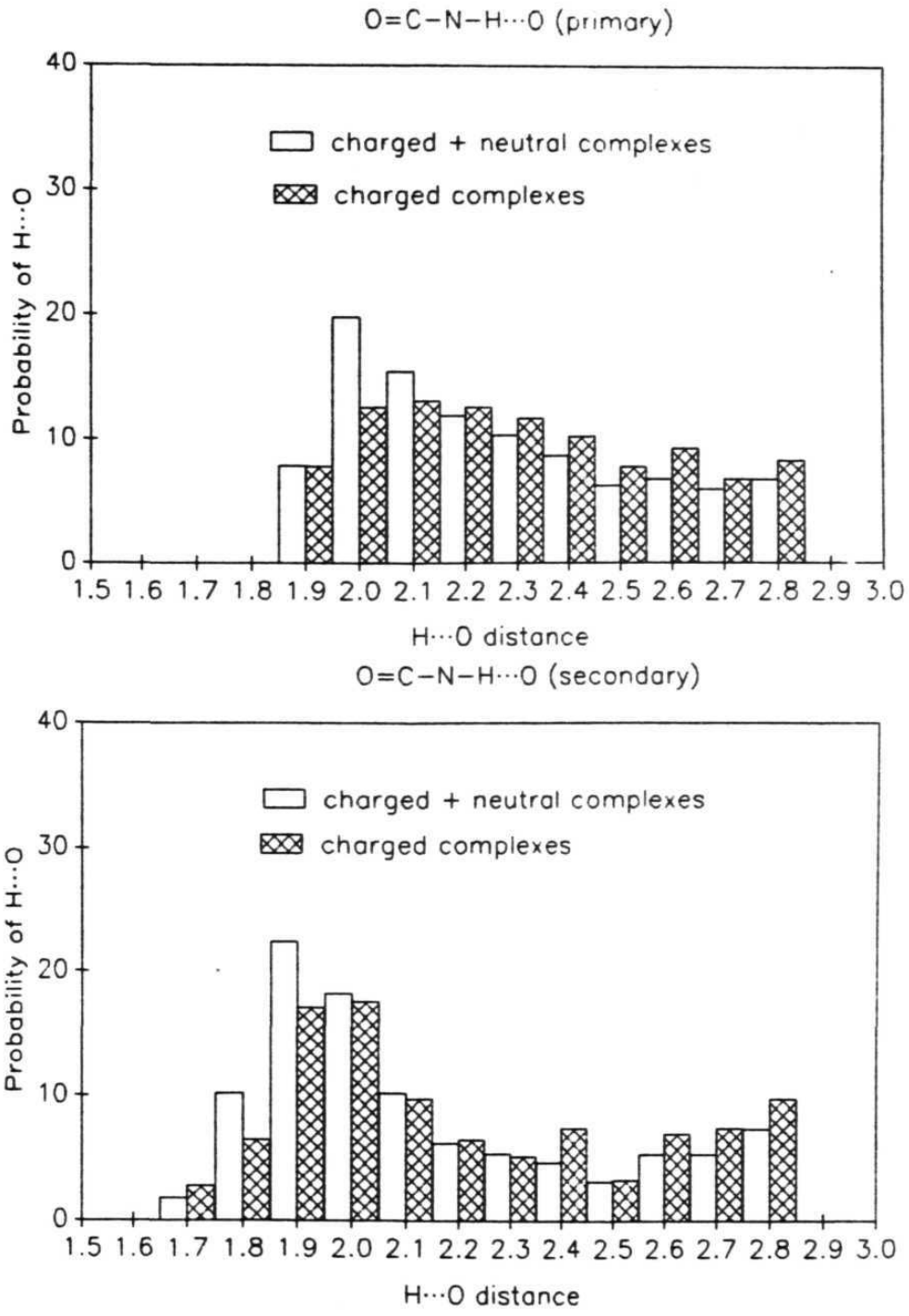

Figure 2. Distributions of the N-H···O distances in ionic and non-ionic complexes of (a) primary OM-amides and (b) secondary OM-amides.

respect to primary amides, although an electronic contributions cannot be confidently ruled out on the basis of pure statistics.

2.2.2 N-H···O angles (θ)

Figures 3 and 4 are scatterplots of the N-H···O [θ] angles versus N-H···O distances in type A primary and secondary amides respectively. In all cases the N-H···O angles span a rather ample range (120-180°) although there is marked tendency to concentrate at higher angles as the distance decreases. For N-H···O distances shorter than 2.0 Å there are no θ-angles smaller than *ca.* 140° and as the hydrogen bonding interaction becomes shorter the angles approaches linearity. These parameters are well correlated and shorter H···O distances are invariably associated with more linear hydrogen bond geometries. This feature, characteristic of strong hydrogen bonding, arises from mutual repulsion of the electronegative atoms N and O which constitute the hydrogen bond and is observed for secondary OM amides as well. These distributions of H···O distances are same as those in 'pure' organic crystals. However, for secondary amides the tendency to afford shorter hydrogen bonds than primary amides can also be appreciated.

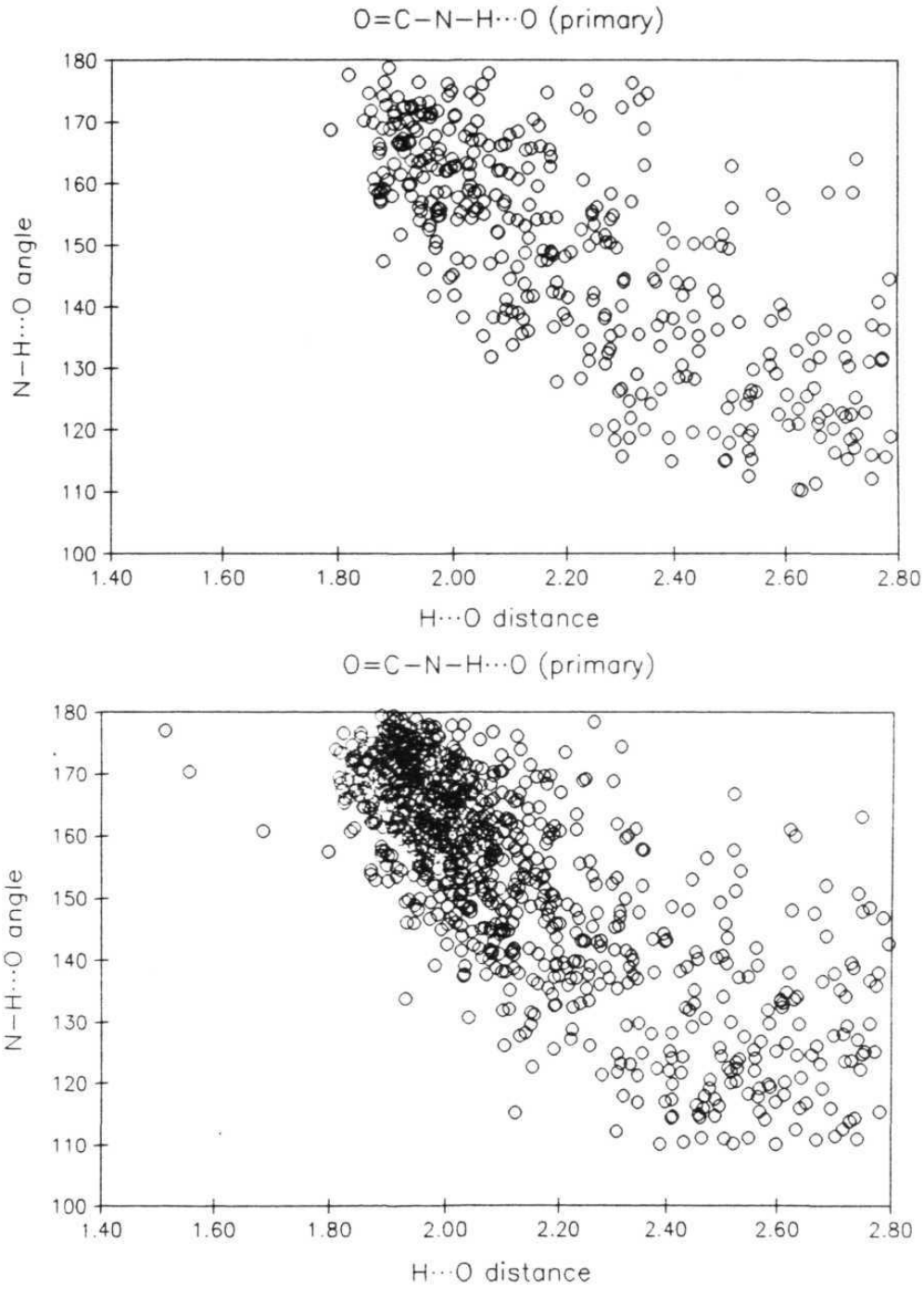

Figure 3. Scatterplot of N-H···O angles (°) versus N-H···O distances (Å); (a) primary OM-amides, (b) primary organic amides.

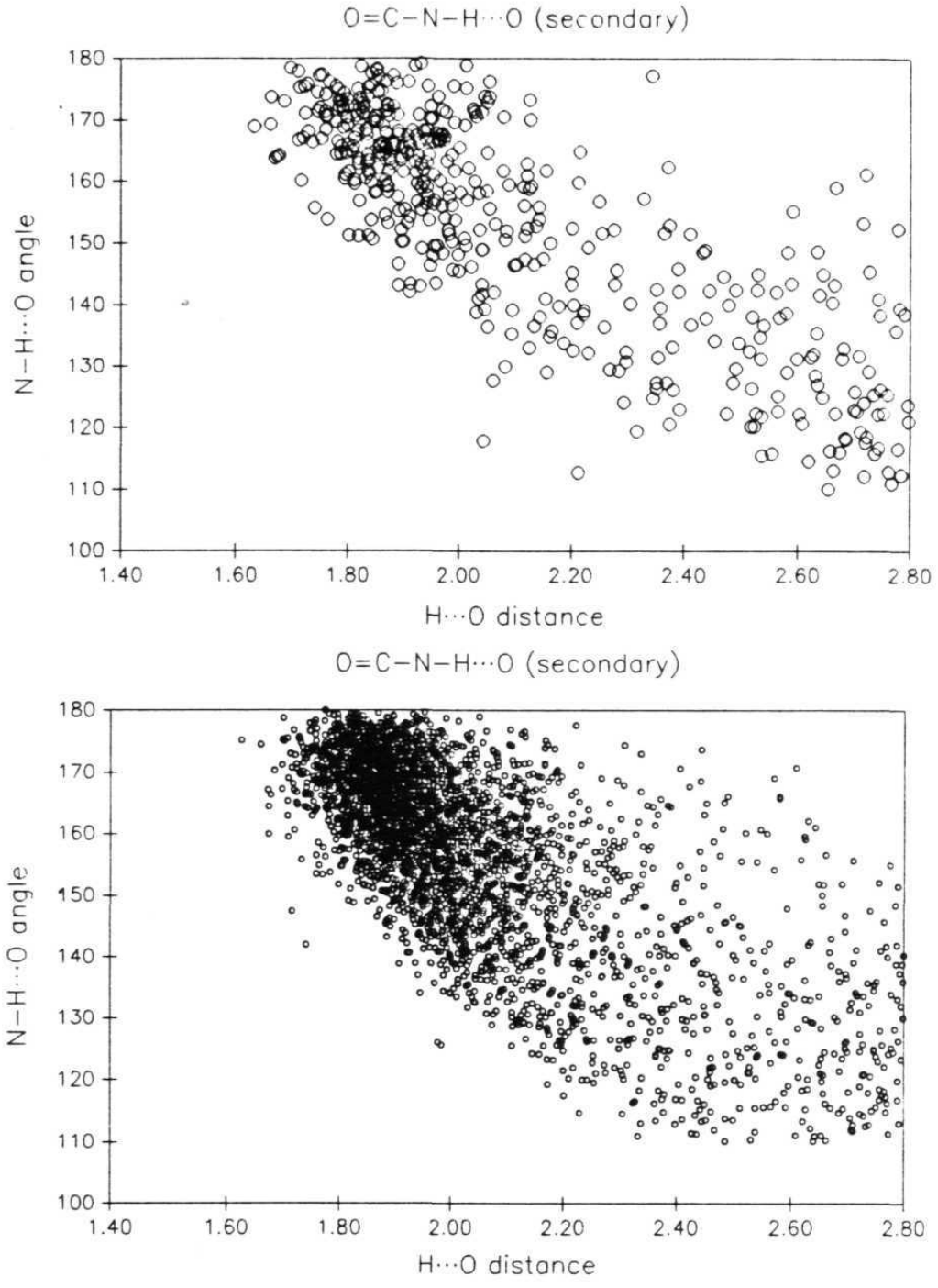

Figure 4. Scatterplot of N-H···O angles (°) versus N-H···O distances (Å)

(a) secondary OM-amides, (b) secondary organic amides

2.2.3 C=O···H angles (ϕ) and hydrogen bond directionality

The distribution of C=O···H angles [ϕ] in category B from OM and organic amides are shown in Figure 5 and 6 respectively. Distinct maxima are observed at 130°. In order to take into account the solid angle correction,[16] the distributions in Figures 5 and 6 are corrected by the sin(ϕ) factor to give the histograms in Figures 7 and 8. The solid angle correction takes into account the different probability of an angular distribution in order to upweight the more linear contacts, which sweep a smaller solid angle. This procedure is more important whenever a comparison is required between calculated and observed angular distributions.

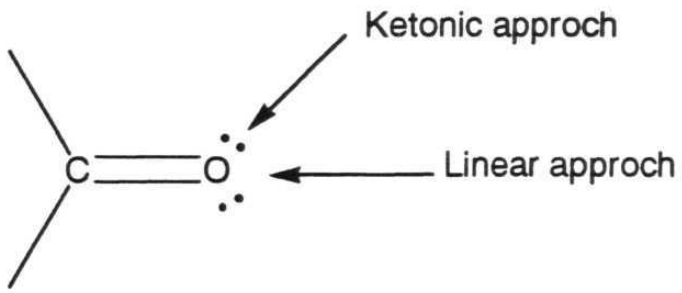

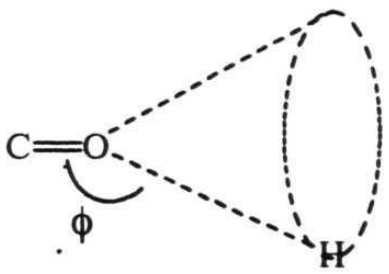

probability of a hydrogen bond to occur with angle ϕ is proportional to sin ϕ

This procedure reveals interesting differences between OM and organic amides, and between primary and secondary amides. While the

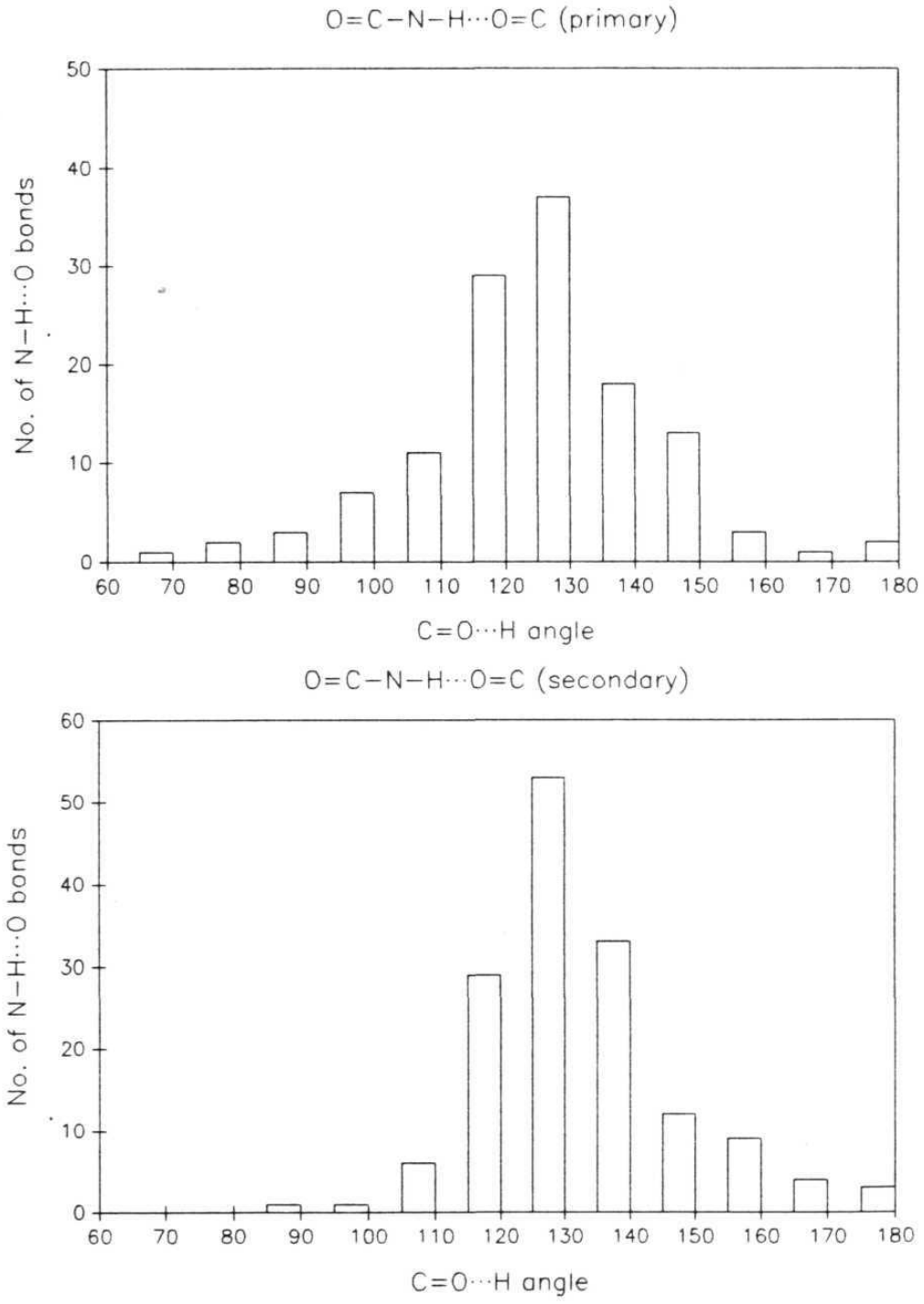

Figure 5. (a) Distribution of C=O···H angles in category B in primary and secondary OM amides. Note the distinct maxima at 130°.

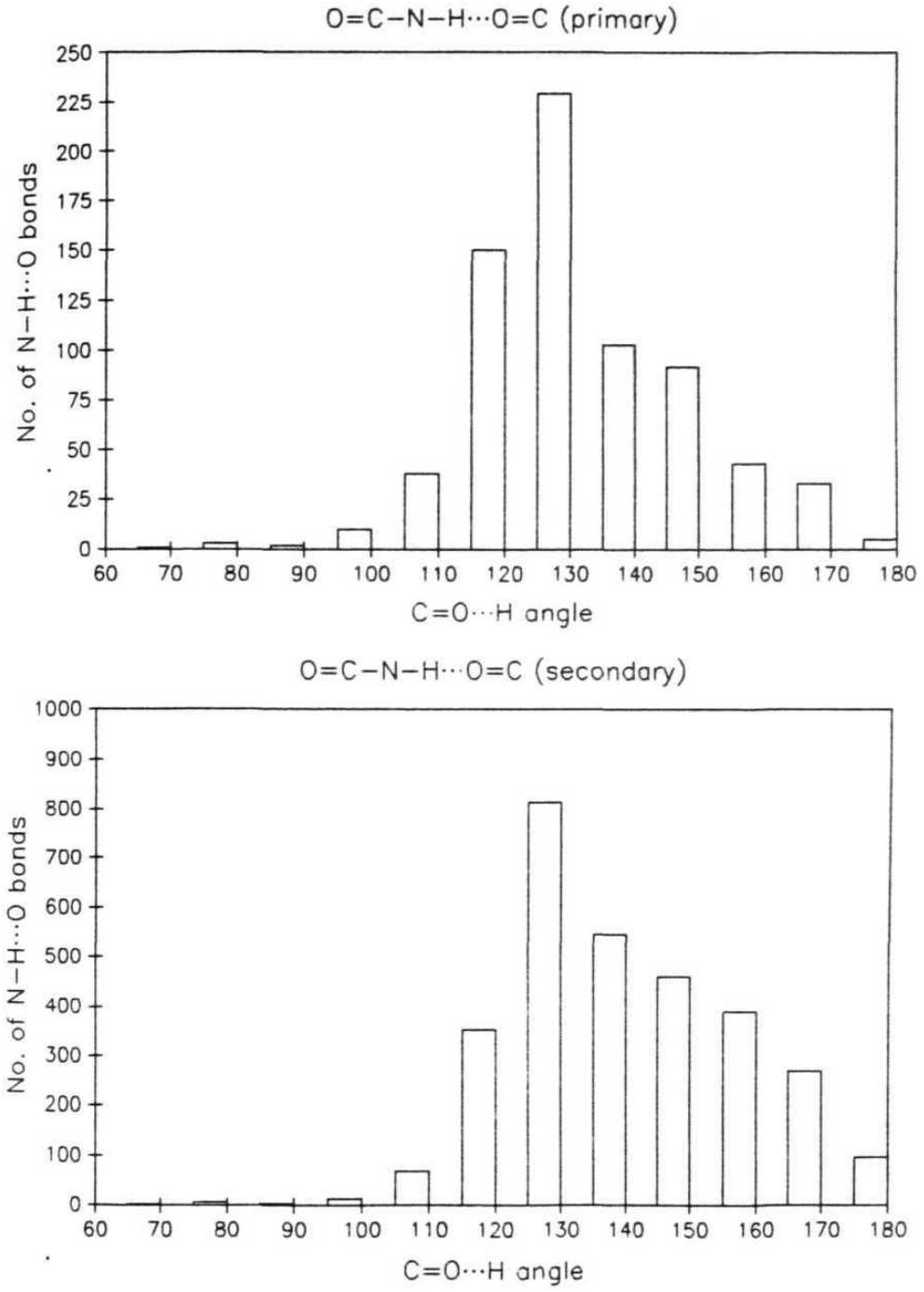

Figure 6. Distribution of C=O···H angles in category B in primary and secondary organic amides. Note the similarities between Figures 5 and 6.

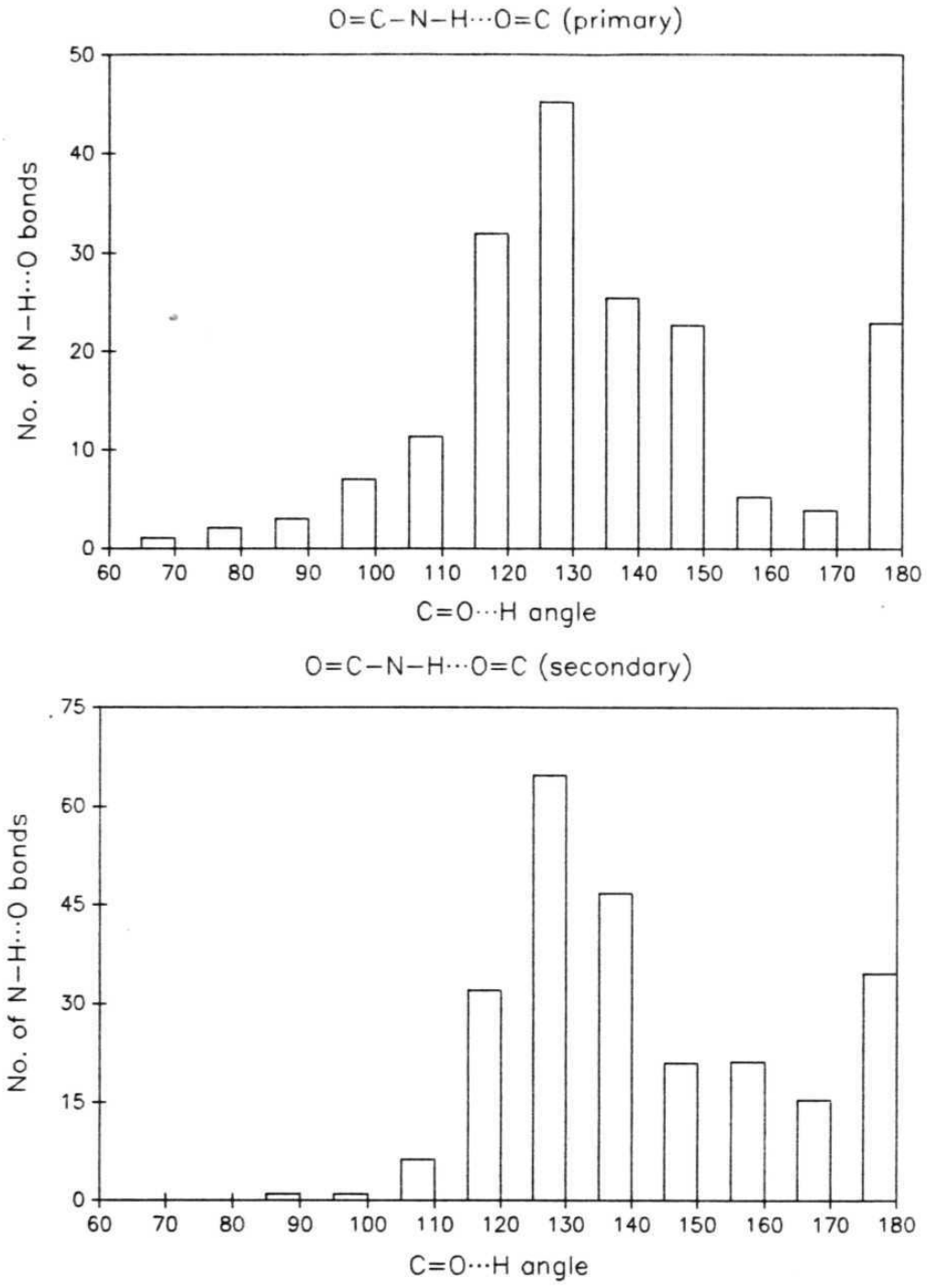

Figure 7. C=O···H angle distribution for OM amides after application of the sin(ϕ) solid angle correction.

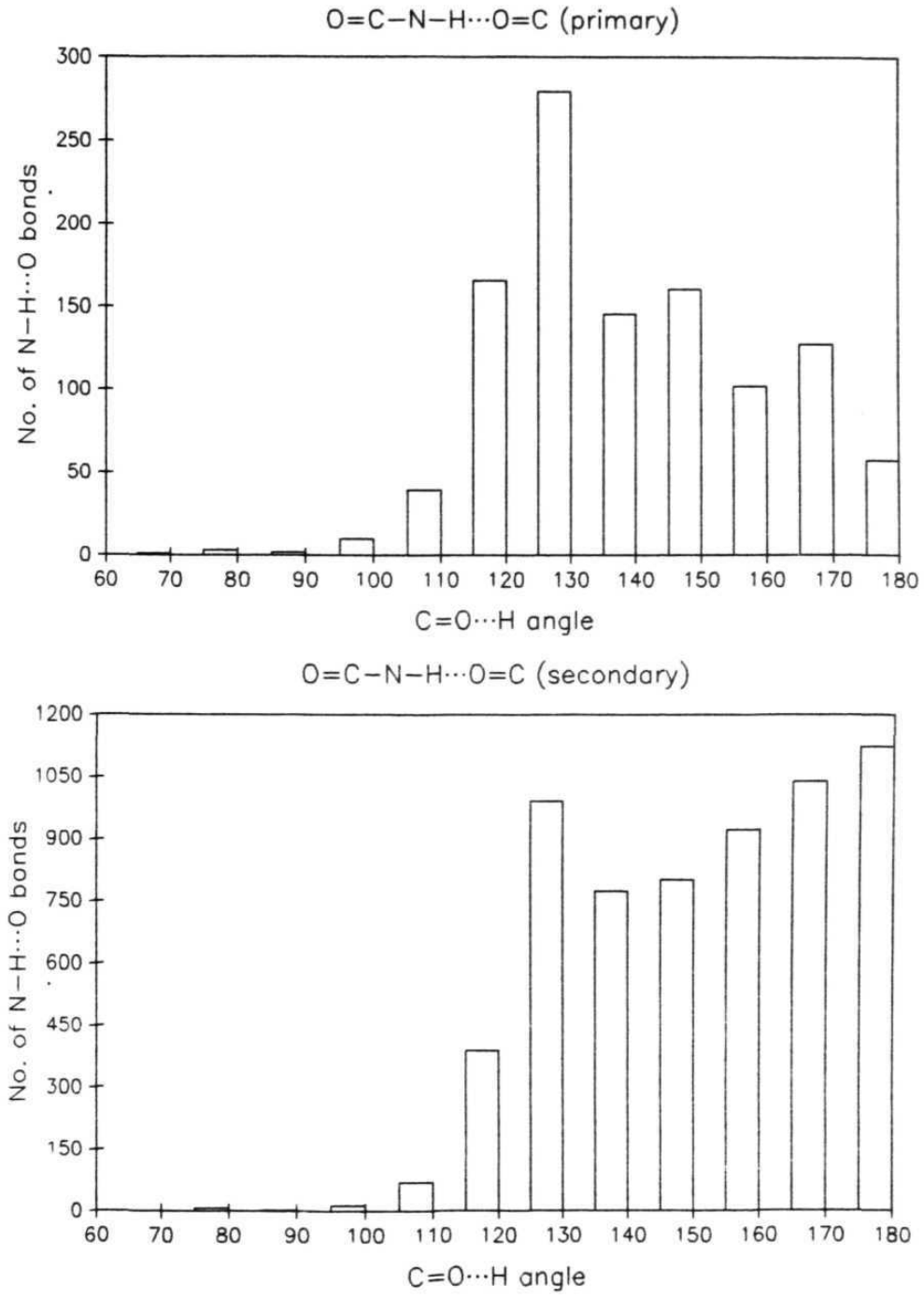

Figure 8. C=O···H angle distribution for organic amides after application of the sin(ϕ) solid angle correction.

distributions for OM amides (both primary and secondary) clearly show double maxima at 130° (corresponding to a 'ketonic' approach of the H-atom) and at 180° (corresponding to a linear approach), that for the pure organic primary amides retains only the single maximum at 130°. These effects are blurred for the organic secondary amides where the distribution of ϕ values is almost uniform in the range 130-180°. These variations again hint that a steric factor is operating. It seems that the more highly hindered OM amides are unable to accommodate the (electronically-favourable) 'ketonic' approach and settle for the linear approach. Again, for the pure organics, secondary amides are by definition more sterically hindered than primary amides and therefore have a greater tendency to adopt the linear hydrogen bond geometry. For primary organic amides the presence of two amido hydrogens, coupled with the absence of steric hindrance in the amide-region of the molecule, results in an optimisation of a large number of hydrogen bonds with the ideal 'ketonic' approach. Figures 9 and 10 are the scatterplots of ϕ versus H···O distances for primary and secondary amides respectively. These plots reveals that these ϕ angle distributions are insensitive to the H···O distance range, that is a particular directionality is preferred for both short and long hydrogen bonds.

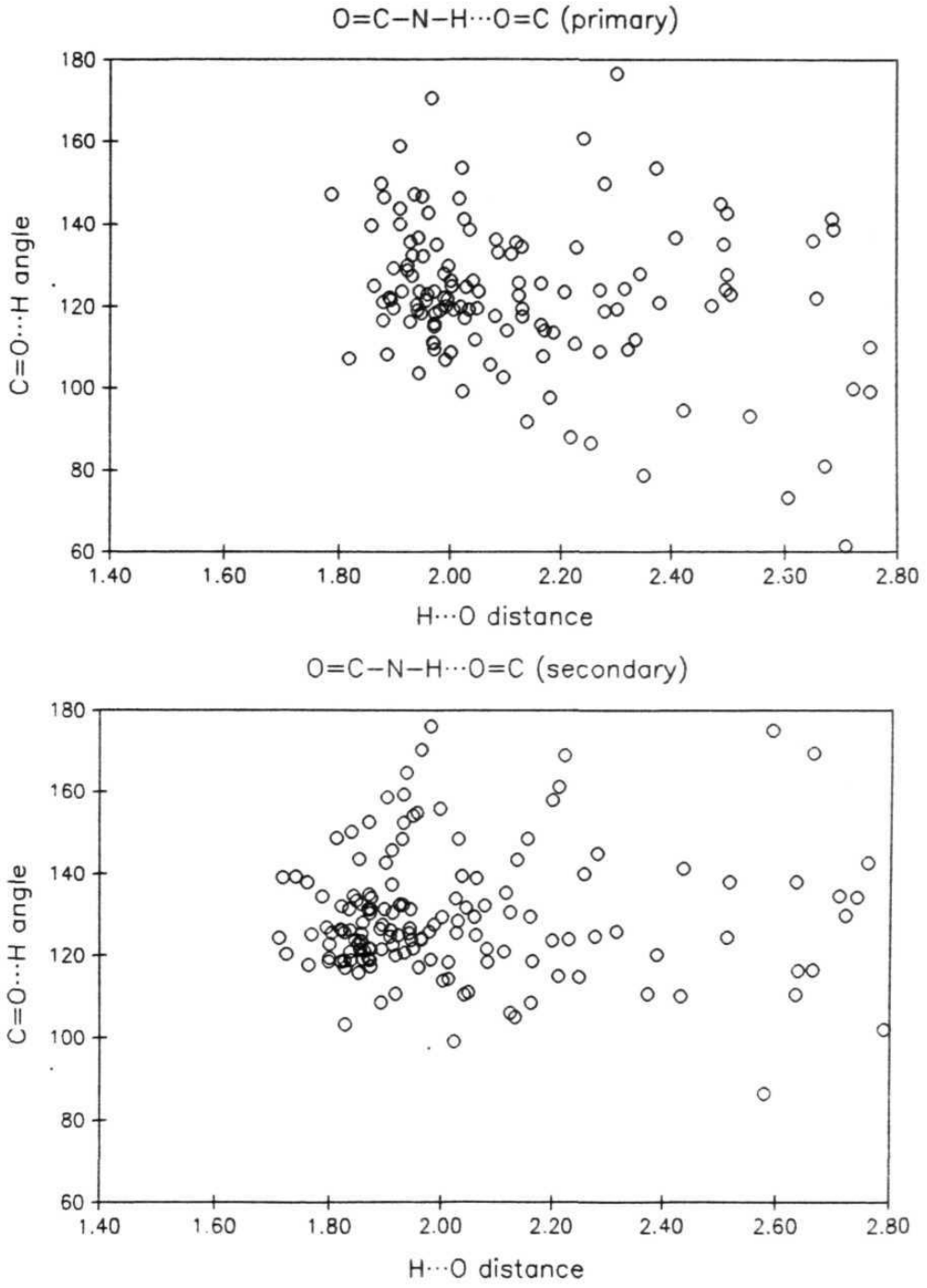

Figure 9. C=O···H angle distributions versus N-H···O distance range for primary and secondary OM. Note that both short and long hydrogen bonds are directional.

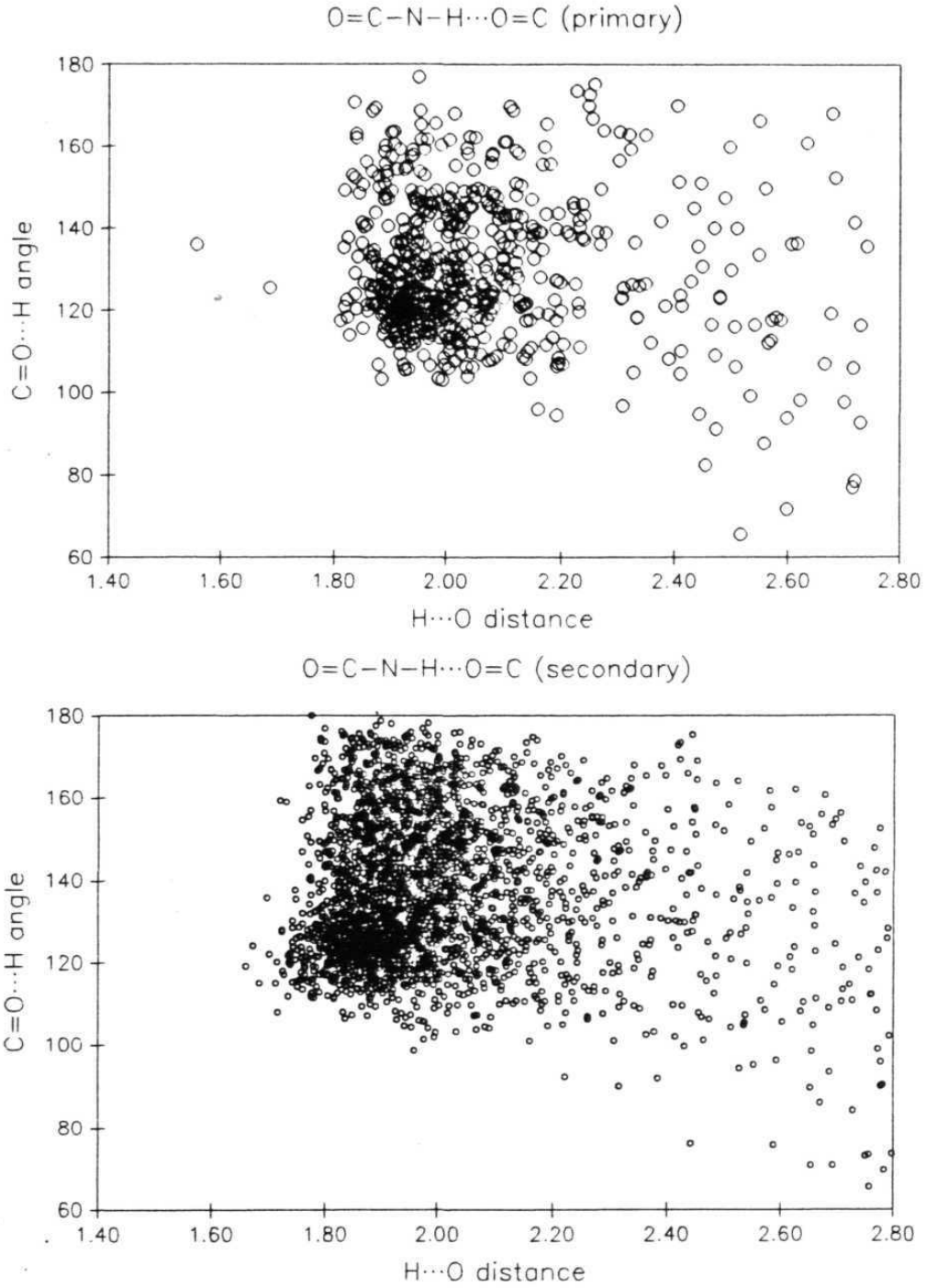

Figure 10. C=O···H angle distributions versus N-H···O distances for primary and secondary organics. Note that both short and long hydrogen bonds are directional.

2.2.4 Tertiary amides

Organometallic complexes containing tertiary amido groups are the most common (510 hits). There is no possibility for hydrogen bonding donors but the groups still carry acceptor oxygen atoms. There are 28 compounds corresponding to structures where the amide oxygen accepts hydrogen bonds from O-H groups (generally belonging to water molecules). These O···H-O bonds are usually short (22 hits below 1.88 Å), the C=O···H angle is spread around 120° (at the amide oxygen) whereas the O-H···O(amide) angle tends to be more linear (above 150°).

2.2.5 Hydrogen bonding patterns in selected crystalline amide complexes

Selected examples will now be discussed. The aim of this section is to provide a direct description of the geometric arrangements of organometallic amide complexes in crystals and of the patterns of hydrogen bonding interactions by means of geometric analysis and graphical representation. Structural parameters for the hydrogen bonds are given as A-H···X, where A = donor, X = acceptor, distances in the sequence A···X, H···X if the H atom position is available, and the angle A-H···X. Atomic labelling form the CSD is maintained. The structural formulae for all the species described in this Section are provided in Scheme 3.

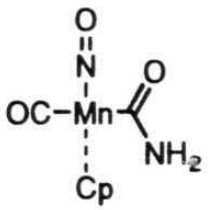

CPCNMN

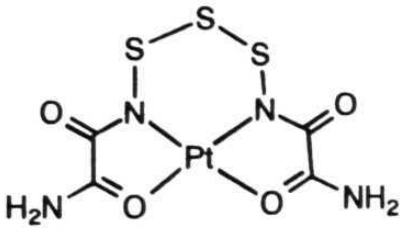

GEHRAM

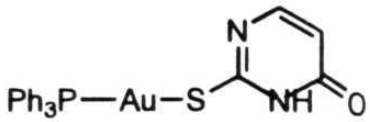

VAMGUL

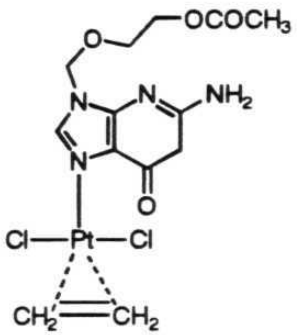

SOFYAB

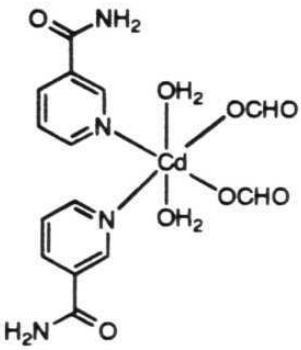

AFNICD

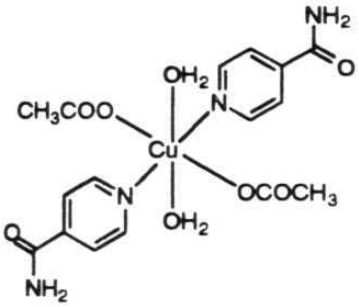

BEXPAV10

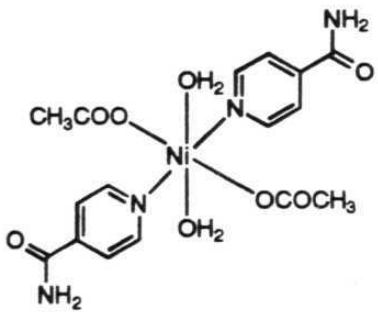

FUWGIN

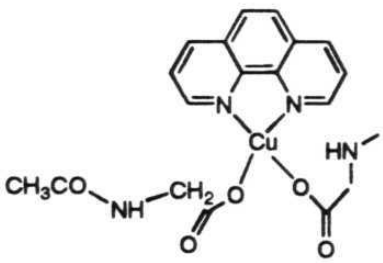

ACGLCU

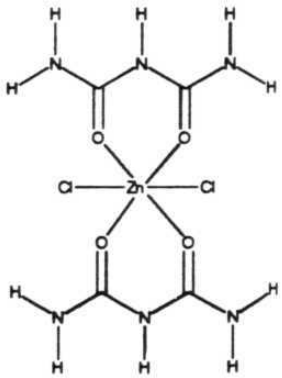

BIUZNC

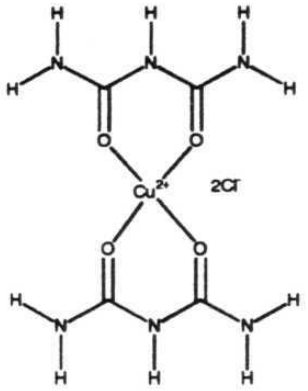

CUCLBU

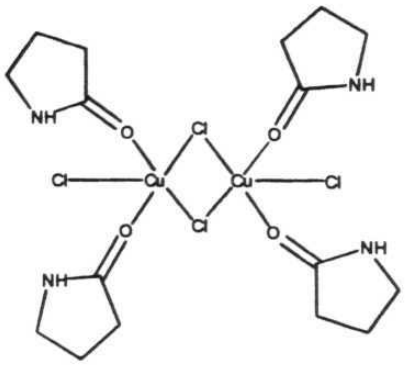

BUZSEU

Scheme 3: Structural formulae of some primary and secondary OM-amides

2.2.5.1 Primary amides

CPCNMN.[17] This Mn complex is a representative example because it forms cyclic dimers in its crystal structure. The metal carries one CO and one NO ligand, one η^5-coordinated C_5H_5 (Cp) ligand and one formamide moiety bound to the metal via a M-C σ-bond. One amide hydrogen [H(7)] establishes a cyclic dimer by interacting with the amide oxygen of a second molecule [N2-H7···O2, 2.95, 1.93 Å, 176.5°] as shown in Figure 11. The second amide hydrogen in CPCNMN does not participate in intermolecular interactions but points towards the N-atom of the NO-group. The amide oxygen, on the contrary, establishes an additional hydrogen bond (which probably takes the place of the second N-H···O interaction commonly observed in primary amides) with an H-atom belonging to the Cp-ligand (C3-H3···O2 3.33, 2.39 Å, 145.2°). A

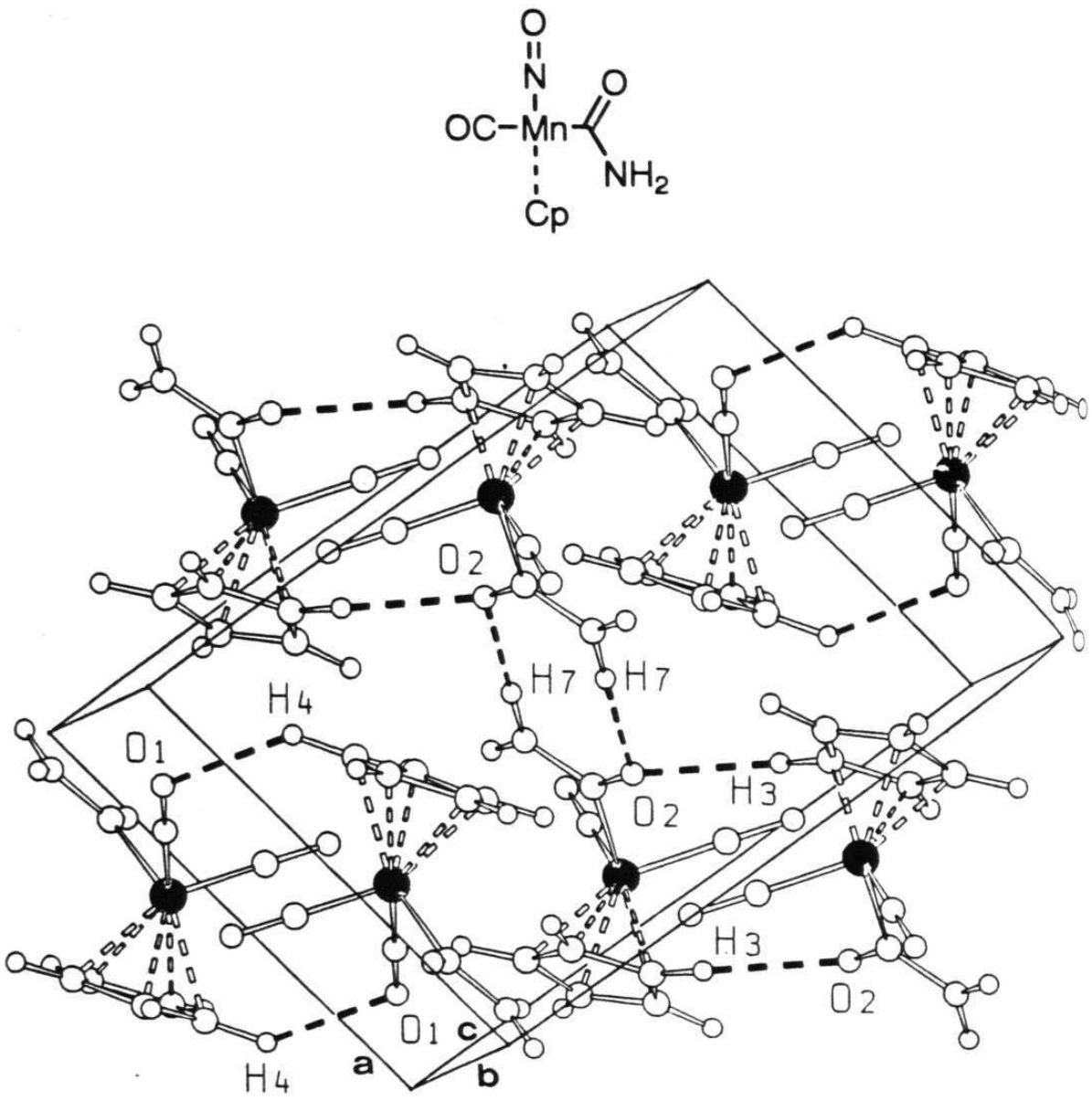

Figure 11. Cyclic amide dimers in crystalline CPCNMN. Notice the two C-H···O hydrogen bonded dimers. One is formed between the CO-ligand and the C-H group of a Cp-ring and other between an amide O-atom and the C-H group of a Cp-ring.

second C-H···O interaction has been found between a CO ligand and a Cp-hydrogen (C4-H4···O1 3.33, 2.44 Å, 139.4°). It is interesting to observe that the crystal structure of formamide[18] is also stabilised by the cyclic dimers of N-H···O and C-H···O hydrogen bonds as shown for comparison in Figure 12.

GEHRAM[19] is a planar Cu-complex, cocrystallising with dimethylformamide. There are two primary amido groups, corresponds to a large macrocycle, which interact directly with the metal atom *via* the two amido oxygens. These atoms participate in two different types of cyclic hydrogen bonds based on the interaction of each O-atom with its own amido group as shown in Figure 13. The first cyclic dimer is formed by N2-H21···O2 (2.99, 2.08 Å, 159.4°) in which O2 is bound to the metal atom; the second cyclic dimer is larger and utilises the ketonic oxygen O3 and the second amido group nitrogen N4. In this ten-membered ring the N···O separation is shorter than within the more conventional N2-H21···O2 six-membered ring (2.84 versus 2.99 Å). The dimethylformamide molecule is found "bridging" two molecules of the complex in the crystal *via* N-H···O(formamide) interactions [N2···O5 2.89, N4···O5 2.91 Å].

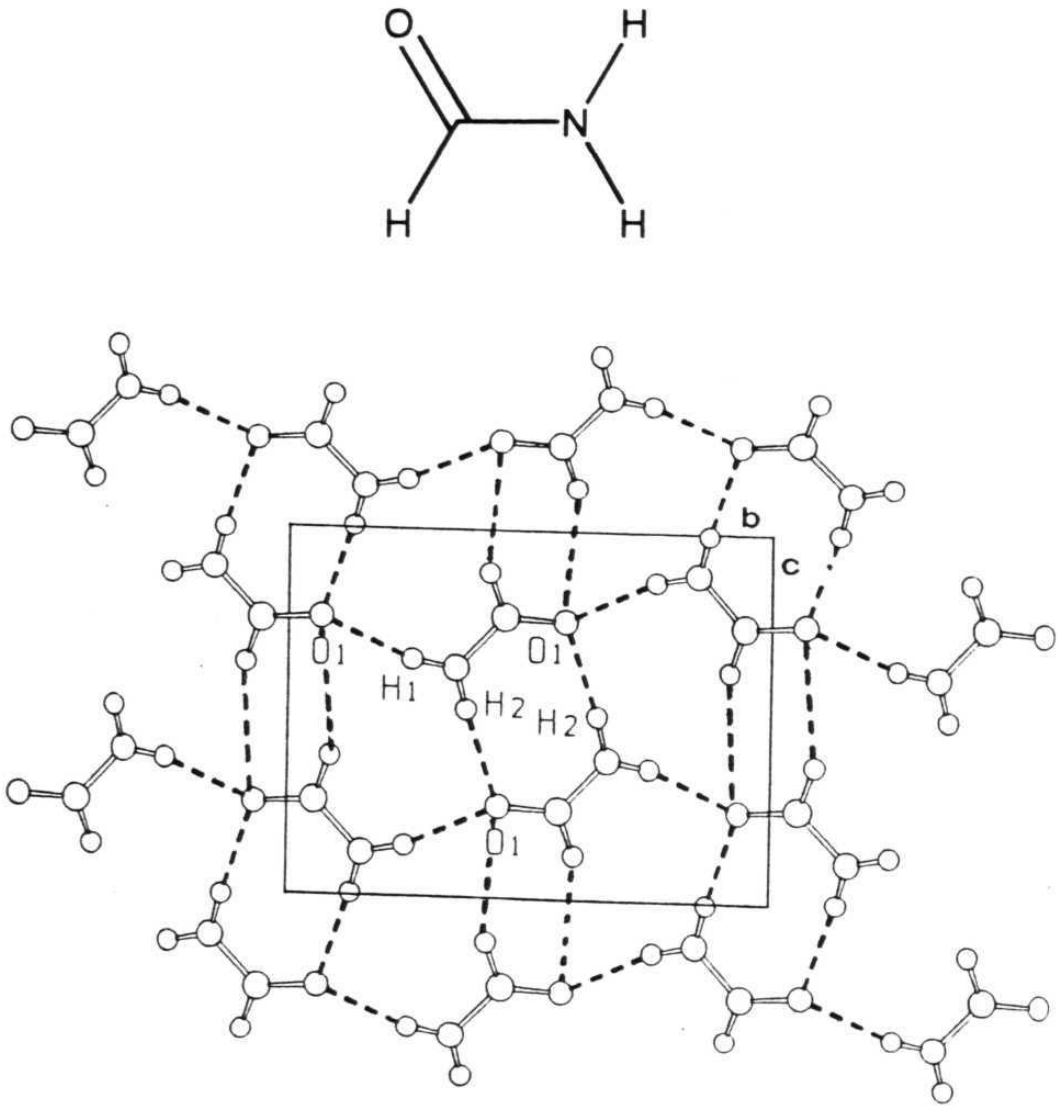

Figure 12. Crystal structure of formamide. Compare the cyclic dimers here with those in figure 11. Notice the cyclic N-H···O and C-H···O dimers.

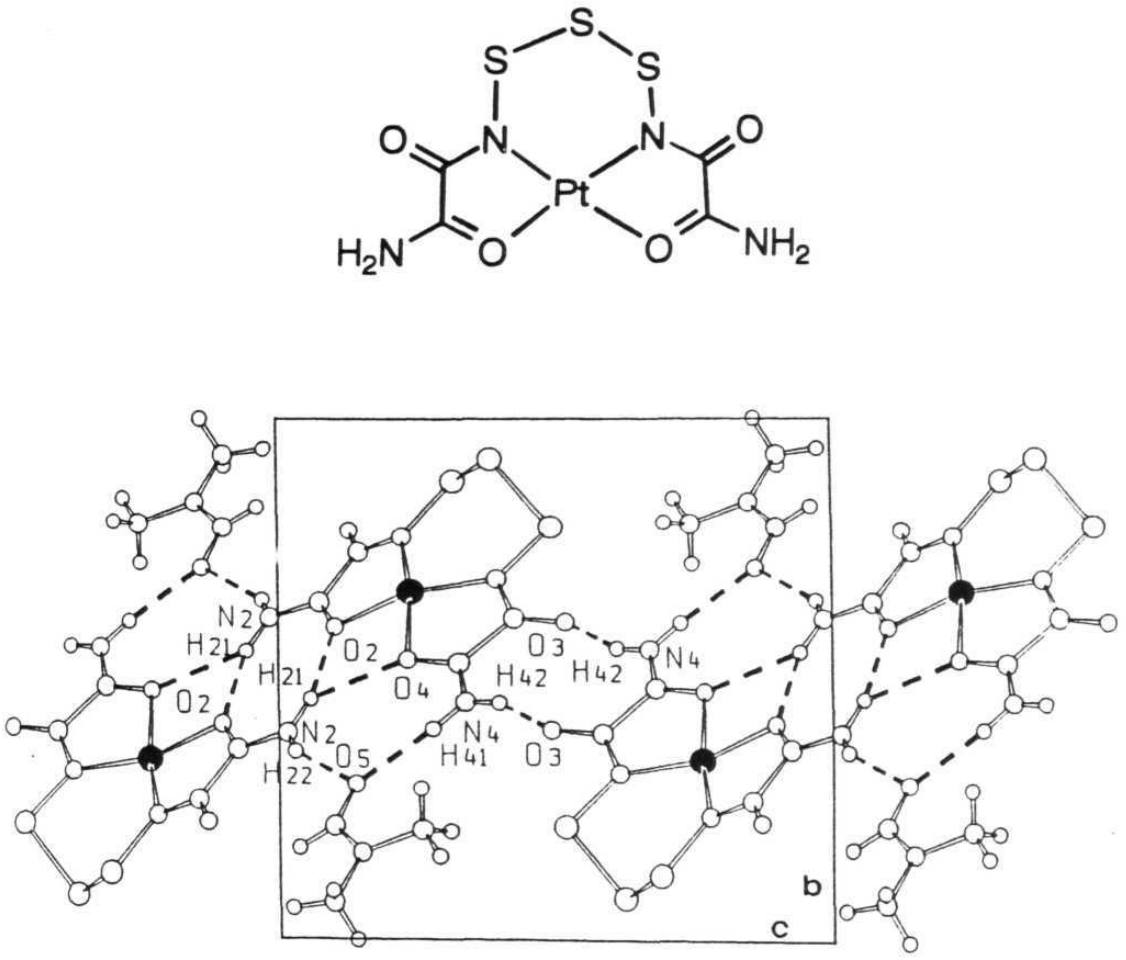

Figure 13. Two different types of cyclic systems present in crystalline GEHRAM: an eight-membered (N2-H21···O2) and a ten-membered ring with the ketonic oxygen O3 and the second amido group N4. Note how the dimethylformamide molecules interact with two molecules of the complex.

2.2.5.2 Secondary amides

VAMGUL.[20] There are two symmetry independent molecules in the asymmetric unit of this Au complex (identified as molecules A and B). This complex carries a secondary amido group belonging to the diazoketonic six-membered ring bound to the S-atom. The amido group of molecule A forms a cyclic dimer between two A-type molecules related by a centre of inversion (N2-H1···O1 2.72, 1.64, 177.9°). However, the same moiety corresponds to molecule B does not form similar cyclic dimer. It forms another type of cyclic dimer with molecule A via C-H···O and N-H···N hydrogen bonds. In other words the interaction A···A is based on an amide-amide cyclic dimer, while the interaction A···B is based on one N-H···N bond and one >C=O···H-C bond (Figure 14). This second cyclic system, however, is not as strong as the amide ring (N4-H19···N1 2.96, 1.94 Å, 156.3°; C4-H3···O2 3.17, 2.27 Å, 139.4°). This complex allows a sort of internal comparison between the three types of hydrogen bonds and allows a ranking of these bonds in terms of geometry if not of energy: N-H···O > N-H···N > C-H···O as expected.

SOFYOB.[21] The secondary amide moiety in this complex also forms cyclic dimers as shown in Figure 15. The geometry of the cyclic dimer is strictly comparable to that in VAMGUL (N1-H5···O1 2.73 Å, 171°). A second aspect of interest is the participation of the Cl-atom

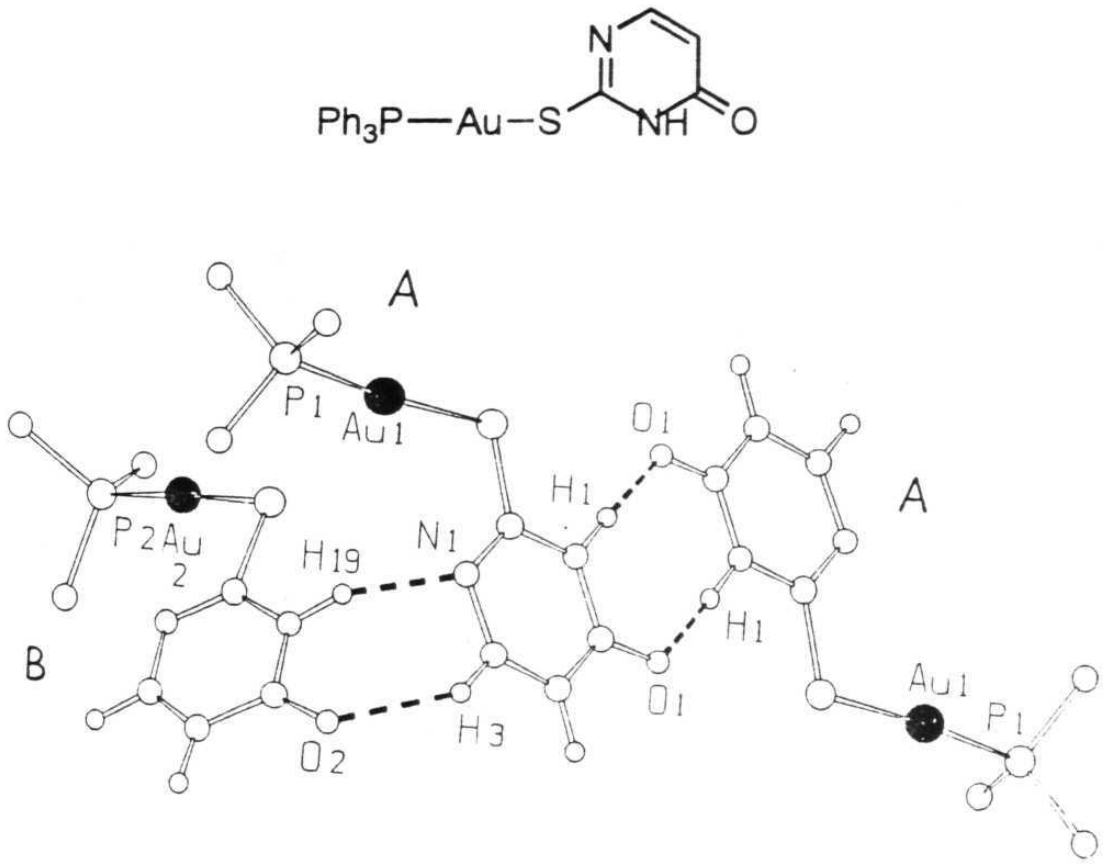

Figure 14. Hydrogen bonding interactions in crystalline VAMGUL: Note the N-H···O hydrogen bonded cyclic dimer between A molecules and N-H···N and C-H···O hydrogen bonded cyclic dimer between A and B molecules. For sake of clarity, only the C-atom bound to phosphorus is shown for each phenyl ring of the PPh_3 ligands.

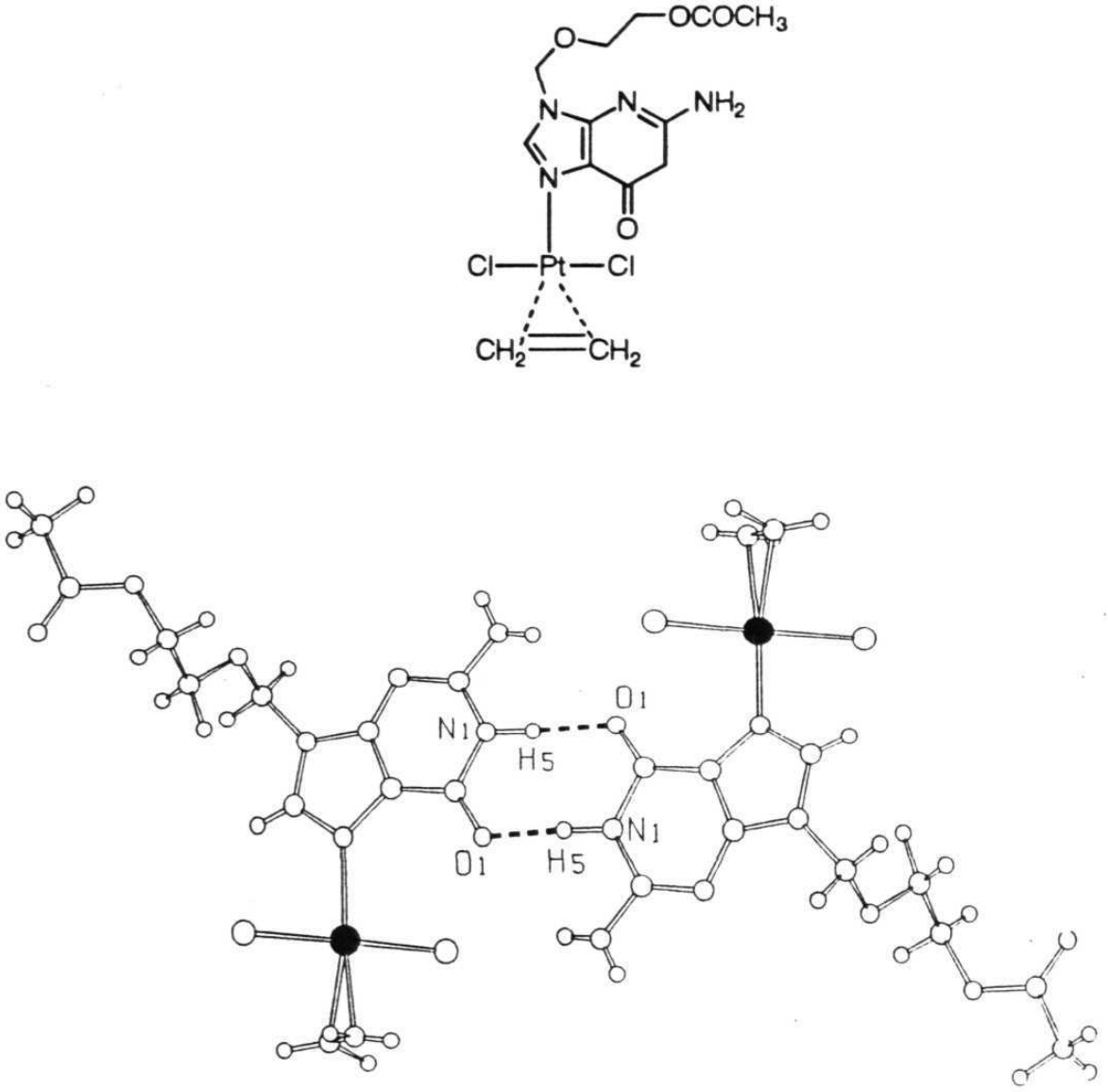

Figure 15. Eight membered amide rings formed by the cis secondary amide moiety in crystalline SOFYOB.

coordinated to the Pt-atom in N-H···Cl bonds involving the NH_2-group protruding from the bicyclic system (H7···Cl2 2.60 Å, 164°).

2.2.5.3 Complexes containing H_2O molecules as ligands

The complex diaqua-diformato-bis(nicotinamide)-cadmium (AFNICD)[22] forms ribbons of centrosymmetric cyclic dimers of the type D as shown in Figure 16a (N2···O1 2.95 Å). Inter-ribbon hydrogen bonds are otherwise formed by the formate and water molecules, which also constitute large cyclic systems (O10···O1 2.84 Å). Although these are the main interactions in crystalline AFNICD, additional hydrogen bonds are formed via the C-H···O interactions between the formate oxygen bound to the metal atom and the C-H groups of the nicotinamide rings. Due to these C-H···O interactions, the molecular layers are connected to form a three-dimensional network in the crystal. It is important to compare this crystal packing with that present in crystalline nicotinamide (NICOAM).[23] NICOAM forms no cyclic dimers and the amide NH_2-group participates in N-H···N bonds with ring N-atom. These N-H···N connected ribbons are interconnected by N-H···O hydrogen bonds as shown in Figure 16b.

The packing in the complex bis(acetato)-bis(amidoisonicotinato)-diaqua-copper(II) (BEXPAV10),[24] whose structure is related to that of AFNICD is not based on usual cyclic dimers (Figure 17). In this structure, however, it can be noted that the crystal packing is optimised with the participation of all the donor and acceptor groups available in the structure

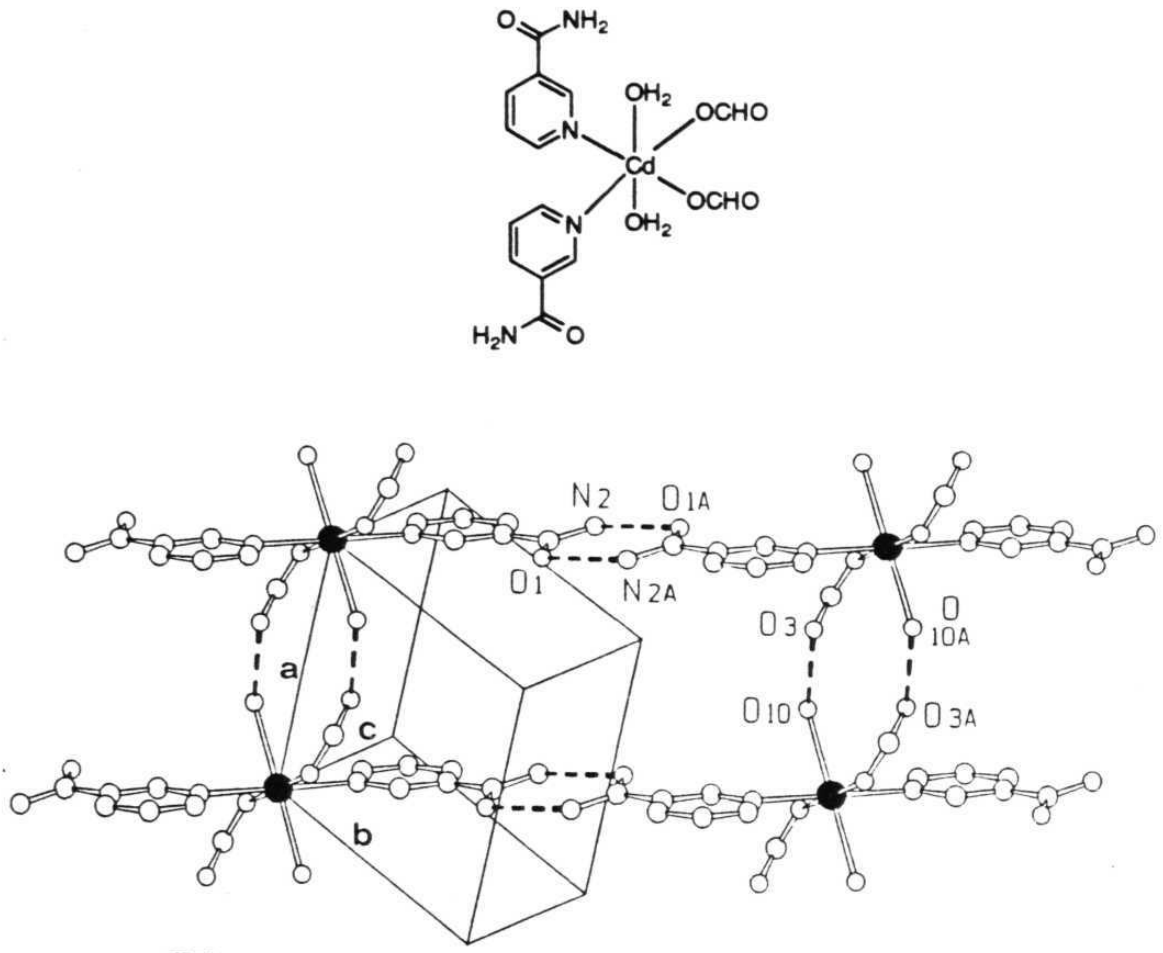

Figure 16a. Ribbons of centrosymmetric cyclic dimers present in crystalline AFNICD. Notice the inter-ribbon hydrogen bonds between the formate and the metal-coordinated water molecules. Molecular layers above and below the plane of the drawing fill in the apparent voids in the network; H-atoms are omitted for clarity.

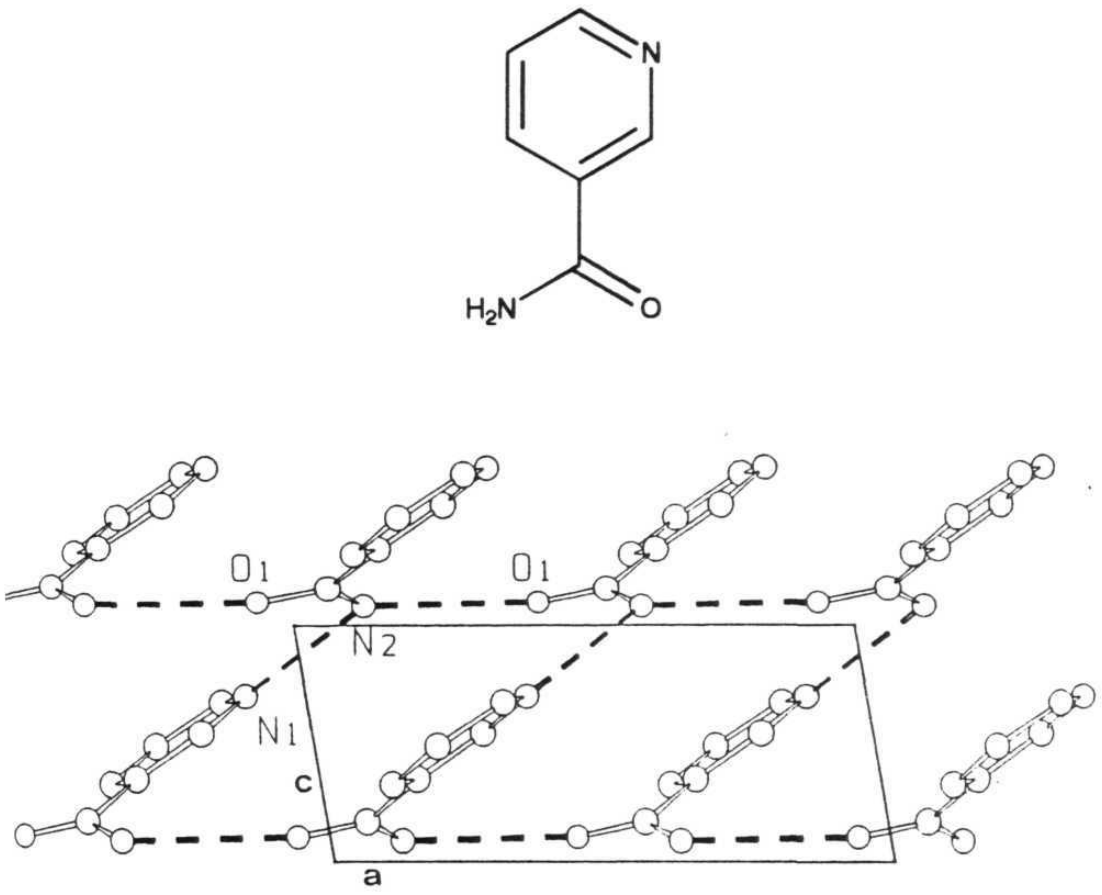

Figure 16b. Crystal structure of nicotinamide (NICOAM). Notice that there are no cyclic dimers but that the amide group forms N-H···N hydrogen bond with N1 and N-H···O hydrogen bond with O1.

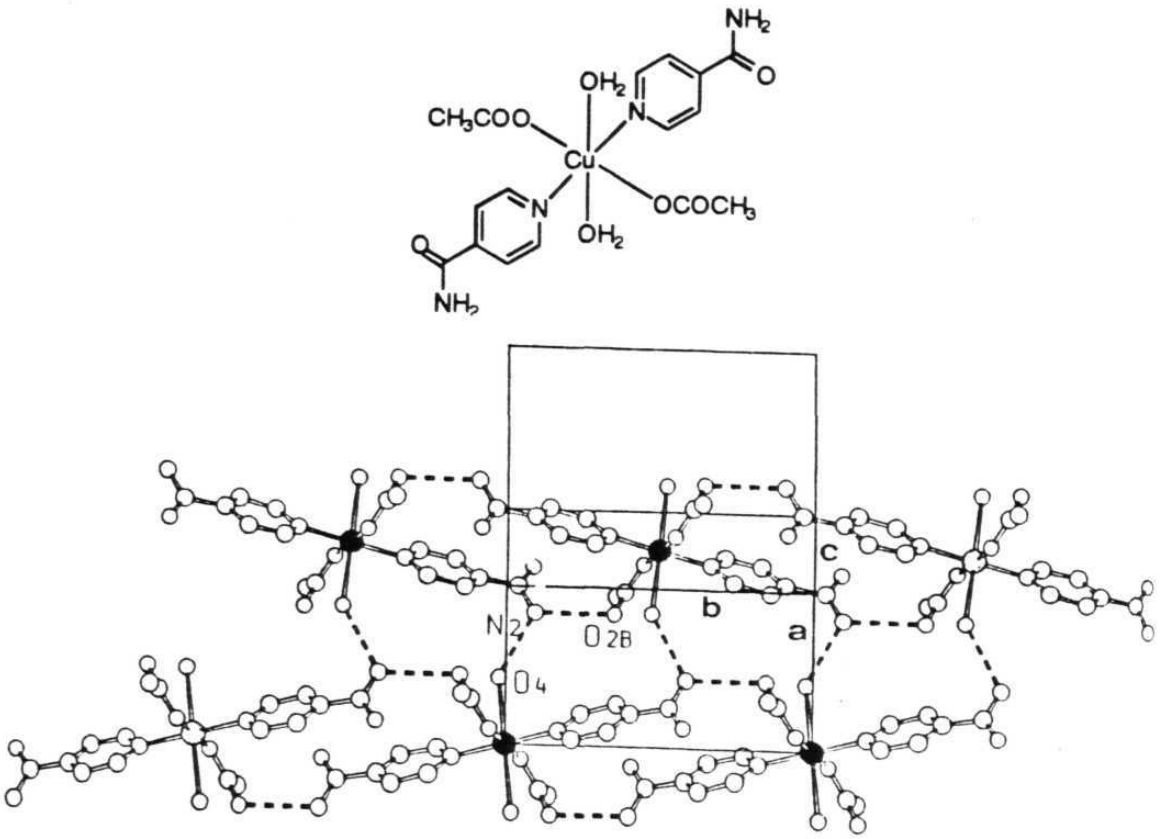

Figure 17. The packing motif in the crystalline complex BEXPAV10. Note how the amide protons do not bind amido oxygen atoms, rather two interactions are formed one with a ligated water molecule and one with the ester oxygen. H-atoms omitted for clarity.

(N-H···O, O-H···O, C-H···O, etc.). In fact the amide protons do not bind amide oxygen atoms, but rather two interactions are formed one with the oxygen of a ligated water molecule (N2···O4 2.92 Å) and one with the ester oxygen (N2···O2B 2.89 Å).

In crystalline bis(acetato)-bis(amidoisonicotinato)-diaqua-nickel(II) (FUWGIN)[25] the packing is the same as in BEXPAV10, with the major difference that the amide proton is also bound to the amide oxygen (H2···O1 2.24 Å). This indicates that, in terms of energy and crystal cohesion, there is ample structural variability when the choice is between amide-amide interactions or amide-water interactions.

The packing in crystalline bis(N-acetylglycinato)-1,10-phenanthroline-copper(II) (ACGLCU)[26] is of interest because the amide O-atom forms a C-H···O hydrogen bonds instead of a N-H···O hydrogen bond with amide N-H group. However, the amide N-H forms a N-H···O hydrogen bond with the ester C=O which is in a position β to it, this results in a cyclic dimer which involves 10 atoms, as shown in Figure 18.

2.2.5.4 Complexes containing metal cooridinated amide O-atoms

Complexes BIUZNC[27] and CUCLBU[28] are of interest because both contain a similar type of ligand and the amide O-atom is coordinated to metal atoms in both the complexes. The major difference between these two complexes is that one is neutral and the other is ionic. The crystal packing of these compounds are shown in Figure 19. In the crystal

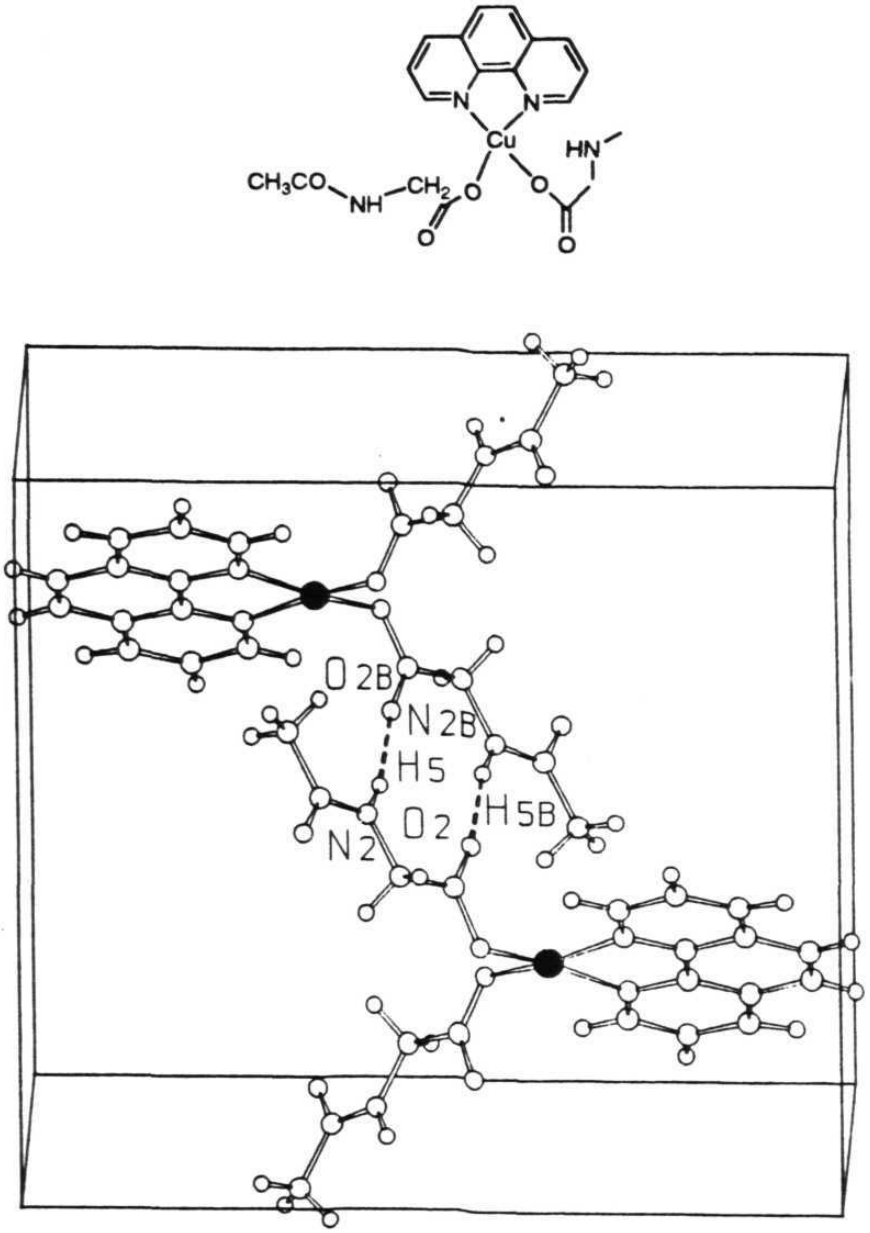

Figure 18. Crystal structure of ACGLCU. Notice that amide O-atom participates in C-H···O hydrogen bond rather than in N-H···O hydrogen bond.

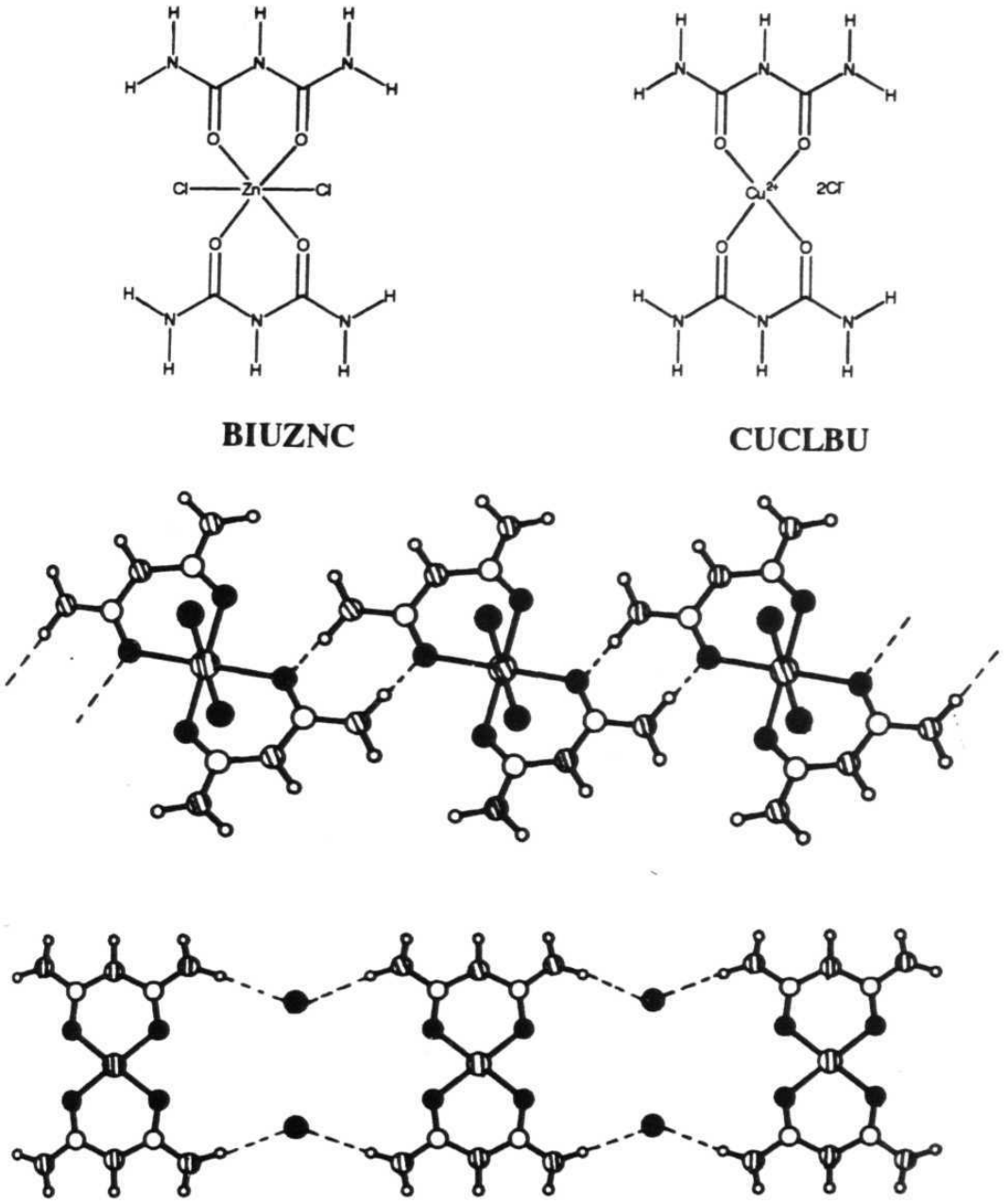

Figure 19. Crystal structure of biuret complexes (a) BIUZNC and (b) CUCLBU. Notice the centrosymmetric dimers in BIUZNC and N-H···Cl interactions in CUCLBU.

structure of BIUZNC one can clearly see that the metal coordinated amide O-atom forms a cyclic dimer to yield a linear chain. While CUCLBU does not form a centrosymmetric dimers because the Cl^- ion disrupts the centrosymmetric dimers by forming N-H···Cl interactions as shown in Figure 19b.

The complex BUZSEU[29] contain secondary amide ligands that are bonded to the metal centre via amide O-atom lone pairs. Figure 20 shows the crystal structure of this compound. In this complex, the molecules are held together by two non-centrosymmetric cyclic dimers (N···O 2.948 and 3.070) of type D to form a linear chain. These examples suggest that even though the amide O-atom is coordinated to metal centre, they accept amide N-H groups to form the usual types of patterns.

2.3 Conclusions

These observations show that much of the knowledge on the intermolecular interactions in organic systems can be transferred to the crystal engineering of organometallic solids with some, far from trivial, differences arising essentially from the presence of typical acceptor and donor groups (such as CO, NO, CN, and the π-bound unsaturated cyclic ligands) in organometallic systems. To summarise, it may be stated that:

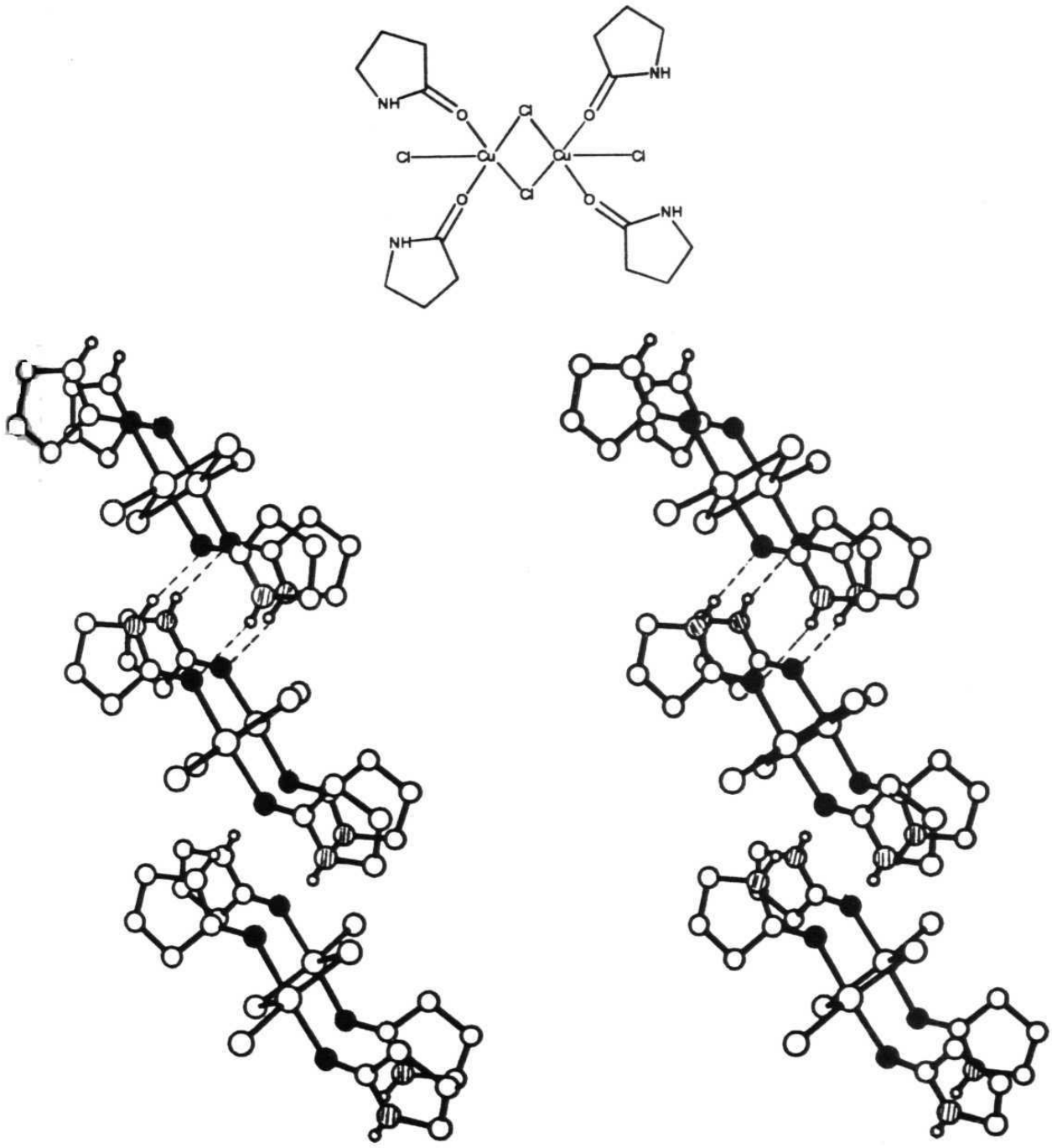

Figure 20. Stereodiagram of the crystal structure of BUZSEU. Notice the two cyclic dimers. The metal atoms are darkened and O-atoms are shaded for clarity.

(i) The 'average' hydrogen bond in OM-amido complexes is longer than in pure organics, although, to compensate, there is a greater number of hydrogen bonds *per* molecule because of the more frequent occurrence of bifurcation.

(ii) The principal hydrogen bonded patterns which are found in organic amides are also observed for organometallic amides, but the presence of water, counterions and more bulky molecular skeletons leads to a greater variability of interactions.

(iii) Coordination of the metal atom to the amide O-atom does not influence the formation of usual N-H···O hydrogen bonded patterns.

(iv) Examination of individual crystal structures shows that, in addition to N-H···O hydrogen bonding, C-H···O interactions confer additional stabilisation as might be expected.

2.4 Experimental section

Cambridge Structural Database (CSD) Analysis: Data were retrieved from the October 1994 update version (5.05) of the CSD (109816 entries) for all crystal structures with an exact match between chemical and crystallographic connectivity. Both neutral and charged species were considered. Only entries where $R < 0.10$ and where atomic coordinates are given were considered. Primary and secondary amido groups were retrieved separately for organic and OM complexes.

Geometrical calculations were performed on these amide subsets for N-H···O hydrogen bonds with H···O distances between 1.40 to 2.80 Å and N-H···O, that is θ angles between 110 to 180°. H-atom positions were invariably normalised to the neutron derived values. Duplicate hits (identified by the same REFCODES) were manually removed by eliminating the structure with the highest R-value in each case. Key examples were selected from the search outputs and were investigated by computer graphics.[30] The computer program PLATON[31] was used to analyse the geometrical features of the hydrogen bonding patterns. Geometrical questions constructed for the organometallic amides are given in the Appendix-A-1.

2.5 References

1. (a) D. Braga and F. Grepioni, *Acc. Chem. Res.,* 1994, **27**, 51. (b) D. Braga and F. Grepioni, *Organometallics,* 1991, **10**, 2563.
2. (a) A.I. Kitaigorodskii, *'Molecular Crystal and Molecules'*, Academic Press, New York, 1973,; (b) G.R. Desiraju, *'Crystal Engineering: The Design of Organic Solids'*, Elsevier, Amsterdam 1989. (c) A. Gavezzotti and M. Simonetta, *Chem. Rev.,* 1982, **82**, 1.
3. (a) D. Braga and F. Grepioni, *Organometallics,* 1992, **11**, 711. (b) D. Braga, F. Grepioni, P. Sabatino and A. Gavezzotti, *J. Chem. Soc., Dalton Trans.,* 1992, 1185.
4. S.S. Pathaneni and G.R. Desiraju, *J. Chem. Soc, Dalton Trans.,* 1993, 2505.
5. (a) D. Braga, F. Grepioni, P. Milne and E. Parisini, *J. Am. Chem. Soc.* 1993, **115**, 5115. (b) D. Braga and F. Grepioni, *Organometallics,* 1992, **11**, 1256. (c) D.M.P. Mingos and A.R. Rohl, *Inorg. Chem.* 1991, **30**, 3769. (d) D.M.P. Mingos, A.R. Rohl and J. Burgess, *J. Chem. Soc., Dalton Trans.* ,1993, 423.
6. (a) D. Braga, *Chem. Rev.,* 1992, **92**, 633. (b) D. Braga and F. Grepioni, *Chem. Commun.,* 1996, .

7. D. Braga, F. Grepioni, P.J. Dyson, B.F.G. Johnson, P. Frediani, M. Bianchi and F. Piacenti, *J. Chem. Soc. Dalton Trans.*, 1992, 2565.

8. (a) G.A. Jeffrey and W. Saenger, "*Hydrogen Bonding in Biological Structures*" Springer-Verlag, Berlin, 1991. (b) P. Murray-Rust and J.P. Glusker, *J. Am. Chem. Soc.* 1984, **106**, 1018. (c) G.A. Jeffrey, H. Maluszynska and J. Mitra,. *Int. J. Biol. Macromol.* **1985**, *7*, 336. (e) T. Steiner and W. Saenger, *Acta Crystallogr. Sect. B*, 1992, **B48**, 819.

9. (a) J.M. Lehn, *Angew. Chem. Int. Ed. Engl.* 1990, **29**, 1304. (b) MacDonald; G.M. Whitesides, E.E. Simanek, J.P. Mathias, C.T. Seto, D.N. Chin, M. Mammen and D.M. Gordon, *Acc. Chem. Res.* 1995, **28**, 37.

10. (a) G.R. Desiraju, *Angew. Chem., Int. Ed. Engl.*, 1995, **29**, 1304. (b) C.V.K. Sharma and G.R. Desiraju,. *Perspectives in Supramulecular Chemistry. The Crystal as a Supramolecular Entity*, Vol. 2, Ed. G.R. Desiraju, Wiley, Chichester, 1996, 31.

11. D. Braga, F. Grepioni, P. Sabatino and G.R. Desiraju,. *Organometallics* 1994, **13**, 3532.

12. (a) L. Leiserowitz and G.M.J. Schmidt, *J. Chem. Soc. A*, 1969, 2372. (b) L. Leiserowitz and A.T. Hagler, *Proc. R. Soc. London*

1983, **388**, 133.(c) A.T. Hagler, E. Huler and S. Lifson, *J. Am Chem. Soc.* 1974, **96**, 5319.

13. (a) P. Dauber and A.T. Hagler, *Acc. Chem. Res.* 1980, **13**, 105. (b) A. Gavezzotti and G. Filippini, *J. Phys. Chem.* 1994, **98**, 4831.

14. 29. F.H. Allen, J.E. Davies, J.J. Galloy, O. Johnson, O. Kennard, C.F. Macrae and D.G. Watson, *J. Chem. Inf. Comp. Sci.* 1991, **31**, 204.

15. Z. Berkovitch-Yellin and L. Leiserowitz, *J. Am Chem. Soc.* 1980, **102**, 7677.

16. A.T. Hagler and L. Leiserowitz, *J. Am. Chem. Soc.* **1978**, *100*, 5879.

15. An interaction is accepted as a bifurcated hydrogen bond if there are at least two O-atoms within 2.80 Å of an amido H-atom and such that both the N-H···O angles lie in the range 110-180°. For a more detailed account of the criteria governing bifurcation, see R. Parthasarthy *Acta Cryst. Sect. B*, 1969, **B25**, 509.

16. J. Kroon and A. Kanters, *J. Mol. Struc.* 1975, **24**, 109.

17. D. Messer, G. Landgraf and H. Behrens, *J. Organomet. Chem.*, 1979, **172**, 349.

18. J. Ladell and B. Post, *Acta Crystallogr.*, 1954, **7**, 559.

19. K. Brunn, H Endres and J. Weiss, *Z. Naturforsch., Teil B,* 1988, **43**, 113.

20. B.F. Hoskins, Lu Zhenrong and E.R.T. Tiekink, *Inorg. Chim. Acta,* 1989, **158**, 7.

21. L. Cavallo, R. Cini, J. Kobe, L.G. Marzilli and G. Natile, *J. Chem. Soc., Dalton Trans.,* 1991, 1867.

22. A.S. Antsyshkina, M.A. Porai-Koshits, M. Kandlovich and V.N. Ostrikova, *Koord. Khim.,* 1981, **7**, 461.

23. W.B. Wright and G.S.D. King, *Acta. Crystallogr.,* 1954, **7**, 283.

24. G.V. Tsintsadze, R.A. Kiguradze and A.N. Shnulin, *Zh. Strukt. Khim.,* 1985, **26**, 104.

25. G.V. Tsintsadze, M.I. Matsaberidze, A.S. Batsanov, Yu Struchkov, T.I. Tsivtsivadze and L.V.G. Verdtsiteli, *Izv. Akad. Nauk. Gruz. SSR, Ser. Khim.,* 1987, **13**, 20.

26. L.P. Battaglia, A.B. Corradi, G. Marcotrigiano and G.C. Pellacani, *Acta. Crystallogr., Sect. B,* 1977, **33**, 3886.

27. M. Nardelli, G. Fava and G. Giraldi, *Acta. Crystallogr.,* 1963, **16**, 343.

28. H.C. Freeman and J.E.W.L. Smith, *Acta. Crystallogr.,* 1966, **20**, 153.

29. S.S. Kukalenko, Y. T. Struchkov, S.I. Shestakova, A.G. Tsybulevskii, A.S. Batsanov and E.B. Nazarova, *Koord. Khim.,* 1983, **9**, 312.

30. E. Keller, SCHAKAL93, Graphical Representation of Molecular Models, University of Freiburg, Germany.

31. A.L. Spek, *Acta Crystallogr.* 1990, **A46**, C31.

Chapter 3

C-H···O Hydrogen Bonds
in Organometallic 1st row
Metal Carbonyl Compounds

3.1 Introduction

The ability of C-H groups to form C-H···O hydrogen bonds has been discussed in Chapter 1.[1] These interactions (energy 1 - 5 kcal mol^{-1}) are well established as significant determinants of crystal packing in some organic structures.[2,3] Anomalies and puzzles in the strong hydrogen bonded patterns of certain crystal structures may be explained on the basis of the interplay of strong (O-H···O, N-H···O) and weak (C-H···O) hydrogen bonds.[4] In general, the strength and effectiveness of a C-H···O hydrogen bond depends on C-H carbon acidity[5] and on O-atom basicity,[6] which is enhanced *via* cooperative effects.[7]

In spite of the interest that the C-H···O hydrogen bond has attracted, little has been done in this context with regard to organometallic solids even though more than 50 % of CSD[8] consists of these structures. Organometallic compounds are of interest in studies of C-H···O hydrogen bonds due to the presence of a different type of potential hydrogen bond acceptor, namely the CO-ligand. Carbonyl complexes of transition metal atoms are common and almost all metals form stable complexes in the low-oxidation states with CO. It is known that the CO-ligand can bind to polynuclear metal complexes in terminal and various bridging fashions. Bridging CO ligands can span a metal-metal bond (μ_2-bonding mode) or cap a triangulated metal face of a higher nuclearity cluster (μ_3-bonding mode). These principal bonding modes are shown in Scheme 1. In all these

bonding modes, CO provides two electrons to the valence electrons of the complex. These CO-ligands are also known to be capable of interacting with metal centres *via* the unsaturated C-O bond. End-on (or isocarbonyl) complexes are also well established.[9] In the previous Chapter, the ability of these CO-ligands to interact with C-H groups rather than with amide N-H groups in the presence of other acceptors has been shown. Recent studies on some of the single crystals of metal carbonyls have shown that the CO-ligands form C-H···O hydrogen bonds.[10]

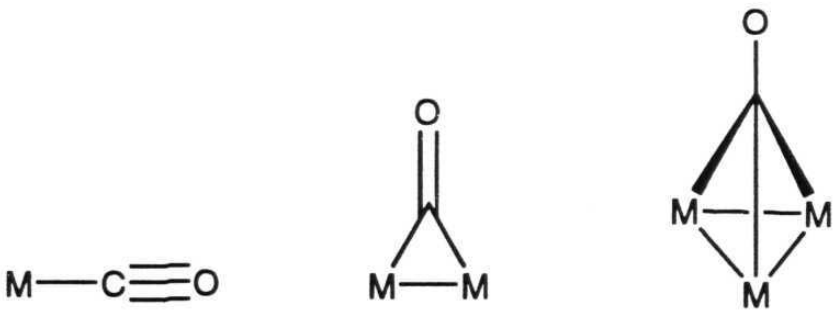

Scheme 1: CO bonding modes

This chapter deals with an extensive study of intramolecular and intermolecular C-H···O hydrogen bonds in organometallic crystal structures of the first row transition metals containing terminal and bridging CO-ligands. In particular, the following questions will be addressed :

i) Does the CO-ligand participate in C-H···O hydrogen bonds either with M-C-H or with an organic ligand, R-C-H?

ii) Do C-H···O hydrogen bonds play a significant role in the stabilisation of crystals formed by neutral mononuclear or polynuclear organometallic complexes? Are these interactions important in supramolecular architecture?

iii) Is there a recognisable difference in hydrogen bonding capability between the two main bonding modes shown by CO-ligands in organometallic complexes, namely terminal (CO-t hereafter) and bridging (CO-b hereafter) which could be related to the different basicity of CO in the two bonding modes?

To answer these questions, the CSD has been searched systematically. Intramolecular and intermolecular C-H···O hydrogen bonds in crystal structures of neutral complexes containing at least one atom among the series Sc-Zn and at least one CO-ligand whether bound in a terminal or in a bridging fashion, have been analysed. From the search outputs, some representative examples have been selected and discussed in detail.

3.2 Results and Discussion

It is known that the basicity of CO-ligand increases on going from the CO-t to the CO-b bonding geometry. Hence, it is anticipated that involvement of the CO-ligand in hydrogen bonding also increases from CO-t to CO-b.[10a] Accordingly, the analysis of C-H···O hydrogen bonds

has been carried out separately for the CO-t and CO-b cases. The descriptors inter and intra will be used to discriminate between intermolecular and intramolecular interactions. Therefore, the four categories which will be discussed are CO-t(inter), CO-b(inter), CO-t(intra) and CO-b(intra).

It was described in Chapter 1 that studies of hydrogen bonds in X-ray derived crystal structures are handicapped by the inaccurate determination of the H-atom positions. In these structures, the C-H distances are systematically shortened by 0.05-0.10Å. Two approaches are commonly used to alleviate this problem. In the first approach, one considers only neutron diffraction structures wherein the H-atom positions are determined with great accuracy.[11] Because of the experimental difficulties in the neutron diffraction studies, this technique cannot be used routinely.[12] In the second approach, the X-Ray derived H-atom position is normalised by extending this position along the C-H vector such that the C-H distance corresponds to the typical neutron-derived value.[13] Such normalisations are expected to yield hydrogen bond geometries which are similar to neutron-derived geometries and this is the procedure which has been employed in this study.

To characterise a particular interaction as a C-H···O hydrogen bond there are two distinct viewpoints: (1) Use a conservative C···O threshold of such as 3.25 or 3.30Å and refer to longer separations as van

der Waals interactions; (2) Use a more liberal threshold.[2] Recent analyses on C-H···O hydrogen bonds show that many longer C-H···O interactions (C···O 3.50 - 4.00Å) have angular characteristics and effects on crystal structures which resemble the effects caused by the shorter interactions (3.10 - 3.50Å).[12] It may be noted that the C-H···O hydrogen bond is not really a van der Waals contact but is primarily electrostatic, falling off much more slowly with distance and hence viable at distances which are equal to or longer than the conventional van der Waals limit. Therefore the outer cut-off C···O distance must be liberal. Additionally, it may be noted that the chemically meaningful distance is the H···O distance rather than the C···O distance. Accordingly, a H···O cut-off of 2.80Å for the H-normalised data has been employed in the present study. This value is close to the van der Waals sum and even longer values have been considered as being justified and necessary.[14]

All average structural parameters from the CSD search for the series Ti - Ni are listed in Table 1. All metals behave very similarly, that is there is no dependence on the nature of the metal which also means there is no dependence on the number of ligands since the number of electrons (that is, of ligands) required by the EAN rule decreases on moving from left to right along the transition row.[15]

Table 1: Mean Geometrical Parameters for C-H···O Hydrogen Bonds in First Row Transition Metal Carbonyls. Values obtained from the CSD (standard deviations are in parentheses).

CO-t (INTER)

	C···O (Å)	H···O (Å)	C-H···O (°)	C-O···H (°)	Unique Refcodes	No.of hits
Ti	3.53(2)	2.63(2)	140(2)	126(4)	7	29
V	3.49(1)	2.65(1)	136(2)	125(3)	22	88
Cr	3.510(3)	2.640(2)	140.1(3)	124.9(0.5)	474	2415
Mn	3.510(4)	2.640(3)	139.4(4)	126.8(0.6)	366	1510
Fe	3.510(2)	2.620(2)	139.8(2)	128.3(0.3)	1137	4205
Co	3.520(5)	2.640(4)	140.3(5)	128.3(0.7)	291	916
Ni	3.52(2)	2.64(2)	141(3)	125(3)	12	30

CO-b (INTER)

	C···O (Å)	H···O (Å)	C-H···O (°)	C-O···H (°)	Unique Refcodes	No.of hits
Ti	------	------	------	------	0	0
V	3.5(1)	2.61(6)	145(12)	126(7)	1	4
Cr	3.56(5)	2.56(4)	155(4)	132(6)	4	9
Mn	3.48(2)	2.58(2)	144(2)	133(3)	23	51
Fe	3.45(1)	2.57(1)	142(1)	133(1)	129	285
Co	3.47(1)	2.59(1)	141(1)	132(1)	110	257
Ni	3.50(2)	2.59(2)	145(2)	128(3)	20	47

Table 1 (continued)

CO-t (INTRA)

	C···O (Å)	H···O (Å)	C-H···O (°)	C-O···H (°)	Unique Refcodes	No.of hits
Ti	3.45(4)	2.62(5)	135(7)	80(1)	2	4
V	3.40(4)	2.660(3)	127(4)	82(2)	10	21
Cr	3.520(7)	2.640(5)	140.1(0.7)	84.6(0.8)	218	456
Mn	3.500(7)	2.650(6)	137.3(0.7)	79.8(0.7)	212	429
Fe	3.500(4)	2.640(3)	138.0(0.4)	82.0(0.4)	599	1272
Co	3.50(1)	2.670(6)	136(1))	83(1))	138	261
Ni	3.60(4)	2.69(2)	143(4))	81(3)	8	15

CO-b (INTRA)

	C···O (Å)	H···O (Å)	C-H···O (°)	C-O···H (°)	Unique Refcodes	No.of hits
Ti	----	----	----	----	0	0
V	3.46(6)	2.62(8)	136(12)	86(3)	1	3
Cr	3.46(8)	2.70(8)	128(9)	104(8)	1	2
Mn	3.34(3)	2.55(3)	132(4)	99(3)	10	22
Fe	3.35(1)	2.56(1)	130(1)	95(1)	45	99
Co	3.32(1)	2.52(1)	131(1)	96(1)	51	128
Ni	3.39(3)	2.59(3)	132(3)	96(3)	13	24

3.2.1 Comparison between CO-t(inter) and CO-b(inter)

Table 1 shows that both C···O and H···O mean distances for CO-t(inter) are generally longer than those of CO-b(inter). Although V and Cr appear to contradict this trend, the number of CO-b in these cases is too small to be of statistical significance. The differences in mean length between CO-t(inter) and CO-b(inter) fall within the range 0.02-0.06Å for the C···O distances, and in the range 0.04-0.08Å for the H···O distances. For Fe and Co, the trend is clear and the confidence level in such an observation is high with the differences in mean length being at least 10σ. For Mn and Ni, the differences in mean length are not significant at the 3σ level because of the standard deviation for the CO-b(inter) values is high. However, the trend is towards longer distances for hydrogen bonds involving CO-t and this behaviour very likely follows from the higher basicity of CO-b with respect to CO-t.[10a]

Although these distance differences are small, there is adequate evidence that mean C···O and H···O distances accurately reflect C-H···O acidity-basicity properties.[5,6] In general, C-H···O distance distributions will always be broad unlike for strong hydrogen bonds (O-H···O and N-H···O). This is inherent in the very weakness of the interaction.[5a] However, when as in this case, the sample sizes run into the several thousands, the values of the means are less likely to be affected by outliers and comparison of mean C···O and H···O distances is reliable.[5d] Further,

these mean C···O distances have been shown to even correlate properly with solution pK_a values.[5c] In support of these arguments, Figure 1 shows histograms of C···O distances for the Fe CO-t(inter) and CO-b(inter) complexes with the populations of structures expressed as probabilities in both cases to facilitate comparison. These histograms represent 4205 and 285 hits respectively. Notice that the entire histogram for CO-t(inter) is offset towards longer C···O distances. Such behaviour has been observed previously for acidity series involving chloroform and dichloromethane[5a] and involving alkynes and alkenes.[5b] The less basic the CO-ligand, the longer the C···O distance. This shows that a consideration of mean C···O and H···O values is a valid approach to monitor O-atom basicity in organometallic complexes.

Similarly, C-H···O angles for CO-t(inter) are smaller than those for CO-b(inter) 139-140° *versus* 142-146°. This difference is small and indeed the trend is again fully satisfactory only for Fe and to some extent Co, but strengthens the idea that CO-b(inter) forms, on the average, more linear and stronger intermolecular bonds than CO-t(inter). It may be noted that steric factors also favour CO-t(inter) over CO-b(inter), the former type of ligands protruding more from the molecular surface. Similar arguments also hold for the C-O···H angles (see Table 1) although these angles are, on the whole smaller, approaching 120°. For metals other than Fe and Co, it should be recognised that the interaction being studied is

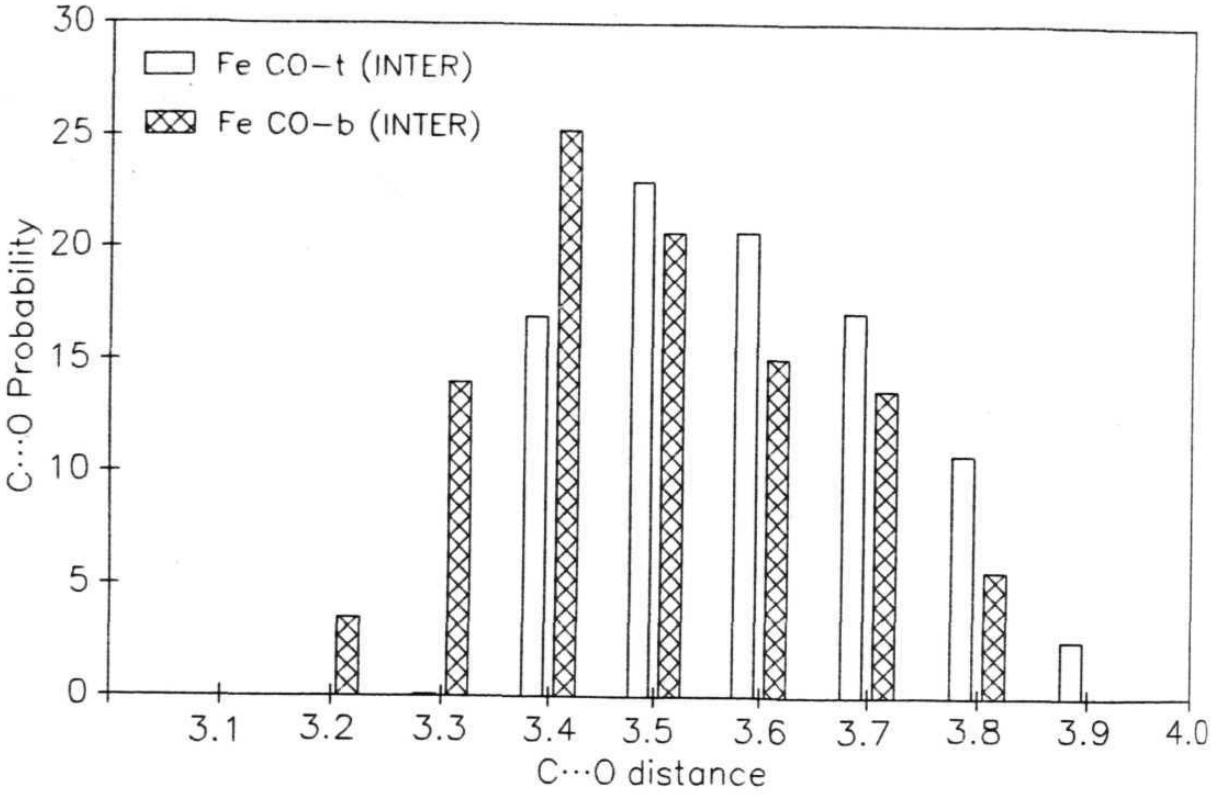

Figure 1. Histograms of C···O distances for the Fe CO-t(inter) and CO-b(inter) complexes. The populations are expressed as probabilities to facilitate comparison. The bars at, say 3.40Å, represent interactions between 3.30Å and 3.40Å. Notice the offset of the CO-t histogram towards longer C···O distances.

really weak and thus the significance level may be low for some of the distance and angle differences. For Cr, Mn and Ni structures, the trends are not statistically significant at the 3σ level. However, they appear similar to the cases of Fe and Co where more data is available. Along these lines, the mean C-H···O angles are calculated for *all* metals for CO-t(inter) and CO-b(inter) to be 139.8(0.3)^{o} and 142.5(1.2)^{o} respectively. Similar C-O···H angles are 127.1(0.5)^{o} and 132.2(1.5)^{o} respectively.

3.2.2 Comparison between CO-t(inter) and CO-t(intra)

C···O and H···O distances for CO-t(intra) and CO-t(inter) have similar mean values. Both C-H···O and C-O···H angles are larger for CO-t(inter) than CO-t(intra). The average values for C-H···O angles is 139 *versus* 137^{o}. The difference in C-O···H angles is even more striking, being of the order of 40-50^{o}. These differences are probably due to the common octahedral coordination of ligands around the metal centres with ligands forming L-Me-L' angles of *ca.* 90^{o}.

3.2.3 Comparison between CO-b(inter) and CO-b(intra)

The relationship observed between CO-t(inter) and CO-t(intra) is also maintained between CO-b(inter) and CO-b(intra). Again, the results for Fe and Co are the most reliable while those for Mn and Ni (though following the same trend) are uncertain. The C-H···O angle difference is

more appreciable while CO···H angles are larger than for CO-t(intra). Thi is very probably due to the fact that CO-b are more embedded in the ligand shell and can get closer to neighbouring ligands.

3.2.4 CO···H directionality and O-atom lone pair orientations

To do this analysis, crystal structures of Cr, Mn, Fe and Co metal complexes were considered for CO-t case as these metals contain more number of hits. Likewise, Fe and Co metal complexes were considered for CO-b case.

3.2.4.1 Intramolecular angles

Plots of CO···H angle *versus* H···O distances in the metal complexes of Cr, Mn, Co and Ni for CO-t (intra) are shown in Figure 2. Similar plots in the crystal structures of Fe and Co complexes for CO-b (intra) are shown in Figure 3. From these scattergrams, it is clear that the CO···H angles in all the metal complexes for both CO-t(intra) and CO-b(intra) cluster around 70-100^{O} with only a very few outliers which exceed 100^{O}. It appears that, as the O···H distance increases, the CO···H angles for CO-t(intra) tend to span a larger range than at shorter distances. The reason for this is perhaps to be found in the normal geometry of a complex or cluster; if ligands have O and H atoms at short contact distances (less than 2.80Å) they must belong to ligands which are bound to the same metal atom or, at most, to two adjacent metal atoms in a dinuclear or

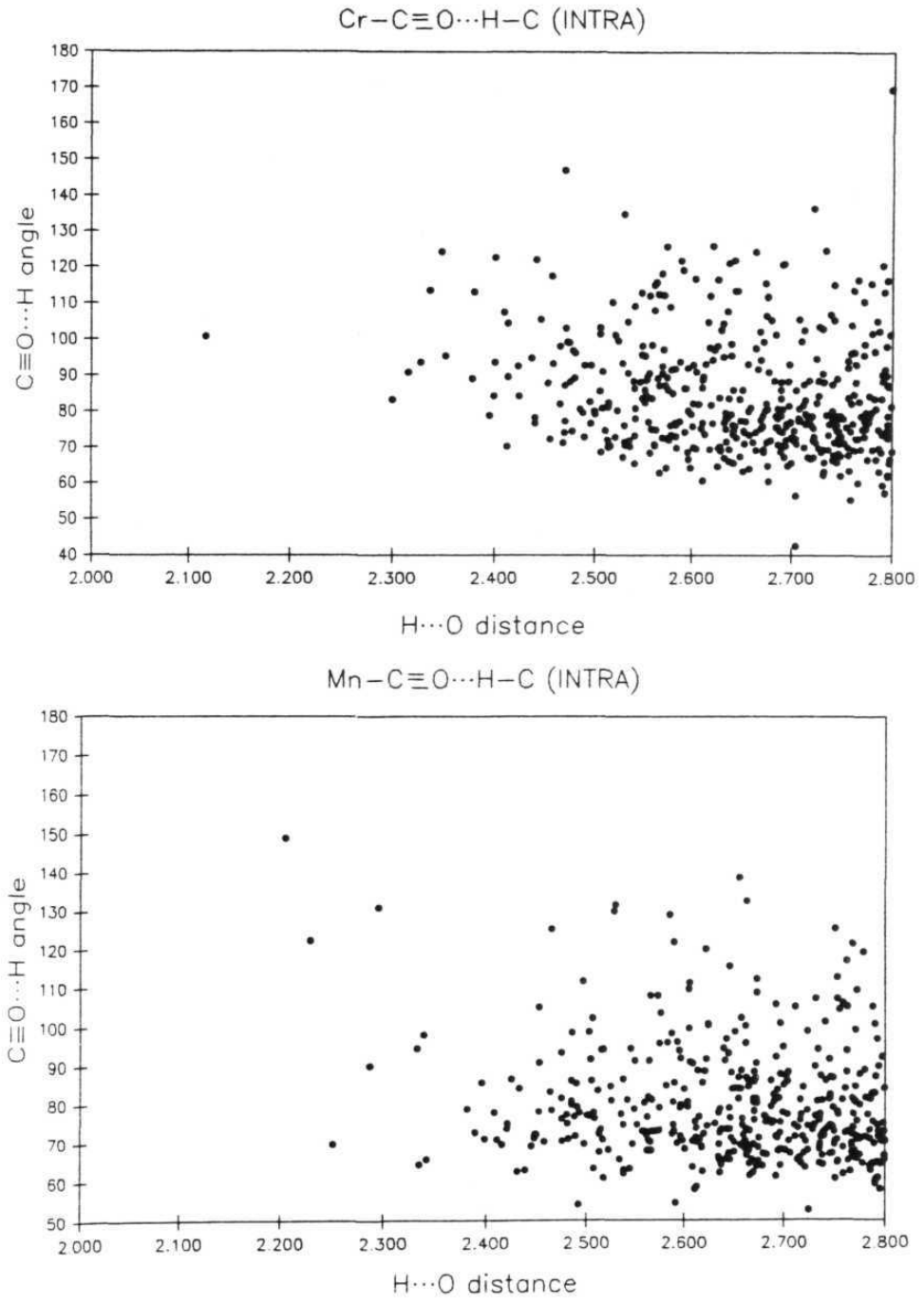

Figure 2. Plots of CO···H angle *versus* H···O distance for intramolecular C-H···O hydrogen bonds in terminal carbonyl (CO-t) (a) Cr and (b) Mn metal complexes.

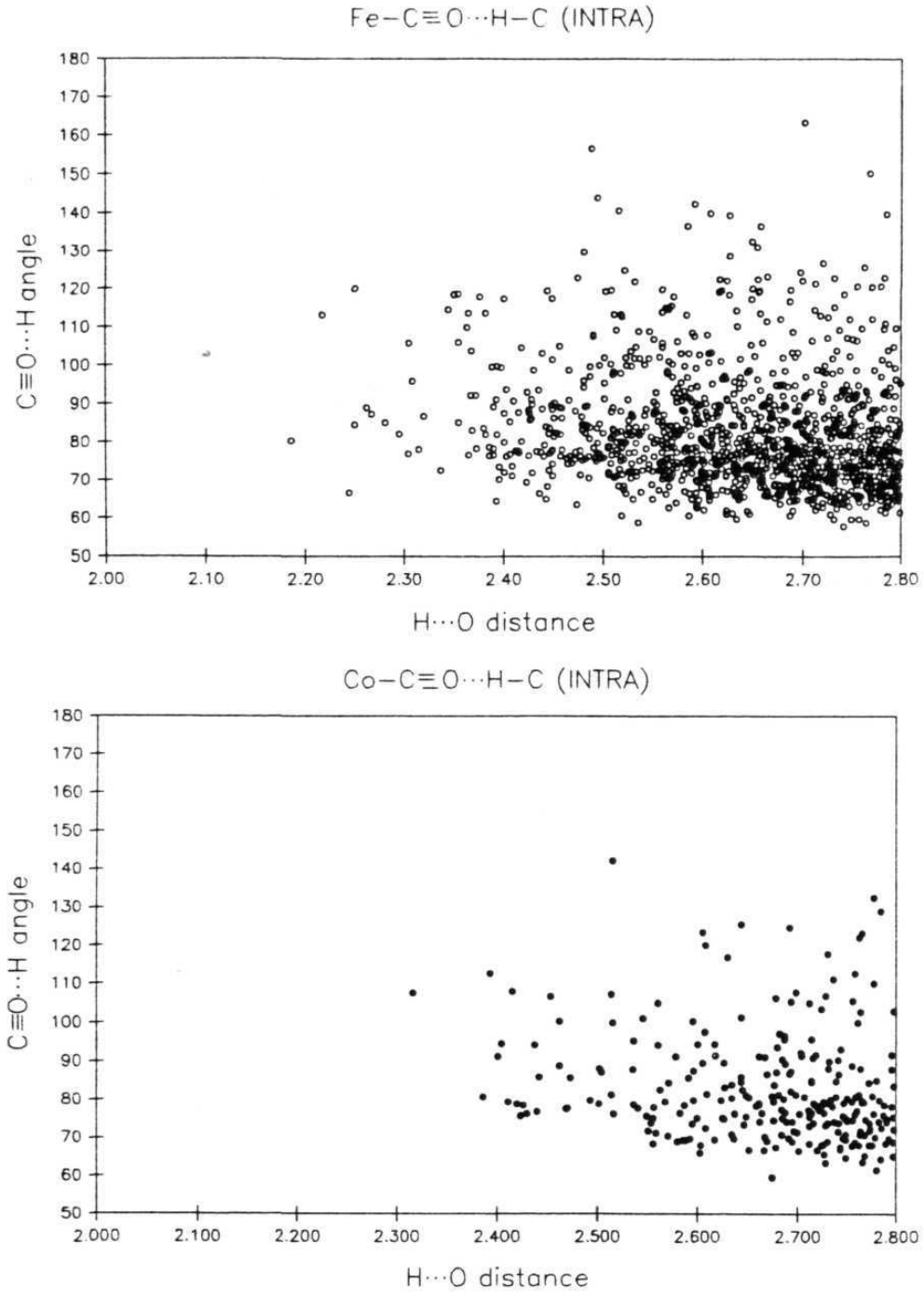

Figure 2. Plots of CO···H angle *versus* H···O distance for intramolecular C-H···O hydrogen bonds in terminal carbonyl (CO-t) (c) Fe and (d) Co metal complexes

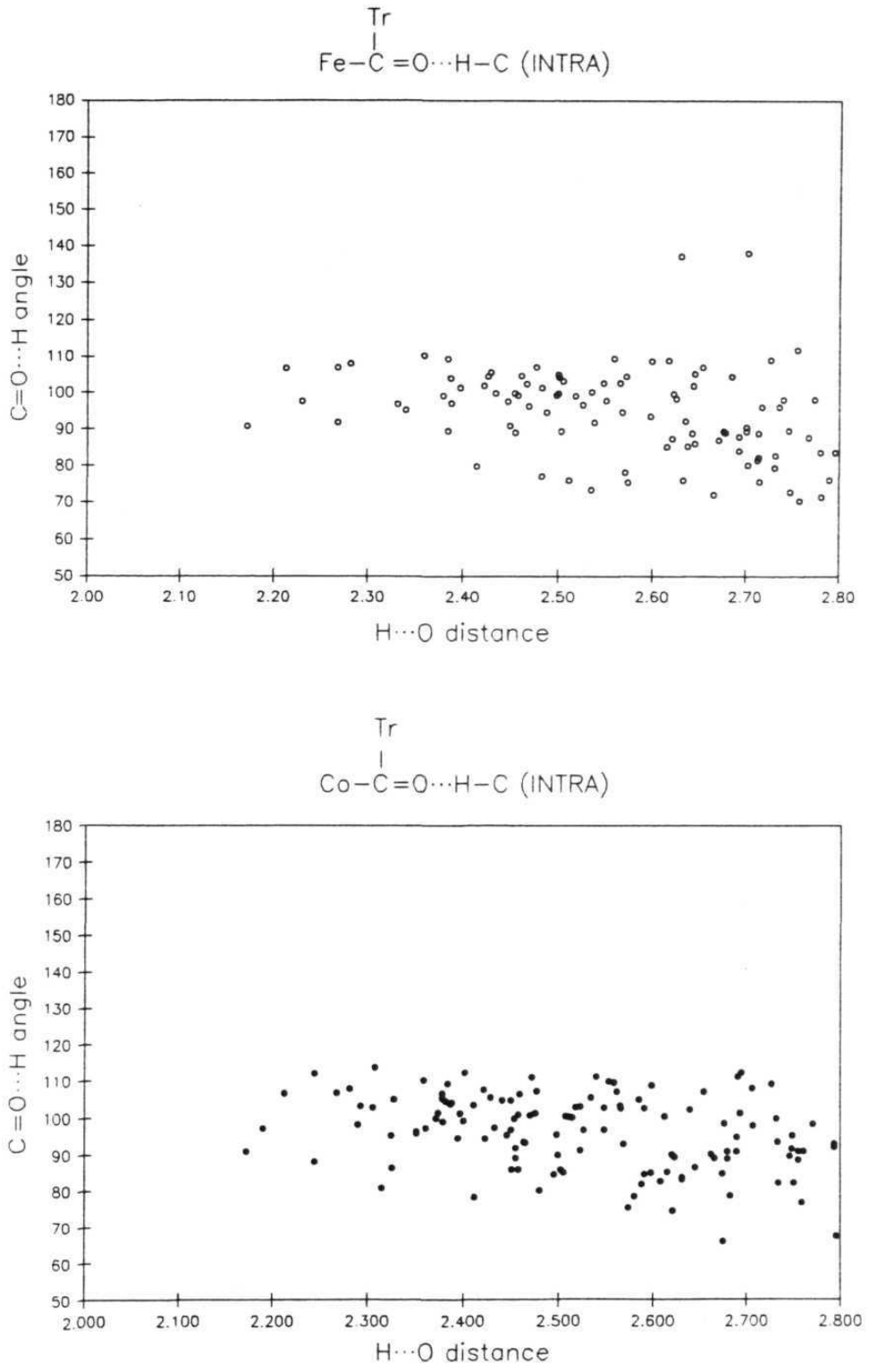

Figure 3. Plots of CO···H angle *versus* H···O distance for intramolecular C-H···O hydrogen bonds in (a) Fe and (b) Co bridged carbonyl (CO-b) complexes.

higher nuclearity complex, as shown in Scheme 2, left. Only when the ligand carrying the C-H unit which is under consideration is very flexible and is capable of folding back towards the CO-ligand (Scheme 2, right) can the CO···H angle be larger.

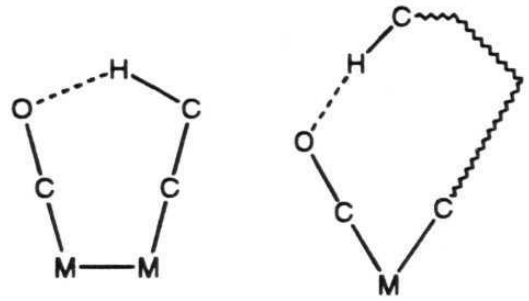

Scheme 2: Intramolecular C-H···O bonding, showing small and large CO···H angles

This could be a reason for the formation of intramolecular six, seven and higher-membered rings rather than the formation of five-membered rings. In order to form five-membered rings, the C-H of interest must be bound directly to the metal. This metal to C-H bond could be either of the uncommon σ-type (M-CH) or it could be a π-type (cyclopentadienyl, arenes etc.) which is found more frequently. In this latter case, intramolecular repulsions between C(π-ligand) and C(CO) arise when the five membered intramolecular C-H···O hydrogen bond is formed as shown in Scheme 3. Hence, the five membered intramolecular C-H···O hydrogen bonds are not found even with C-H group of cyclopentadienyl ligand also.

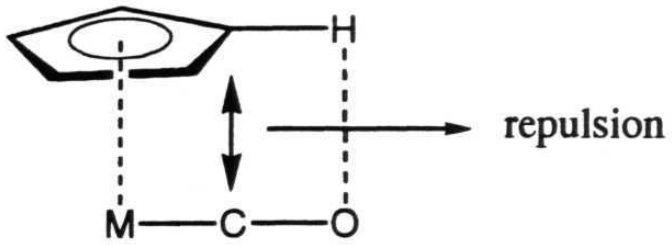

Scheme 3

3.2.4.2 Intermolecular angles

A consideration of the CO···H angles in the CO-t(inter) case is more interesting. Scattergrams of CO···H angle *versus* H···O distances in the metal complexes of Cr, Mn, Co and Ni for CO-t (inter) are presented in Figure 4. Similar plots in the crystal structures of Fe and Co for CO-b (inter) are shown in Figure 5. These plots provide information on O-atom directionality, a subject which has not been studied rigorously for C-H···O bonding. For strong hydrogen bonds, the directionality of X-H···O (X=N, O) that is, the preference of the X-H vector to point towards the lone pair direction of the O atom has been found to depend on whether the O atom is sp^2 or sp^3 hybridised.[1d] For carbonyl acceptors, there is a marked preference for the hydrogen bond to lie in the lone pair direction, or in other words with an X-H···O=C< angle of around 120^0. In the previous Chapter the directionality of amide carbonyl group in organic and organometallic complexes has been discussed. For ether acceptors, however, the directionality is not so pronounced; while there is some preference for hydrogen bonding in the plane containing the O-lone pairs ('rabbit ears' plane), there is no favoured trajectory within the plane.[13a] In

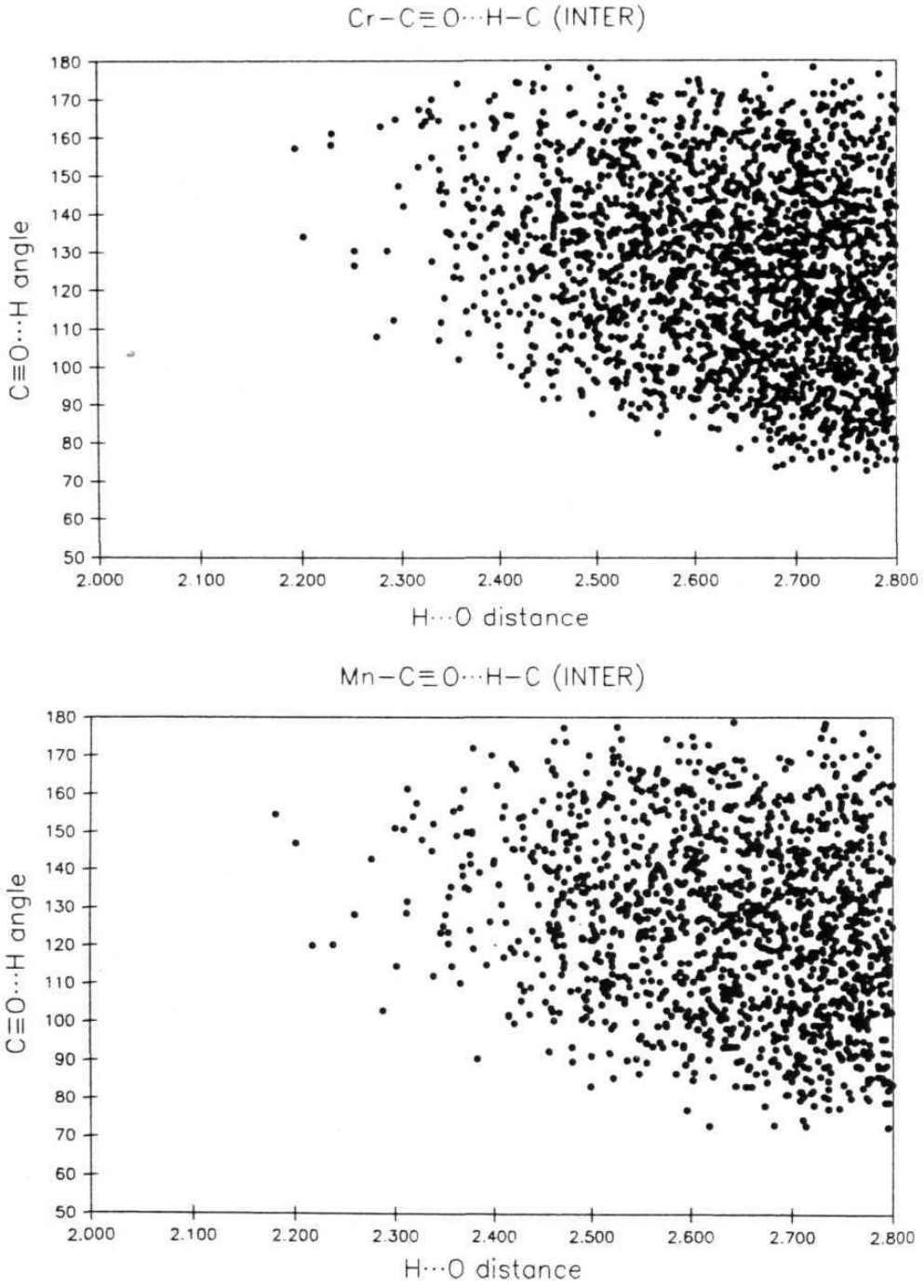

Figure 4. Plots of CO···H angle *versus* H···O distance for intermolecular C-H···O hydrogen bonds in terminal carbonyl (CO-t) (a) Cr and (b) Mn metal complexes.

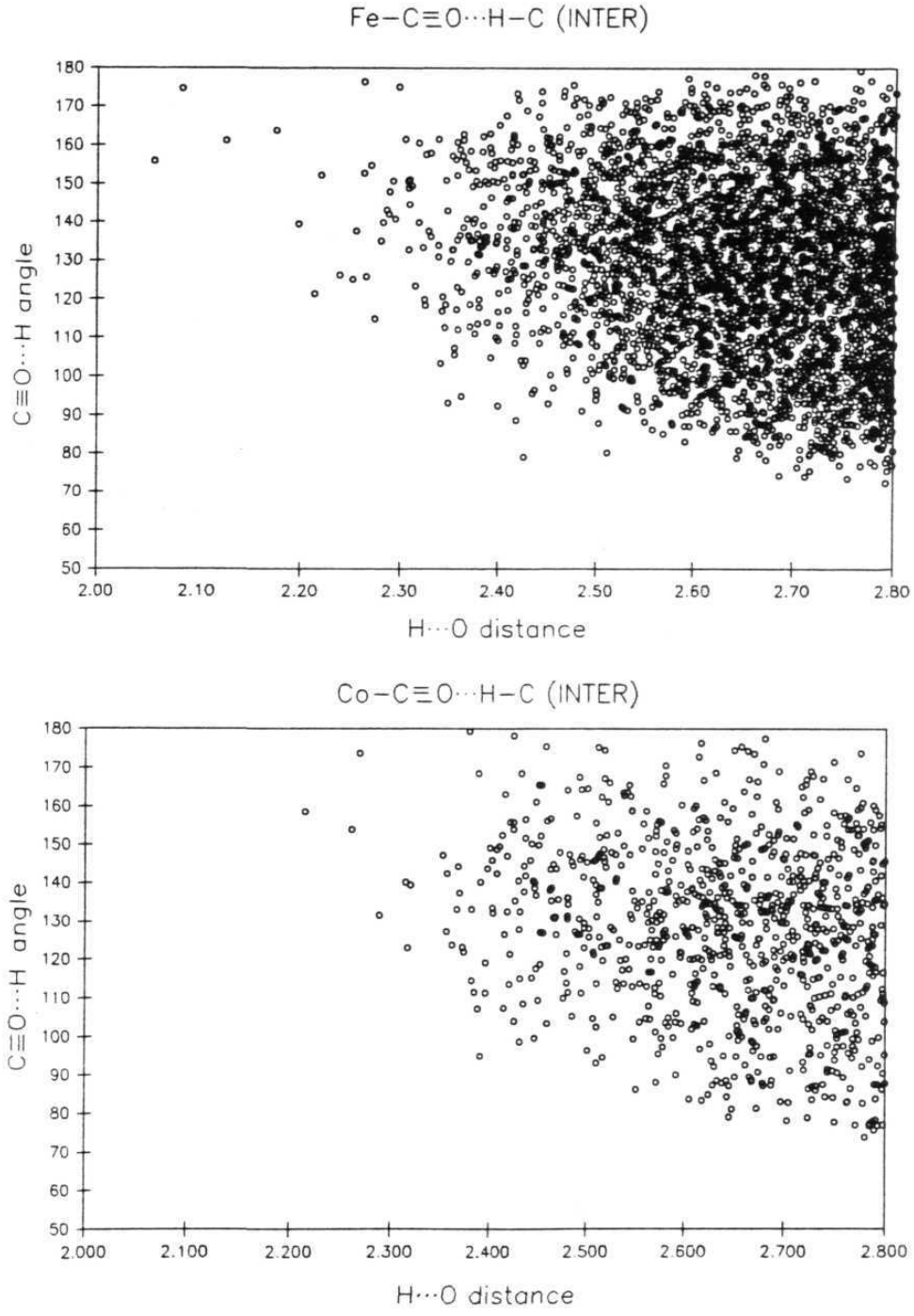

Figure 4. Plots of CO···H angle *versus* H···O distance for intermolecular C-H···O hydrogen bonds in terminal carbonyl (CO-t) (c) Fe and (d) Co metal complexes

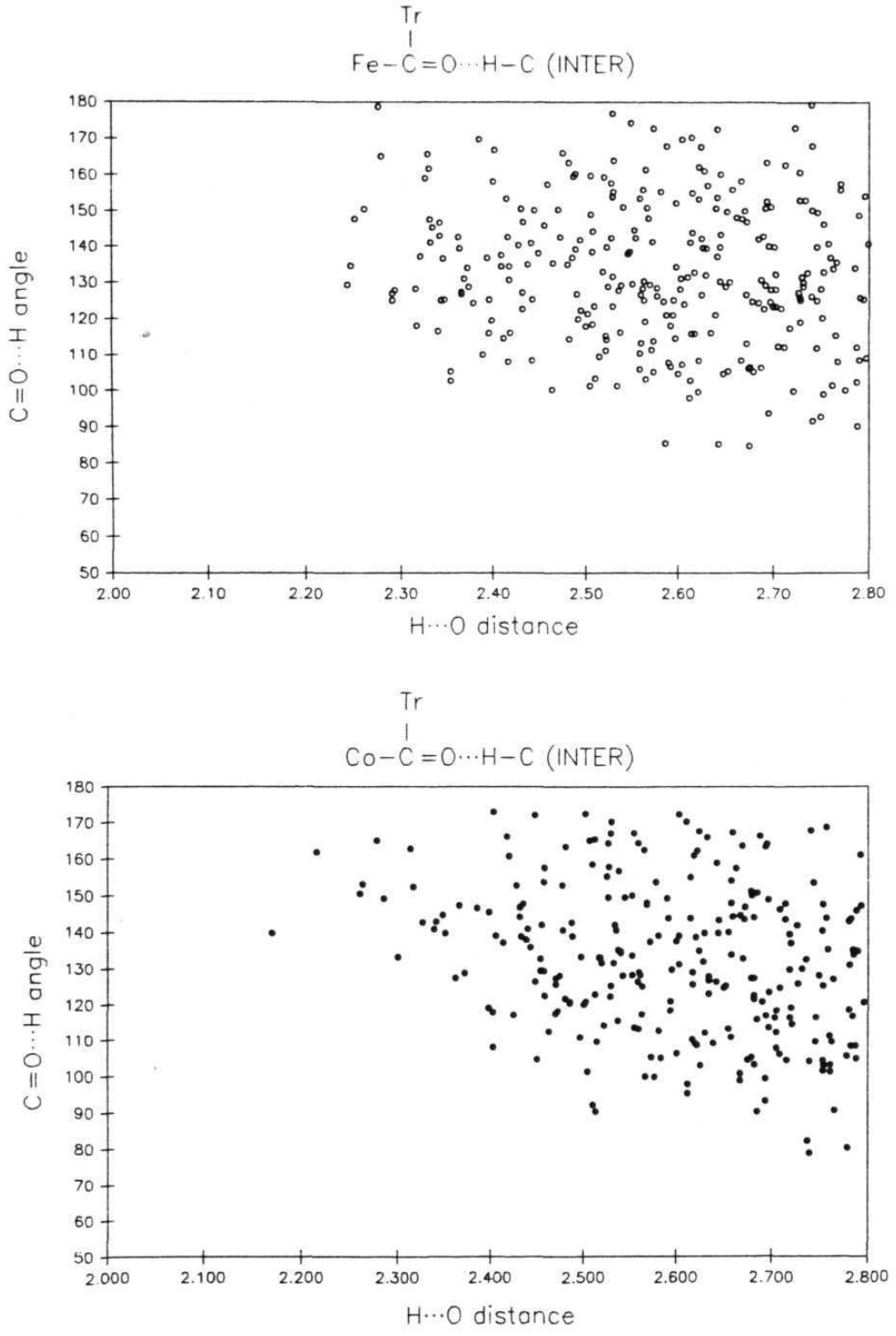

Figure 5. Plots of CO···H angle *versus* H···O distance for intermolecular C-H···O hydrogen bonds in (a) Fe and (b) Co bridged carbonyl (CO-b) complexes.

general, C-H···O directionality has been found to be similar, that is C-H···O hydrogen bonds to carbonyl O are more directional than those to ether O. The extent of CO···H-C directionality among the organometallic compounds studied here is therefore of relevance because it may be used to obtain evidence for the shapes of lone-pairs on the O-atoms of CO-t and CO-b ligands.

CO-t(inter) plots of all the metals suggests that the directional preference decreases as H···O distance increases. This aspect is studied further by examining the CO-t(inter) plot of Fe complexes. The most significant feature of this plot is that data on as many as 4205 hits from 1137 Fe-atom containing crystal structures are included. There is a large angular distribution (90 - 180^{O}) at long O···H separations (> 2.60Å) which narrows as the O···H separation decreases, focussing around 125-135^{O} for the strongest C-H···O hydrogen bonds. This feature is quantified in Figure 6 which is a plot of the percentage (probability) of hits in the range 125-135^{O} *versus* the H···O distance. It may be noted that 25% of the hits have CO···H angles in this range when the H···O distance is around 2.30Å whereas this percentage falls to around 16% at a distance of 2.80Å. Is this result significant and does Figure 6 really confirm that the CO···H approach is angular? This question is studied further by using the method of solid angle correction that was described in Chapter 2.[13b] Figure 7a is a histogram of observed CO···H angles. The populations in each 10 deg

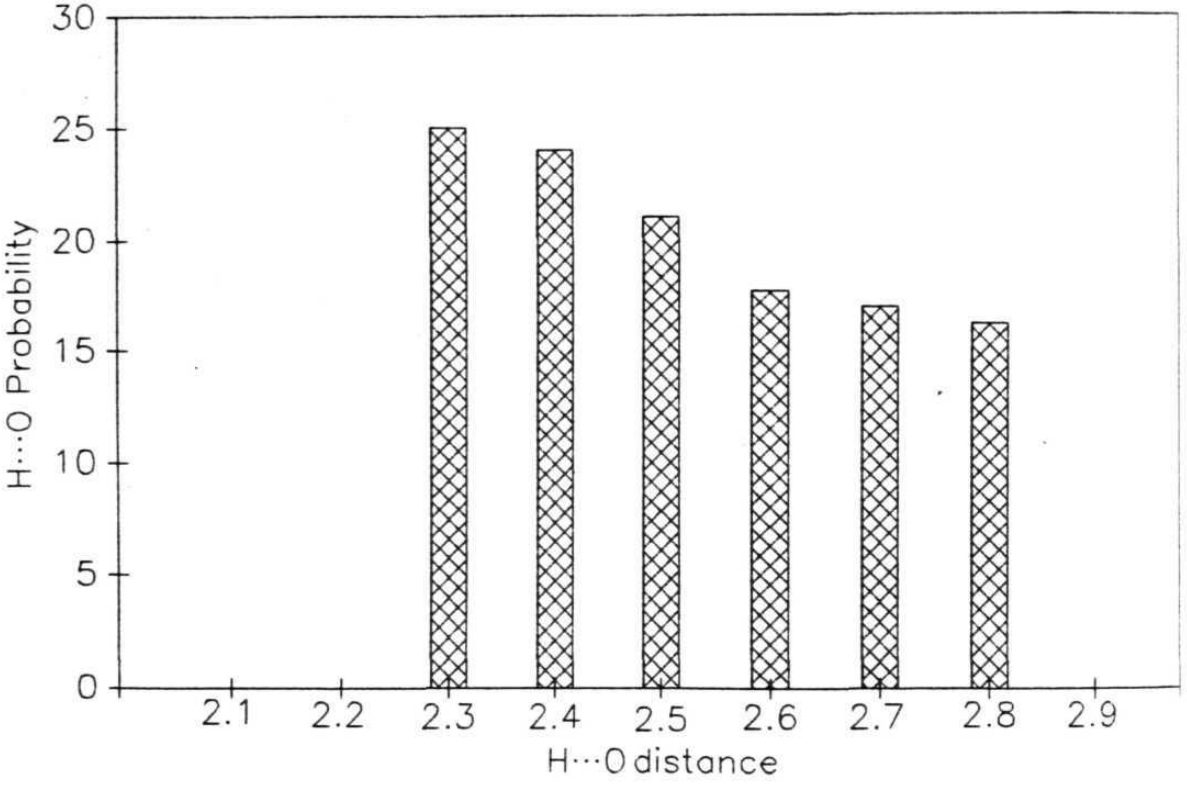

Figure 6. Populations of CO···H angles (expressed as probabilities) in the 125-135^{o} range as a function of H···O distances for Fe CO-t (inter). Notice that the probability decreases smoothly from 25% to 15% as the H···O distance increases.

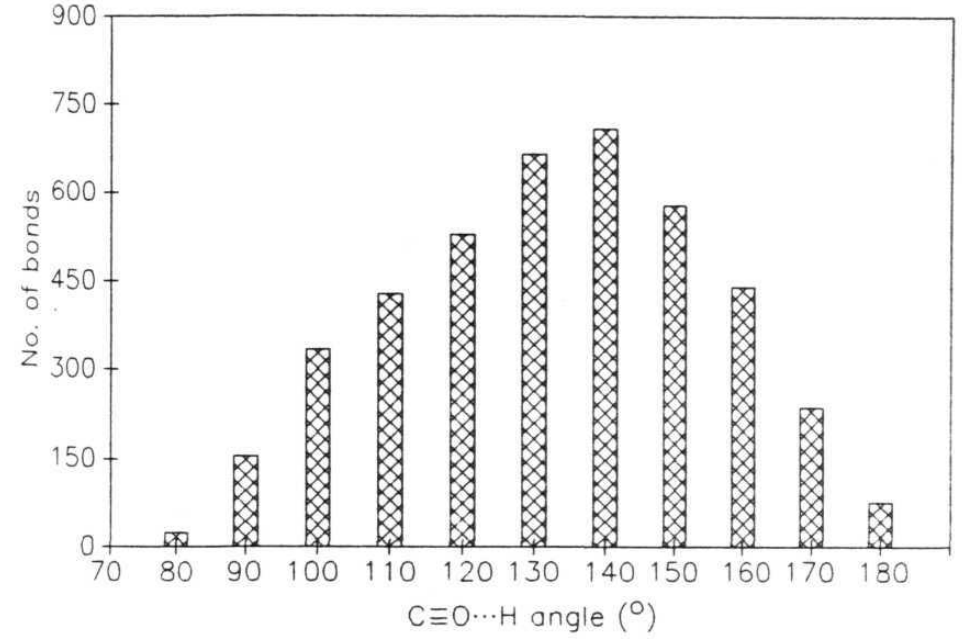

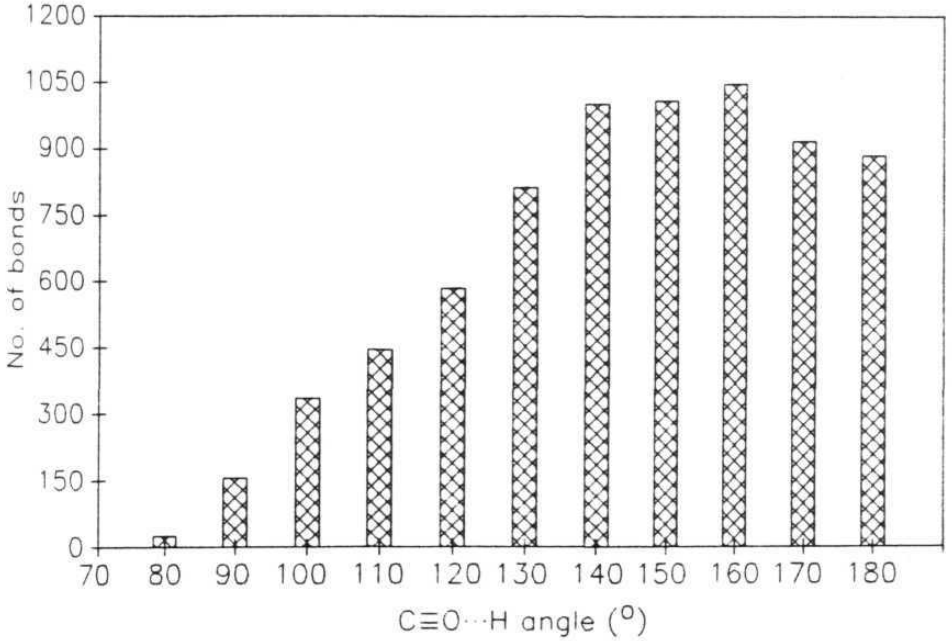

Figure 7. (a) Histogram of CO···H angles, ϕ for Fe CO-t(inter). (b) Histogram of CO···H angles, ϕ for Fe CO-t(inter) with the populations corrected by a factor of sin ϕ.

range of ϕ were then normalised for the above geometrical bias by division by sin ϕ, and the corrected histogram is shown in Figure 7b. Significantly, the maximum population for ϕ occurs around 140-160^{o} and not around 180^{o} though the preference for such a bent approach is only just discernible. This is in contrast to the results of Kroon et al. and also of Taylor and Kennard (who applied a similar geometrical correction on C-H···O angles)[1d] and found that the 'observed' maximum for θ at around 150^{o} became, in effect, a true maximum at 180^{o} (showing incidentally the linearity of the O-H···O and C-H···O approaches). All the results and especially Figure 7b reveals a tendency for a bent CO···H approach. This effect is somewhat less pronounced for CO-b(inter) as is seen in Figure 5. It is significant that the CO-t cases display an O-atom directionality suggestive of a ketonic >C=O group because in a valence bond picture, this should be true only for the bridging CO group where there are presumably two lone pairs on the O-atom available to accept H-bonds at around 120^{o}. According to such a depiction there should be a potential for the formation of only one hydrogen bond in a terminal CO-group, that is towards the single lone pair along the M-C≡O vector (CO···H angle ~ 180^{o}). So, while the observed directionality of the CO-b(inter) bonds may be thus rationalised, that of the CO-t(inter) bonds is unexpected and suggests the presence of resonance form II (Scheme 4).

I II

Scheme 4: Resonance forms for CO-t

3.2.5 Hard and soft hydrogen bonds

This study has shown that CO-ligands of both terminal and bridging varieties form a profusion of C-H···O hydrogen bonds. However, in Chapter-2 it has been described that CO-ligands do not act as efficient hydrogen bond acceptors in strong hydrogen bonding situations. The reason for this observation could lie in the hardness and softness of these interactions. One might consider O-H···O and N-H···O as hard hydrogen bonds and C-H···O, O-H···π[16] and C-H···π[17] as soft hydrogen bonds with perhaps N-H···N being a borderline case. Accordingly, it might be argued that the soft acceptor CO prefers to hydrogen bond with the soft donor C-H or alternatively the hard donor O-H prefers to form bifurcated or solvated hydrogen bonds with hard acceptors rather than waste itself on the soft acceptor CO. As in molecular chemistry, hardness and strength need not always be correlated. A recent study of C-H···Se hydrogen bonding shows that this interaction can affect molecular structure and conformation significantly.[18] All these observations suggests that the C-H group is a soft acid and that the C-H···O hydrogen bond is a soft hydrogen bond. This concept is in agreement with the work of Koch and Popelier who have shown recently that for C-H···O hydrogen bonds, the nonbonded

charge density on the H-atom is penetrated more than that on the O-atom.[19]

3.2.6 Discussion of selected examples

Geometrical details of C-H···O hydrogen bonds and references to the original structural papers are given in Table 2.[20-27] Only those C-H···O hydrogen bonds which are shown in Figures 8 to 15 are mentioned in Table 2. The structural formulae of these compounds are shown in Scheme 5.

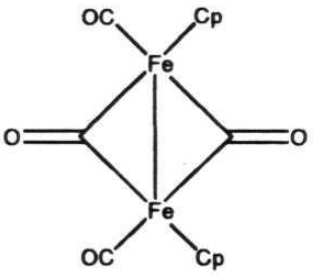

CPFECO10

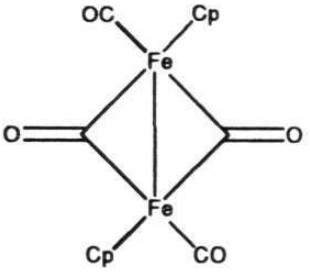

CYPFEC03

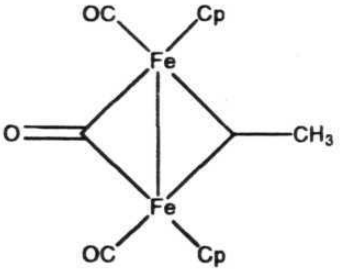

CMCPFE10

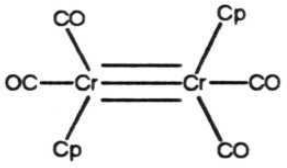

CPCOCR

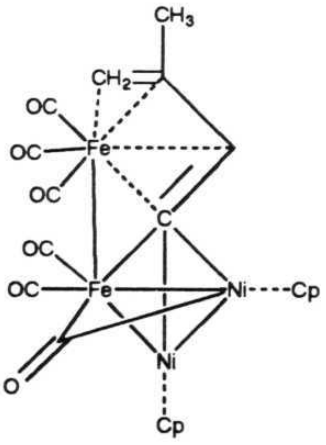

COBGEF

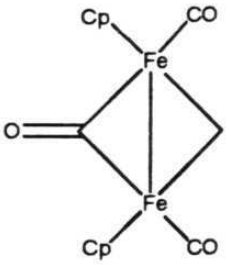

BEBSAC01

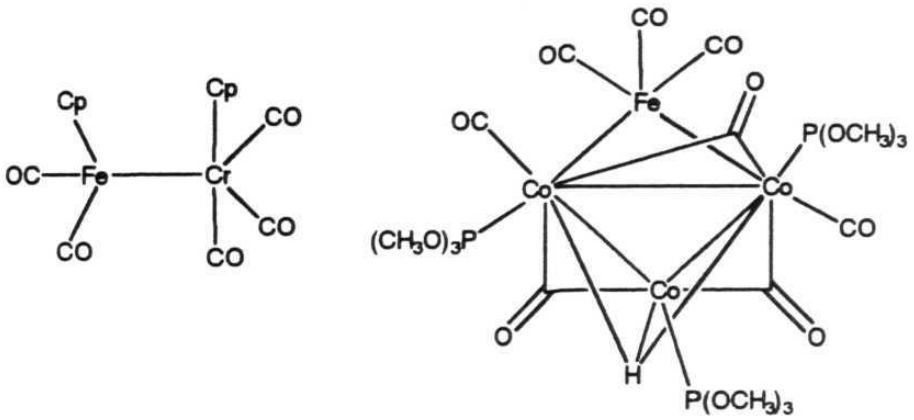

FERLOD **HMPCIC01**

Scheme 5: Structural formulae of the selected examples

cis-, trans-$(\eta^5\text{-}C_5H_5)_2Fe_2(CO)_2(\mu\text{-}CO)_2$, CPFECO10 and CYPFEC01

These two complexes are the cis- and trans- isomers of the dinuclear Fe complex (CPFECO10, and CYPFEC01, respectively) and are of interest because they carry two terminal and two symmetrically bridging CO-ligands each. The C-H···O hydrogen bonding patterns are shown in Figures 8 and 9 for the crystals of cis- and trans-complexes respectively. The neutron derived crystal structure at 74K is also available for the trans-isomer (CYPFEC03). A comparison of the room and low temperature structures (with the X-ray determined H-atom positions being normalised) allows one to see the effect of temperature on the hydrogen bonds.

Figure 8 clearly shows that both CO-t and CO-b are involved in the C-H···O network. The strongest interaction is associated with O1 of the CO-b ligand and H8 of the Cp-ligand (H···O 2.34Å C-H···O 157.9^o)

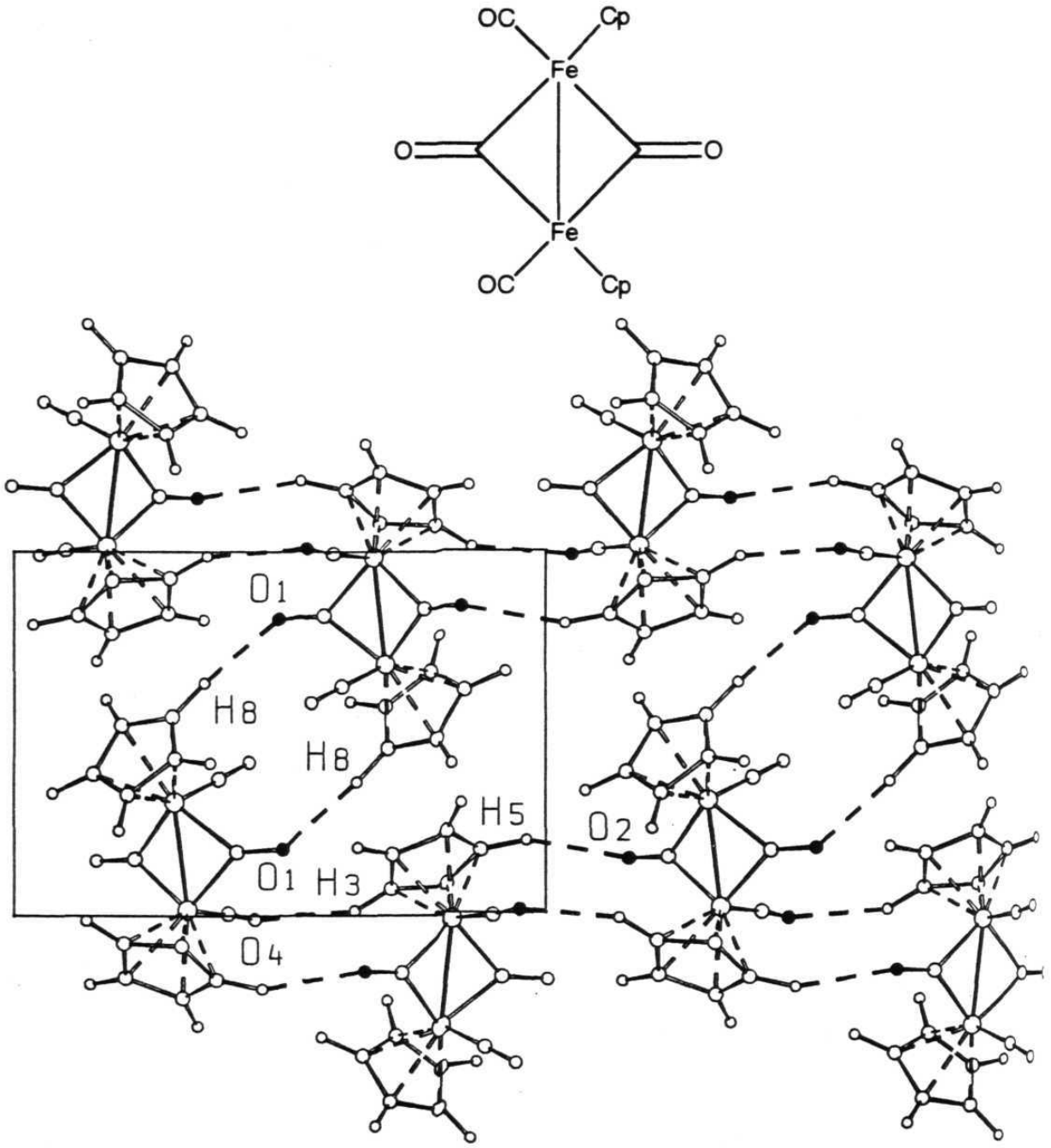

Figure 8. Hydrogen bonding networks in the cis-isomer of the dinuclear complex $(\eta^5\text{-}C_5H_5)_2Fe_2(CO)_2(\mu\text{-}CO)_2$, CPFECO10 both CO-t and Co-b are in the C-H···O network. Note how the two Cp rings are involved in a different number of interactions.

Table 2: Geometrical parameters of C-H···O hydrogen bonds in selected organometallic crystals.

Refcode	Type	C-H···O	C···O (Å)	H···O (Å)	C-H···O (°)	Ref.
CPFECO10	CO-t	C(4)-H(3)···O(4)	3.24	2.36	137.7	20
	CO-b	C(6)-H(5)···O(2)	3.48	2.53	145.7	
	CO-b	C(10)-H(8)···O(1)	3.36	2.34	157.9	
CYPFEK01	CO-b	C(5)-H(5)···(O2b)	3.34	2.53	131.5	21a
CYPFEK03 47K	CO-b	C(6)-H(4)···(O2)	3.16	2.42	124.8	21b
CMCPFE10	CO-b	C(5)-H(5)···O(3)	3.21	2.48	123.6	22
CPCOCR	CO-t	C(2)-H(1)···O(3)	3.55	2.50	164.0	23
	CO-t	C(6)-H(5)···O(2)	3.40	2.49	141.7	
COBGEF	CO-t	C(12)-H(7)···O(4)	3.60	2.55	162.0	24
	CO-b	C(15)-H(10)···O(1)	3.49	2.46	158.9	
	CO-b	C(20)-H(15)···O(1)	3.47	2.41	166.6	
BEBSAC01	CO-b	C(5)-H(5)···O(3)	3.62	2.57	164.0	25
	CO-b	C(6)-H(6)···O(3)	3.42	2.35	170.0	
	CO-b	C(10)-H(10)···O(3)	3.40	2.37	160.4	
	CO-b	C(11)-H(11)···O(3)	3.40	2.40	152.3	
FERLOD	Intra	C(6)-H(1)···O(3)	3.12	2.60	109.1	26
	Intra	C(9)-H(4)···O(5)	3.11	2.59	109.0	
	CO-t	C(11)-H(6)···O(3)	3.33	2.28	164.3	
	CO-t	C(14)-H(9)···O(3)	3.57	2.50	176.1	
HMPCIC01 neutron	Intra CO-b	C(10)-H(4)···O(6)	3.45	2.52	150.1	27
	Intra CO-b	C(13)-H(13)···O(5)	3.26	2.51	126.2	
	CO-b	C(18)-H(28)···O(5)	3.57	2.56	158.3	
	CO-t	C(10)-H(3)···O(9)	3.40	2.54	140.1	
	CO-t	C(11)-H(7)···O(8)	3.32	2.48	135.8	
	CO-t	C(13)-H(11)···O(2)	3.12	2.59	109.2	

between two molecules related by the inversion centre. This results in a centrosymmetric dimer which shows some resemblance to O-H···O dimers in carboxylic acids and C-H···O dimers in α,β-unsaturated carbonyl compounds. These dimers are interconnected by two other C-H···O hydrogen bonds. One of these bonds is formed in between O4 of CO-t and H3 of the other Cp-ligand of the molecule (H···O 2.36Å) whereas the second C-H···O is formed in between O2 of CO-b and H5 of the same Cp-ligand. This is an important difference between the packing environments around the two Cp-rings, and accounts clearly for the different librational and reorientational motion shown by the two ligands in the solid state. This dynamic process has been studied by ^{13}C CPMAS NMR, ^{1}H spin-lattice relaxation time measurements, packing potential energy barrier calculations and thermal motion analysis.[28]

The trans-isomer forms a different kind of C-H···O hydrogen bonded network as shown in Figure 9. At both room temperature and 74K only the CO-b ligands are involved in hydrogen bonds (O···H 2.53Å C-H···O 131.5^{o} at room temperature; 2.42Å; 124.8^{o} at 74K). Because of the site symmetry (the molecule is located on a crystallographic centre of inversion placed midway along the Fe-Fe bond) both Cp-ligands have crystallographically identical surroundings and experience the same type of interactions. Each molecule interacts with other four surrounding molecules *via* identical CO-b···H(Cp) interactions. The shortest H···O

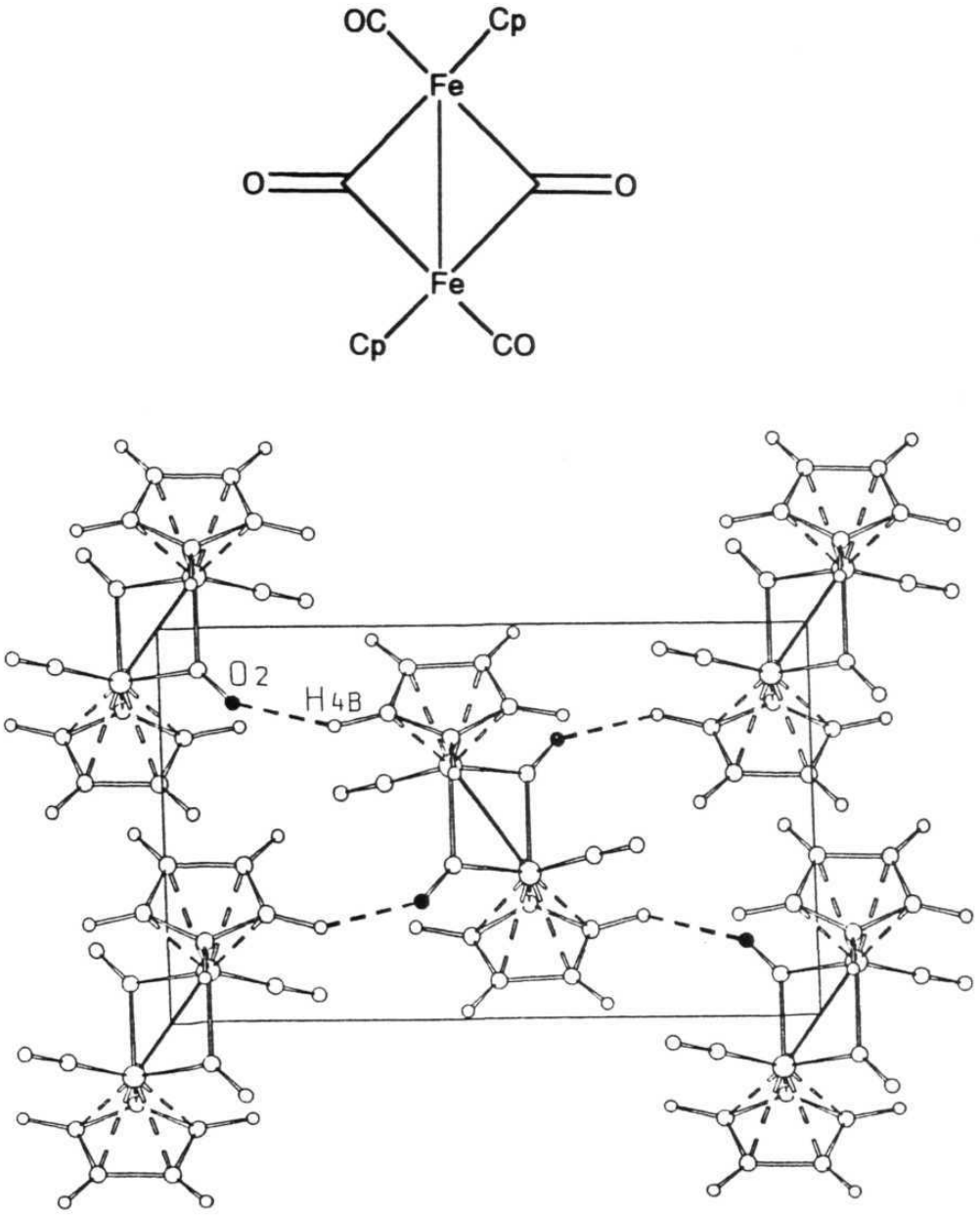

Figure 9. Hydrogen bonding networks in the trans-isomer CYPFEC03 shows that only CO-b are involved in the C-H···O network. Note the differences between 6 and 7.

interaction involving the terminal CO is above the threshold of interest (2.81Å) at room temperature but shortens significantly on going down to 74K (2.65Å).

$(\eta^5\text{-}C_5H_5)_2Fe_2(CO)_2(\mu\text{-}CO)(\mu\text{-}CHCH_3)$, CMCPFE10

Figure 10 shows the bifurcated-acceptor interaction established by the bridging CO-ligand in crystalline CMCPFE10. Because of the crystallographic and molecular symmetry, the unique bridging CO-ligand is at equal interaction distance from both Cp ligands of a neighbouring molecule along the c-axis (H···O 2.48Å, C-H···O 123.6^{o}). With these bifurcated hydrogen bonds, the crystal structure can be described as being formed by chains of molecules joined *via* C-H···O hydrogen bonded interactions. This bifurcation interaction is a common motif in crystals of 'pure' organics and is found with both strong and weak hydrogen bonds. For example, very similar bifurcated-acceptor C-H···O hydrogen bonds may be observed in the crystal structure of 2,5-dibenzylidenecyclopentenone[29] while the N-H···O topological equivalent may be identified in the crystal structure of urea.[30]

$(\eta^5\text{-}C_5H_5)_2Cr_2(CO)_6$, CPCOCR

This complex is of importance as it contains terminal CO-ligands only. The C-H···O bonded network is shown in Figure 11. This network is based on centrosymmetric dimers connected by pairs of C-H···O interactions. A second type of interaction is also present to connect these

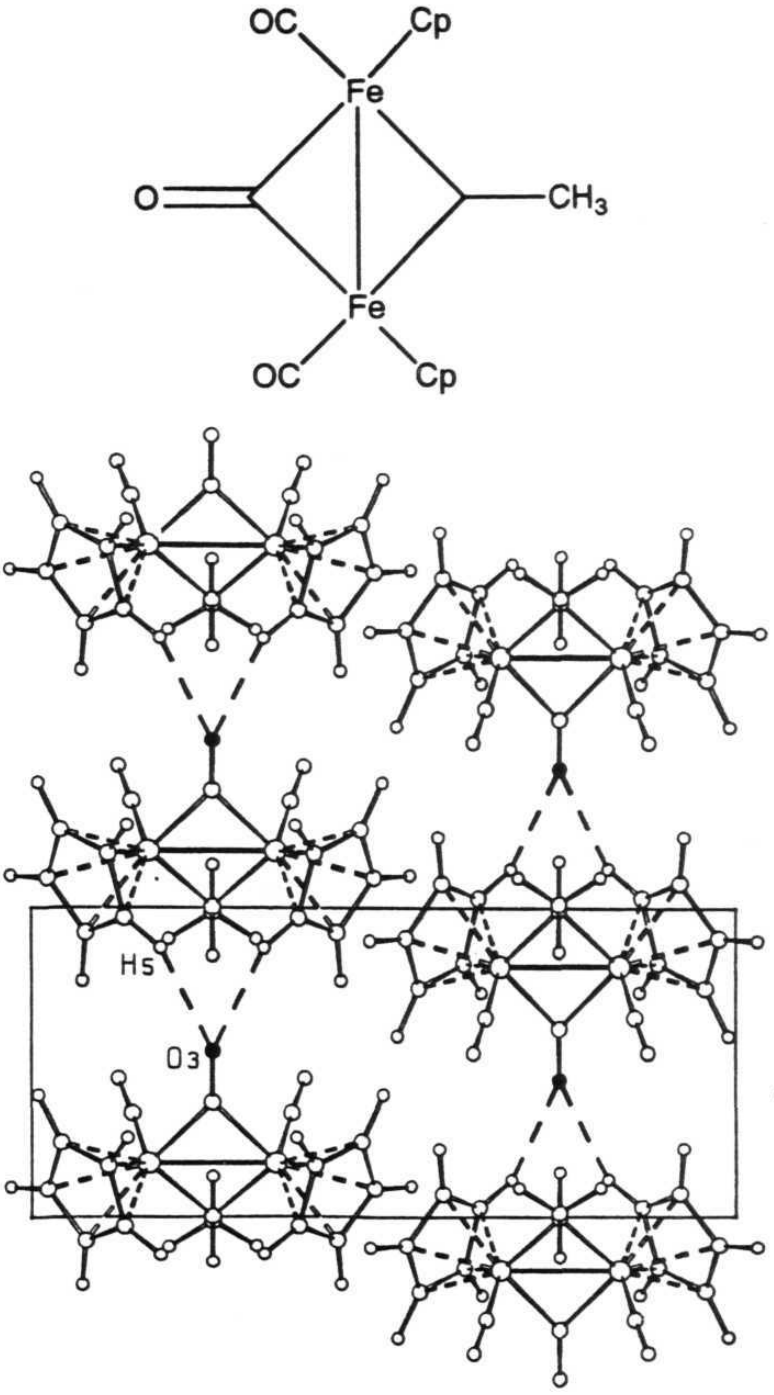

Figure 10. The bifurcated interaction established by the bridging CO in $(\eta^5\text{-}C_5H_5)_2Fe_2(CO)_2(\mu\text{-}CO)(\mu\text{-}CHCH_3)$, CMCPFE10.

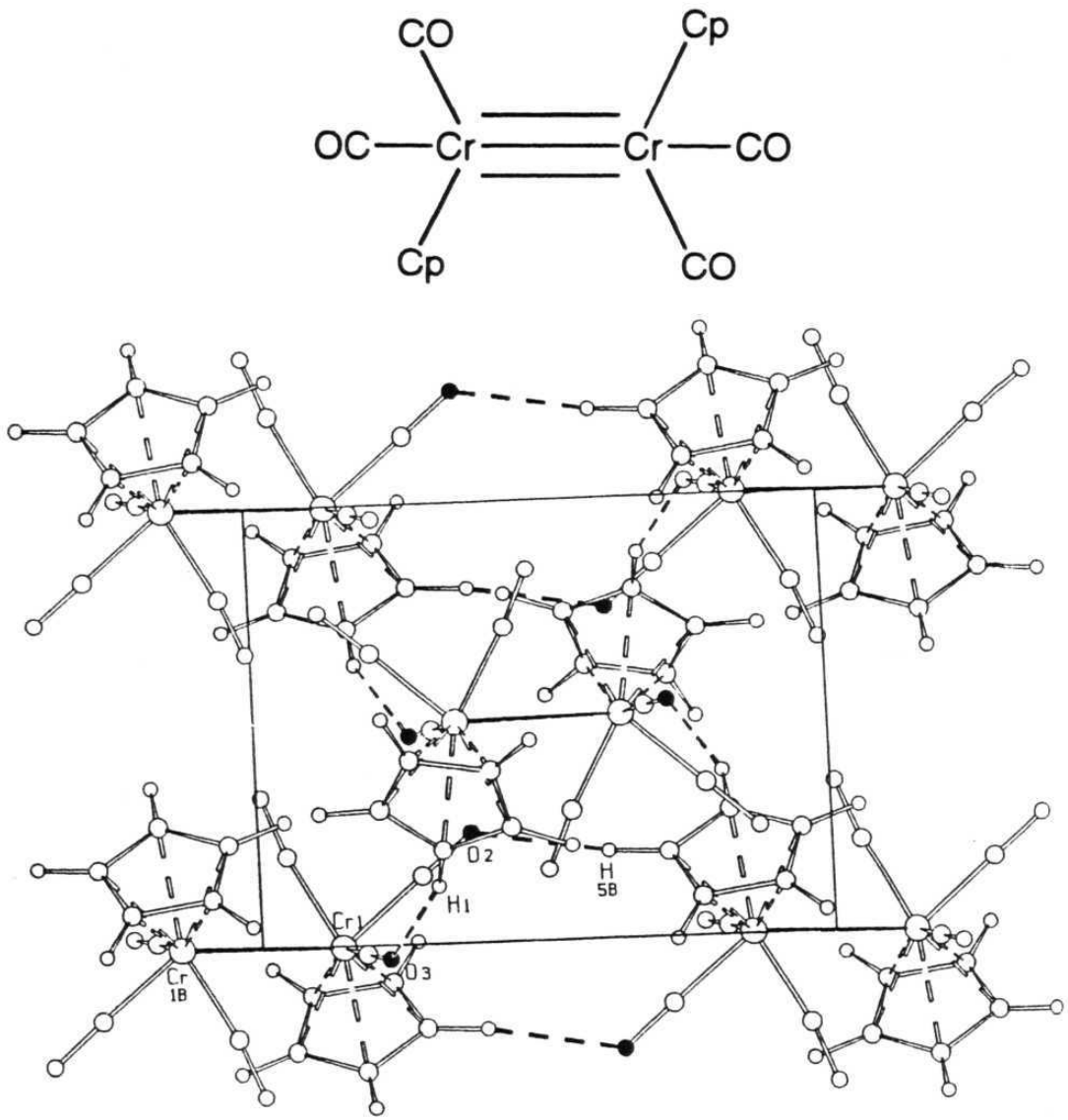

Figure 11. Intermolecular C-H···O interactions in crystalline $(\eta^5\text{-}C_5H_5)_2Cr_2(CO)_6$, CPCOCR. The network is based on centrosymmetric 'dimers' joined by pairs of C-H···O interactions.

dimers in an extended network. Such extended dimer structures are known in strong hydrogen bonded networks. A general conclusion of this study is that the basic packing motifs - rings and chains - adopted by strong hydrogen bonds are also established by these weak interactions.

$(\eta^5\text{-}C_5H_5)_2Ni_2Fe_2(\mu_3\text{-}CO)(CO)_5(\mu_4\text{-}\eta^3\text{-}$Methylbutenyl-1-1'-ylidine), COBGEF

The triply bridging CO-ligand in crystalline COBGEF participates in a bifurcated hydrogen bonds with H-atoms of the Cp ligands of a neighbouring molecule which is related by a crystallographic centre of inversion (Figure 12). Both interactions are short (H···O 2.46 and 2.41Å) and linear (158.9 and 166.6°). Although the terminal ligands are also involved in C-H···O interactions (Table 2) the triply bridging CO is sufficiently effective to form the strongest interactions despite their bifurcated nature.

$(\eta^5\text{-}C_5H_5)_2Fe_2(CO)_2(\mu\text{-}CO)(\mu\text{-}CH_2)$, BEBSAC01

In this complex, the unique CO-b ligand is involved in a tetrafurcated C-H···O hydrogen bonded interactions with the H···O distances below 2.60 Å (Figure 13). The bridging CH_2-group is not involved in C-H··· hydrogen bonds. In general, in C-H···O bonded crystals, there may be a tendency for several (greater than three) C-H groups to approach a single O-atom.[31] As a result there is a loss of directionality. This loss of directionality must be accompanied by a loss of bonding

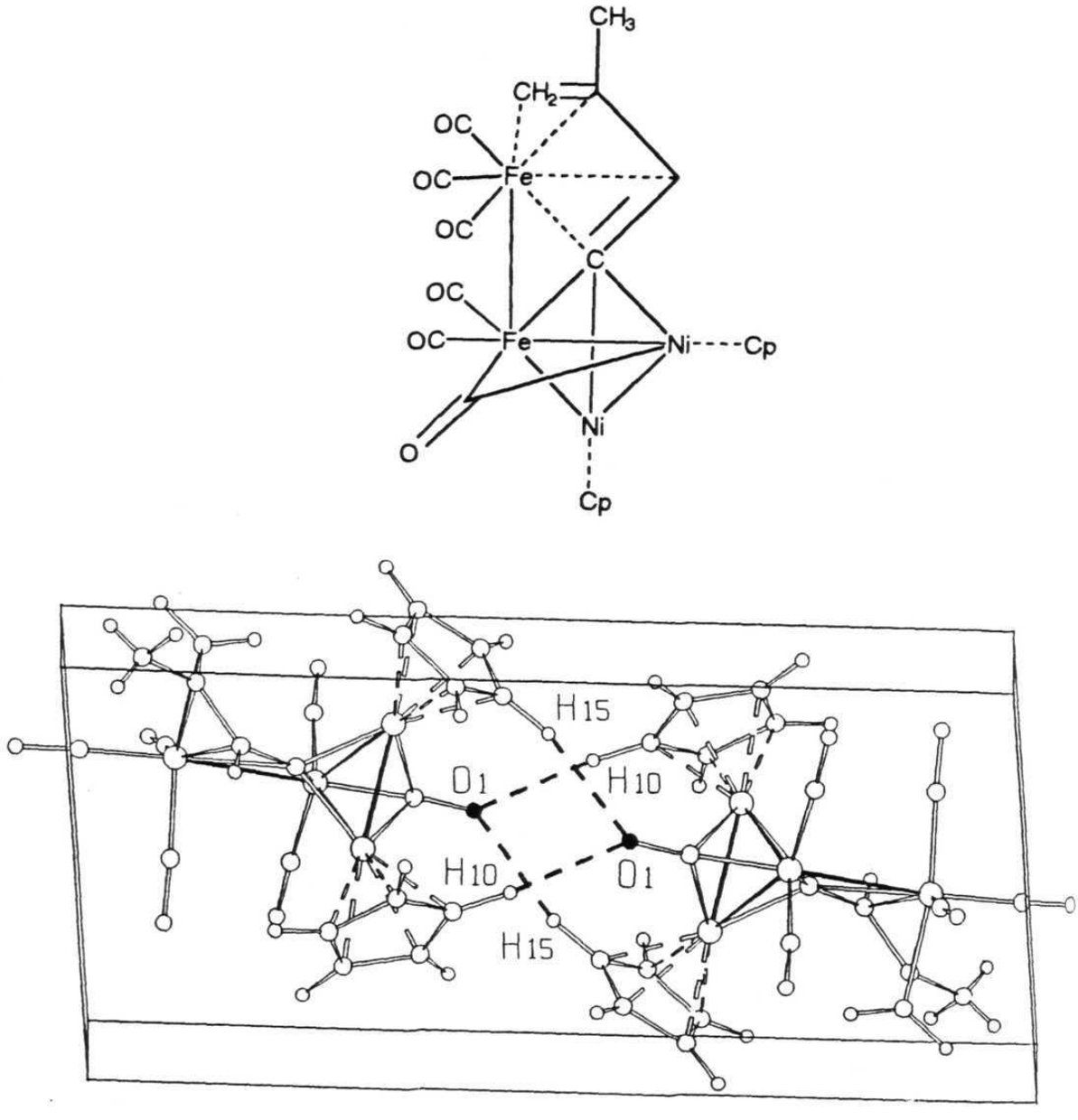

Figure 12. The triply bridging CO-ligand in crystalline (η^5-$C_5H_5)_2Ni_2Fe_2(\mu_3$-CO)(CO)$_5(\mu_4$-η^3-Methylbutenyl-1-1'-ylidine), COBGEF interacts with the Cp ligands of neighbouring molecules related by a crystallographic centre of inversion.

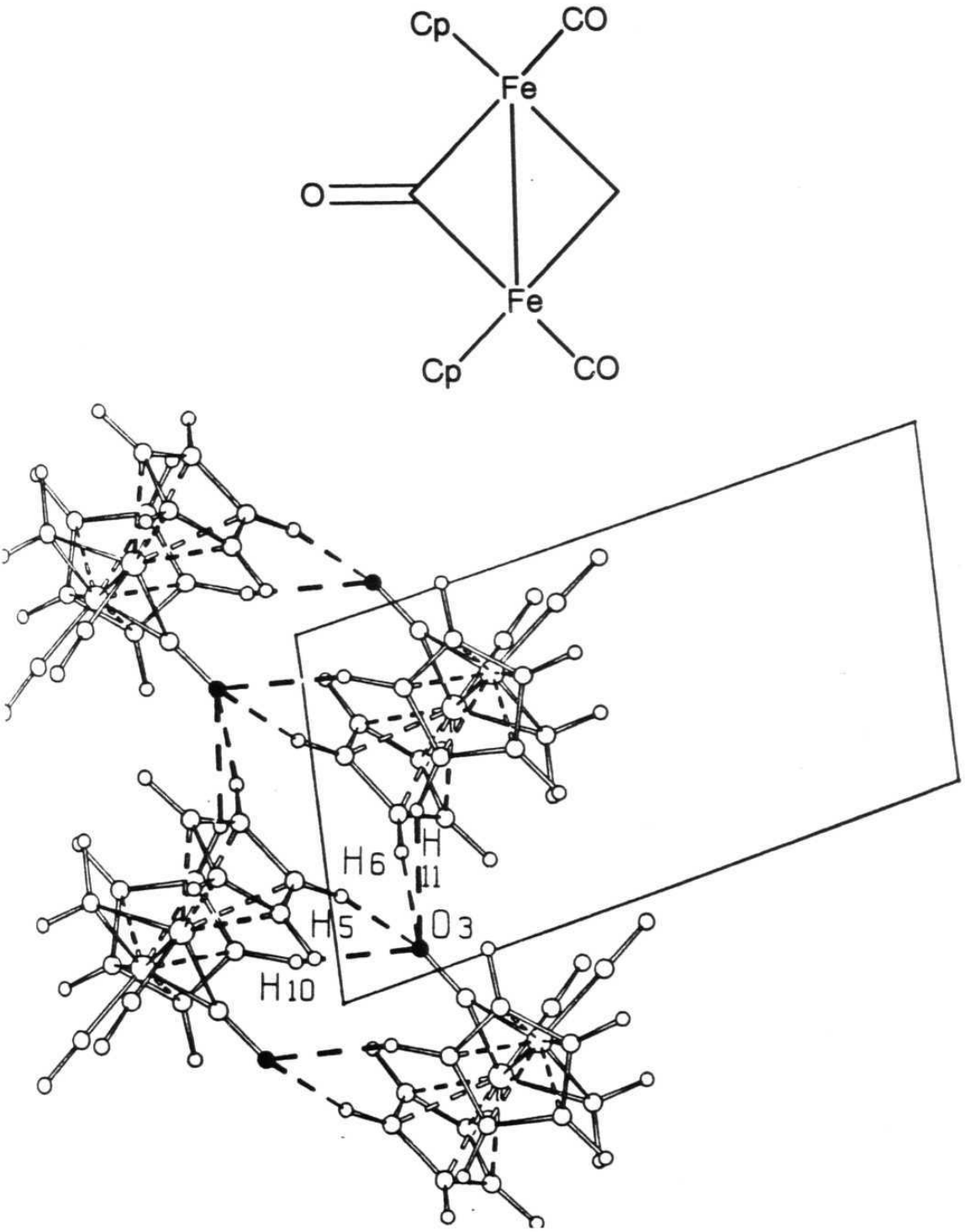

Figure 13: The C-H···O hydrogen bonded network in the crystal structure of $(\eta^5\text{-}C_5H_5)_2Fe_2(CO)_2(\mu\text{-}CO)(\mu\text{-}CH_2)$, BEBSAC01. The unique CO-b ligand participates in a total of four CO···H-C interactions below 2.60 Å.

character and is compensated for by a greater number of interactions. This tendency towards non-directionality is distinctly more pronounced for the weak C-H···O bonds when compared to the strong O-H···O and N-H···O bonds. This hints at the differing relative importance of bonding and electrostatic effects in weak and strong hydrogen bonds.

$(\eta^5\text{-}C_5H_5)_2FeCr(CO)_5$, FERLOD

In this complex, the shortest C-H···O (O3···H6) joins together two molecules in a centrosymmetric fashion. The same CO(3) ligand participates in hydrogen bonded network with a second C-H···O interaction. These two patterns are shown in Figure 14. This CO(3) ligand also forms an intramolecular C-H···O hydrogen bond. O3 is, in effect, a trifurcated-acceptor. From Table 2, it may be noted that the C···O distance for the intramolecular hydrogen bond is shorter than those for the intermolecular hydrogen bonds although the actual H···O distance is longer. This reflects a different angular relationship between the M-C≡O vectors and the donor C-H groups in the inter and intra patterns.

$(\mu_3\text{-}H)FeCo_3(CO)_9(P(OMe)_3)_3$, HMPCIC01.

The crystal structure of HMPCIC01 has been determined by neutron diffraction at 90 K.[27] The C-H···O bond network in this crystal is of interest because it contains all four of the bond types that have been discussed in this chapter so far, namely CO-t(inter), CO-b(inter), CO-t(intra) and CO-b(intra) and also because all the C-H···O hydrogen bonds involve only methoxy H-atoms. Of the nine CO-ligands in the molecule,

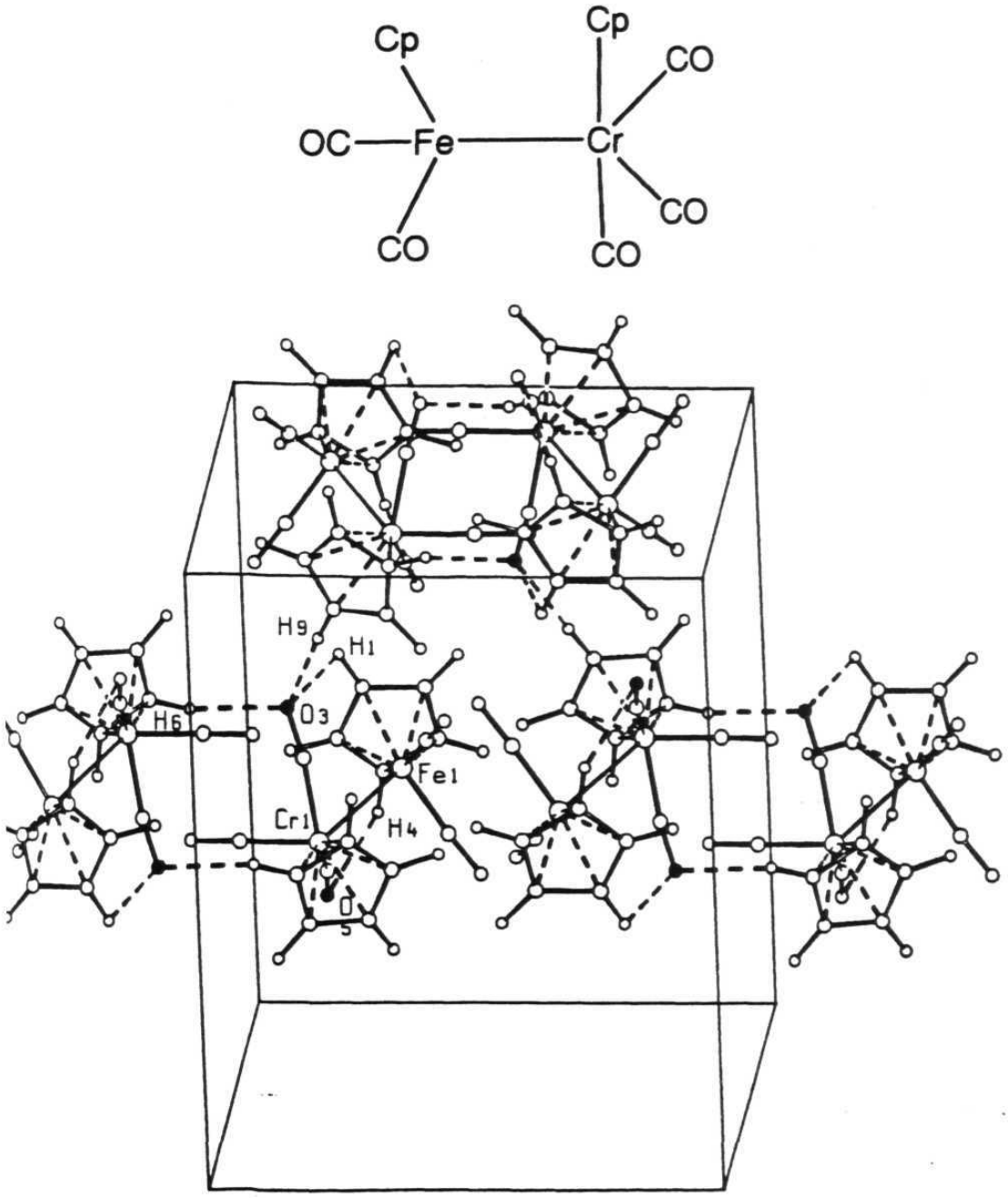

Figure 14: The shortest H···O interaction in crystalline (η^5-$C_5H_5)_2FeCr(CO)_5$, FERLOD (O3···H9) joins the two molecules in the usual centrosymmetric pair. The same CO(3) ligand participates in a slightly weaker interaction to form a network with second set of molecules.

only one is not C-H···O hydrogen bonded. The individual molecule ORTEP is given in Figure 15a and the packing diagram in Figure 15b shows only the intermolecular contacts. All three terminal CO-ligands on Fe are intermolecularly C-H···O bonded. The ligands on Co are weakly hydrogen bonded; one of them forms an intramolecular bond (H···O 2.69Å), another is intermolecularly bonded (2.71Å) while the third is the free C-H group. As for the bridging CO-ligands, while all three form intramolecular hydrogen bonds, two of them are additionally involved in intermolecular bonds (Table 2). Because neutron data are available for the C-H···O hydrogen bonds in this structure and in particular because the anisotropic displacement parameters (ADP) are known accurately (see the ORTEP diagram), additional information on the bonding nature of C-H···O interactions can be obtained. This was done with a modification of the method of Steiner who showed in a recent study of C-H···O bonded alkyne C≡C-H groups that while the ADPs of the terminal alkyne C-atom are generally larger than those of the internal alkyne C-atom, the *ratio* of these parameters decreases with decreasing C···O distance.[14] This is presumably the case because the terminal atom is more constrained by the hydrogen bonding. In any event, it is assumed that the stronger the C-H···O bonding, the less would be the thermal vibration of atoms in the vicinity of the bond. The results are given in Table 3 and in Figure 16.

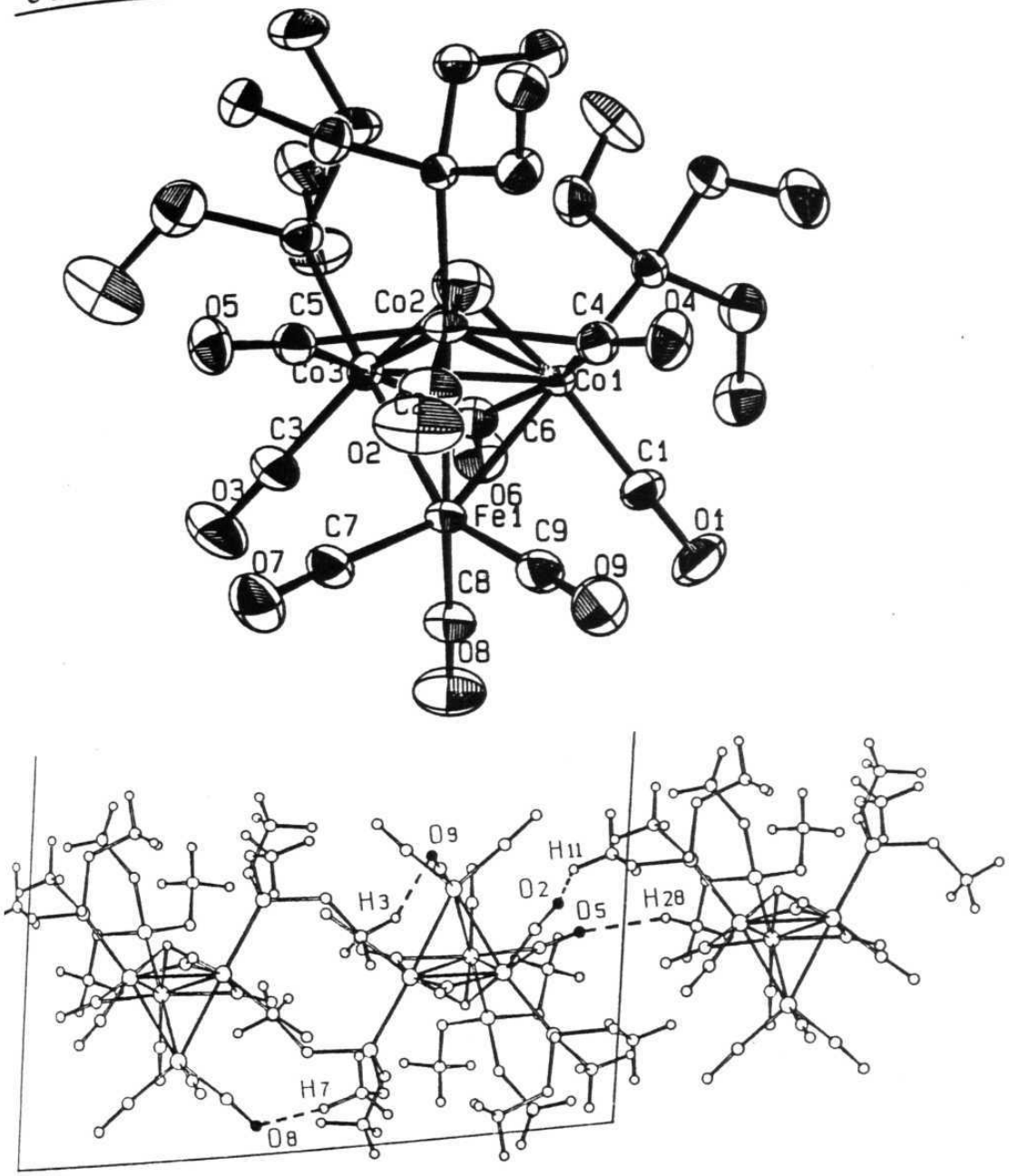

Figure 15. (a) ORTEP drawing of the neutron determined crystal structure of $(\mu_3\text{-H})FeCo_3(CO)_9(P(OMe)_3)_3$, HMPCIC01. The $P(OMe)_3$ ligands and H-atoms are unlabelled. (b) The intermolecular hydrogen bonding network in crystalline $(\mu_3\text{-H})FeCo_3(CO)_9(P(OMe)_3)_3$, HMPCIC01.

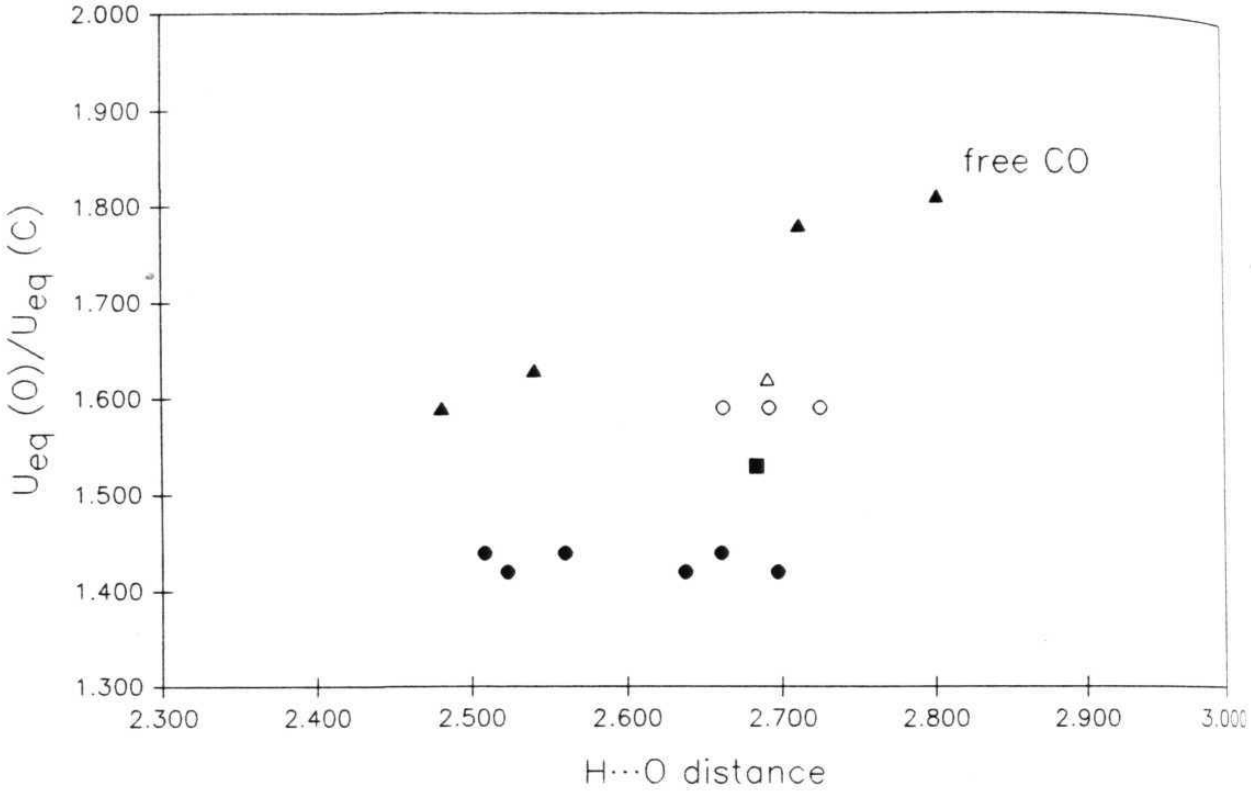

Figure 16. Plot of $U_{eq}(O)/U_{eq}(C)$ or U-ratio, *versus* H···O distance for the C-H···O hydrogen bonds in crystalline $(\mu_3$-H)$FeCo_3(CO)_9(P(OMe)_3)_3$, HMPCIC01. (Δ) CO-t (inter) non-bifurcated, (Δ) CO-t(intra), (❍) CO-t single acceptor trifurcated to three CH groups, (■) CO-b(intra), (●) CO-b(inter and intra) bifurcated.

Table 3 gives the values of the $U_{eq}(O)/U_{eq}(C)$ ratio (U-ratio) for the nine CO-ligands in the molecule while Figure 16 is plot of these ratios versus the fourteen H···O distances formed by eight of these ligands. The plot and the Table show that there is a separation between CO-t and CO-b. The CO-b ratios are lower, in the range 1.42 - 1.53 while the CO-t ratios are higher, in the range 1.59 - 1.78. This means that there is lower relative motion of O with respect to C for CO-b as compared to CO-t as might be expected since CO-t protrude more from the surface and have a larger soft bending motion. More interestingly, for the non-bifurcated-acceptor CO-t bonds, there is a very good correlation between the U-ratio and the H···O distance with the non-hydrogen bonded ligand (U-ratio 1.81) also following the same trend. This demonstrates clearly that as the C-H···O bond gets stronger, the O-atom is able to vibrate less. The bifurcated-acceptor CO-t bonds are shifted to longer H···O distances as would be expected and yet the O-atoms are still relatively immobile. All the CO-b bonds are of the bifurcated-acceptor variety (intra and intermolecular), and they follow a trend similar to the bifurcated CO-t case. This exercise, which becomes highly reliable with neutron data, shows that an analysis of ADPs is effective in assessing the bonding character of a C-H···O interaction.[32] In this respect, subtle differences between CO-t and CO-b bonds and between bifurcated and non-bifurcated

bonds are revealed. Significantly, these shades of difference are apparent even for C-H···O hydrogen bonds formed by C(sp^3)-H atoms.

Table 3: U_{eq} (O)/U_{eq} (C) and H····O distances for C-H···O hydrogen bonds in the crystal structure of HMPCIC01.

	H···O (Å)	U_{eq}(O)/U_{eq}(C)
CO-t (Inter)		
C(3)-O(3)···H(14)	2.71	1.78
C(7)-O(7)···H(14)	2.69	1.59
C(7)-O(7)···H(16)	2.72	1.59
C(7)-O(7)···H(23)	2.66	1.59
C(8)-O(8)···H(7)	2.48	1.59
C(9)-O(9)···H(3)	2.54	1.63
CO-b (Inter)		
C(5)-O(5)···H(14)	2.66	1.44
C(5)-O(5)···H(28)	2.56	1.44
C(6)-O(6)···H(2)	2.70	1.42
C(6)-O(6)···H(6)	2.64	1.42
CO-t (Intra)		
C(1)-O(1)···H(2)	2.69	1.62
CO-b (Intra)		
C(4)-O(4)···H(6)	2.68	1.53
C(5)-O(5)···H(13)	2.51	1.44
C(6)-O(6)···H(4)	2.52	1.42

3.3 Conclusions

This work shows the importance of intramolecular and intermolecular C-H···O hydrogen bonds in the crystal structures of compounds containing metal-coordinated CO-ligands. The results of the analysis can be summarised as follows:

i) Metal coordinated CO-ligands take part in the formation of clearly recognisable hydrogen bonds with the C-H groups of ligands.

ii) Bridging COs establish preferential interactions with respect to the terminal bonding mode and on average these H-bonds are shorter and more linear. Both bridging and terminal COs seem to favour C-H···O bond formation with CO···H angles around 140^{o} suggesting similar lone pair directionality in the two cases.

iii) From the examination of individual crystal structures it is understood that the CO ligands accept more than one C-H group to form bifurcated and trifucated hydrogen bonds. It is also observed that CO-t and CO-b form centrosymmetric dimers of the type III and IV respectively. It is possible that one could use these C-H···O hydrogen bonded patterns as supramolecular synthons in crystal engineering studies.

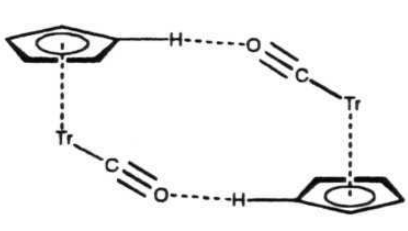

III

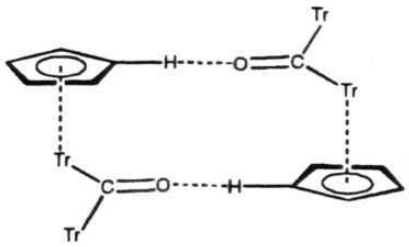

IV

iv) Triply bridging CO-ligands also form C-H···O hydrogen bonds.

v) The effects of different metal atoms or of the nuclearity of the complex on C-H···O hydrogen bonding is not observed.

vi) The effectiveness of these C-H···O hydrogen bonds in the crystal structure is also reflected in a reduction of the thermal motion of the atoms involved in the C-H···O hydrogen bond.

vii) The C-H···O hydrogen bond is an example of a soft intermolecular interaction.

3.4 Experimental Section

Cambridge Structural Database (CSD) Analysis: Data were retrieved from the 1993 update of Version 5.05 of the CSD (109816 entries) for all the ordered crystal structures with an exact match between chemical and crystallographic connectivity and containing at least one of the first row transition metal atoms (Sc-Zn). Polymeric and charged species were excluded. No R-factor restriction was employed because the structures were found to be of good accuracy with R-factors very rarely in excess of 0.10. Geometrical calculations were performed on the retrieved data for intramolecular and intermolecular C-H···O interactions separately for each metal atom using QUEST3D-GSTAT, an automatic graphics non-bonded search program of the CSD. Duplicate hits (identified by the same REFCODE) were removed manually by eliminating all but the

structure with the lowest R-value in each case. Unique contacts were considered up to an H···O distance of 2.80Å (van der Waals sum). A bonafide C-H···O hydrogen bond was considered to be one where, in addition to this distance stipulation, the C-H···O angle lies in the range 110-180^{o}. C-H bond lengths were normalised to 1.08Å. The queries were constructed such that the O atom of the C-H···O bond belongs to a CO group attached to a metal atom. Calculations were performed separately for the CO-t (C-H···O≡C-M) and CO-b (C-H···O=C<) cases. Geometrical questions constructed for the Mn case are given in the Appendix-A-2 as representative examples. Key examples were then selected from the search outputs and were investigated by computer graphics.[33a] The computer program PLATON[33b] was used to analyse the geometrical features of the hydrogen bonding patterns.

3.5 References

1. (a) D.J. Sutor, *Nature*, 1962, **68**, 195. (b) J. Donohue, in *'Structural Chemistry and Molecular Biology'*, Eds. A. Rich, N. Davidson, W.H. Freeman, San Francisco, 1968, pp 443-465. (c) R.D. Green, 'Hydrogen Bonding by C-H Groups', Wiley, New York, 1974. (d) R. Taylor and O. Kennard, *J. Am. Chem. Soc.*, 1982, **104**, 5063. (e) G.R. Desiraju, *'Crystal Engineering: The Design of Organic Solids'*, Elsevier, Amsterdam, 1989, pp 142-173. (f) G.A. Jeffrey and W. Saenger, *'Hydrogen Bonding in Biological Structures'* Springer-Verlag, Berlin, 1991.

2. (a) G.R. Desiraju, *Acc. Chem. Res.* , 1991, **24**, 290. (b) G.R. Desiraju, *Acc. Chem. Res.*, 1996, **29**, 000 (in press) and references cited therein.

3. (a) C.V.K. Sharma, K. Panneerselvam, T. Pilati and G.R. Desiraju, *J. Chem. Soc., Chem. Commun.*, 1992, 832. (b) K. Biradha, C.V.K. Sharma, K. Panneerselvam, L. Shimoni, H.L. Carrell, D.E. Zacharias and G.R. Desiraju, *J. Chem. Soc., Chem. Commun.*, 1993, 1473. (c) D.S. Reddy, D.C. Craig and G.R. Desiraju, *J. Chem. Soc., Chem. Commun.*, 1994, 1457. (d) V.R. Thalladi, K. Panneerselvam, C.J. Carrell, H.L. Carrell and G.R. Desiraju, *J. Chem. Soc., Chem. Commun.* **1995**, 341.

4. C.V.K. Sharma, K. Panneerselvam, T. Pilati and G.R. Desiraju, *J. Chem. Soc., Perkin Trans. 2,* 1993, 2209.

5. (a) G.R. Desiraju, *J. Chem.Soc., Chem. Commun.,* 1989, 179; (b) G.R. Desiraju, *J. Chem. Soc., Chem. Commun.,* 1990, 454; (c) V.R. Pedireddi and G.R. Desiraju, *J. Chem. Soc., Chem. Commun.,* 1992, 988. (d) R. Taylor and F.H. Allen, in *'Structure Correlation'*, Eds. H.-B. Bürgi and J.D. Dunitz, VCH, Weinheim, 1994, Vol. 1, p 128-130.

6. T. Steiner, *J. Chem. Soc., Chem. Commun.,* 1994, 2341.

7. C.V.K. Sharma and G.R. Desiraju, *J. Chem. Soc., Perkin Trans. 2,* 1994, 2345.

8. F.H. Allen, J.E. Davies, J.J. Galloy, O. Johnson, O. Kennard, C.F. Macrae and D.G. Watson, *J. Che. Inf. Comp. Sci.* 1991, **31**, 204.

9. C.P. Horwitz and D.F. Shriver, *Adv. Organomet. Chem.,* 1984, **23**, 218.

10. (a) D. Braga, F. Grepioni, P. Sabatino and G.R. Desiraju, *Organometallics,* 1994, **13**, 3532. (b) S. Aime, L. Cordero, R. Gobetto, S. Bordoni, L. Busetto, V. Zanotti, V.G. Albano, D. Braga and F. Grepioni, *J. Chem. Soc. Dalton Trans.,* 1992,

2961.(c) D. Braga and F. Grepioni, *J. Chem. Soc., Dalton Trans.*, 1993, 1223. (d) D. Braga, F. Grepioni, E. Parisini, B.F.G. Johnson, M.C. Martin, J.G.M. Nairn, J. Lewis and M. Martinelli, *J. Chem. Soc. Dalton Trans.*, 1993, 1891.

11. G.A. Jeffrey in *'Accurate Molecular Structures'*, Eds., A. Domenicano and I. Hargittai, Oxford University Press, 1992, Oxford, pp 270 - 298.

12. T. Steiner and W. Saenger, *J. Am. Chem. Soc.*, 1992, **114**, 10146.

13. (a) P. Murray-Rust and J.P. Glusker, *J. Am. Chem. Soc.* 1984, **106**, 1018.; (b) J. Kroon, J.A. Kanters, J.G.C.M. van Duijneveldt-van de Rijdt and J. Vliegenhardt, *J. Mol. Str.*, 1975, **24**, 109.

14. T. Steiner, *J. Chem. Soc., Chem. Commun.*, 1994, 101.

15. However, many stable complexes of the early and late transition metals possess fewer electrons than predicted by the EAN rule.

16. (a) M.A. Viswamitra, R. Radhakrishnan, J. Bandekar and G.R. Desiraju, *J. Am. Chem. Soc.*, 1993, **115**, 4868. (b) F.H. Allen, J.A.K. Howard, V.J. Hoy, G.R. Desiraju, D.S. Reddy and C.C. Wilson, *J. Am. Chem. Soc.*, 1996, **118**, 4081.

17. (a) M. Nishio and M. Hirota, *Tetrahedron,* 1989, **45**, 7201. (b) T. Steiner, E.B. Starikov, A.M. Amado and J.J.C. Teixeira-Dias, *J. Chem. Soc., Perkin Trans. 2*, 1995, 1321.

18. M. Iwaoka and S. Tomoda, *J. Am.Chem.Soc.,* 1994, **116**, 4463.

19. U. Koch and P.L.A. Popelier, *J. Phys. Chem.* **1995**, 99, 9747.

20. R.F. Bryan, P.T. Greene, M.J. Newlands and D.S. Field, *J. Chem. Soc. A,* 1970, 3068.

21. (a) R.F. Bryan and P.T. Greene, *J. Chem. Soc. A.,* 1970, 3064; (b) A. Mitschler, B. Rees and M.S. Lehmann, *J. Am. Chem. Soc.,* 1978, **100**, 3390.

22. A.G. Orpen, *J. Chem. Soc., Dalton Trans.,* 1983, 1427.

23. R.D. Adams, D.M. Collins and F.A. Cotton, *J. Am. Chem. Soc.,* 1974, **96**, 749.

24. M.L.N. Marchino, E. Sappa, A.M.M. Lanfredi and A. Tiripicchio, *J. Chem. Soc., Dalton Trans.,* 1984, 1541.

25. M.I. Altbach, F.R. Fronczek and L.G. Butler, *Acta. Crystallogra.,* 1992, **C48**, 644.

26. W.A. Herrmann, J. Rohrmann, E. Herdtweck, C. Hecht, M.L. Ziegler and O. Serhadli, *J. Organomet. Chem.*, 1986, **314**, 295.

27. R.G. Teller, R.D. Wilson, R.K. McMullan, T.F. Koetzle and R. Bau, *J. Am. Chem. Soc.* 1978, **100**, 3073.

28. (a) D. Braga, F. Grepioni, P. Milne and E. Parisini, *J. Amer. Chem. Soc.* 1993, **115**, 5115; (b) D. Braga and F. Grepioni, *Organometallics* 1992, **11**, 1256. (c) D.M.P. Mingos and A.R. Rohl, *Inorg. Chem.*, 1991, **30**, 3769. (d) D.M.P. Mingos, A.R. Rohl and J. Burgess, *J. Chem Soc., Dalton Trans.*, 1993, 423.

29. G.R. Desiraju, J. Bernstein, K.V.R. Kishan and J.A.R.P. Sarma, *Tetrahedron Lett.*, 1989, **30**, 3029.

30. C.W.M. Mak and G.-D. Zhou, *'Crystallography in Modern Chemistry'*, Wiley, 1992, New York, pp 175-181.

31. G.R. Desiraju, S. Kashino, M.M. Coombs and J.P. Glusker, *Acta. Crystalogra.*, 1993, **B49**, 880.

32. This exercise was repeated with ADP values from the X-ray structure (134K) published in B.T. Huie, C.B. Knobler and H.D. Kaesz, *J. Am. Chem. Soc.*, 1978, **100**, 3059. However, the

correlation failed and this could indicate that neutron data are a prerequisite for this sort of subtle analysis.

33. (a) E. Keller, SCHAKAL93, 'Graphical Representation of Molecular Models', University of Freiburg, Germany. (b) A.L. Spek, *Acta Crystallogr.*, 1990, **A46**, C31.

Chapter 4

M-H···O Hydrogen bonds in Organometallics

4.1 Introduction

In organometallic chemistry, the capacity to form hydrogen bonds is not confined to the "traditional" acceptor and donor groups of organic molecules. It has been described in Chapter 1 that the electron rich transition metals can act as proton acceptors to form O-H···M, N-H···M and C-H···M hydrogen bonds. This chapter deals with a problem where the transition metal centres act as proton donors to form M-H···O interactions. H-bonding to metal can be viewed as an "arrested protonation", similar to the arrested oxidative addition found in non-classical dihydrogen compounds.[1] In Chapter 3 it has been shown that C-H groups actively participate in C-H···O hydrogen bonds with CO-ligands. It is known that both the M-H and C-H groups are of low polarity and can react as H^+, H· or H^- donors. Therefore M-H···O hydrogen bonds that are similar to C-H···O hydrogen bonds might be anticipated.

The hydrogen atom can bind to mono- and poly-nuclear metal complexes in terminal or bridging fashions. Bridging hydrides can span a metal-metal bond (μ_2-bonding mode) or cap a triangulated metal face of a higher nuclearity cluster (μ_3-bonding mode). These principal bonding modes are shown in Scheme-1. The terminal bonding mode occurs in mononuclear complexes and only rarely in polynuclear complexes (metal clusters). The bridging mode predominates in polynuclear complexes.

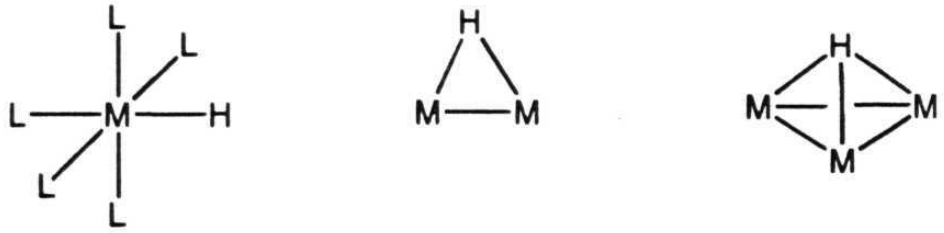

Scheme-1: Hydride ligand bonding modes

As described in Chapter 1, there is accumulated evidence that electron rich metal atoms can act as acceptors towards proton donors.[2] However, direct involvement of a metal bound "hydride" ligand in intermolecular interactions with the CO ligand has been reported only in very few cases such as $(\mu_2\text{-H})Fe_4(\mu\text{-}\eta^2\text{-CH})(CO)_{11}L$(L=CO,[3a,b] PPh_3[3c]), $[(C_5H_5)_2Mo(H)CO]$ $[(C_5H_5)Mo(CO)_3]$.[4] Recently a W-H···O intramolecular hydrogen bond has been found in the crystal structure of $WH_3(\eta^1\text{-OCOME})(Ph_2PCH_2CH_2PPh_2)_2$.[5]

In general, the ability of a group to participate in any specific intra- or intermolecular hydrogen bond depends on the interplay of steric and electronic factors. The crucial role of these factors in hydrogen bond formation has been demonstrated in the case of the C-H group.[6] For the M-H group, the steric factors arise from the distribution of the ligands around the metal bound hydrogen atoms and also from the extent that these H-atoms are screened from the surrounding molecules. The electronic factors depend on the number and type of other ligands, oxidation state of the metal(s) and nuclearity of the complex. Studies on the Brønsted acidity of transition metal hydride suggest that there is a

trend of increasing acidity on going from left to right along the periods.[7,8] For example, $HCo(CO)_4$ behaves as a strong acid. The acidity of the metal hydride also depends on the hardness and softness of other ligands attached to it. Soft, electron delocalising ligands attached to the metal atom weaken the M-H bond and increase the Brϕnsted acidity. Hard ligands increase the hydridic nature of the bond.

4.2 Results and Discussion

In the hydrogen bonding studies (Chapters 2 and 3), the inaccurate determination of hydrogen atom position in X-ray studies has been tackled by normalising X-H distances to neutron derived values. However, this is not possible with metal hydrides where the M-H geometry is much more variable depending on the shape, size and mode of coordination of the other ligands in the molecule. In many of these complexes, and especially in the most polynuclear systems, the location of hydrogen atom is not even attempted. These positions are calculated either on the basis of the geometry of the surrounding ligands of the hydride ligand or on the basis of atom-atom potential energy minimisation procedures. In the present study the H-atom positions are considered as given in the CSD. However, it was observed that most of the M-H distances of X-ray data are consistent with those of neutron data. Further, the results obtained are also in agreement with those obtained spectroscopically.

The CSD search yielded 962 metal carbonyl hydride structures determined by neutron and X-ray diffraction. In 204 cases, M-H···O intermolecular interactions shorter than 3.2 Å were observed. Compounds having interactions shorter than 2.8 Å are listed in Table 1 together with the relevant geometrical information.

From the analysis of Table 1, the following general considerations can be made:

i) Although most structures are based on X-ray data, the M-H distances fall within a rather narrow range and are consistent with the available neutron structures.

ii) All the complexes in Table 1 are μ_2-bridged hydride ligand complexes with the exception of $[Cp_2Mo(H)CO][CpMo(CO)_3]$ (CPCBMO) where the hydride ligand is attached in terminal fashion.

iii) The M-H···O distances can be as short as 2.446 Å in $(\mu\text{-}H)_3Os_3Ni(CO)_9Cp$ (BOBTAN10) and 2.507 Å in $Os_4(CO)_{13}(\mu\text{-}SCH_2CMe_2CH_2Cl(\mu\text{-}H)$ (VUPPAX) and appear to be comparable in length with the interactions established by C-H groups and CO ligands (Table 1) which are described in previous chapter.

iv) The complexes $(\mu\text{-}H)(\mu\text{-}NCHCF_3)Os_3(CO)_{10}$ (BAJXIT) and $(\mu\text{-}H)Os_3(CO)_9$ (MeCCHCMe) (DEVZEP) allow one to compare the M-H···O and C-H···O interactions.

v) The average M-H···OC angle is 133.6^{o} and is in agreement with the angularity observed in Chapter 3 for C-H···OC interactions.

vi) H-atoms spanning M-C (agostic systems, Chapter 5) or M-B bonds also participate in short intermolecular H···O interactions as shown by the three examples selected from Table 1.

4.2.1 Selected examples of intermolecular M-H···O bonds

In this section, the M-H···O hydrogen bonding networks for some of the complexes reported in Table 1 will be discussed. When present, C-H···O hydrogen bonds will also be shown and compared with M-H···O hydrogen bonds. Some examples of the complexes which do not form M-H···O hydrogen bonds were also examined to demonstrate that steric hindrance is most often responsible for the absence of the M-H···O interactions.

The structure of $(\mu\text{-H})(\mu\text{-NCHCF}_3)\text{Os}_3(\text{CO})_{10}$ (BAJXIT) has been determined by neutron diffraction.[9] As shown in Figure 1, the M-H···O interactions connect the molecules along a row via a direct interaction between the edge bridging hydride and a terminally bound CO while the C-H···O hydrogen bonds interconnect these rows through centrosymmetric dimers. It is important to stress that the two types of interactions are of comparable length (hence, presumably, strength) and both involve the same type of base, namely terminally bound CO ligand.

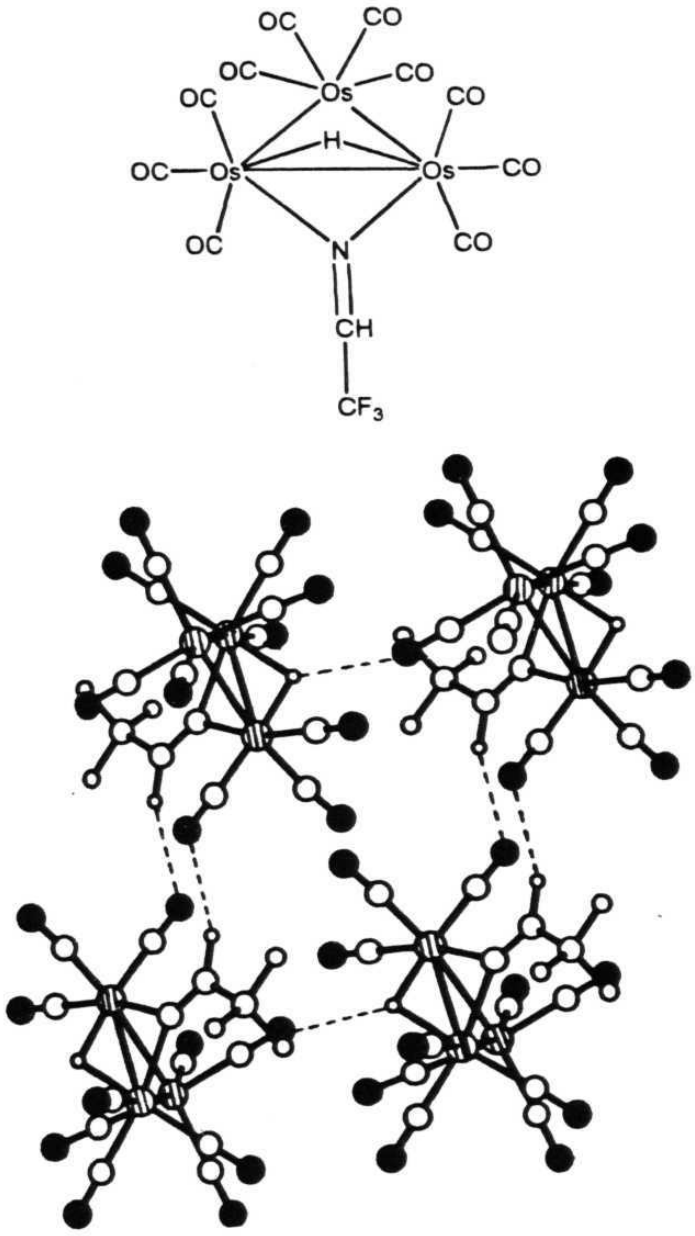

Figure 1. Crystalline $(\mu\text{-H})(\mu\text{-NCHCF}_3)\text{Os}_3(\text{CO})_{10}$ (BAJXIT). Each cluster molecule participate in hydrogen bonds of the M-H···O and C-H···O types of comparable length (Os-H11···O21 2.594 Å, H1···O31 2.571 Å). Note that the hydride-CO interactions forms molecular rows whereas the C-H···O bonds form rings between molecules related by a centre of symmetry. O=●, Os=○

Table 1: Compound REFCODES and relevant geometrical parameters for M-H···O and C-H···O interactions with M-H···O distance < 2.8 Å.

REFCODE	Diffraction method	T(K)	M-H (Å)	M-H···O (Å)	H···O-C (°)	C-H···O (Å)
BAJXIT	Neutron	20	1.837	2.594	136.4	2.571
BOBTAN10	X-ray	296	1.972	2.446	141.0	2.613
BOXGUQ	X-ray	298	1.798	2.616	113.1	2.316 (intra)
BUWGEF10	X-ray	297	1.798	2.576	117.5	
CPCBMO	X-ray	148	1.798	2.511	131.0	2.225 2.554 2.386 2.379 2.509
DEVPEZ	X-ray	298	1.861	2.556	166.7	2.637
HANTIZ	X-ray	298	1.825	2.637	112.8	2.426
HMYCFE01	Neutron	26	1.670 1.754 1.717	2.660 2.700	138.0 125.9 138.0 125.9	2.576[b] 2.482[b]
HMYCFE	X-ray	173		2.680 2.702	170 143	2.718[b] 2.739[b]
KIWVOB	X-ray	298	1.9 8	2.587 2.582 intra	156.48	
KIWVUH	X-ray	298	1.7 3	2.636	140.90	
VESGAB	X-ray	296	2.163	2.601	121.39	2.599
VUPPAX	X-ray	298	1.9 3	2.507	163.53	2.354
DEXCUE	X-ray	298	1.856	2.635	130.1	2.548 2.588
JEMDEK	X-ray	298	1.846	2.621[c]	125.3	
SOBTEI	X-ray	123	1.623	2.884[c]	118.3	

(a) C-H···O distances based on normalised C-H distances, (b) Intermolecular M-H···O interactions involving metal bound hydrogen atoms participating in agostic interactions, (c) Intermolecular M-H···O interactions involving hydrogen atoms spanning B-M bonds.

Similarly in the crystal structure of $(\mu\text{-H})_3Os_3Ni(CO)_9C_I$ (BOBTAN10), both M-H···O and C-H···O hydrogen bonds are present.[1] Figure 2a and 2b show two projections of the molecular arrangements i the crystals. The M-H···O hydrogen bonds (H11···O22 2.446 Å) join th molecules in chain-like fashion (Figure 2a) while a C-H group belonging t a Cp ring and a terminally bound CO (2.434 Å) form a centrosymmetri dimers (Figure 2b). The C-H···O interactions connect rows of molecul linked by the H(hydride)···O bonds in a crystal.

Centrosymmetric dimers via M-H···O hydrogen bonds which ar formed in between terminal CO and bridging H-ligand are found in th crystal structure (Figure 3) of $(\mu\text{-H})Os_3(CO)_{10}(\mu_3\text{-CH})$ (BOXGUQ)[11] Similar centrosymmetric dimers are also observed in the crystal structur of [CpMo(H)CO] [CpMo(CO)] (CPCBMO)[4], but these M-H···C hydrogen bonds are formed between terminal H-ligands and terminal CO ligands (Figure 4). CPCBMO contains two ionic derivatives o molybdenum, one is the cationic species, bearing the ligand, and the othe anionic. Further, this structure also contains a diffuse network of C-H···O shown in detail in Table 1. The M-H···O dimer **I** observed in thes structures is almost similar to that of O-H...O dimer **II** in carboxylic acids.

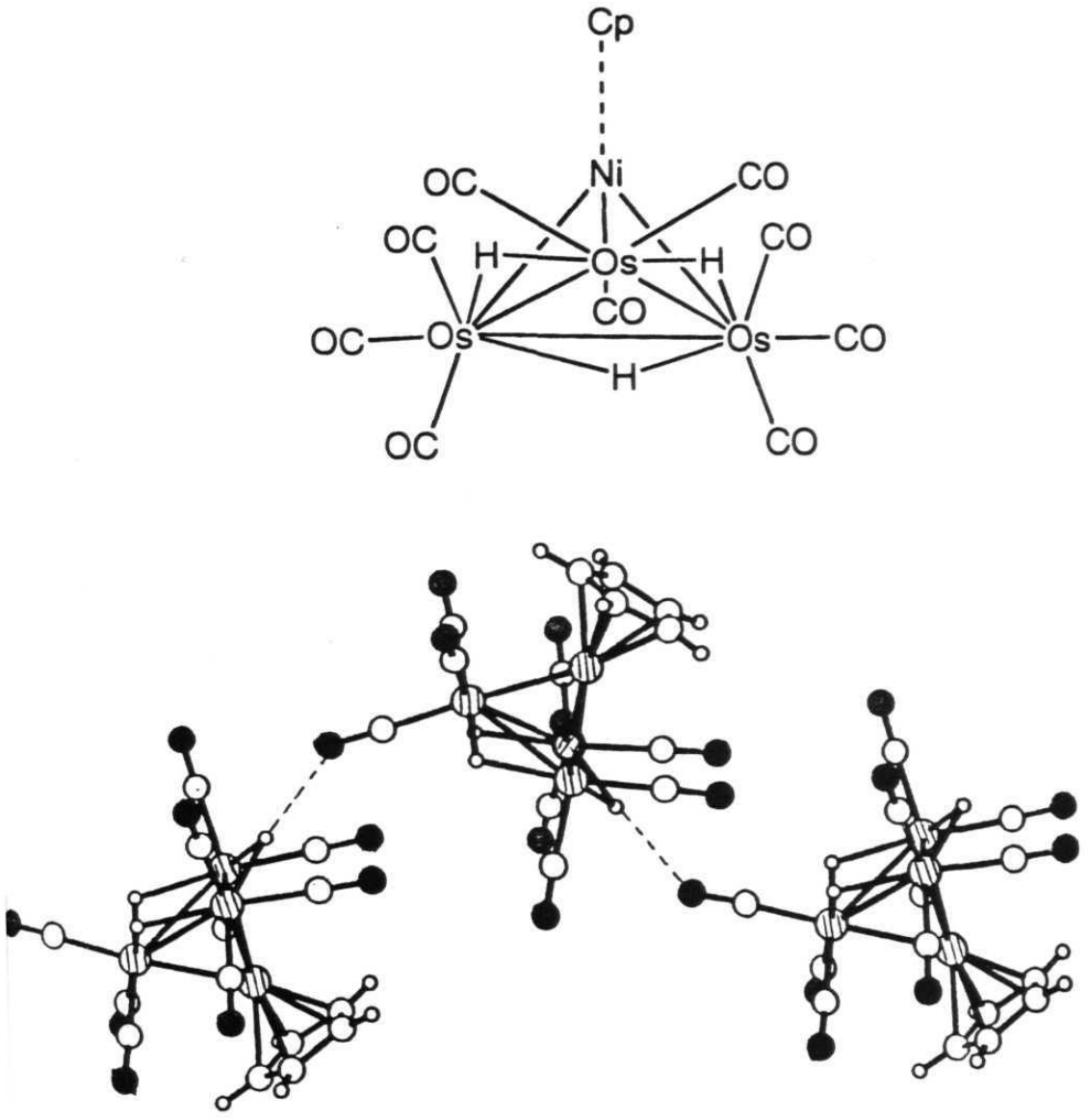

Figure 2a. Molecular rows in crystalline $(\mu\text{-H})_3Os_3Ni(CO)_9Cp$ (BOBTAN10). M-H···O hydrogen bonds are formed between terminally CO ligands and bridging H ligands. O=●, Os,Ni=◐

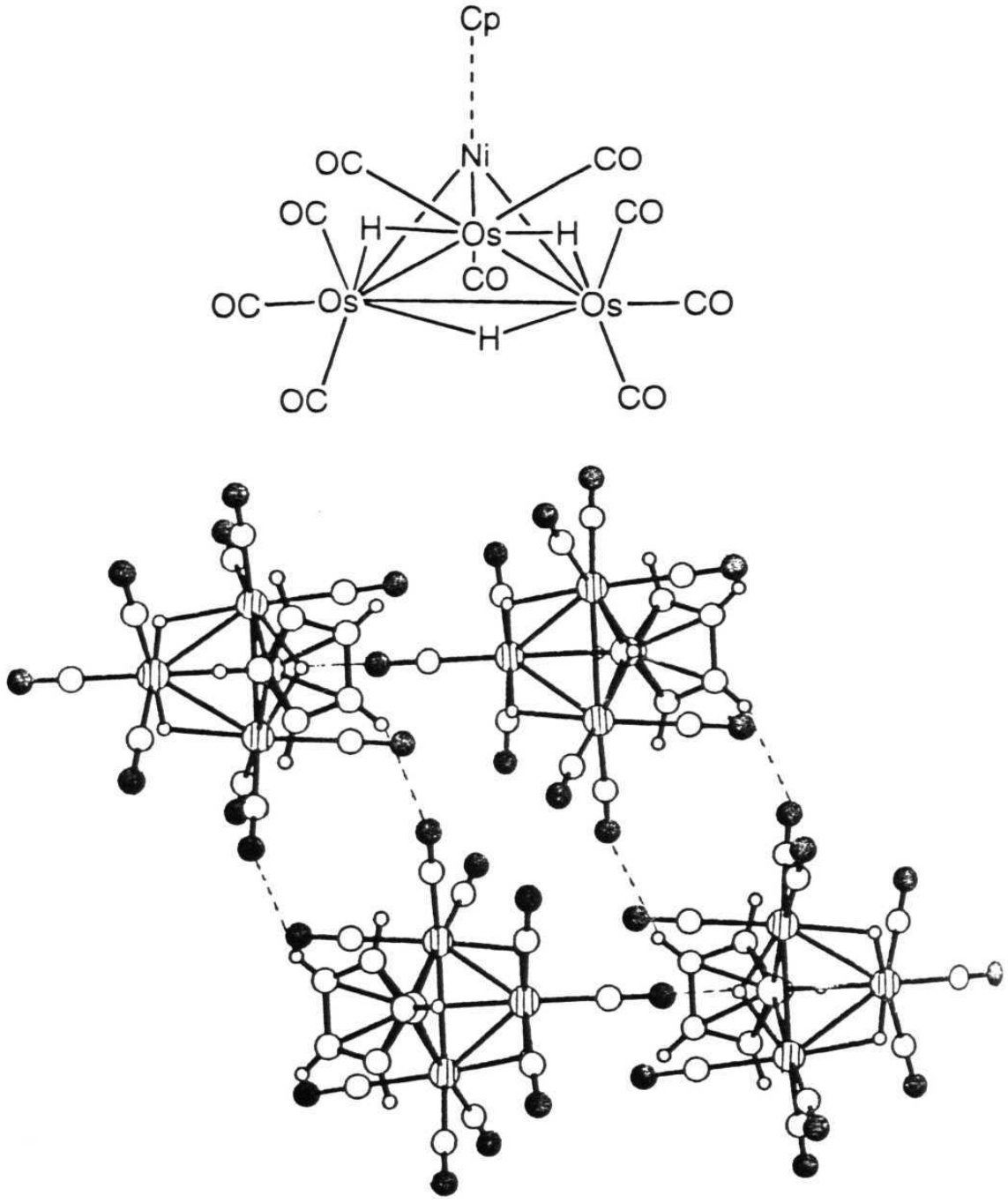

Figure 2b. Centrosymmetric dimers of C-H···O hydrogen bonds (BOBTAN10) between CO ligands and H atoms of the Cp rings. Note how the C-H···O hydrogen bonds joining the molecular rows formed by M-H···O bonds. O=●, Os,Ni=❶

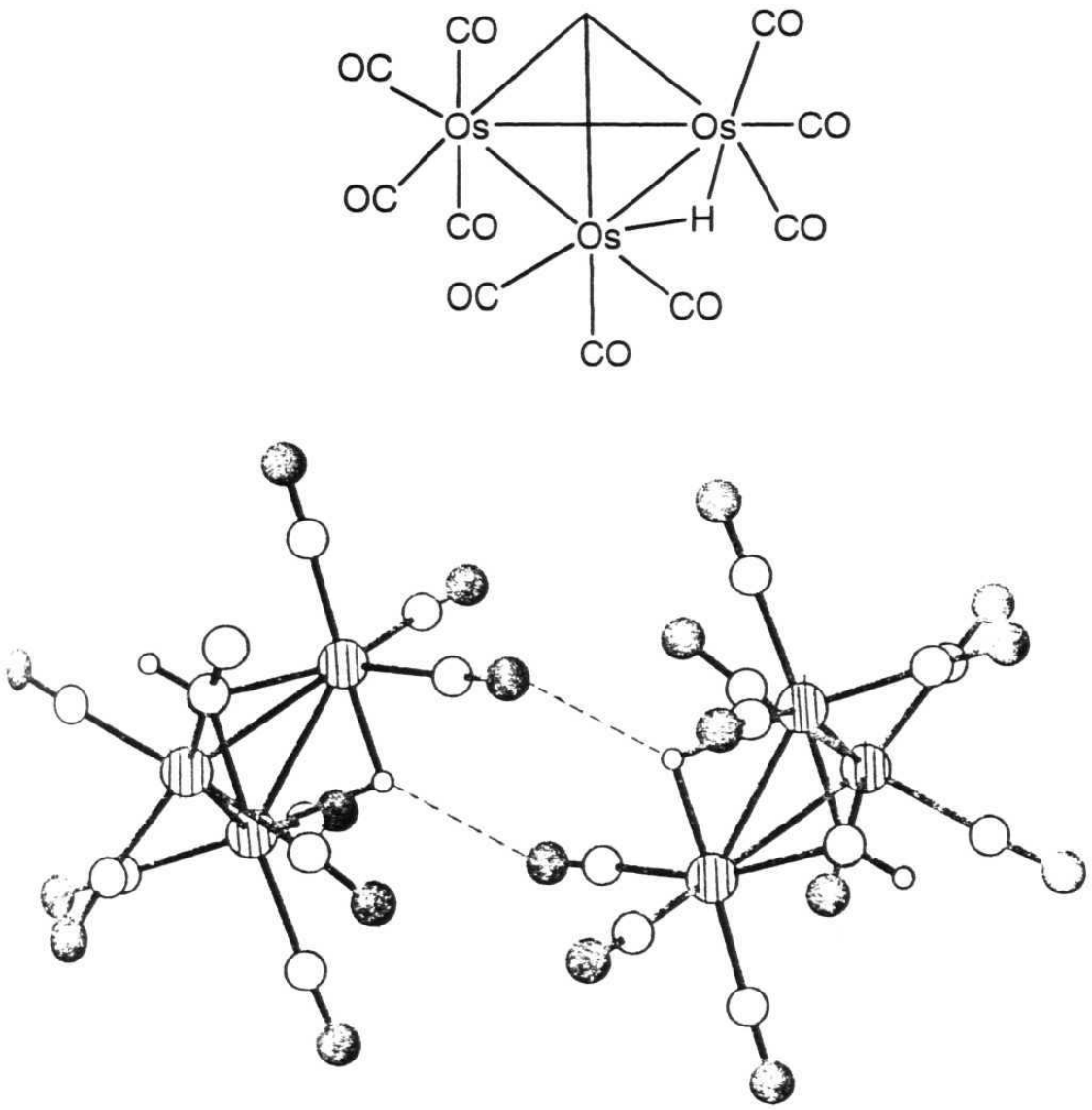

Figure 3. Centrosymmetric rings are formed by CO and bridging hydride ligands in crystalline $(\mu\text{-H})Os_3(CO)_{10}(\mu_3\text{-CH})$, (BOXGUQ). O=●,Os=◑

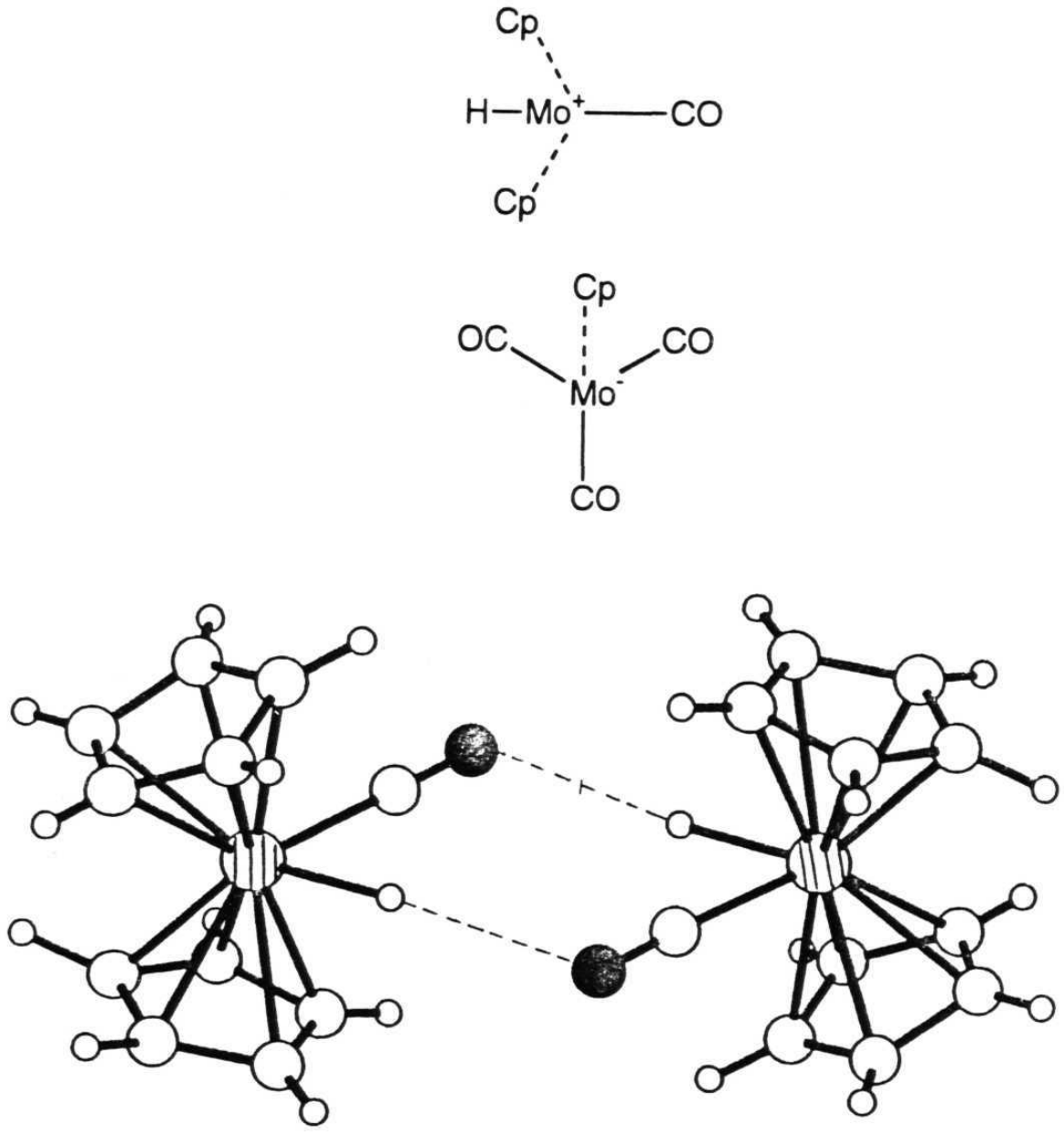

Figure 4. Centrosymmetric dimers in the crystal structure of $[Cp_2Mo(H)CO]$ $[CpMo(CO)_3]$ (CPCBMO). Notice that the M-H···O interaction is formed between the terminal H-ligand and the terminal CO-ligand. The $CpMO(CO)_3$ species omitted for clarity. O=●, Mo=❍

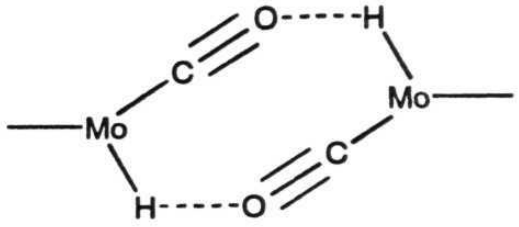

I

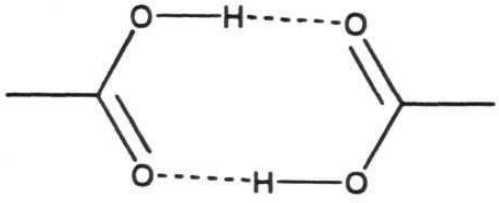

II

The trinuclear cluster $(\mu\text{-H})_2Os_3(CO)_9(\mu_3\text{-COO})$, (BUWGEF10)[12] is disordered in the solid state. The asymmetric unit in the crystal contains two half molecules. One molecule is ordered and the hydride positions are well located, whereas the hydride positions are disordered in the second molecule. In order to model this disorder on the basis of the metal cluster geometry following the discussion on the Os-Os bond length distribution in the original paper, the disordered crystal packing is considered as the average of two alternative ordered models. In both models only the hydrides ligands belonging to the ordered cluster appear to be involved in hydrogen bond interactions whereas the second independent molecule is not. This indicates that the hydride position of one molecule is disordered due to its dynamic nature while in the ordered molecule the hydrides are frozen out in one fixed conformation because of the additional constraints arising from the intermolecular interactions.

The crystal packing and intermolecular H(hydride) bonds present in crystalline $(\mu\text{-H})Os_3(CO)_9(MeCCHCMe)$, (DEVPEZ)[13] are shown in

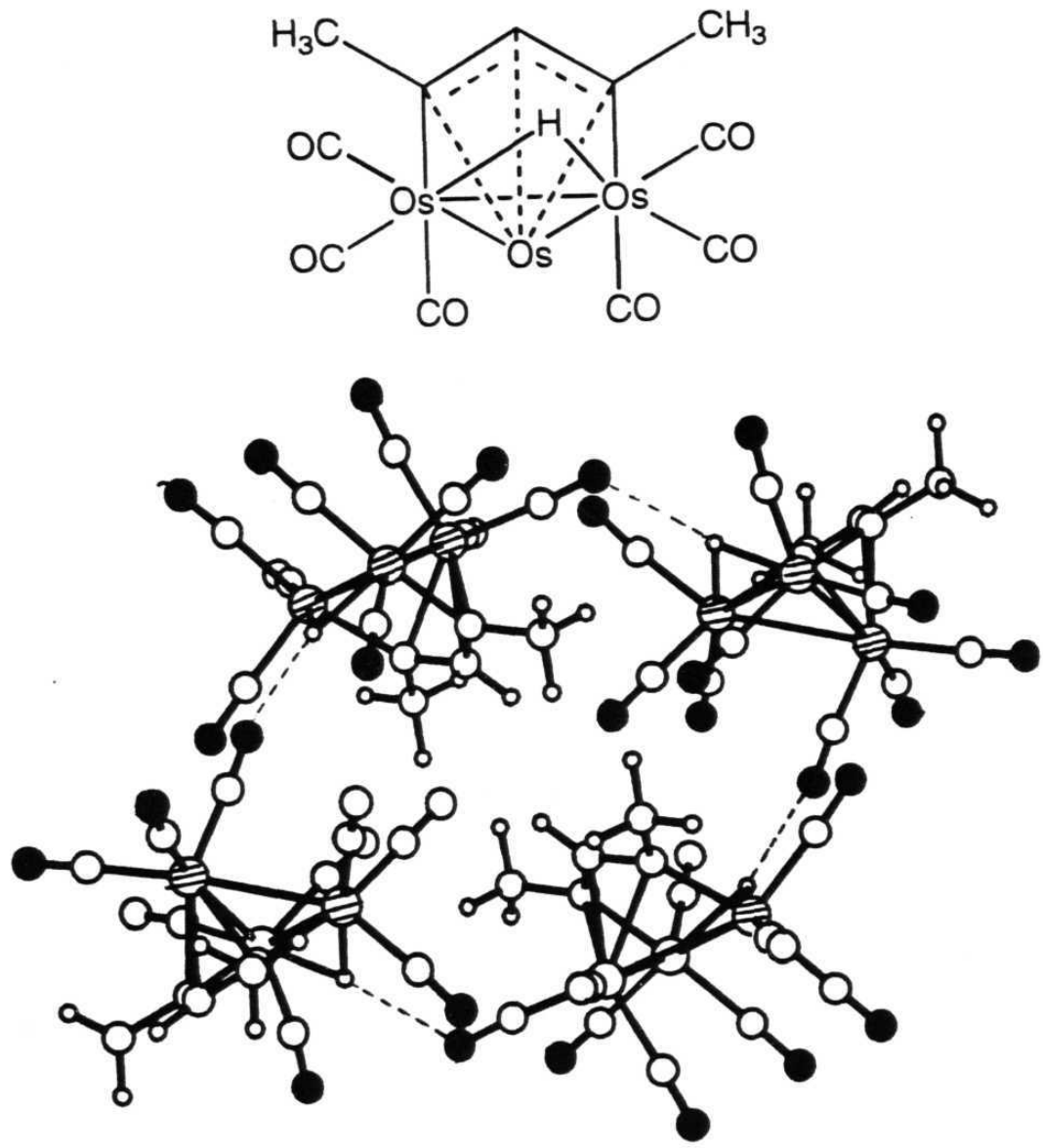

Figure 5. The tetramolecular systems formed by via Os-H···O interactions in crystalline (μ-H)$Os_3(CO)_9$(MeCCHCMe), (DEVPEZ). O=●, Os=❶

Figure 5. The bridging hydride ligand interacts with a terminal CO of a neighbouring molecule forming tetramolecular systems (H···O2 2.556 A).

As observed above for BOBTAN10 and BOXUGQ, two different types of interactions are present in crystalline (μ-H)$Os_3(CO)_{10}(CNPr)(OCOCF_3)$, (HANTIZ)[14] (see Table 1). The first interaction is between the unique H(hydride) and a CO ligand, while the second interaction is formed between H of the CNPr ligand and an oxygen of the carboxylic ligand of the other molecule (in fact the M-H···O distance, H1···O31 2.637 is longer than the carboxylic one, H2-O12 2.426)

The crystal structures of $(\mu\text{-H})_8Pt_2Os_7(CO)_{23}$ (KIWVOB)[15a] and $(\mu\text{-H})_8PtOs_6(CO)_{18}$ (KIWVUH)[15b] have been determined in the same study and short M-H···O interactions (2.636 and 2.587 Å respectively) are present in both the crystals. However in crystalline KIWVOB, there is simultaneous presence of both intramolecular and intermolecular M-H···O interactions (see Figure 6). In both cases terminal CO ligands are involved and the M-H···O distances have comparable length (2.587 and 2.582 Å).

The pattern of intermolecular hydrogen bonds in crystalline $Os_4(CO)_{13}(\mu\text{-}SCH_2CMe_2CH_2Cl)(\mu\text{-H})$ (VUPPAX)[16] recalls that formed by typical organic acids (see Figure 7). Two molecules form a centrosymmetric dimer and are connected by two M-H···O interactions.

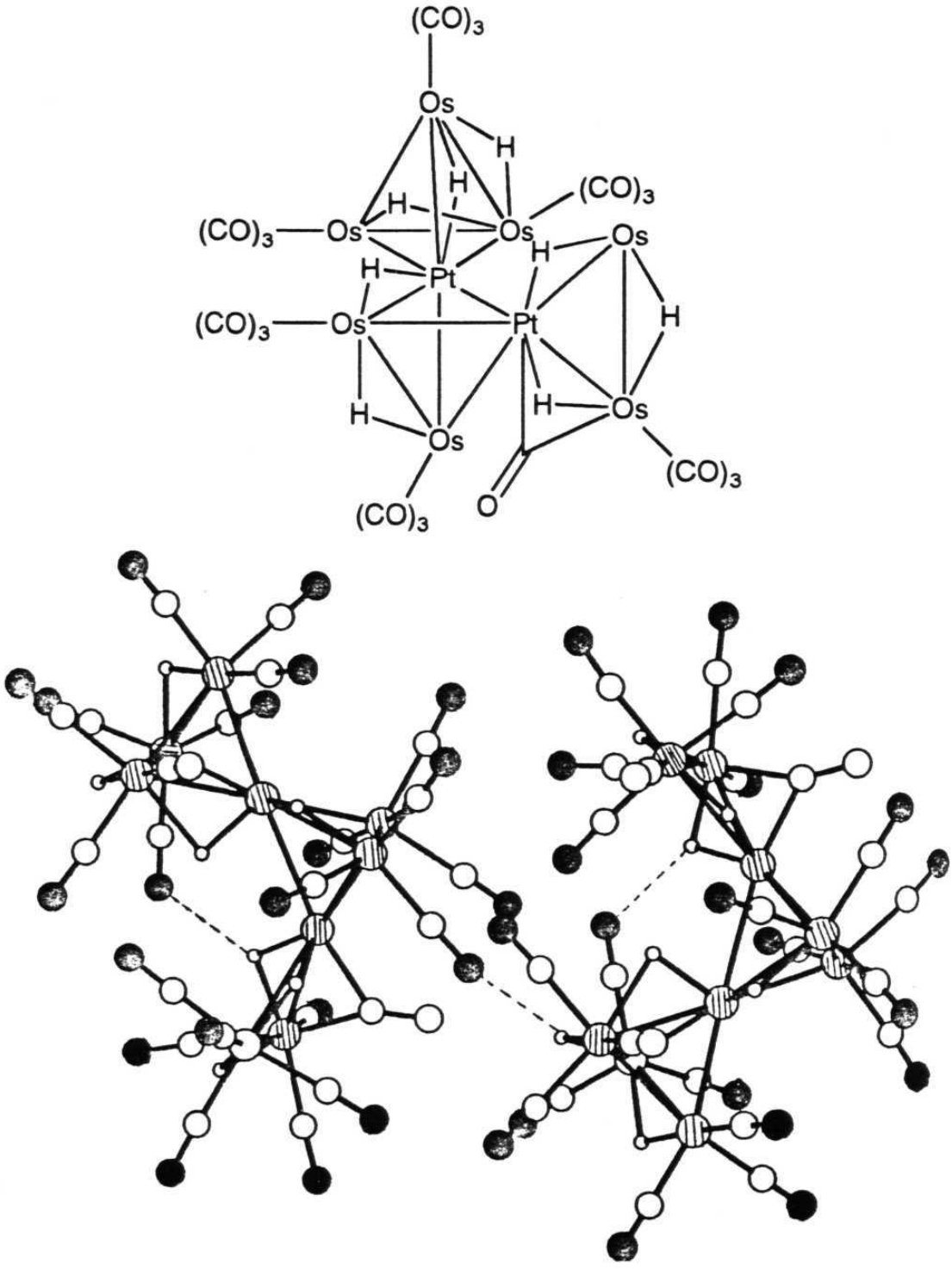

Figure 6. The intramolecular and intermolecular M-H···O interactions present in crystalline $(\mu\text{-H})_8Pt_2Os_7(CO)_{23}$ (KIWVOB). O=●, Os=○

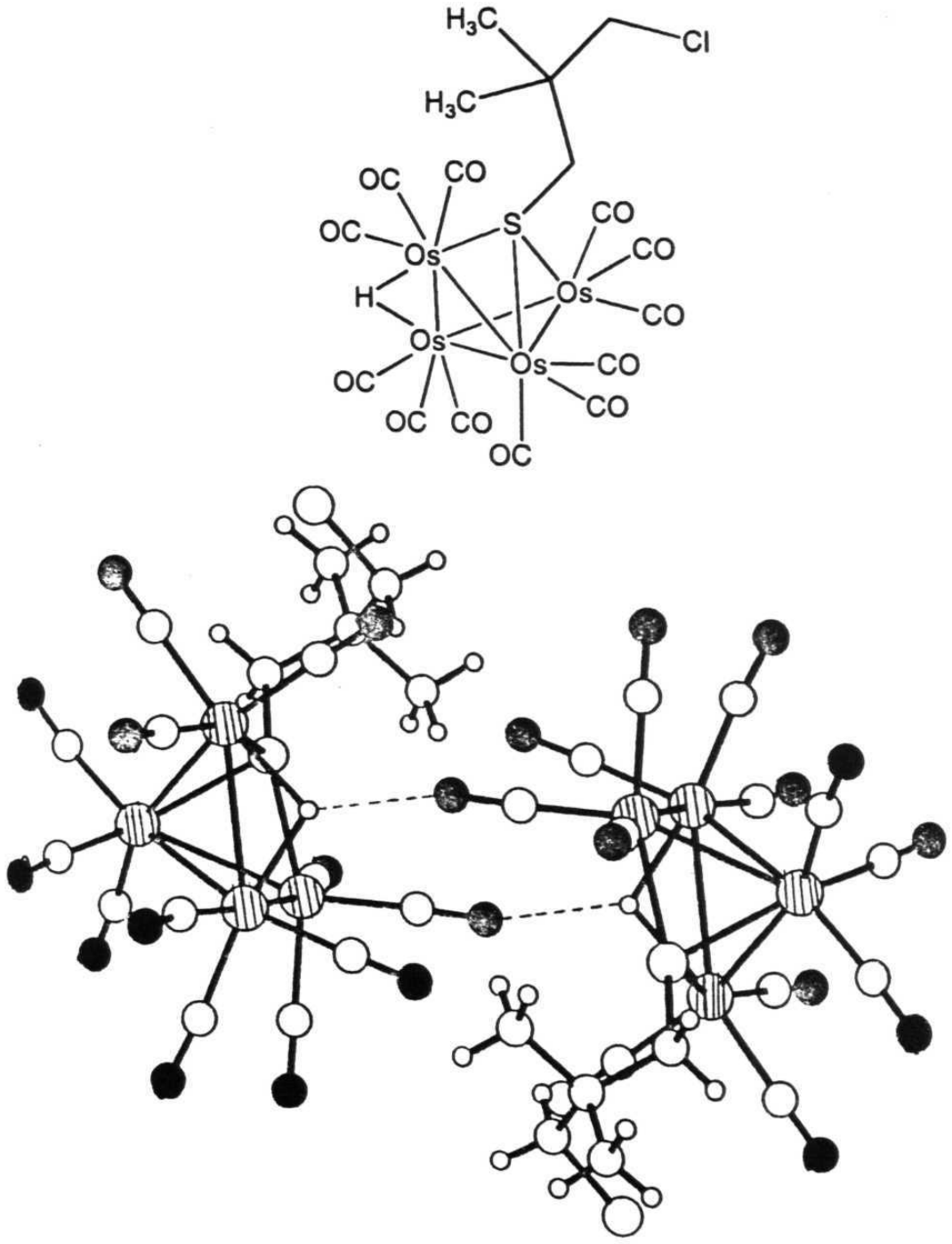

Figure 7. The cyclic dimer in crystalline $(\mu\text{-H})Os_4(CO)_{13}(\mu\text{-}SCH_2CMe_2CH_2Cl)$ (VUPPAX). Geometrical parameters H1···O10 2.507

A . O=● Os=O

The length and directionality of these interactions is strictly comparable to those observed in many crystals of carbonyl complexes where similar dimers are formed between hydrogen atoms of cyclopentadienyl rings and CO ligands.

Intermolecular M-H···O interactions are established also by metal bound hydrogen atoms participating in agostic interactions. However, the electronic nature of the M-H interaction in agostic M···H-C and in hydride M-H systems is fundamentally different. Nonetheless, it is found that in some of the hydride ligands, some agostic hydrogen atoms, when not sterically screened from the surroundings by other ligands can form intermolecular hydrogen bonds with CO bases. The H···O separations are comparable to those of the most acidic C-H···O and to some M-H···O interactions. For example, in the mononuclear complex $Cr(CO)_2(PMe_3)(\eta^4\text{-}C_7H_{10})$ DEXCUE[17] where the agostic hydrogen participates in an interaction with a neighbouring CO (2.635 Å), two shorter C-H···O interactions are also present within the same crystal (2.548 and 2.588 Å). HMYCFE01[18] is an another example in which M-H···O hydrogen bonds are formed by the agostic hydrogen. Intermolecular M-H···O interactions involving hydrogen atoms spanning B-M bonds are observed in crystalline $WRh_2Au_2(\mu_3\text{-}CC_6H_4Me_4)(CO)_6(\eta^5\text{-}C_5H_5)(\eta\text{-}C_2B_9H_9Me_2)_2$ (JEMDEK)[19] and $(\mu\text{-}H)_6H_2B_4Fe_4(CO)_{12}$ (SOBTEI).[20]

4.2.1.1 Sterically hindered hydride complexes:

Some examples of the hydride complexes that do not form intermolecular M-H···O hydrogen bonds will be discussed. This discussion relates to the connection between steric problems and the formation of hydrogen bonds between hydride ligands and acceptors. It is known that the hydride atom in polynuclear metal complexes is acidic. However, in these polynuclear metal complexes the hydride ligands are, in most cases, embedded in the ligand envelope close to the metal atoms. Even though the carbon monoxide acceptor group protrudes from the cluster surface, the metal bound hydrogen atoms are generally not available for a close approach by these ligands.

One of the prototypical polyhydride clusters is $H_4Ru_4(CO)_{12}$ (FOKPAW).[21] This ruthenium cluster has been extensively studied and is known to have four long and two short Ru-Ru edges, the four long edges being very likely spanned by the H-bridges. A 3% disorder in the orientation of the cluster was also detected. A recent spectroscopic study of solid $H_4Ru_4(CO)_{12}$ has shown that the ^{13}C-$\{^1H\}$ CP MAS, ^1H-MAS and ^1H wide-line spectral features can be interpreted in terms of a dynamic process involving either the motion of H_4Ru_4 as a whole or the motions of the hydrides over the metal cluster. The calculated H···O distances between hydride ligands, placed in calculated positions along bridging sites by XHYDEX,[22] and next neighbouring COs falls in the range 2.787-2.775

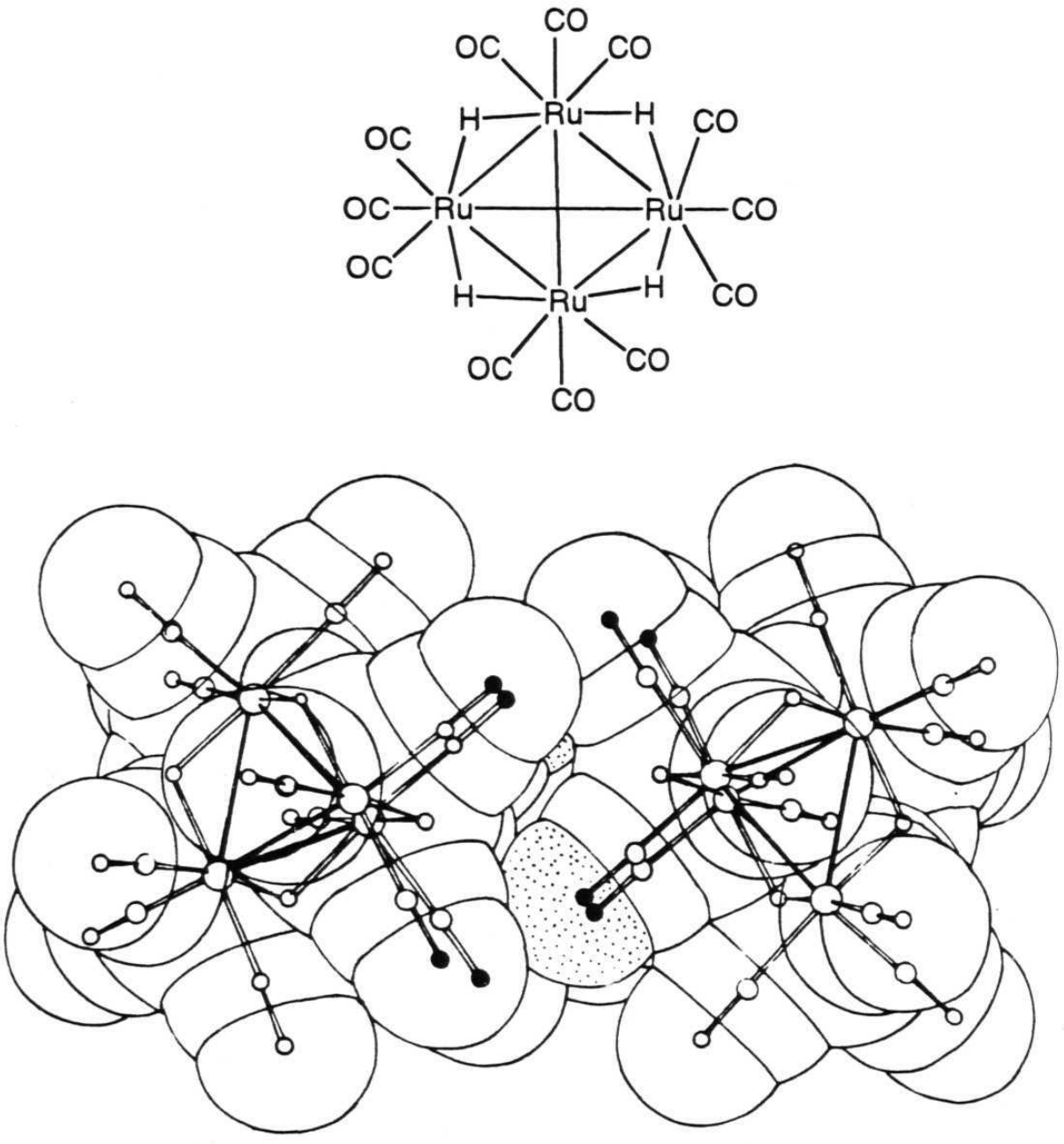

Figure 8. Space filling representation of two first neighbouring $H_4Ru_4(CO)_{12}$ molecules showing how the CO-ligands are interlocked.

Å. These distances are longer than in the cases discussed above where the hydrogen atoms could be located directly. One may think that dynamic behaviour detected by NMR arises from the lack of intermolecular stabilisation of the bridging sites due to the difficult intermolecular interpenetration of molecules carrying twelve terminal COs beside the hydride ligands. Figure 8 shows a space filling representation of two-interlocking $H_4Ru_4(CO)_{12}$ molecules with the modeled hydride atom positions. The other three sites have similar interactions with neighbouring molecules. All intermolecular C···C, C···O, and O···O interactions between first neighbours pairs of atoms belonging to the two molecules correspond to "normal" van der Waals contacts, that is to say that a decrease in the Ru-H···O distances would lead to tighter intermolecular interpenetration and of atom-atom repulsions among the outer atoms.

Another example of hydride ligand encapsulation is shown in Figure 9a wherein the space filling representation of the complex $HW_2(CO)_9(NO)$ (FUZROH)[23] is reported. The hydride ligand is surrounded by three terminal COs, which do not leave enough space for hydrogen bonding with neighbouring molecule via W-H···O interactions (the nearest oxygen atom is at 3.500 Å). A similar situation is seen in $HMn_2(Re)(CO)_{14}$(VITMIU)[24] (see Figure 9b). This mixed cluster has the hydride completely embedded within the CO-ligand envelope.

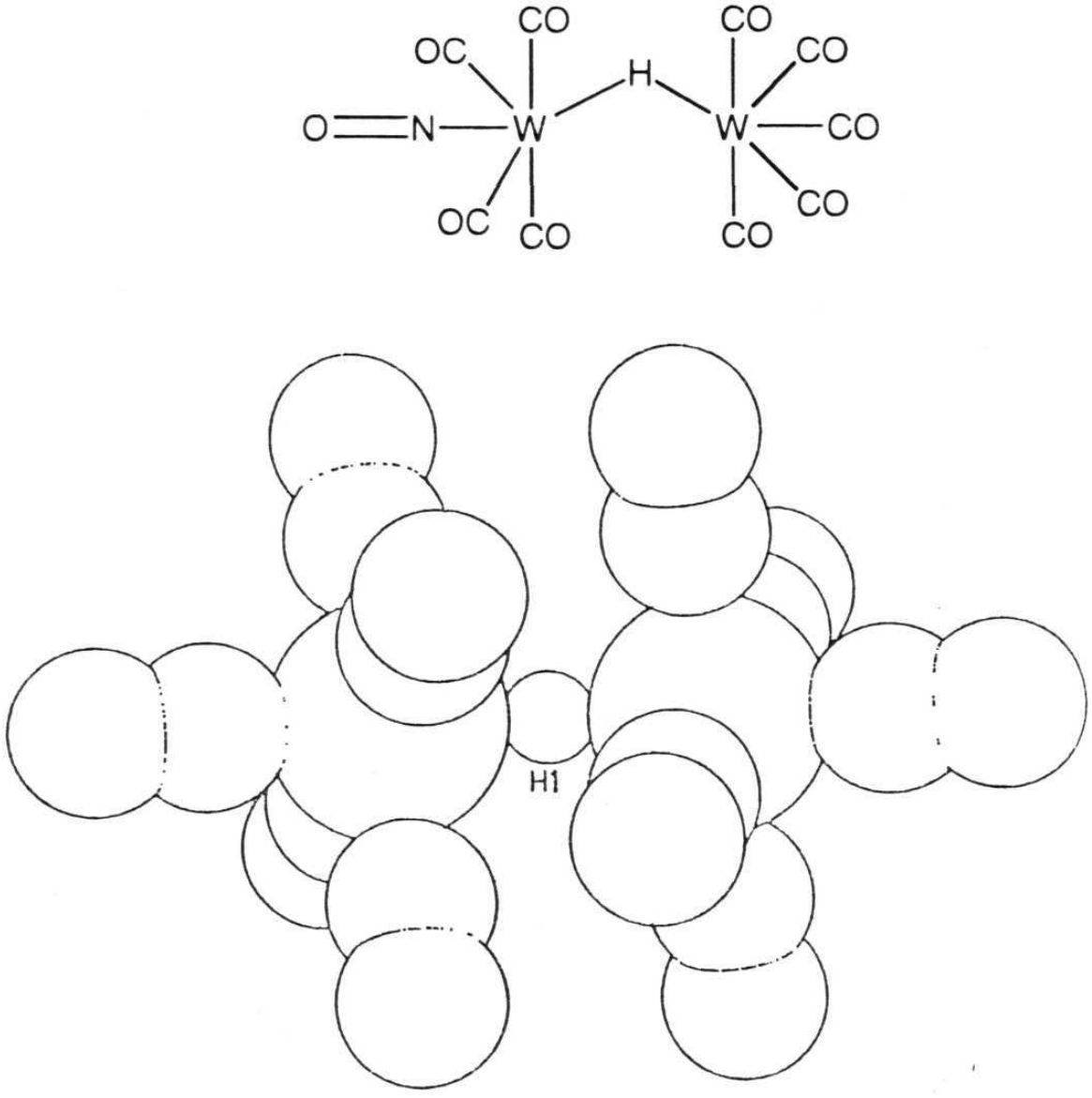

Figure 9a. Space filling representation of the molecular structures of $HW_2(CO)_9(NO)$ (FUZROH)

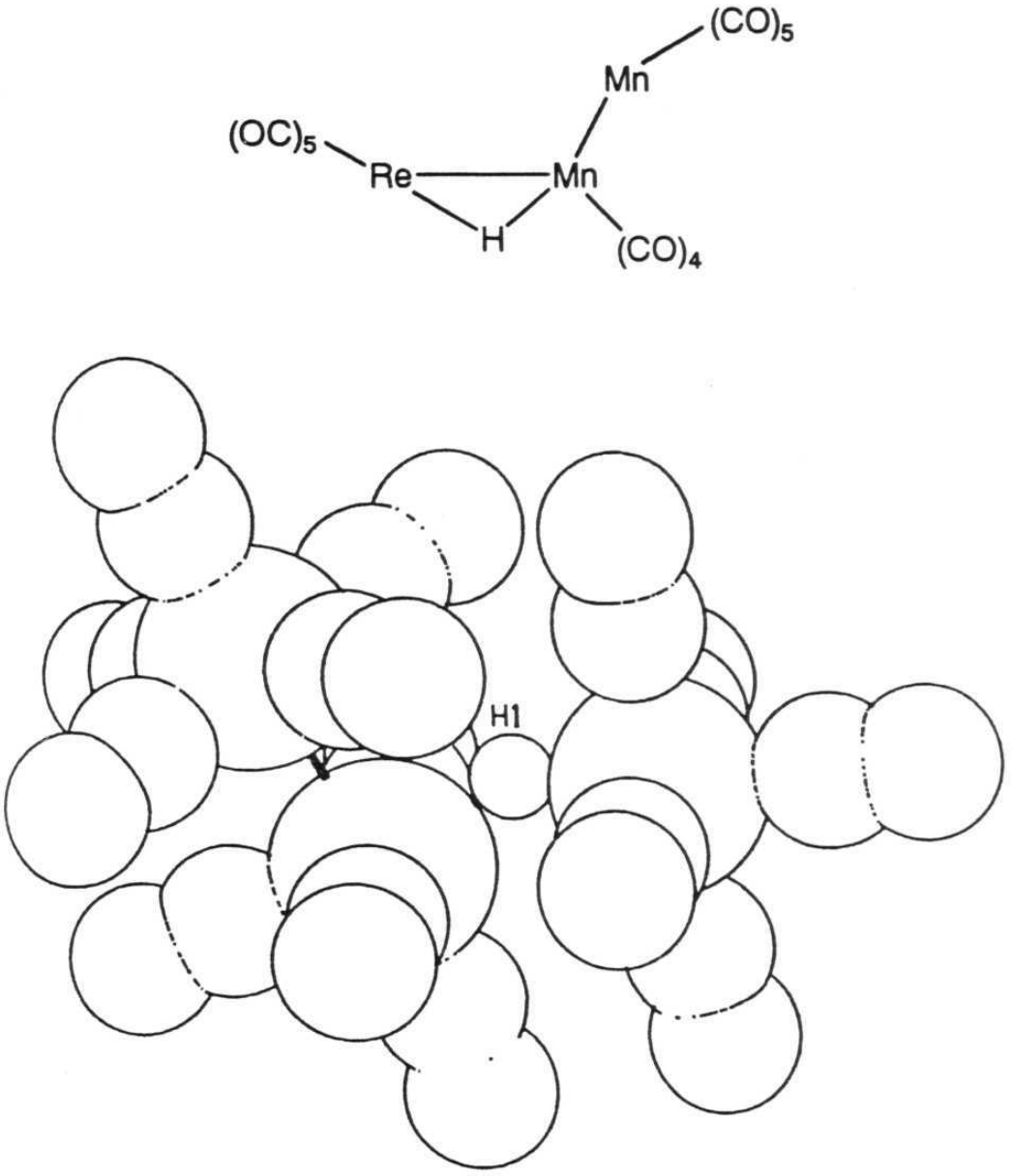

Figure 9b. $HMn_2Re(CO)_{14}$ (VITMIU) to show how the ligands are completely surrounded by other ligands and are not available for intermolecular interactions.

4.3 Conclusions

The results of the analysis described in this chapter suggest that hydrogen atoms bound to metal atoms chiefly in polynuclear systems can be sufficiently acidic to establish hydrogen bonds in the solid state. This has been demonstrated on the basis of a CSD search which has provided evidence of the existence of M-H···O cohesive interactions in which the transition metal atoms act as donors in intermolecular hydrogen bonds with the oxygen atoms of the ligands, mostly CO. From this study it appears that the M-H group, like the C-H group, can act as a soft donor in the presence of soft acceptors, such as CO. These results are in agreement with the information already available on the Brønsted acidity of the hydride atom and on its tendency to interact with weak bases (such as CO). This capacity depends on the other ligands and on the type of the metal(s) forming the complex and on the relative stability of the associated deprotonation anion. Steric factors which are important in determining hydrogen bond formation in organic systems become crucial in the case of metal-"hydride" complexes in which the hydrogen ligands are bound to the metal core, hence are most often completely embedded within the ligands. In general, these M-H···O bonds are comparable in distances (strengths) to those formed between C-H groups, mainly belonging to sp^2 hybridised carbon atoms (as in cyclopentadienyl ligands, arenes etc.,) and CO. Interactions of the C-H···O type are, for obvious reasons far more

abundant than M-H···O interactions. As pointed out by Pearson the Tr-H bond appears to be very similar to the C-H bond.[8b] Both bonds, for example, react as H^+,H· and H^- depending on the relative stability of the resulting species. Importantly, these results also lead to the same conclusion starting from a completely different source of data and suggests that the word "hydride" is misleading for the type of complexes discussed here and should be replaced with a more general "hydrogen ligand" definition.

4.4 Experimental Section

Cambridge Structural Database (CSD) analysis: Data were retrieved from the April 1995 version of the CSD (137527 entries)[25] for all crystal structures with an exact match between chemical and crystallographic connectivity. Both neutral and charged species were considered. Only entries where R<0.10 and where atomic coordinates (including those of the hydride atoms) are given were considered. Geometrical calculations were performed on these hydride subsets for M-H···O hydrogen bonds with H···O distances between 2.0 and 3.2 Å. Duplicate hits (identified by the same REFCODES) were manually removed by eliminating the structure with the highest R-values. Unique contacts were considered up to an H···O distance of 2.80 Å (van der Waals sum). A bonafide M-H···O hydrogen bond was considered to be one

where, in addition to this distance stipulation, the M-H···O angle lies in the range 110-180°. M-H···O bond lengths were taken as such and were not normalised. The queries were constructed such that the O atom of the M-H···O interaction belongs to CO group attached to a metal atom. CSD query was given in Appendix A-3. Key examples were selected from the search outputs and were investigated by computer grap`hics.[26a] The computer program PLATON[26b] was used to analyse the hydrogen bonding patterns.

4.5 References

1. S.G. Kazarian, P.A. Hamley and M. Poliakoff, *J. Am. Chem. Soc.,* 1993, **115**, 9069.
2. L. Brammer, D. Zhao, F.T. Ladipo and J. Braddock-Wilking, *Acta. Crystgr. Sect. B* 1995, **B51**, 632.
3. (a) M.A. Beno, J.M. Williams, M. Tachikawa and E.L. Muetterties, *J. Am. Chem. Soc.,* 1980, **102**, 4542. (b) M.A. Beno, J.M. Williams, M. Tachikawa and F.L. Mutterties, *J. Am. Chem. Soc.,* 1981, **103**, 1485. (c) H. Wadepohl, D. Braga and F. Grepioni, *Organometallics*, 1995, **14**, 24.
4. M.A. Adams, K. Folting, J.C. Huffman and K.G. Caulton, *Inorg. Chem,* 1979, **18**, 3020.
5. S.A. Fairhurst, R.A. Henderson, D.L. Hudhes, S.K. Ibraham and C.J. Pickett, *J. Chem. Soc., Chem. Commun.,* 1995, 1569.
6. V.R .Pedireddi and G.R. Desiraju, *J. Chem. Soc., Chem. Commun.,* 1992, 988.
7. B.E. Bursten and M.G. Gatter, *Organometallics* 1984, **3**, 895.
8. (a) D.F. Shriver, *Acc. Chem. Res.,* 1970, **3**, 231. (b) R.G. Pearson, *Chem. Rev.,* 1985, **85**, 41.
9. Z. Dawoodi, M.J. Mays and A.G. Orpen, *J. Organomet. Chem.,* 219, **251**,1981
10. M.R. Churchill and C. Bueno, *Inorg. Chem.,* 1983, **22**, 1510.

11. J.R. Shapley, M.E. Cree-Uchiyama, G.M.St. George, M.R. Churchill and C. Bueno, *J. Am. Chem. Soc.,* 1983, **105**, 140.

12. M.R. Churchill and C. Bueno, *J. Organomet. Chem.,* 1990, **396**, 327.

13. M. Castiglioni, R. Giordano, E. Sappa, A. Tiripicchio and M.T. Camellini, *J. Chem. Soc., Dalton Trans.,*1986, 23.

14. C.-J. Su, M.-L. Chung, H.-M. Gau, Y.-S. Wen and K.-L. Lu, *J.Organomet.Chem.,* 1993. **456**, 271.

15. (a) R.D. Adams, M.P. Pompeo and W. Wu, *Inorg. Chem.,* 1991, **30**, 2425. (b) R.D. Adams, M.P. Pompeo and W. Wu, *Inorg. Chem.,* 1991, **30**, 2425.

16. R.D. Adams, J.A. Belinski and M.P. Pompeo, *Organometallics,* 1992, **11**, 3129.

17. G. Michael, J. Kaub and C.G. Kreiter, *Chem. Ber.,* 1985, **118**, 3944.

18. M.A. Beno, J.M. Williams, M. Tachikawa and E.L. Muetterties, *J. Am. Chem. Soc.,* 1981, **103**, 1485.

19. N.Carr, M.C. Gimeno, J.E. Goldberg, M.U. Pilotti, F.G.A. Stone and I. Topaloglu, *J. Chem. Soc., Dalton Trans.,* 1990, 2253.

20. C.S. Jun, X. Meng, K.J. Haller and T.P. Fehlner, *J. Am. Chem. Soc.,* 1991, **113**, 3603.

21. R.D. Wilson, S.M. Wu, R.A. Love and R. Bau, *Inorg. Chem.*, 1978, **17**, 1271.

22. A.G. Orpen, XHYDEX, A Program for locating Hydrides, Bristol University, 1980; see also A.G. Orpen, *J. Chem. Soc., Dalton Trans.*, 1980, 2509.

23. J.P. Olsen, T.F. Koetzle,S.W. Kirtley, M. Andrews, D.L. Tipton and R. Bau, *J. Am. Chem. Soc.*,1974, **96**, 6621.

24. A. Albinati, R.M. Bullock,B.J. Rappoli and T.F. Koetzle, *Inorg. Chem.*, 1991, **30**, 1414.

25. F.H. Allen, J.E. Davies, J.J. Galloy, O. Johnson, O. Kennard, C.F. Macrae and D.G. Watson, *J. Che. Inf. Comp. Sci.*, 1991, **31**, 204.

26. (a) E.Keller, SCHAKAL93, Graphical Representation of Molecular Models, University of Freiburg, Germany. (b) A.L.Spek, *Acta Crystallogr.*, 1990, **A46**, C31.

Chapter 5

Agostic Interactions in Transition Metal Complexes

5.1 Introduction

In Chapter 3 the ability of C-H groups to act as proton donors in hydrogen bonding stituations was shown. This chapter deals with different type of interactions of C-H groups where the C-H bond pair electrons interact with electron deficient transition metal atoms. Brookhart and Green termed these interactions "agostic" interactions. Agostic interactions have been well-studied with crystallographic and spectroscopic techniques.[1] The bonding in these C-H···M interations is similar to that of the bridging hydrogen systems which occur in B-H-B, M-H-M and B-H-M groups. The strengths of agostic interactions are estimated to be of the order of 30-60 kJ mol^{-1} and are of comparable strength to those of conventional hydrogen bonds (10-65 kJ mol^{-1}).[2] These interactions are 3-centre 2-electron interactions (3c-2e). This is in contrast to the interactions described in Chapter 1 where the electron rich transition metals or late transition metals can act as proton acceptors to form 3c-4e electron interactions, that is hydrogen bond like interactions with O-H, N-H and C-H groups.[3]

In agostic interactions, lengthening of the C-H bond will occur if the backbonding from the metal atom ($d\pi$) to the C-H group (σ^*) is strong. The acidity and electrophilicity of the C-H group will also increase due to this backbonding. To determine the kinetic pathway of these interactions, Crabtree and co-workers studied a series of

structures of complexes containing C-H···M interactions by the method of structure correlation[4] and proposed that the C-H bond initially approaches the metal atom with a C-H···M angle of around 130°, resulting in a strong M-H interaction. The C-H bond then rotates, bringing the carbon atom close to the metal centre preparing it for oxidative addition.[5]

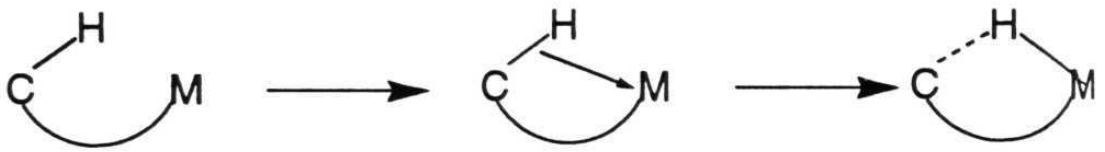

Organolithium complexes are known to form short H···Li contacts with the C-H bonds. These C-H···Li interactions play an important role in stabilising the crystal structures of some organolithium compounds like $LiB(CH_3)_4$, $LiCH_3$, LiC_2H_5, and cyclohexyl lithium.[6] Theoretical studies on these interactions suggests that although the primary reason for these short C-H···Li contacts is ionic, the overlap interactions of the Li orbitals with the carbon lone pair and those with the σ C-H orbitals play a non-negligible role.[7,8] These studies also show that a lengthening of C-H bond occurs when it makes several C-H···Li contacts close to right angle arrangements.

The importance of the CSD in exploring hydrogen bonding interactions like O-H···O, N-H···O and C-H···O[4] has been demonstrated in the previous chapters. Though the agostic interaction is different from a hydrogen bond, in that it is a 3c-2e rather than a 3c-

4e interaction, it can be similarly approached with the CSD. Accordingly, this chapter deals with CSD studies on agostic interactions in IVB, VB and Li metal complexes. In particular, attention is paid to lengthening of the C-H bond with H···M shortening and the similarity in behaviour of C-H···Li interactions to C-H···Tr interactions.

5.2 Results and Discussion

In the studies of C-H···O hydrogen bonds (Chapter 3), the X-ray derived C-H distances were normalised to neutron derived values. However, in the studies of agostic interactions such normalisation is not really justified because the C-H distances are subject to considerable variations by the effect which is being studied, namely the agostic effect. So, in the present study, all available neutron structures were first analysed (irrespective of the metal atom) and then X-ray structures with $R \leq 0.075$ (containing group IVB and VB metals) were considered *without* normalising the H atom positions. Before an X-ray structure was accepted for the analysis, the method of location and refinement of the H-atom positions and their esd's were scrutinised in the original papers. It was found that in almost all the (Ta and Zr) X-ray structures, the H atom positions had been located from difference Fourier maps and refined isotropically. The esd's of these H atoms have

been published in only a few cases but these were found to be satisfactory.

All average structural parameters from the CSD search for the IVB, VB and Li metals are given in Table 1.

Table 1: Mean Geometrical Parameters for C-H···M Interactions in IVB, VB and Li Metal Complexes

Metal	H···M (Å)	C···M (Å)	C-H···M (°)	No. of hits	No. of compounds
Ti	2.36(2)	2.20(4)	68(3)	30	20
Zr	2.32(2)	2.53(5)	93(5)	26	21
Hf	2.28(5)	2.29(3)	79(3)	7	6
V	2.33(3)	2.37(8)	83(7)	23	16
Nb	2.35(4)	2.24(4)	72(5)	7	4
Ta	2.28(4)	2.10(3)	67(2)	23	16
Li(Intra)	2.07(1)	2.34(1)	94(1)	77	36
Li(Inter)	2.09(1)	2.35(3)	93(3)	26	10

5.2.1 Agostic interactions (C-H···Tr)

For neutron structures, there is a total of six compounds which contain eight agostic interactions C-H···Tr (Tr = Ti, Ni, Fe, Ta).[9-14] Of these eight agostic interactions, four each are formed by sp^2 and sp^3 C-H groups. Geometrical parameters for these six compounds are given in Table 2. Chemical formulae of these compounds are shown in Scheme 1. Both α and β agostic interactions are found. There are two

agostic interactions in HMYCFE01, corresponding to the two molecules in the asymmetric unit. Here, the C-atom of the C-H group which forms the agostic interaction bridges the four Fe atoms in a μ4 fashion. In addition to this agostic interaction, the C-H group is also involved in an intermolecular C-H···O hydrogen bond with one of the C≡O ligands (Figure 1).

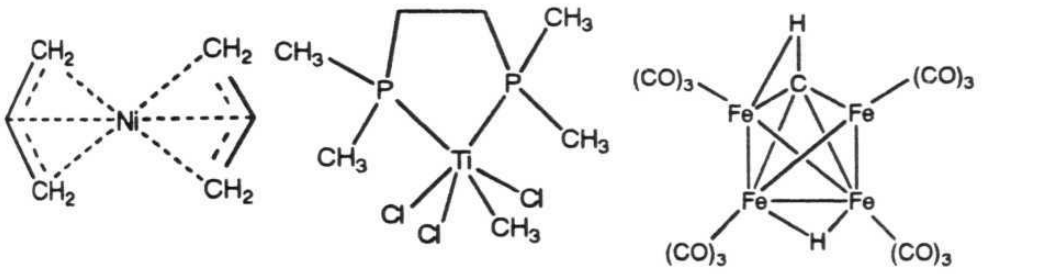

BIPJEP01 **BODRER01** **HMYCFE01**

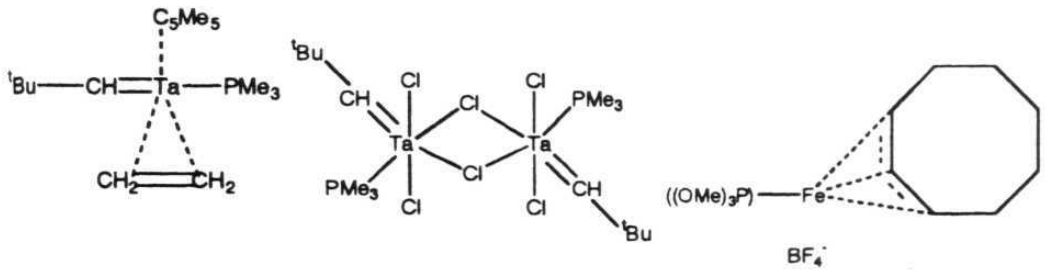

NPNTAB **NPYTAQ10** **OCMPFE03**

Scheme 1: Chemical formulae of neutron derived crystal structures.

In principle, several geometrical parameters may be used to monitor the efficacy of the agostic interaction. The C, H and M atoms may be considered as forming a triangular array. The dimensions of any

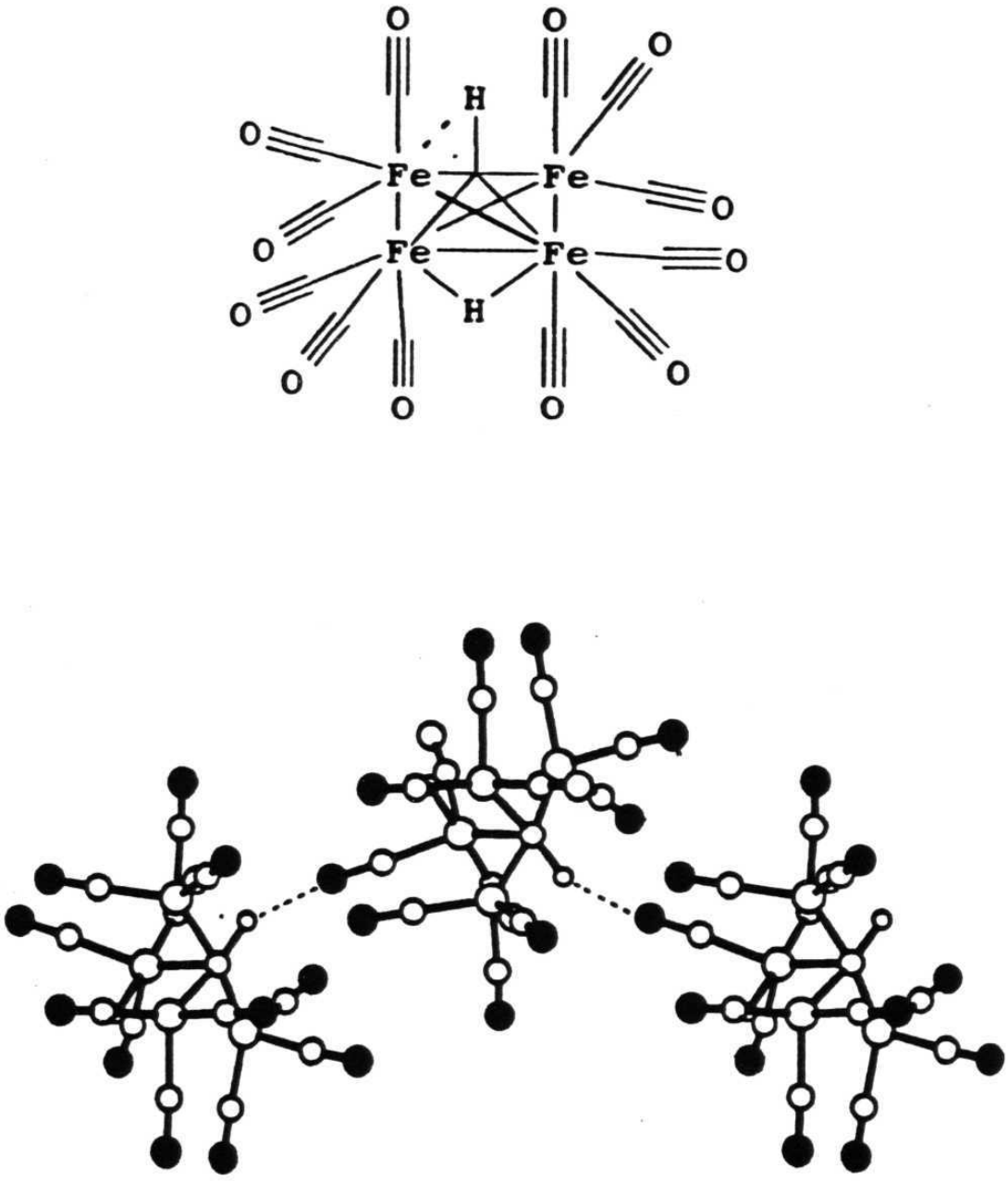

Figure 1. Plot of the C-H···O hydrogen bond network and C-H agostic bond in the neutron derived crystal structure of HMYCFE01.

Table 2: Geometrical Parameters for C-H···M Interactions in Neutron Structures

REFCODE	T (K)	C-H (Å)	H···Tr (Å)	C···Tr (Å)	CHTr (°)	Ref
BIPJEP01	100	1.094(2)	2.466	2.026	54.0	9
		1.090(2)	2.452	2.030	54.8	
BODRER01	20	1.095(2)	2.448	2.123	60.0	10
HMYCFE01	26	1.190(4)	1.754	1.927	79.2	11
		1.175(5)	1.747	1.921	79.6	
NPNTAB	20	1.134(5)	2.041	1.946	68.9	12
NPYTAQ10	110	1.131(3)	2.120	1.898	63.1	13
OCMPFE03	30	1.165(3)	1.873	2.362	99.4	14

The values in the parentheses are the esd's of the C-H distances which were taken from their original structural papers.

triangular array may be defined by three geometrical parameters (one or more distances and two or less angles). The choice of which parameters are to be used is based on the chemical usefulness of these parameters. In this study the C-H and H···M distances and the C-H···M angle were chosen as being chemically meaningful.

Figure 2a is a plot of H···Tr distance versus C-H distance for the eight agostic interactions retrieved. The correlation between these parameters is excellent and shows that as the H···Tr separation decreases, the C-H bond is weakened. In order to better compare these H···Tr distances which arise from different metals, the atomic radius of

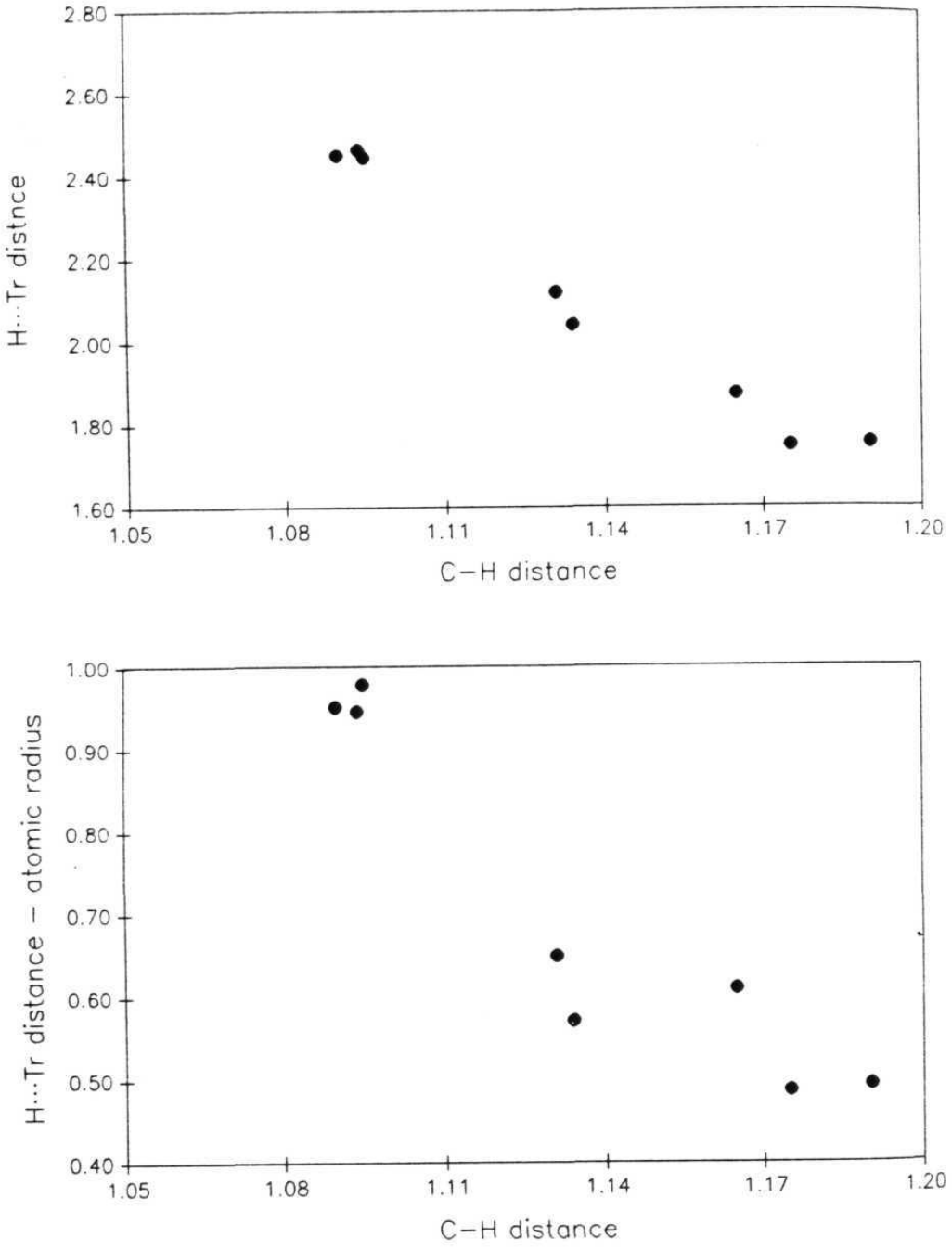

Figure 2. (a) Plot of H···Tr distance versus C-H distance for eight neutron-derived C-H···Tr agostic geometries. (b) Plot of the difference values (H···Tr - atomic radius of Tr) versus C-H distance for eight neutron-derived C-H···Tr agostic geometries. A strengthening of the H···Tr interaction is accompanied by a weakening of the C-H bond.

the particular metal (Tr = Ta 1.47, Fe 1.26, Pt 1.39, Ti 1.47 and Ni 1.25 Å)[15] can be subtracted from the corresponding H···Tr distance. When these distance differences are plotted versus the C-H distances (Figure 2b), a behaviour similar to that seen in Figure 2a was found. Figures 2a and 2b therefore represent a structure correlation[4] of the breaking of the C-H bond by an adjacent electron-deficient Tr-metal atom and its general appearance is similar to structure correlation diagrams of the O-H···O[16] and N-H···N[17] interactions wherein a shortening of one of the bonds formed by the H-atom is accompanied by a concomitant lengthening of the other. Yet it must again be emphasised that the nature of the agostic interaction, C-H···Tr which involves an electron-rich species (the C-H bond) and an electron-deficient species (the Tr-atom) is quite different from that of a hydrogen bond, A-H···B which may be viewed, in the broadest sense, as the positioning of an electron-deficient H-atom between two electron-rich atoms, A and B.[3] Figure 3 which is an overlap diagram of the C, H and Tr-atom positions in these structures, shows that the C-H···Tr angle increases with a strengthening of the agostic H···Tr bond (and the weakening of the C-H bond). To summarise, Figures 2a, 2b and 3 are representations of the trajectory of the H-atom as it moves between the C and Tr-atoms.

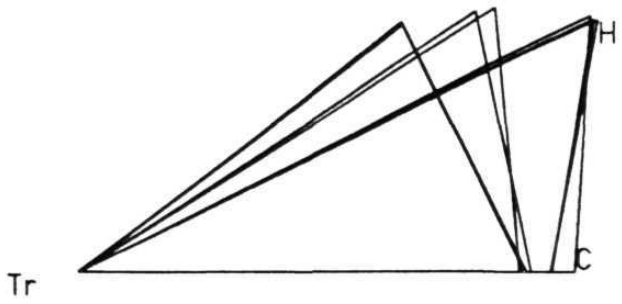

Figure 3. Superposition plot of the seven C-H···Tr α-agostic bonds in Figure 2. The metal atom is at the origin and the M-C vector along the x-axis.

While the neutron results are adequate in themselves, it would be much more satisfying if the CSD-based approach could also be applied to the more numerous X-ray structures available which contain agostic interactions. The main problem with such an extrapolation, from neutron to X-ray derived information, is the inaccuracy in the determination of H-atom positions in X-ray studies. Therefore a direct correlation between C-H and H···Tr distances cannot be attempted. Even so, it may be observed from the neutron derived data (Figure 4a), that the C-H distances and C-H···Tr angles are linearly correlated. The errors associated with the C-H···Tr angles are expected to be lower than those associated with the C-H distances, because the C-H vector direction is determined more exactly than the C-H distance. H···Tr distances were therefore plotted versus C-H···Tr angles in Figure 4b.

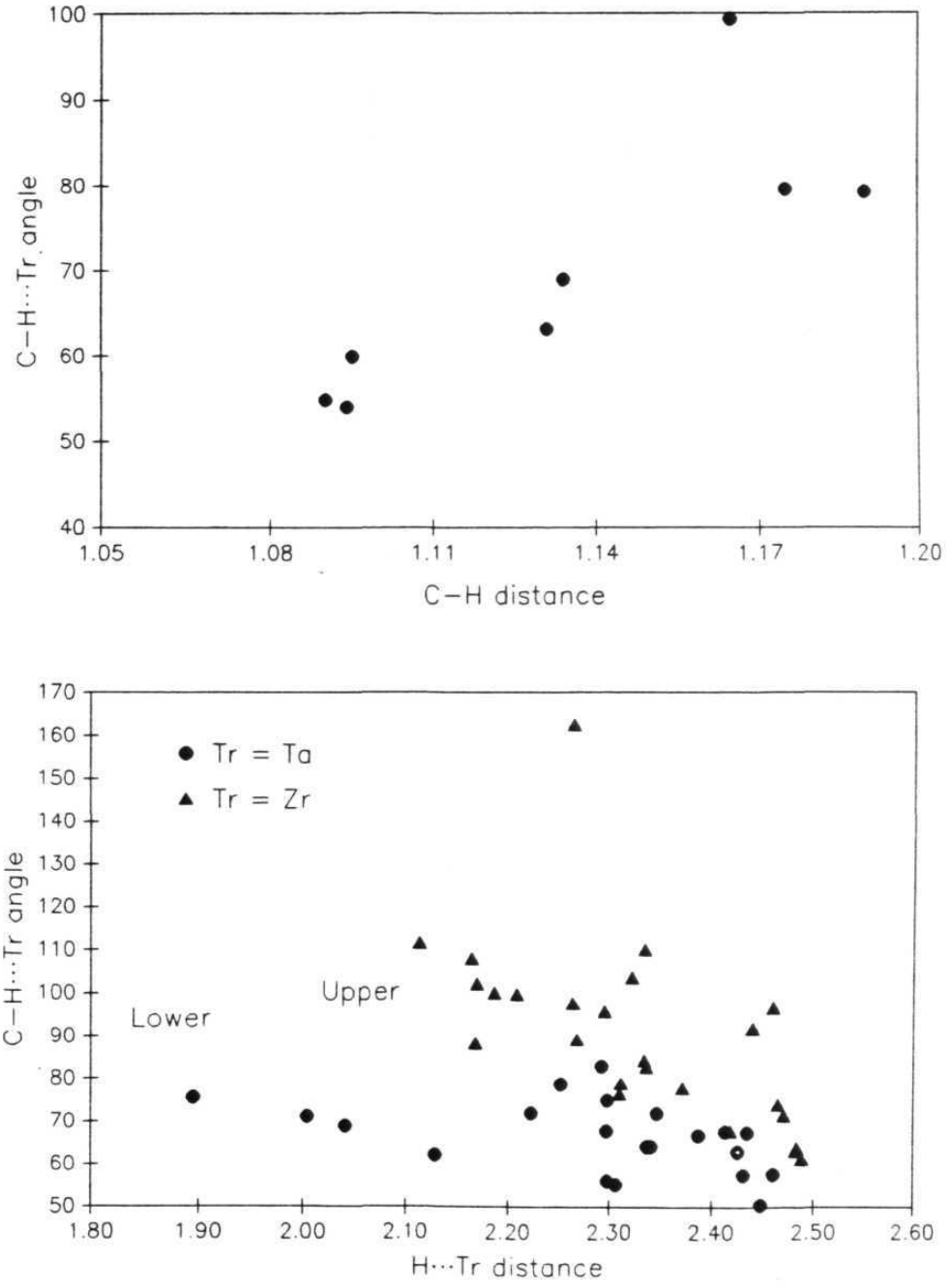

Figure 4. (a) Plot of C-H···Tr angle versus C-H distance for neutron-derived agostic geometries. (b) Plot of C-H···Tr angle versus H···Tr distance for 26 and 23 X-ray-derived agostic geometries of Zr and Ta-complexes. Note the two populations (Lower and Upper diagonals) for the Ta-complexes.

Figure 4b is a plot of these X-ray derived parameters for the 26 and 23 agostic interactions formed by Zr and Ta-atoms respectively. Figure 4b shows two populations for Ta-complexes. One of them contains 7 data points from 5 compounds and lies roughly along the lower diagonal and shows a greater shortening of the H···Ta distance.[12,18-21] Interestingly, all these points represent agostic interactions formed by the neopentylidene moiety, $=CH\text{-}C(CH_3)_3$. CSD Refcodes and geometrical parameters for these 6 compounds are given in Table 3. Chemical formulae of these compounds are shown in Scheme 2. It is known that in these complexes, the expected carbene geometry I is distorted to the geometry II with remarkably small M-C-H angles as low as 78°, and correspondingly large M-C-C angles as high as 170°. Theoretical calculations on these systems shows C-H bond activation and carbene pivoting with the bulky substituents on both the C-atom of the carbene and the metal atom being responsible for these distortions.[22] Figure 5 is a neutron derived crystal structure of the complex $Ta(\eta^5\text{-}C_5Me_5)(CHCMe_3)(\eta^2\text{-}C_2H_4)(PMe_3)$ (NPNTAB) showing the C-H···Ta interaction and geometry of the neopentylidene moiety.

I II

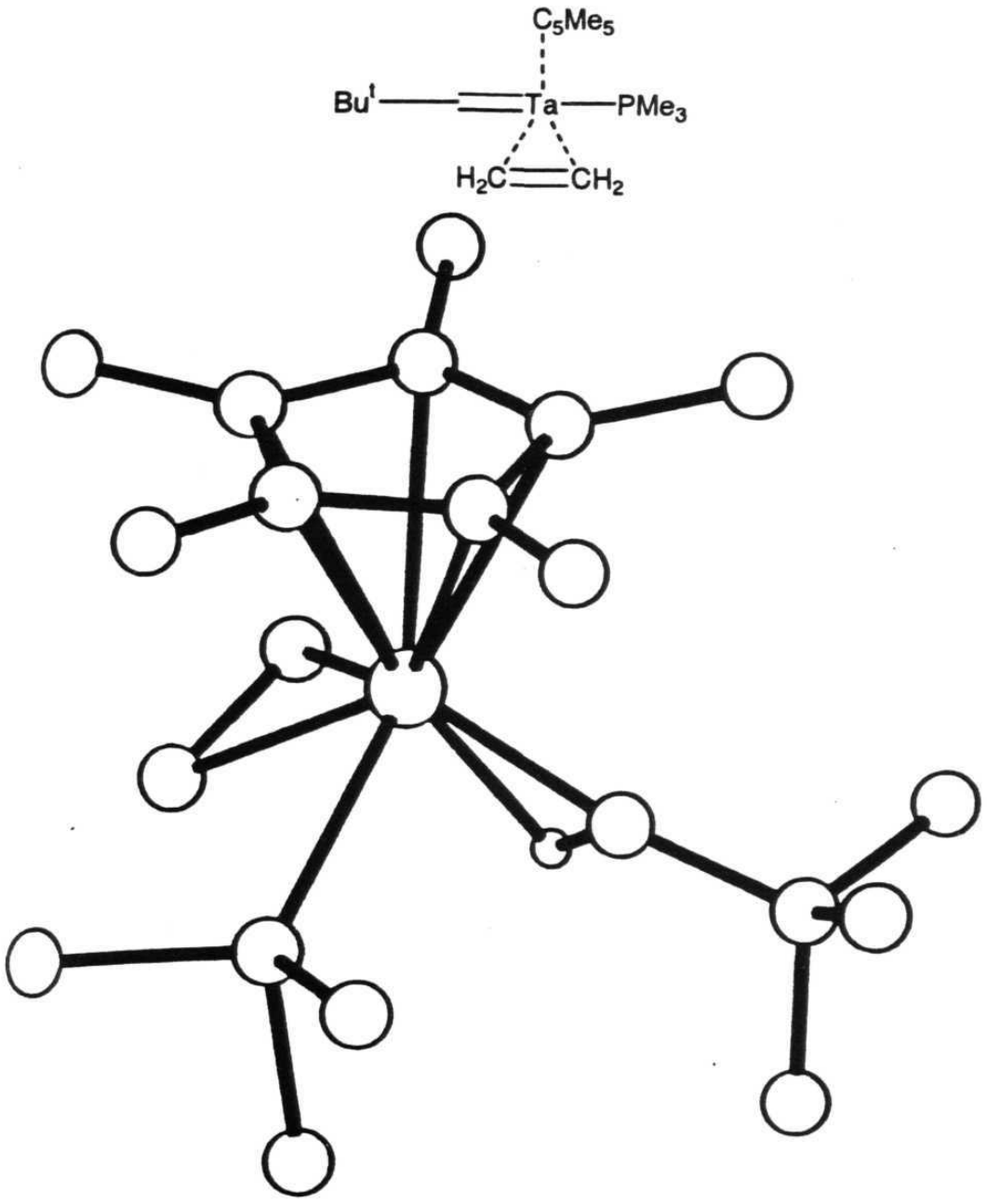

Figure 5. Plot of the neutron derived crystal structure of the complex $Ta(\eta^5\text{-}C_5Me_5)(CHCMe_3)(\eta^2\text{-}C_2H_4)(PMe_3)$ (NPNTAB). Notice the distortion in the Ta-C-H and Ta-C-C angles. Only the hydrogen atom which is involved in the agostic interaction is shown. All the remaining hydrogen atoms are omitted for clarity.

The upper diagonal corresponds to 'weaker' agostic interactions and the points are not so tightly bunched. This region contains agostic C-H groups in a variety of chemical environments. For Zr-complexes, all 26 points correspond to the 'weaker' population but even here the correlation between C-H···Zr and H···Zr is quite satisfactory. Similar plots for Ti, Hf, V and Nb metals are shown in Figure 6. It is understood from Figure 4b and Figure 6 that the agostic interaction geometries are identical for all the metals. It may be noted that an analysis of X-ray derived geometries in Figure 4b and Figure 6 is almost as reliable as the neutron analysis in Figure 2.

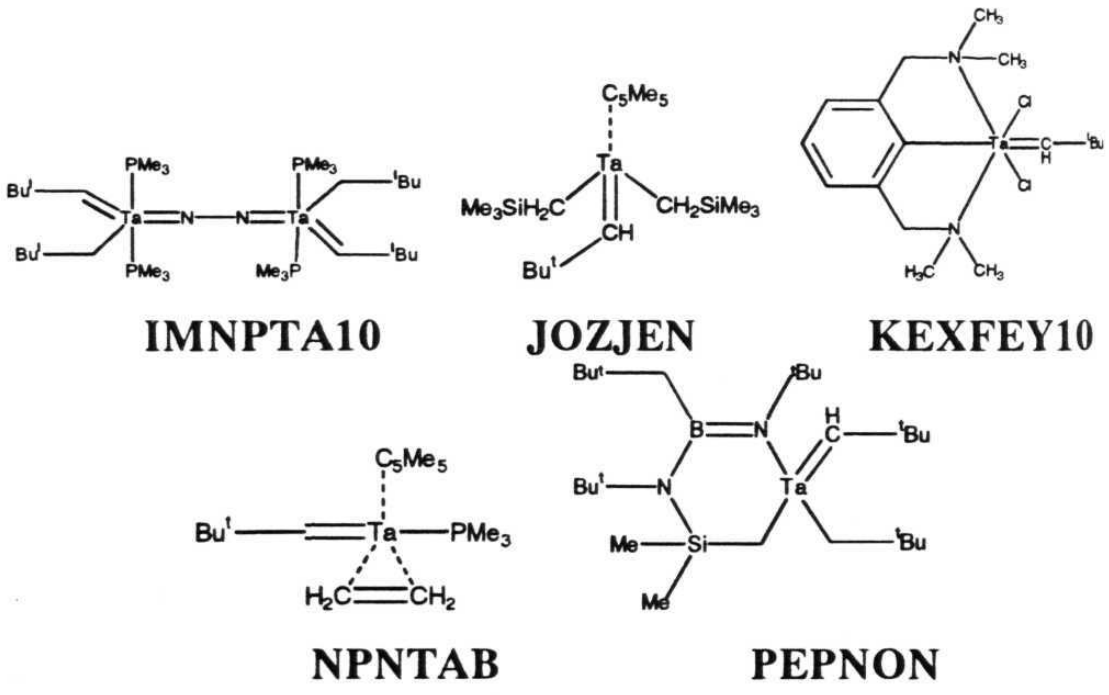

Scheme 2: Chemical formulae of Tantalum neopentylidene complexes

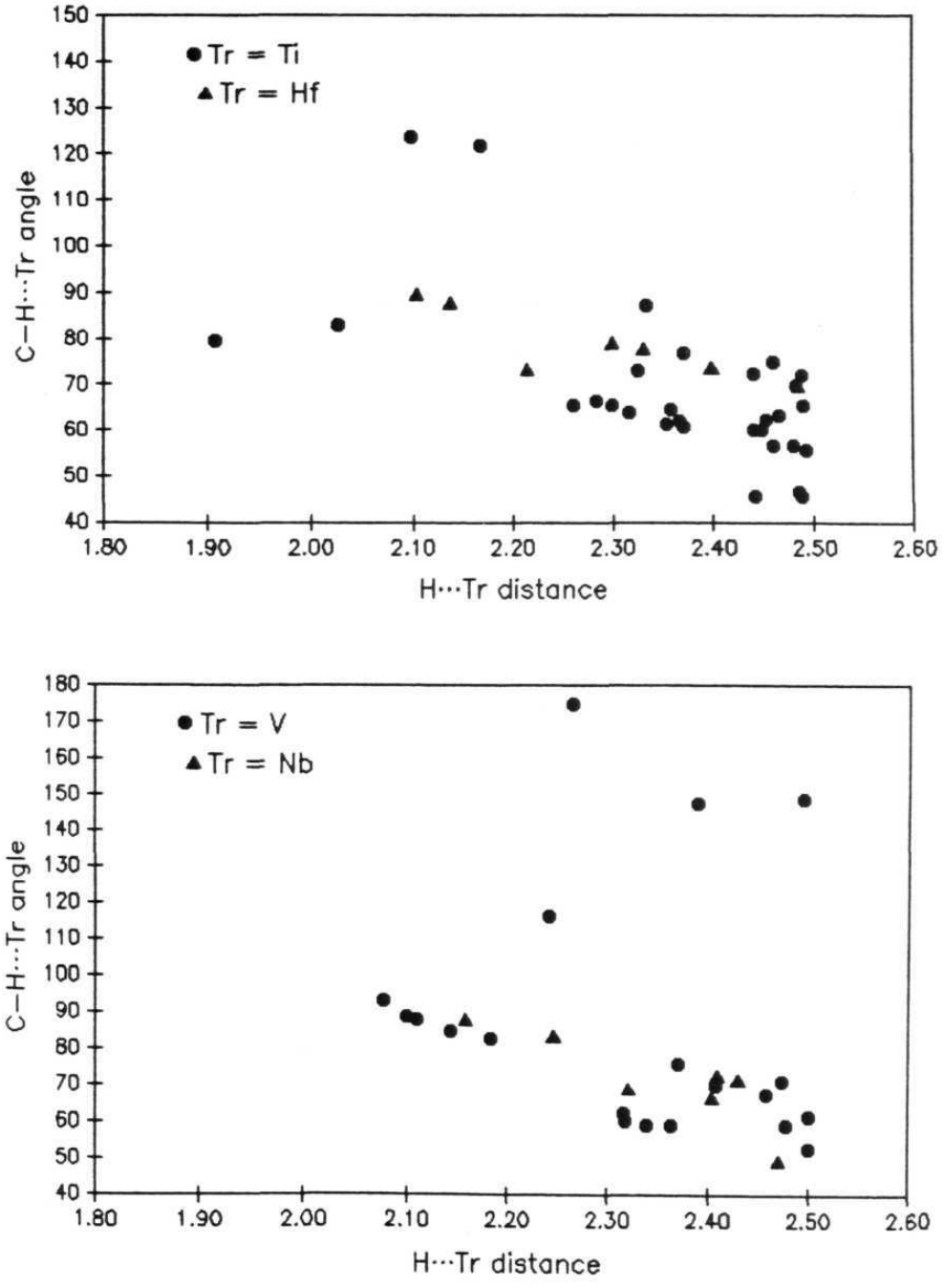

Figure 6. Plot of C-H···Tr angle versus H···Tr distance for X-ray-derived agostic geometries of Ti, Hf, V and Nb complexes.

Table 3: Geometrical Parameters for C-H···M interactions with Neopentylidene C-H group in Ta Complexes

REFCODE	H···Tr (Å)	C···Tr (Å)	CHTr (°)	Ref
IMNPTA10	2.31	1.93	55.5	18
	2.30	1.94	56.2	
JOZJEN	2.43	2.17	63.0	20
	2.00	1.92	71.1	
KEXFEY	1.90	1.94	75.6	20
NPNTAB	2.04	1.95	68.9	12
PEPNON	2.13	1.89	62.2	21

5.2.2 Carbon-Hydrogen-Lithium Interactions:

This CSD analysis was extended to intra and inter molecular C-H···Li interactions which have been recognised as the Li-analogues of the C-H···Tr agostic bond.[7] The Li atom can bind a C-H bond in three types of structural configurations shown below, i.e., mono bridged, dibridged and tribridged geometries (Scheme 3). These types of dibridged and tribridged geometries are not found in the IVB and VB transition metal complexes.

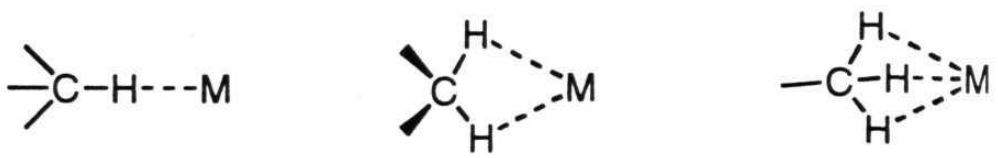

Scheme 3

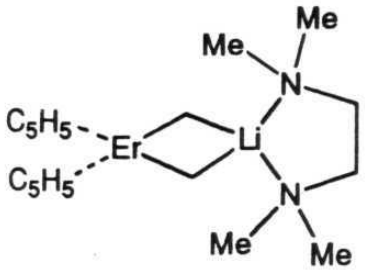

CUDXII

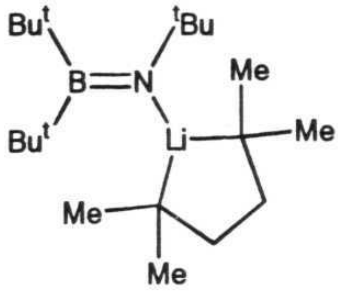

FOZSOC

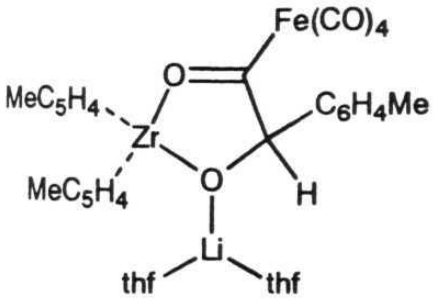

HEMCOR

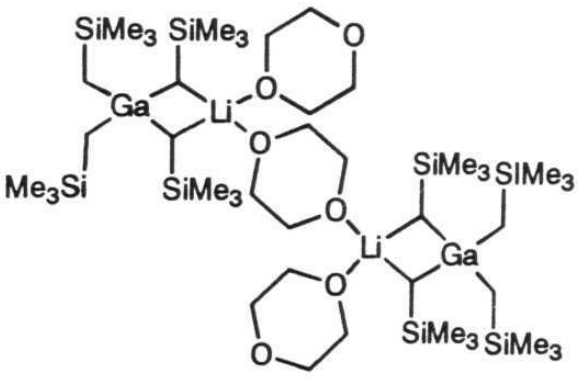

KIMJAR

Scheme 4: Chemical formulae of Li complexes that form dibridged C-H···Li intramolucular interactions

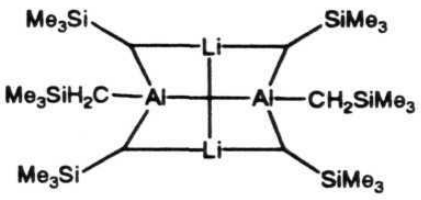

KIZDEC

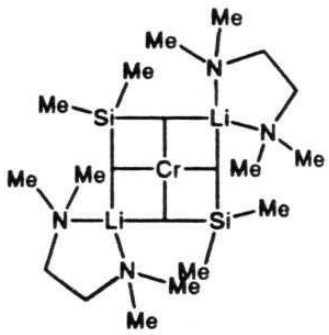

PIXYAM

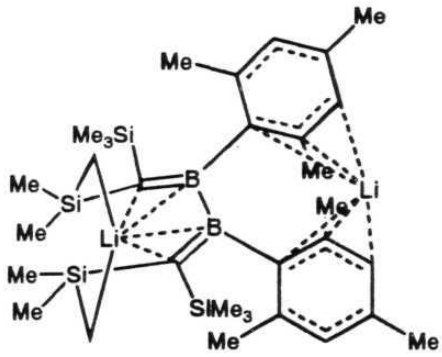

SIJZUG

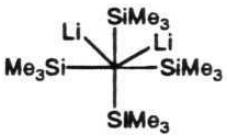

TMSIHH10

$\{Li_2(MnOMe_3)2Li_2(Meacac)(TMED)_2\}_2$

JIBXEX

$\{CH_3C(CH_2NLiCH(CH_3)_2)_3\}_2$

PEBJAH

Scheme 4: Contd...

There are 77 intramolecular C-H···Li agostic geometries in 36 X-ray derived crystal structures with the H···Li distance less than 2.20Å. In these 36 structures, 10 compounds form a dibridged configuration and none forms a tribridged C-H···Li geometry.[23-33] CSD refcodes and relevant geometrical parameters for these 10 compounds are given in Table 4. Chemical formulae of these compounds are given in Scheme 4. In 5 of the 10 dibridged geometries, C-H···Li interactions are formed by the $-CH_2-$ group which acts as a bridge between Li and M (Er, Ga, Al, Cr, Si) (Scheme 5). The bridging of the alkyl group between Li and M may accordingly be stabilised by these C-H···Li interactions.

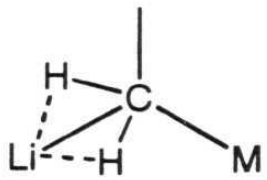

Scheme 5

Figure 7a is a plot of C-H···Li angles versus H···Li distances for the 77 intramolcular C-H···Li geometries. The correlation between C-H···Li angles and H···Li distances holds good at shorter distances (i.e. upto 2.10Å) but it is less obvious at longer distances. It is evident from Figures 4, 6 and 7a that the geometries of C-H···Tr and C-H···Li are identical. The similarity in behaviour of Li to the heavier transition

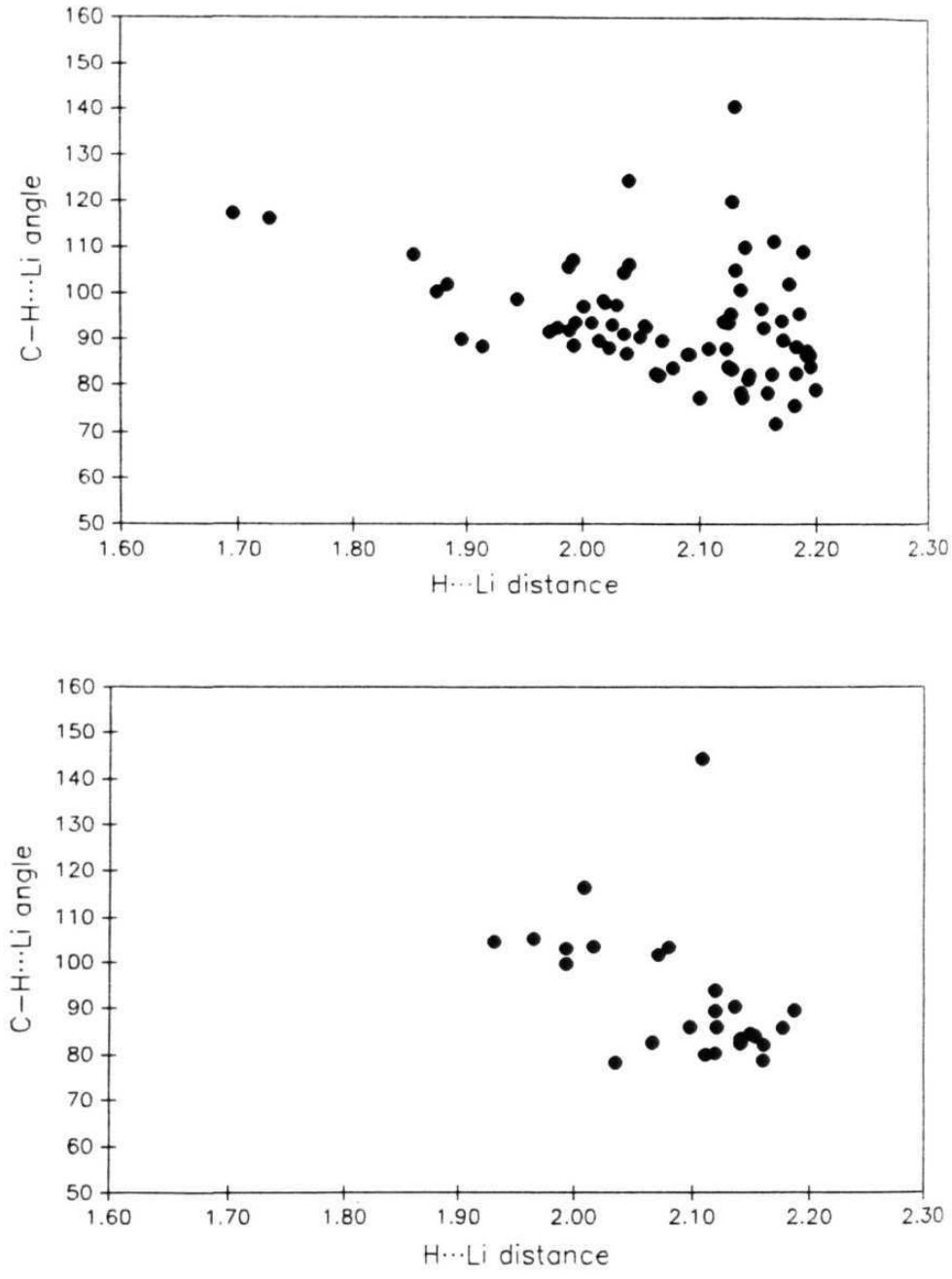

Figure 7. (a) Plot of intramolecular C-H···Li angle versus H···Li distance for 77 X-ray-derived agostic geometries. (b) Plot of intermolecular C-H···Li angle versus H···Li distance for 26 X-ray-derived agostic geometries. Notice the similarity between Figures 4 and 6.

metals in these agostic bonds is noteworthy and in the extreme of the H-atom trajectory, it is known that alkyl lithium compounds, RCH_2Li thermally decompose to LiH and alkenyl derivatives.[7] The dibridged C-H···Li geometries are similar to that of monobridged geometries unlike the bifurcated hydrogen bonds in which the average geometry of the bifurcated hydrogen bond differs from that of the non bifurcated hydrogen bonds.[8c]

Table **4:** Geometrical Parameters for Dibridged C-H···Li Intramolecular Interactions in Li Complexes

REFCODE	Li···H1 (Å)	Li···H2 (Å)	C···Li (Å)	CH1Li (°)	CH2Li (°)	Ref
CUDXII	2.02	2.20	2.26	88.0	79.1	23
FOZSOC	1.99	2.17	2.43	105.9	94.0	24
HEMCOR	1.98	1.99	2.24	92.5	91.8	25
	2.12	2.12	2.39	93.9	93.6	
JIBXEX	2.09	2.09	2.25	86.6	86.6	26
	2.18	2.18	2.36	88.5	88.4	
KIMJAR	2.20	1.99	2.32	84.1	107.3	27
	2.17	2.07	2.30	89.8	89.7	
KIZDEC	2.13	1.89	2.19	77.6	89.9	28
PEBJAH	2.03	2.19	2.35	97.6	87.5	29
PIXYAW	2.14	2.18	2.16	78.5	75.9	30
SIJZUG	2.20	2.19	2.34	86.5	86.5	31
	2.19	2.19	2.34	86.5	86.5	
TMSIHH10	2.00	2.18	2.32	93.5	82.6	32

Intermolecular C-H···Li contacts are less common than the intramolecular ones. There are 26 hits from 10 compounds for intermolecular C-H···Li interactions. Figure 7b is the plot of C-H···Li angles versus H···Li distances for these 26 hits. The geometries of intermolecular interactions are similar to that of the intramolecular C-H···Li interactions. Intermolecular dibridged geometries were found in three structures.[32-34] Refcodes and relevant geometrical parameters are given in Table 5. Chemical formulae are given in Scheme 6. The tribridged geometry is found in only one structure, $LiB(CH_3)_3$ (LITMEB10). This structure was confirmed in both X-ray and neutron diffraction studies. Figure 8 is the neutron derived structure of this compound. In this structure, the $B(CH_3)_4$ units are linked together by one tribridged and two dibridged C-H···Li geometries to form a linear chain.

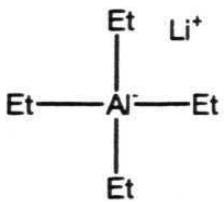

LIALET

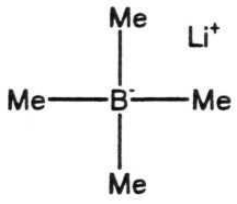

LITMEB01

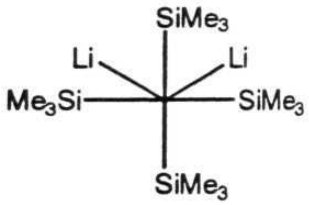

TMSIHH10

Scheme 6: Chemical formulae of Li complexes that form dibridged C-H···Li intermolucular interactions

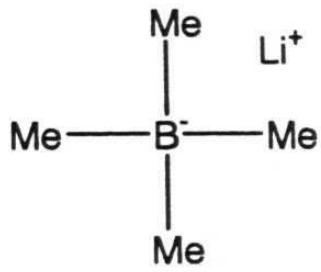

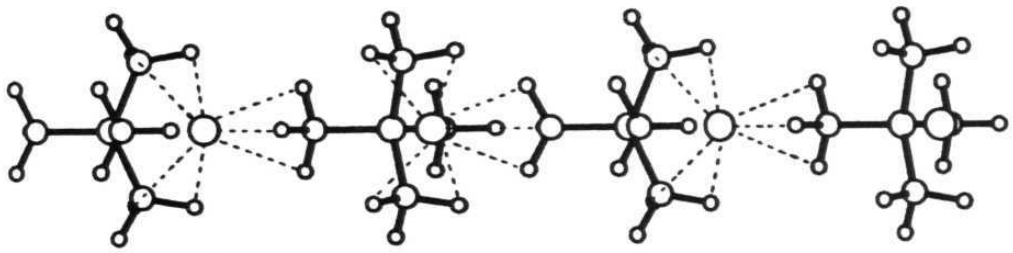

Figure 8. Plot of the C-H···Li agostic bond network in the neutron derived crystal structure of $LiB(CH_3)_4$ (LITMEB10). Notice the tribridged and dibridged C-H···Li geometries.

Table 5: Geometrical Parameters for Dibridged C-H···Li Intermolecular Interactions in Li Complexes

REFCODE	Li···H1 (Å)	Li···H2 (Å)	C···Li (Å)	CH1Li (°)	CH2Li (°)	Ref
LIALET	2.15	2.15	2.30	84.5	84.5	33
LITMEB01	2.11	2.11	2.21	80.4	80.0	34
	2.18	2.18	2.36	85.9	85.9	
LITMEB10	2.16	2.07	2.19	78.9	82.8	
TMSIHH10	2.19	1.99	2.45	89.6	103.2	32

5.3 Conclusions

This work is a confirmation that a strengthening of the H···M (M = Li, Tr) agostic bond is systematically accompanied by a weakening of the corresponding C-H bond. The dynamic profile of the C-H···M trajectory, conveyed by a simultaneous examination of geometries from several crystal structures, may be extrapolated towards the ultimate scission of the C-H bond and is of relevance to studies of C-H bond activation. The similarity in geometries of C-H···Li interactions to the C-H···Tr interactions confirms that the C-H···Li interaction is the organolithium analogue of the agostic interactions of transition metal complexes.

5.4 Experimental Section

Data were retrieved from the 1995 update of Version 5.09 of the CSD (137527 entries)[35] for all ordered crystal structures with an exact match between chemical and crystallographic connectivity and containing at least one of the IVB or VB group metal atoms. Only entries where the R-value is less than or equal to 0.075 and where atomic coordinates are given, were considered. A bonafide agostic interaction was considered to be one where the H···Tr distance is between 1.80-2.50Å. Structures in which the Tr-atoms have more than 16 electrons were removed manually.[1] Li atom containing structures were retrieved separately with the all above constrains and with a C-H···Li contact assumed when the H···Li distance lies between 1.80 and 2.20Å. Geometrical calculations were performed separately for each metal atom using QUEST3D-GSTAT, an automatic graphics nonbonded search program of the CSD. Geometrical questions constructed for the Ta case are given in Appendix A-4 as a representative example.

5.5 References

1. (a) M. Brookhart, M.L.H. Green and L.-L. Wong, *Prog. Inorg. Chem.*, 1988, **36**, 1; R.H. Crabtree, *Chem. Rev.,* 1985, **85**, 245, (b) R.H. Crabtree, *Angew. Chem. Int. Ed. Engl.,* 1993, **32**, 789.
2. (a) K. Zhang, A.A. Gonzalez and C.D. Hoff, *J. Am. Chem. Soc.,*1989, **111**, 3627, (b) K. Zhang, AA. Gonzalez, S.L. Mukerjee, S.-J. Chou, C.D. Hoff, K.A. Kubat-Martin, D. Barnhar and G.J. Kubas *J. Am. Chem. Soc.,* 1991, **113**, 9170.
3. L. Brammer, D. Zhao, F.T. Ladipo and J.B. Wilking, *Acta. Cryst.,* 1995, **B51**, 632.
4. *Structure Correlation*, eds. H.-B.Bürgi and J.D.Dunitz, VCH, Weinheim, 1994, Vols. 1 and 2.
5. R.H. Crabtree, E.M. Holt, M.E. Lavin and S.M. Morehouse, *Inorg. Chem.* 1985, **24**, 1986.
6. (a) R. Zerger, W.E. Rhine, G.D. Stucky and S.W. Peterson, *J. Am. Chem. Soc.,* 1974, **96**, 6048, (b) R.S. Hay-Motherwell, G. Wilkinson, B. Hussain and M.B. Hursthouse, *J. Chem. Soc., Chem. Commun.,* 1989, 1436, (c) G.D. Stucky, M.M. Eddy, W.H. Harrison, R. Lagow and D.E. Cox, 1990, **112**, 2425.
7. E. Kaufmann, K. Raghavachari, A.E. Reed and P.v.R. Schleyer, *Organometallics,* 1988, **7**, 1597.

8. J.J. Novoa, M.-H. Whangbo and G.D. Stucky, *J. Org. Chem.*, 1991, **56**, 3181.

9. R. Goddard, C. Kruger, F. Mark, R. Stansfield and X. Zhang, *Organometallics*, 1985, **4**, 285.

10. Z. Dawoodi, M.L.H. Green, V.S.B. Mtetwa, K. Prout, A.J. Schultz, J.M. Williams and T.F. Koetzle, *J. Chem. Soc., Dalton Trans.*, 1986, 1629.

11. M.A. Beno, J.M. Williams, M. Tachikawa and E.L. Muetterties, *J. Am. Chem. Soc.,* 1981, **103**,1485.

12. A.J. Schultz, R.K. Brown, J.M. Williams and R.R. Schrock, *J. Am. Chem. Soc.,* 1981, **103**, 169.

13. A.J. Schultz, R.K. Brown, J.M. Williams and R.R. Schrock, *J. Am. Chem. Soc.*, 1981, **103**, 169.

14. R.K. Brown, J.M. Williams, A.J. Schultz, G.D. Stucky, S.D. Ittel and R.L. Harlow, *J. Am. Chem. Soc.,* 1980, **102**, 981.

15. A.F.Wells, *Structural Inorganic Chemistry*, Oxford University Press, Oxford, 1975, pp. 1022.

16. J.D.Dunitz and H.-B.Bürgi, *Acc. Chem. Res.,* 1983, **16**, 153.

17. T.Steiner, *J.Chem.Soc., Chem. Commun.,* 1995, 1331.

18. M.R. Churchill and H.J. Wasserman, *Inorg. Chem.,* 1981, **20**, 2899.

19. I. De Castro, J. De La Mata, M. Gomez, P. Gomez-Sal, P. Royo and J.M. Selas, *Polyhedron,* 1992, **11**, 1023.

20. H.C.L. Abbenhuis, D.M. Grove, P. van der Sluis, A.L. Spek and G. van Koten *Rec. Trav. Chim. Pays-Bas (Rec.J.R.Neth.Chem.Soc.)*, 1990, **109**, 446.

21. H. Braunschweig, P. Paetzold and T.P. Spaniol, *Chem. Ber.,* 1993, **126**, 1565.

22. R.J.Goddard, R. Hoffmann and E.D. Jemmis *J. Am. Chem. Soc.,* 1980, **102**, 7667.

23. H. Schumann, H. Lauke, E. Hahn, M.J. Heeg and D. van der Helm, *Organometallics,* 1985, **4**, 321.

24. P. Paetzold, C. Pelzer, R. Boese, *Chem. Ber.,* 1988, **51**, 121.

25. F.R. Askham, K.M. Carroll, P.M. Briggs, A.L. Rheingold and B.S. Haggerty *Organometallics*, 1994, **13**, 2139.

26. R.J. Morris and G.S. Girolami, *Polyhedron,* 1988, **7**, 2001.

27. W. Uhl, K.-W. Klinkhammer, M. Layh and W. Massa, *Chem. Ber.,* 1991, **124**, 279.

28. W. Uhl, M. Layh and W. Massa, *Chem. Ber.,* 1991, **124**, 1511.

29. L.H. Gade and N. Mahr, *J. Chem. Soc., Dalton Trans.,* 1993, 489.

30. P.M. Morse, M.D. Spencer, S.R. Wilson and G.S. Girolami, *Organometallics,* 1994, **13**, 1646.

31. M. Pilz, J. Allwohn, P. Willershausen, W. Massa and A. Berndt, *Angew. Chem., Int. Ed. Engl.,* 1989, **19**, 3577.

32. W.H. Ilsley, M.J. Albright, T.J. Anderson, M.D. Glick and J.P. Oliver, *Inorg. Chem.,* 1980, **19**, 3577.

33. R.L. Gerteis, R.E. Dickerson and T.L. Brown, *Inorg. Chem.,* 1964, **3**, 872.

34. W.E.Rhine, G.Stucky and S.W.Peterson, *J. Am. Chem. Soc.,* 1975, **97**, 6401.

35. F.H.Allen, J.E.Davies, J.J.Galloy, O.Johnson, O.Kennard, C.F.Macrae, and D.G.Watson, *J. Chem. Inf. Comput. Sci.,* 1991, **31**, 204.

Chapter 6

Multi-point Supramolecular Synthons that Contain C-H···O Hydrogen Bonds.

6.1 Introduction

Crystal engineering with conventional (or strong) hydrogen bonds such as O-H···O and N-H···O may appear sufficiently reliable, but is in reality incomplete if weak intermolecular interactions are not considered.[1] The advantage of using weak intermolecular interactions in crystal engineering is that the variety of compounds that can be used to construct supermolecules can be dramatically increased. Among weak intermolecular interactions, C-H···O hydrogen bonds have attracted attention. The ability of C-H groups in organometallic cluster compounds to form C-H···O hydrogen bonds with CO-ligands has been shown in Chapter 3. These studies also reveal that the stability of these interactions depends on the basicity of the CO ligand and that they are directional with the preferred C ≡O···H angle being around 140°. The studies available on C-H···O hydrogen bonds so far suggest that these hydrogen bonds, though weak, show properties similar to those of strong hydrogen bonds.[2] To summarise, C-H···O hydrogen bonds can be used in the design of supramolecular synthons. However, owing to the inherent weakness of these interactions, multi-point recognition rather than single point recognition is the preferred strategy.

Multi-point recognition is of importance in biology. It is known that nucleosides in DNA are held together by three-point recognition between purines and pyrimidines. These three-point recognition patterns

are well studied for strong O-H···O, N-H···O and N-H···N hydrogen bonds.[3] In general, there are three different possible arrangements for three-point recognition. They are ADA:DAD, AAD:DDA and AAA:DDD, where A and D represent hydrogen bond acceptor and donor groups respectively. Experimental data on association constants of these systems shows that the increasing order of stability is AAA:DDD > AAD:DDA > ADA:DAD.[4] This order of stability can be explained by considering secondary interactions. Scheme I shows the primary and secondary interactions that are involved in these three systems. Primary interactions are shown as dashed lines and secondary attractive and repulsive interactions are shown as solid lines and double-headed arrows respectively. In the AAA:DDD system all the four secondary interactions are attractive, in AAD:DDA system two are attractive and two are repulsive and in ADA:DAD system all the four are repulsive. However, theoretical calculations on these systems also shows that cooperative effects can enhance the stability of ADA:DAD and DDA:AAD systems, but not of AAA:DDD systems.[5]

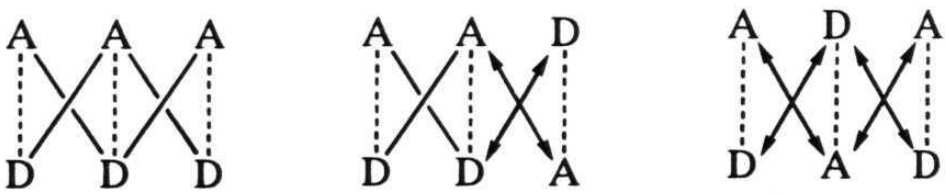

Scheme-I: Possible arrangements of donor and acceptors in three-point synthons.

It is known that the 2,4,6-triaminopyridines and barbituric acid derivatives form a variety of patterns through the three point synthon II.[6] This chapter discuss the design and the robustness of the three point recognition synthon I (ADA:DAD type) which is a C-H···O hydrogen bonded mimic of the strong hydrogen bonded synthon II. For this purpose the crystal structures of complexes **3a**, **3b**, **3c**, **3d**, **3e**, **3f** and **3g** have been solved and analysed. Synthon I is found in **3a**, **3b**, **3c**, **3d** and **3e** but not in **3f** and **3g**. The CSD was used to analyse the patterns observed in these structures and in other α, β-unsaturated carbonyl compounds.

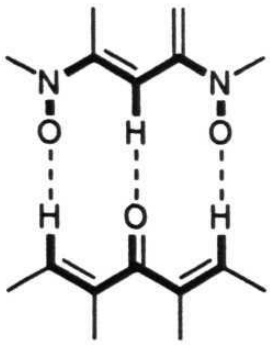

I

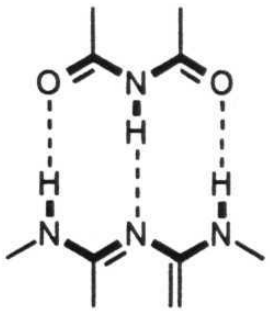

II

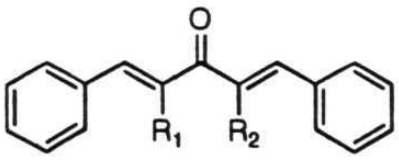

1

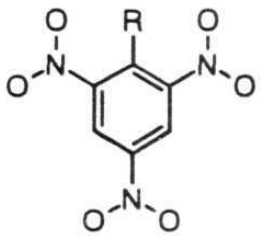

2

1a. $R_1 = R_2 = H$

1b. R_1-R_2 = -CH_2-CH_2-

2a. R = H

2b R = Cl

1c. R_1-R_2 = -CH_2-CH_2-CH_2 2c. R = OH
1d. R_1-R_2 = -CH=CH-

3a. 1a:2a (1:2) 3e. 1d:2b (1:2)
3b. 1b:2a (1:2) 3f. 1b:2c (1:1)
3c. 1c:2a (1:2) 3g. 1a:2c (1:1)
3d. 1b:2b (1:2)

6.2 Results and discussion

The choice of trinitrobenzene **2a** as one of the supramolecular components to form supramolecular synthon I is due to the high acidity of its C-H group and the capability of nitro groups to form C-H···O hydrogen bonds. The choice of dibenzylideneketones as a second supramolecular component is made by matching complementary groups. The observation of C-H···O hydrogen bonded interactions III and IV formed by α,β-unsaturated carbonyl compounds elsewhere[7] also strengthened the idea for the choice of dibenzylideneketones. Geometrical parameters of the C-H···O hydrogen bonded patterns which will be discussed are given in Table-1

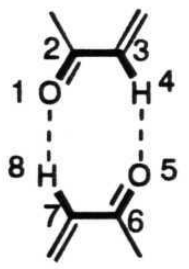

III

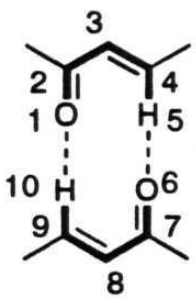

IV

6.2.1 Synthon I in complexes of 2a:

Compound **2a** forms 2:1 crystalline complex **3a**, with dibenzylideneketone **1a** and also yields synthon I as expected. Among the two **2a** molecules, one molecule forms I with molecule **1a** while the second molecule forms an alternative C-H···O hydrogen bonded pattern with the other side of **1a** as shown in Fig. 1a. To avoid this alternate C-H···O hydrogen bonded pattern, compounds **1b**, and **1c** were also considered instead of **1a** to complex with **2a**. Compound **2a** also forms 2:1 crystalline complex **3b** and **3c** with **1b** and **1c** respectively. Synthon I is found in both the complexes and the alternative C-H···O hydrogen bonded pattern which involves the hydrocarbon side of the molecule is found again in complex **3b** but not in **3c**. Curiously the **1b** molecules in complex **3b** are disordered because of the alternative C-H···O hydrogen bonded pattern. The occupancies of the two orientations of **1b** in this complex are constrained by crystallographic symmetry to be 0.5 and 0.5 indicating that the I and the alternate C-H···O hydrogen bonded pattern are of comparable significance. The C-H···O hydrogen bond recognition pattern V is found in complexes **3b** and **3c** but not in **3a**. Synthons I and V are shown in Figs. 1b and 1c respectively.

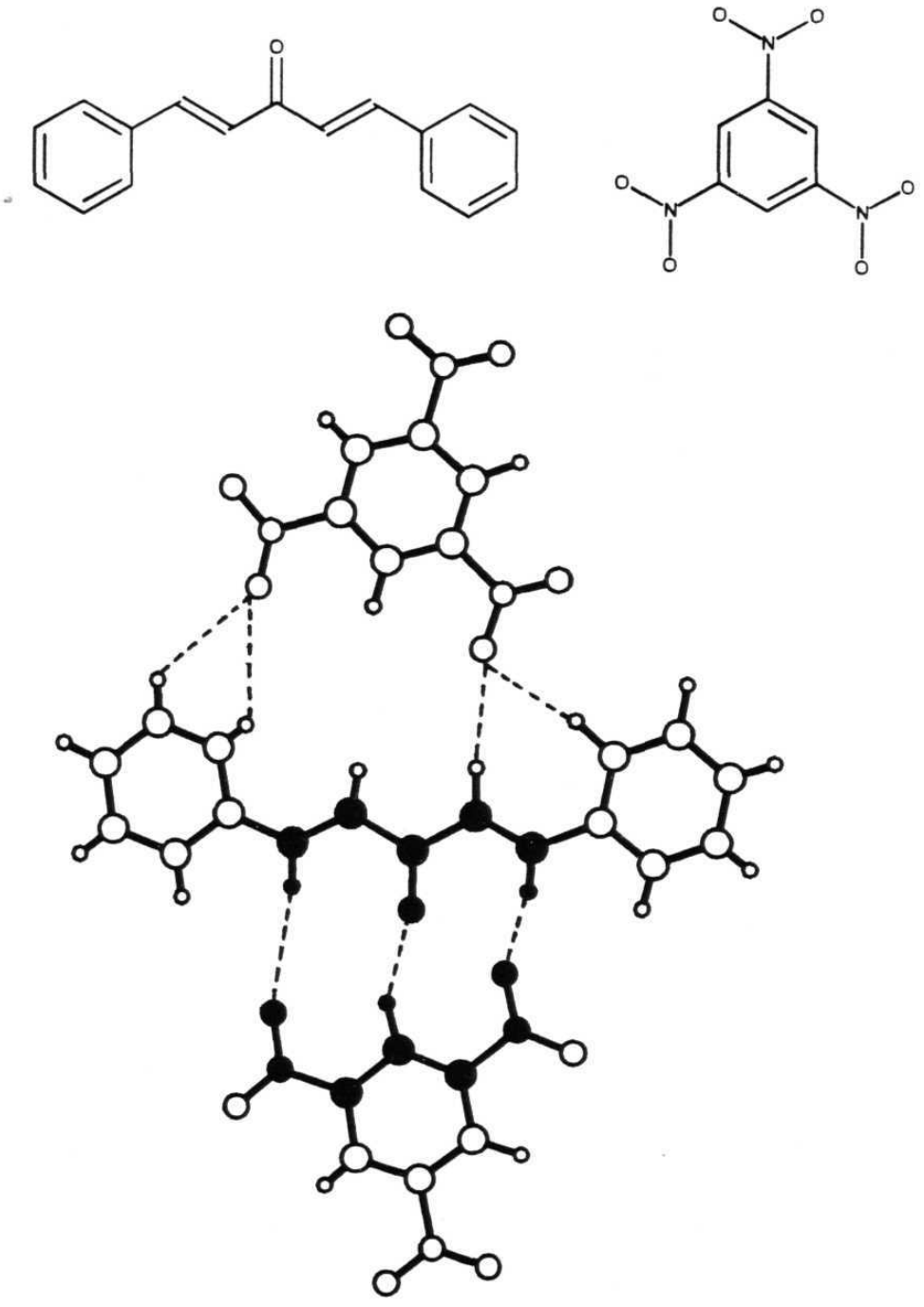

Figure 1a. Crystal structure of complex **3a** to show synthon I, and an alternative C-H···O hydrogen bonded pattern;

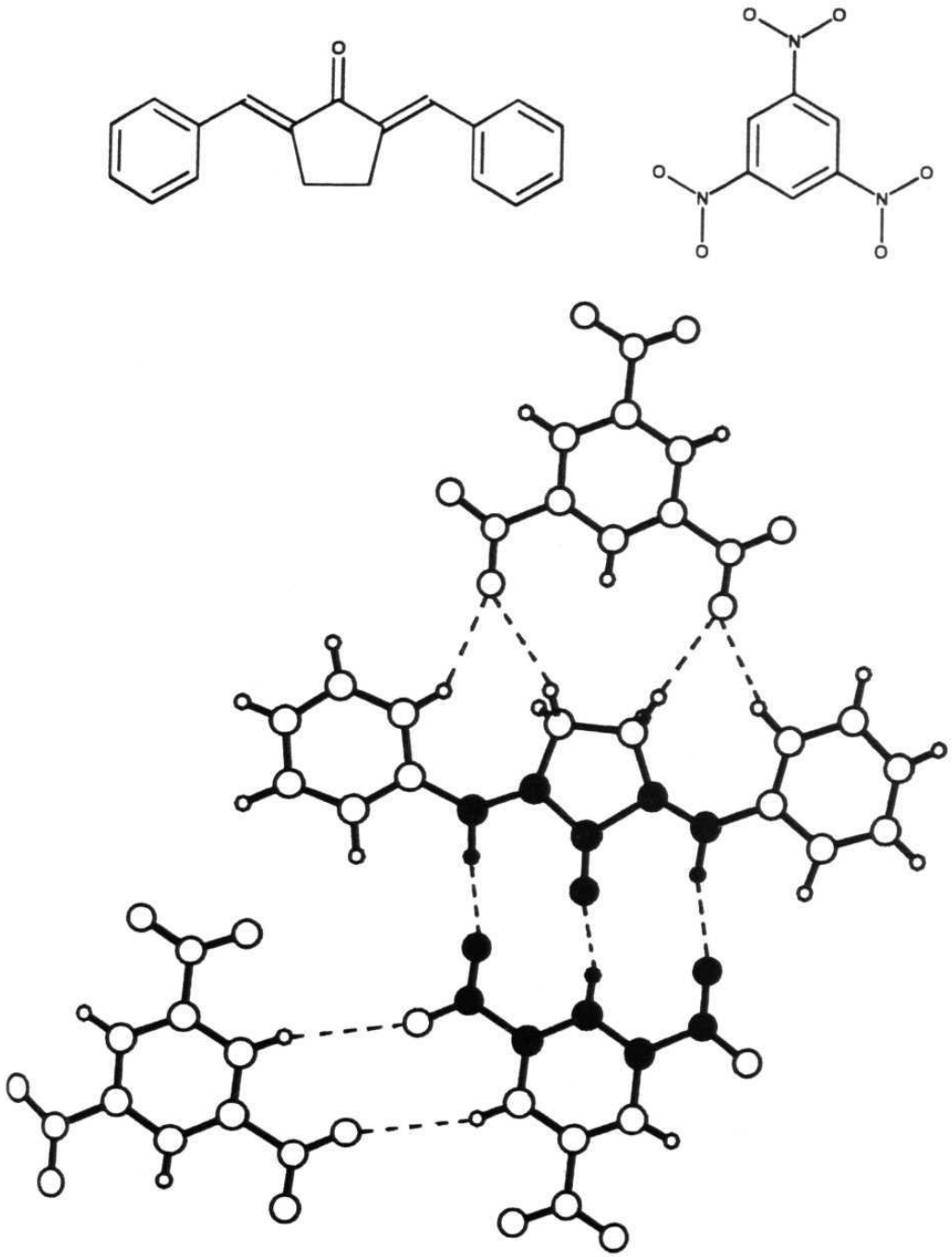

Figure 1b. Crystal structure of complex **3b** to show I, V and an alternative C-H···O hydrogen bonded pattern.

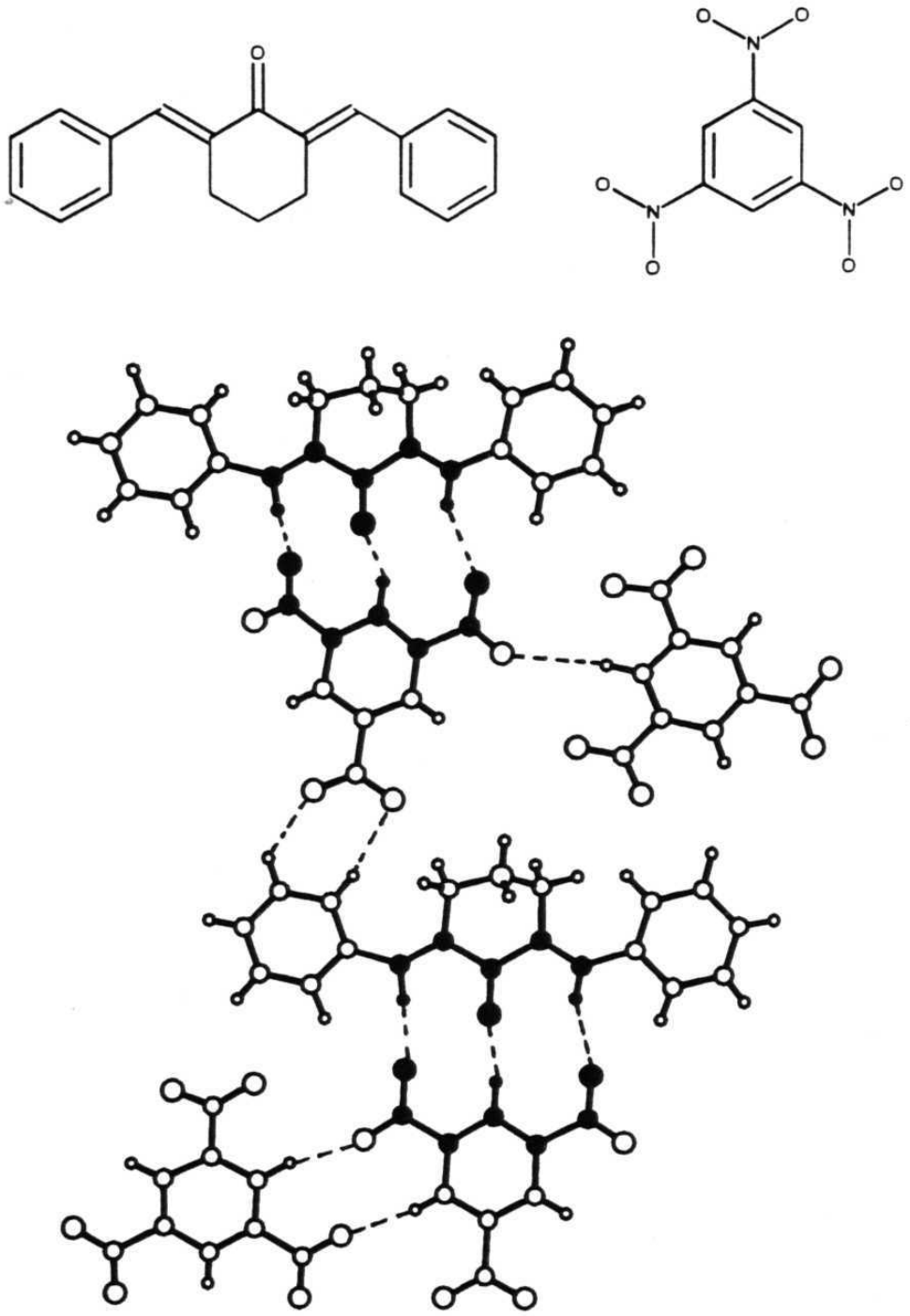

Figure 1c. Crystal structure of complex **3c** to show I and V . Notice the symmetry independent molecules.

Table 1: Geometrical parameters of C-H···O hydrogen bonds in I, V and VIII.

Complex	Synthon	C···O (Å)	H···O (Å)	C-H···O (°)
3a	I	3.34	2.59	132
		3.66	2.81	155
		3.17	2.45	137
3b	I	3.44	2.48	157
		3.18	2.30	160
		3.31	2.39	156
	V	3.61	2.69	162
3c	I	3.39	2.61	141
		3.16	2.50	131
		3.31	2.51	149
	I	3.34	2.40	158
		3.34	2.45	151
		3.47	2.63	149
	V	3.26	2.55	139
		3.48	2.56	154
3d	I	3.39	2.43	165
		2.97	2.37	124
		3.36	2.43	155
	V	3.56	2.67	133
3e	I	3.47	2.86	125
		2.93	2.40	116
		3.39	2.69	133
	V	3.49	2.72	141
3g	VIII	3.35	2.58	139
		3.40	2.58	145

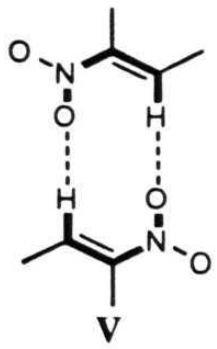

V

To analyse the C-H···O hydrogen bonds in the above complexes, plots of the C···O distances versus the C-H···O angles are obtained (Fig. 2). Circles, triangles and squares represent the C-H···O hydrogen bonds in complexes **3a**, **3b** and **3c** respectively. The C-H···O hydrogen bonds which are involved in synthon I are shown as filled symbols. From this plot, one notes that the C-H···O hydrogen bonds of synthon I are shorter and more linear and that they constitute the essence of these crystal structures. This observation strengthens the idea that the significance of a C-H···O hydrogen bond increases if it is part of a multi-point synthon.

6.2.2 Synthon I in presence of -Cl and -OH functional groups:

In order to test the robustness of the C-H···O hydrogen bonded synthon I in the presence of the other functional groups like -Cl and -OH, compounds **2b** and **2c** are considered instead of **2a** to complex with **1.** It is well-known that **2c**, picric acid forms stable complexes with various aromatic compounds through π-π interactions[8] and that it may be used in crystal engineering experiments to design a three-point synthon VI that

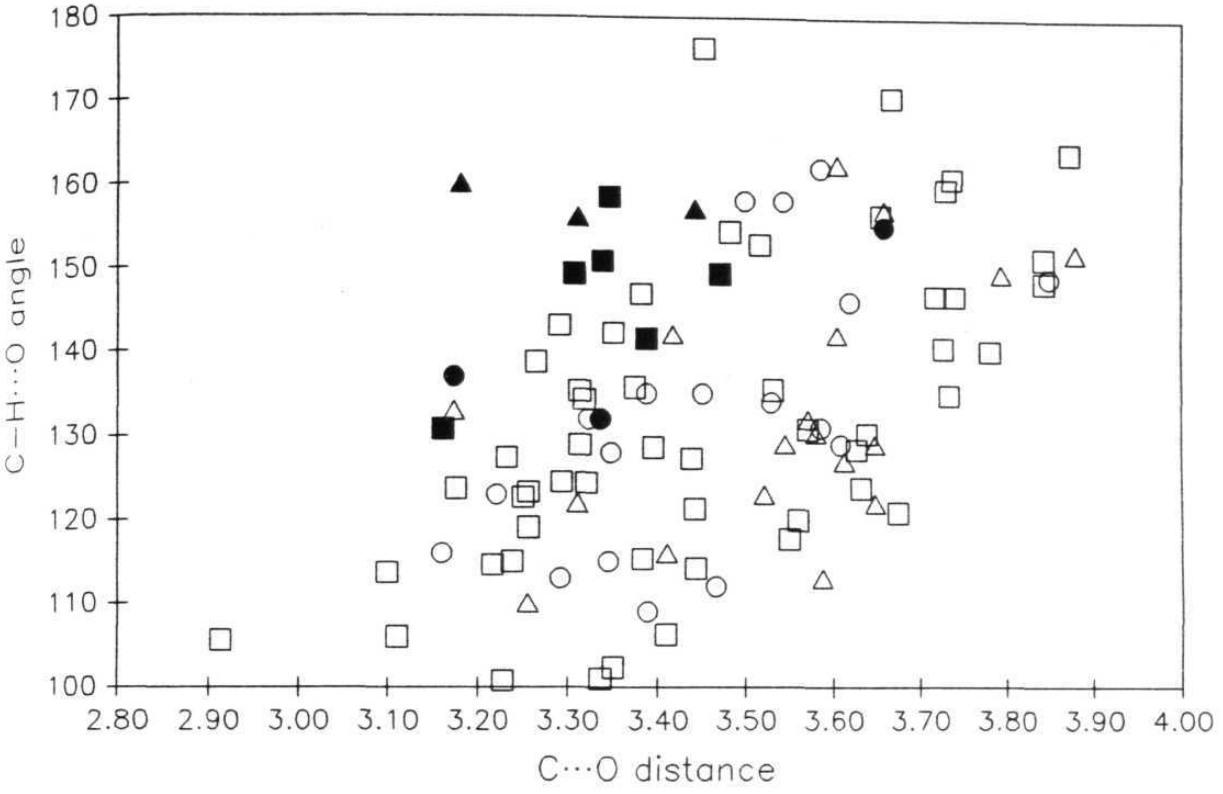

Figure 2. Scatterplot of C-H···O interactions in the complexes of **3a**, **3b** and **3c**. Filled symbols are the C-H···O hydrogen bonds involved in synthon I. Notice that all the filled symbols are in the strong hydrogen bonds region.

contains two C-H···O and one N-H···O hydrogen bonds.[9] Further, from the examination of the crystal structures of pure **2b** and **2c**, it is found that the three nitro groups are coplanar with the aromatic ring in **2b** whereas in **2c**, the ortho nitro group which is not involved in intramolecular O-H···O hydrogen bond is out of the plane of the aromatic ring. Therefore, **2b** and **2c** are anticipated to form complexes with dibenzylideneketones to yield synthon I.

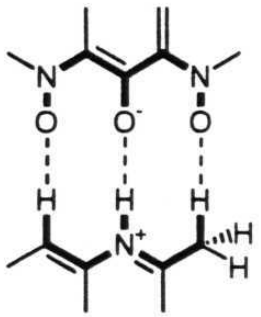

VI

6.2.2.1 Synthon I in the complexes of 2b:

Compound **2b** forms 2:1 crystalline complexes **3d** and **3e** with ketones **1b** and **1d** respectively. Even though compounds **1b** and **1d** are chemically different, they form isostructural complexes with **2b** due to the disorder in the dibenzylidene moiety. The C-H···O hydrogen bonded synthon I was found in both complexes. This indicates that the Cl group does not interfere in the formation of I. These crystal structures are almost reminiscent to those of **3a**, **3b** and **3c** except that these structures form synthon VI through O···Cl interactions. The nitro group oxygens which

are involved in **VI** are disordered. The crystal structures of these complexes **3d** and **3e** are shown in Fig. 3a and 3b respectively. Further, the dibenzylidene moiety in these two complexes mimics the pentacenedione moiety due to the presence of disorder (Scheme I). In order to model this disorder pentacenedione and compound **2b** were taken together for cocrystallisation experiments. However, due to the mismatch of solubilities of pentacenedione and compound **2b**, they failed to co-crystallise.

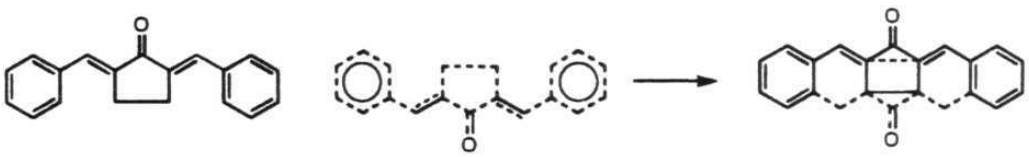

Scheme I: disorder of molecule **1b** and **1d** in the complexes of **3d** and **3e**.

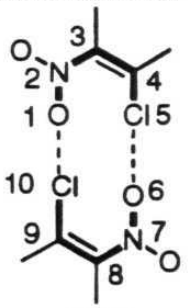

VII

6.2.2.2 Absence of synthon I in complexes of 2c:

Compound **2c** forms 1:1 molecular complexes **3f** and **3g** with compounds **1b** and **1a** respectively. In both the complexes the C-H···O hydrogen bonded synthon I is absent. Interestingly in complex **3f**, the O-H

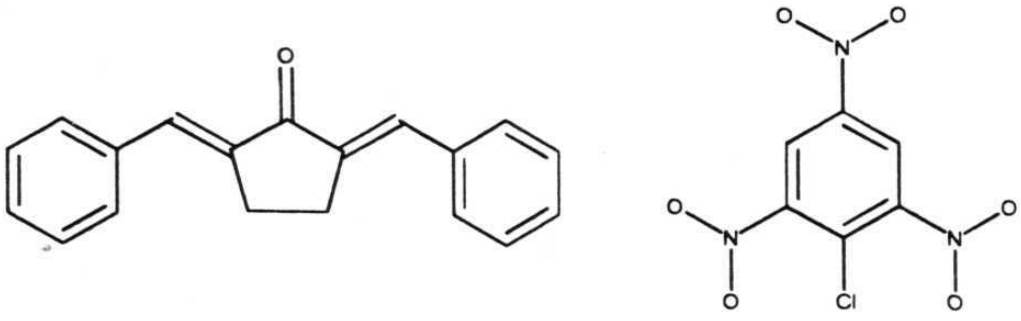

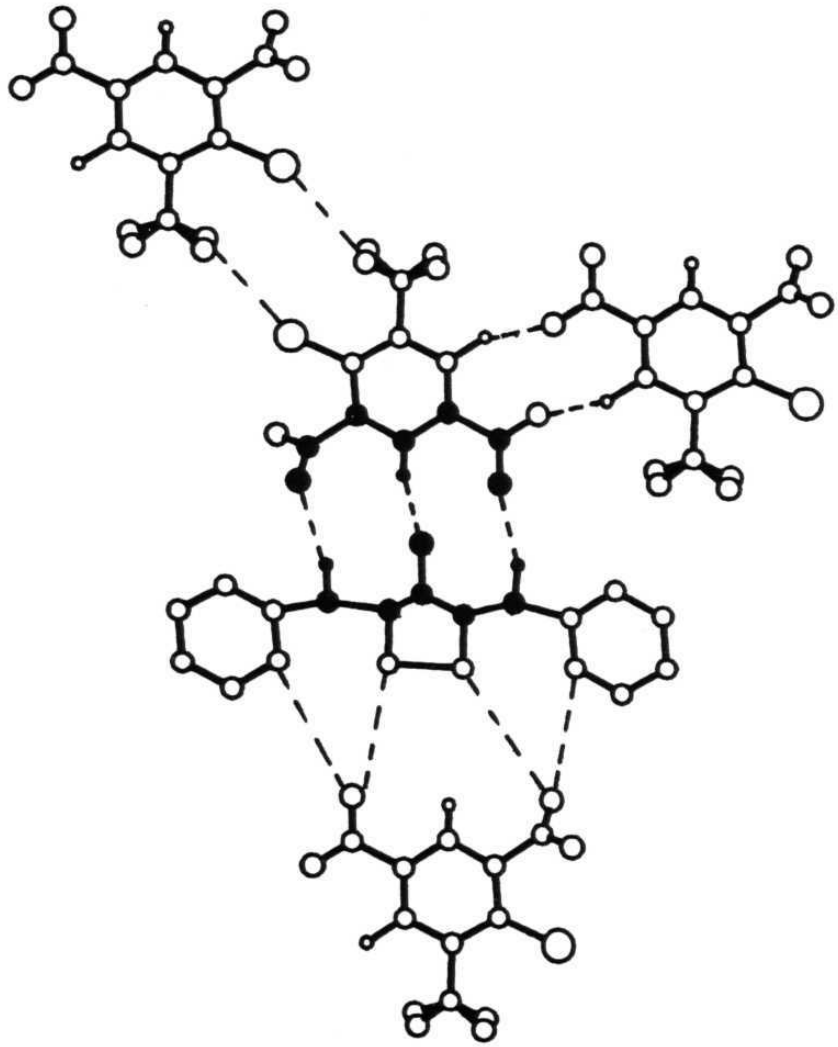

Figure 3a. Crystal structure of **3d** to show synthons I, V and VII. Note that one of the nitro groups of molecule **2b** is disordered and that the cyclopentanone moiety also distorted due to the disorder.

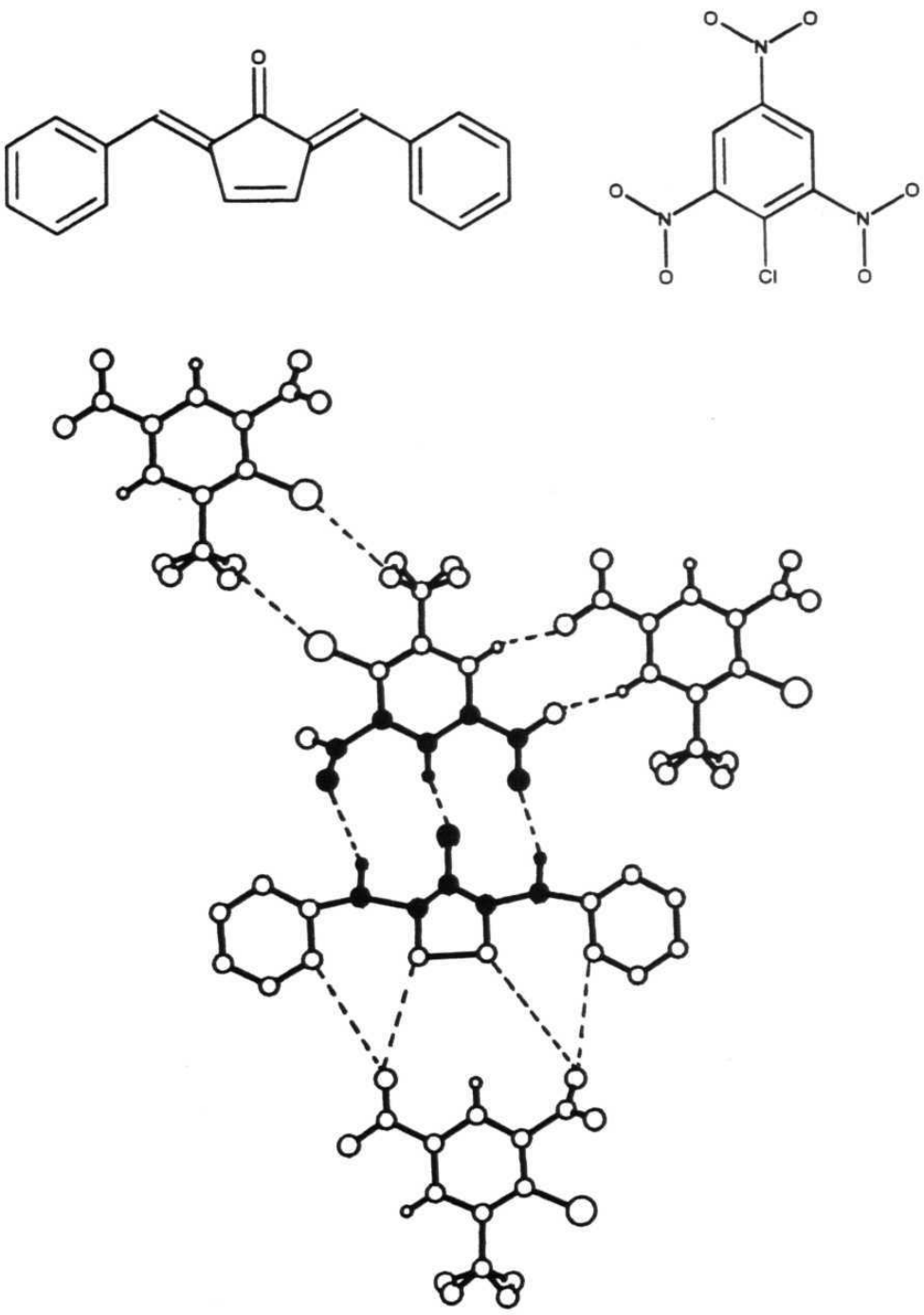

Figure 3b. Crystal structure of **3e** to show synthons I, V and VII. Note that one of the nitro groups of molecule **2b** is disordered and that the cyclopentenone moiety also distorted due to the disorder. Note the similarities between **3a** and **3b**.

group forms an intermolecular hydrogen bond with the keto group of molecule **1b** (O···O, H···O, O-H···O; 2.90 Å, 2.06 Å, 123°). It also forms two C-H···O hydrogen bonds (C···O, H···.O, C-H···O 3.18 Å, 2.98 Å, 164° and 3.42 Å, 2.23 Å, 156°) to form a supermolecule of **1b** and **2c** which is held together by one O-H···O and two C-H···O hydrogen bonds as shown in Fig. 4a. Further, these supermolecules are packed in three dimensions with herringbone interactions as shown in Fig 4b.

In complex **3g**, the situation is entirely different from the other complexes in that it does not form an intermolecular O-H···O hydrogen bond with a keto group as in complex **3f**. Instead one finds centrosymmetric dimers of **1a** and **2c**. These dimers are in turn connected by C-H···O hydrogen bonds as shown in Figure 5 to form a 2-dimensional sheet. Dimer of **2c** is associated with tandem hydrogen bonds[10] where as that of **1a** is associated with C-H···O hydrogen bonded interactions network VIII. VIII is an another example of three-point C-H···O hydrogen bonded recognition.

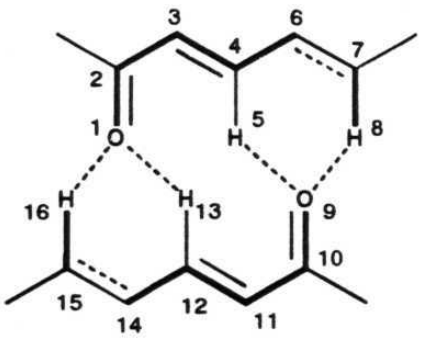

VIIIa

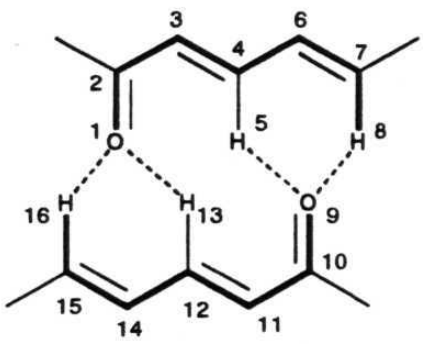

VIIIb

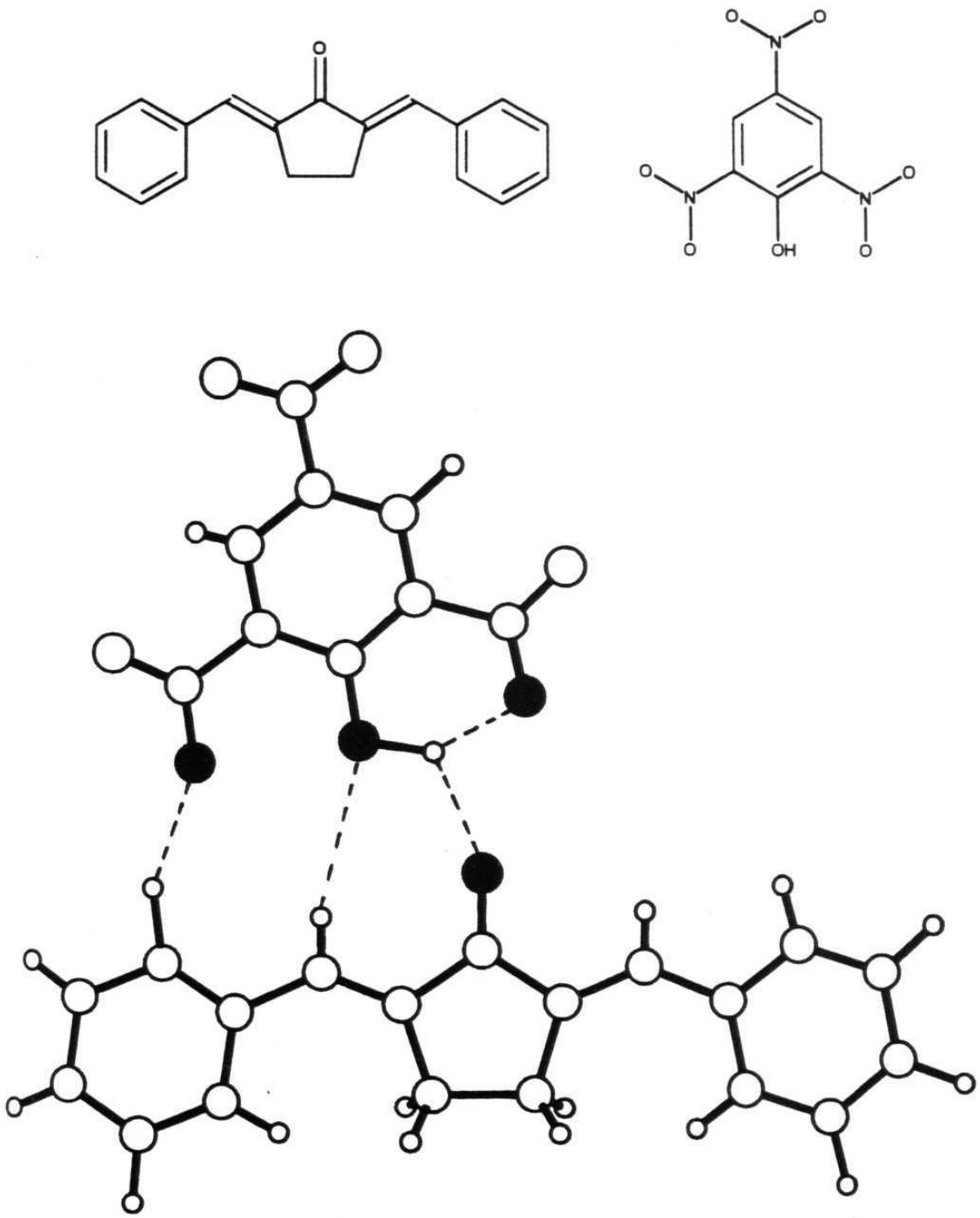

Figure 4a. Crystal structure of complex **3f** to show the supermolecule which involves one intermolecular O-H···O and two C-H···O hydrogen bonds.

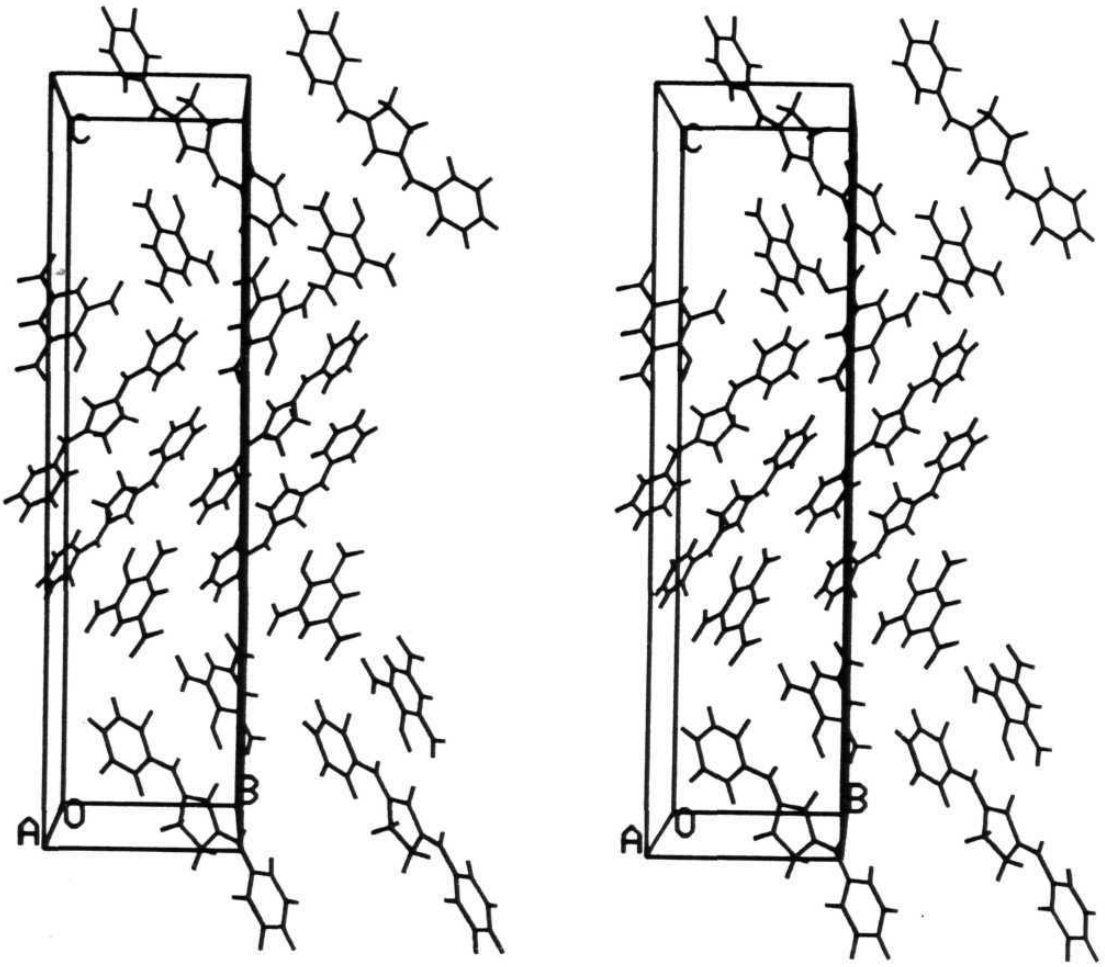

Figure 4b. Packing diagram of the crystal structure of complex **3f**.

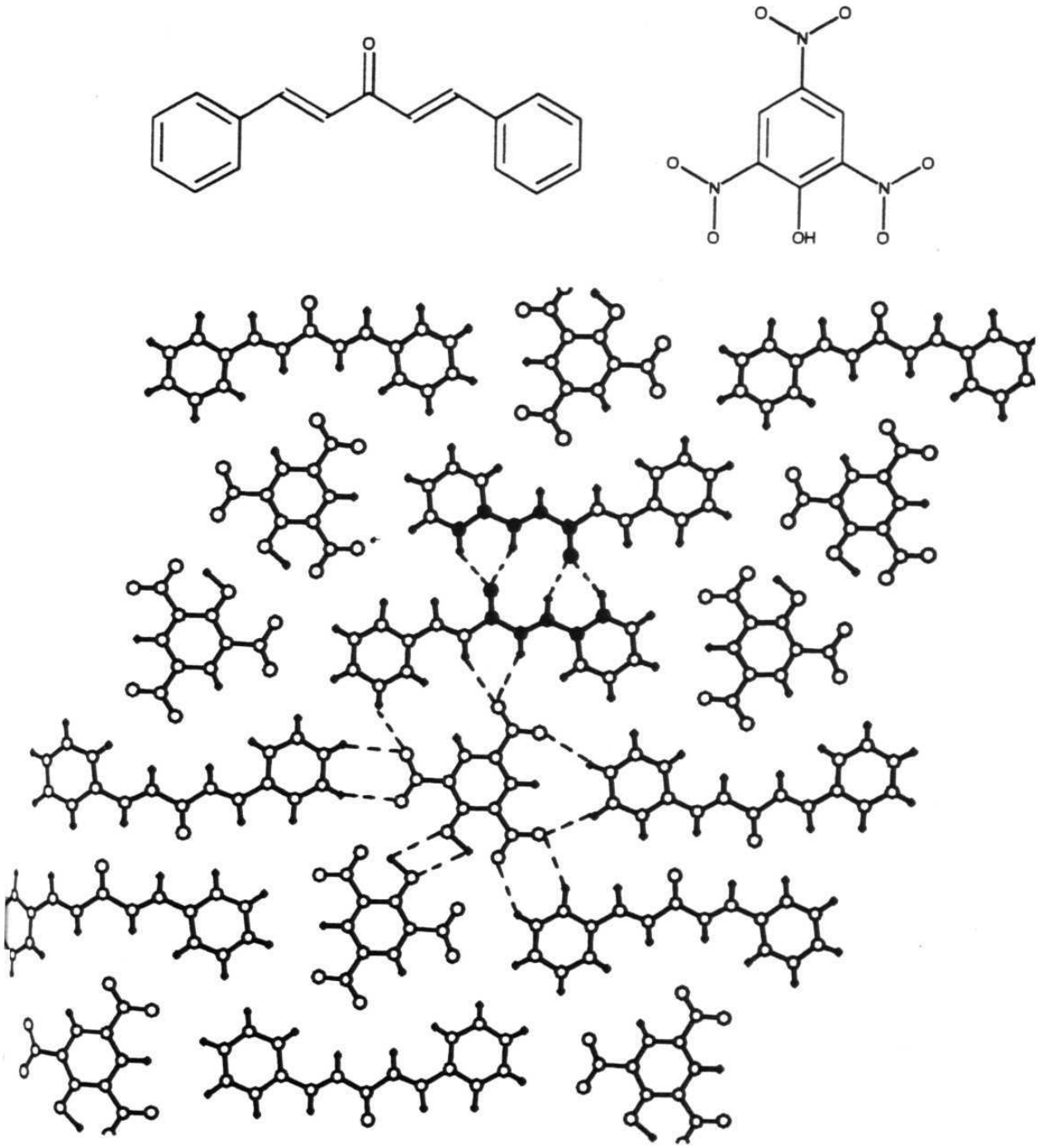

Figure 5. Packing diagram of the crystal structure of the complex **3g** to show the dimers of molecules **1a** and **2c** which are formed by C-H..O hydrogen bonded interactions VIII and tandem hydrogen bonds respectively.

The differences in the packing of these two molecular comple of **2c** can be examined by looking at the NIPMAT plots.[11] A pictor matrix is formed using the atoms of a molecular skeleton (A_1, A_2··· A_m A_n) and the matrix element $A_m A_n$ which is defined by the short intermolecular contact A_m···A_n is shown in terms of a grey scale. T shorter the contact, the greyer the square which represents that particul contact. The scale of this greyness with respect to the A_m···A_n distance represented at the bottom of the figure. The dark line in this scale indicat the sum of the van der Waals radii of A_m and A_n. Further, if there are tv molecular skeletons (A_1, A_2,··A_m··A_n) and (B_1, B_2··· B_i··· B_j) in tl structure, the interactions will be shown in four distinct rectangl separated by darker lines. The upper left and lower right rectangl indicate the A···B interactions while the lower left and upper rig rectangles indicate A···A and B···B interactions respectively. Therefor the plot obtained is a simultaneous visual representation of all tl intermolecular interactions in the crystal. Figure 6a and 6b are NIPMA plots of complexes **3f** and **3g** respectively. In Fig 6b the overall greyne in the upper left and lower right rectangles, which represents the C-H··· interactions and stacking interactions between molecules **2c** and **1a**, more when compared with that of Fig 6a. From these figures it is clear th complex **3g** is stabilised by the C-H···O hydrogen bonds and stackii interactions. In complex **3f**, the intermolecular O-H···O hydrogen boi

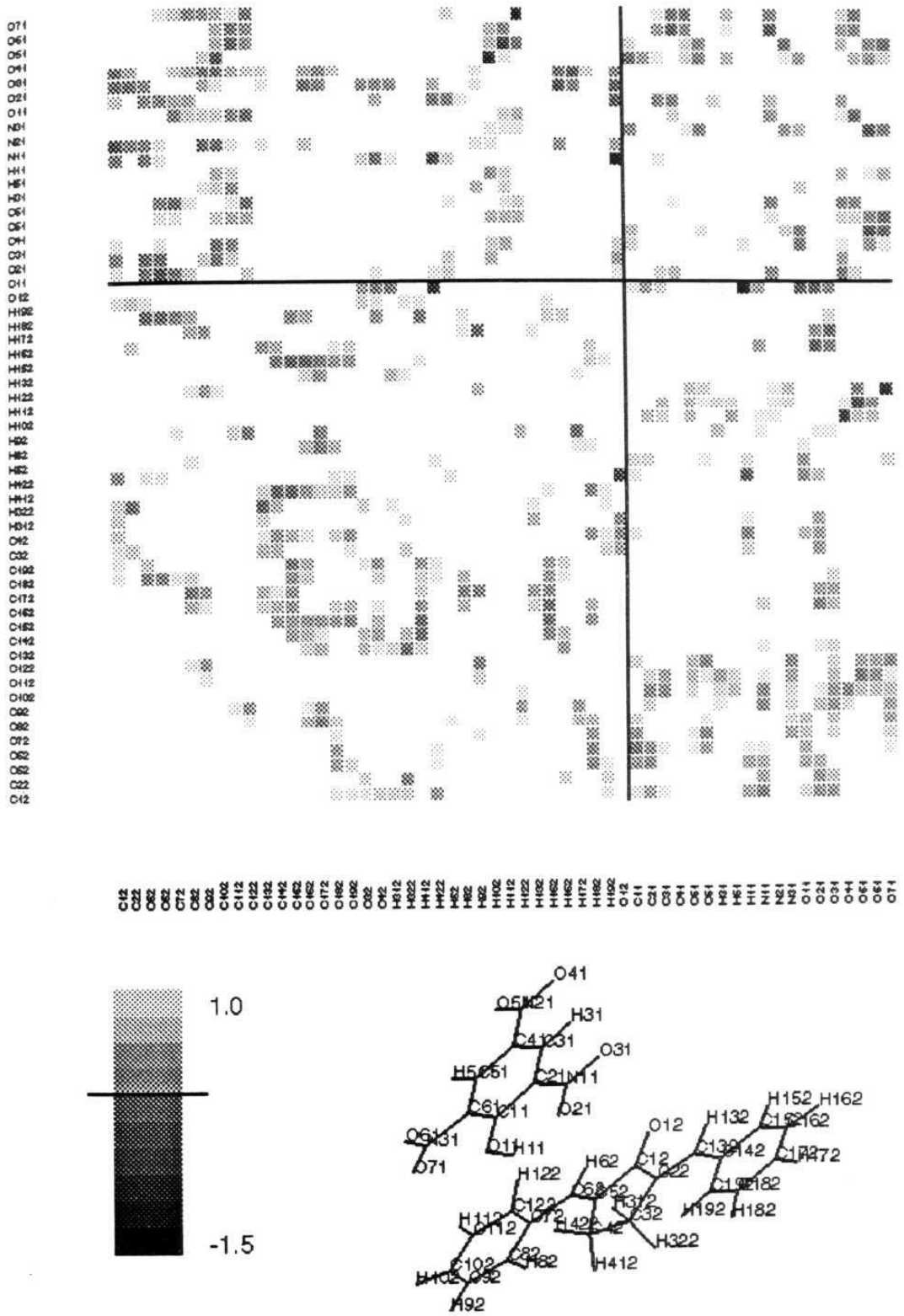

Figure **6a**. NIPMAT plot for complex **3f**. Compare with Figure 6b.

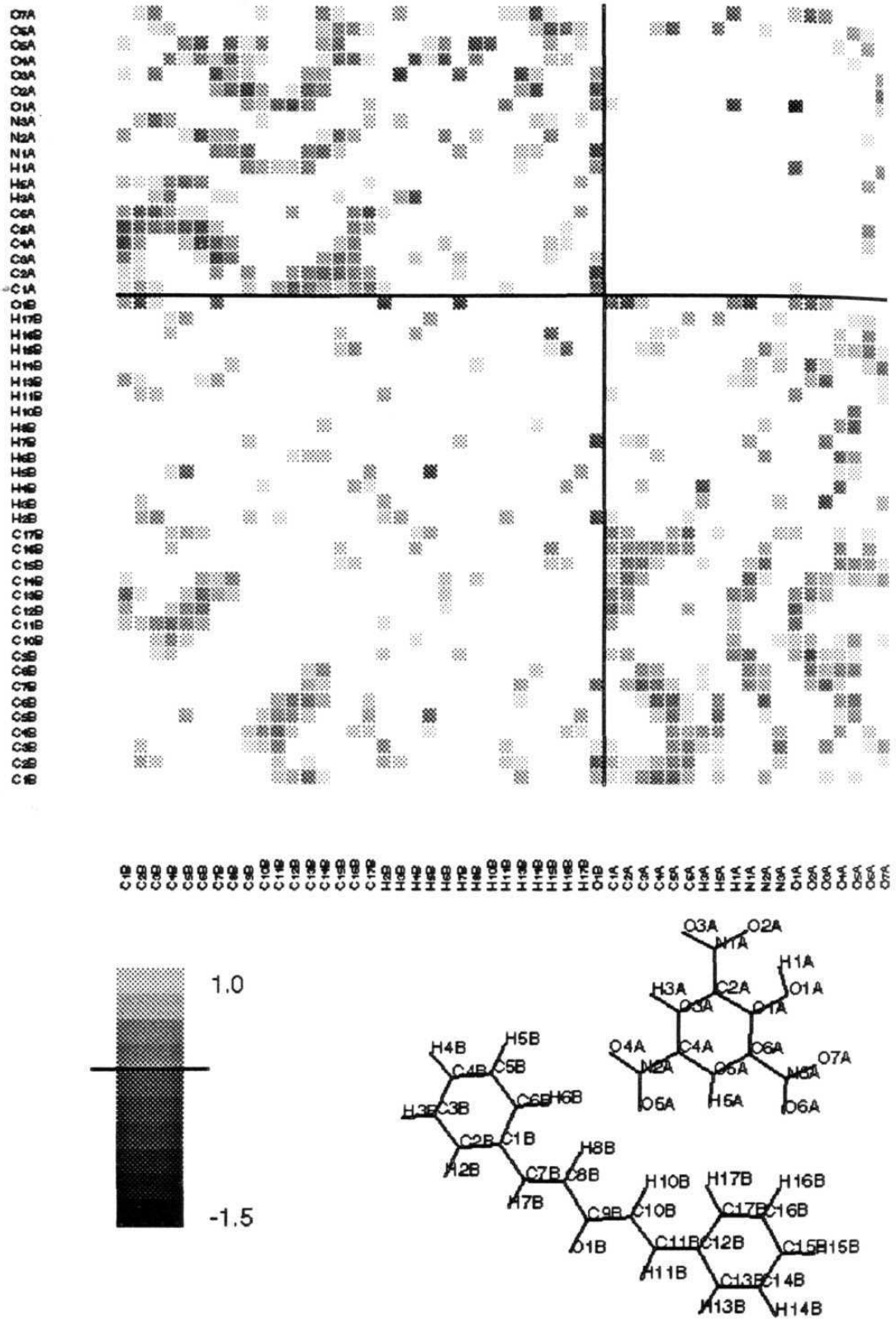

Figure 6b. NIPMAT plot for complex **3g**. Compare with Figure 6a.

takes the lead due to the presence of the relatively less acidic sp^3 C-H groups of compound **1b**.

6.2.3 π-π stacking

The formation of 1:2 molecular complexes **3a**, **3b**, **3c**, **3d** and **3e** from solutions containing equimolar amounts of **1** and **2** can be justified by considering π-π stacking. Molecule **1** contains two phenyl rings and can accommodate two molecules of **2**. It is well known that aryl groups prefer to interact either edge-to-face or offset, face-to-face orientation[12] and compound **2a** forms charge transfer complexes with aromatic compounds.[13] Recently, compound **2a** also has been used as a guest for chiral molecular tweezers through these interactions.[14] It is found that all the above molecular complexes of **2a** and **2b** forms these interactions with slightly offset stacking as shown in Fig. 7. The centroid to centroid distances (X1X2) and plane to plane angles (P1P2) in these complexes range from 3.64 to 4.83 Å and 0.81 to 10.4° respectively. The values of X1X2 and P1P2 are given in Table 2. However, these stacking interactions are different in complexes **3f** and **3g**. Complex **3f** is stabilised by π-π interactions and herringbone interactions whilst complex **3g** is stabilised by only π-π interactions. The change in the stoicheometries of complexes **3f** and **3g** from those of **3a**, **3b**, **3c**, **3d** and **3e** may be a consequence of changes in the interactions between aromatic rings.

a

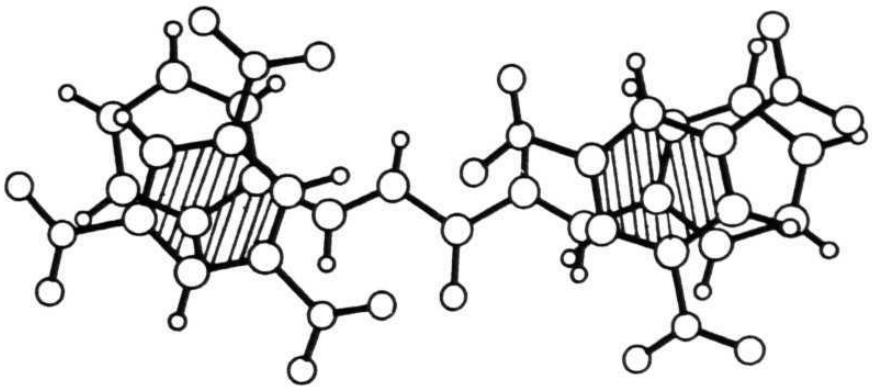

b

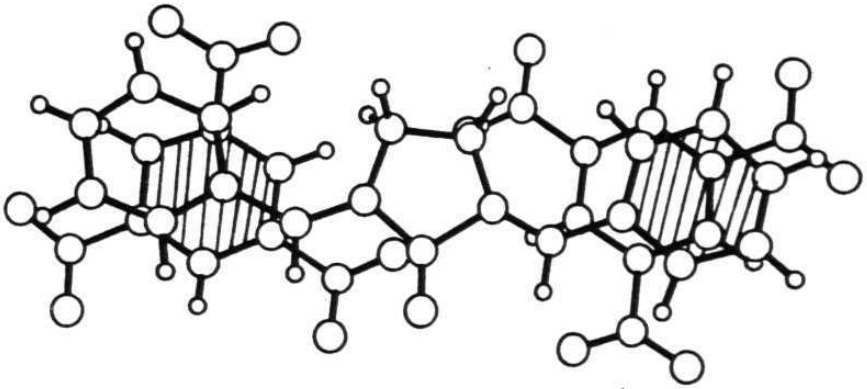

c

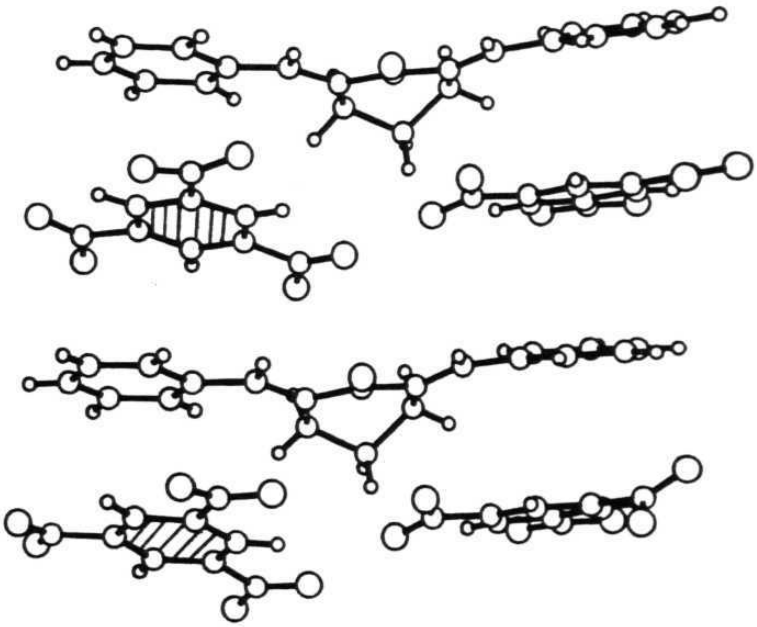

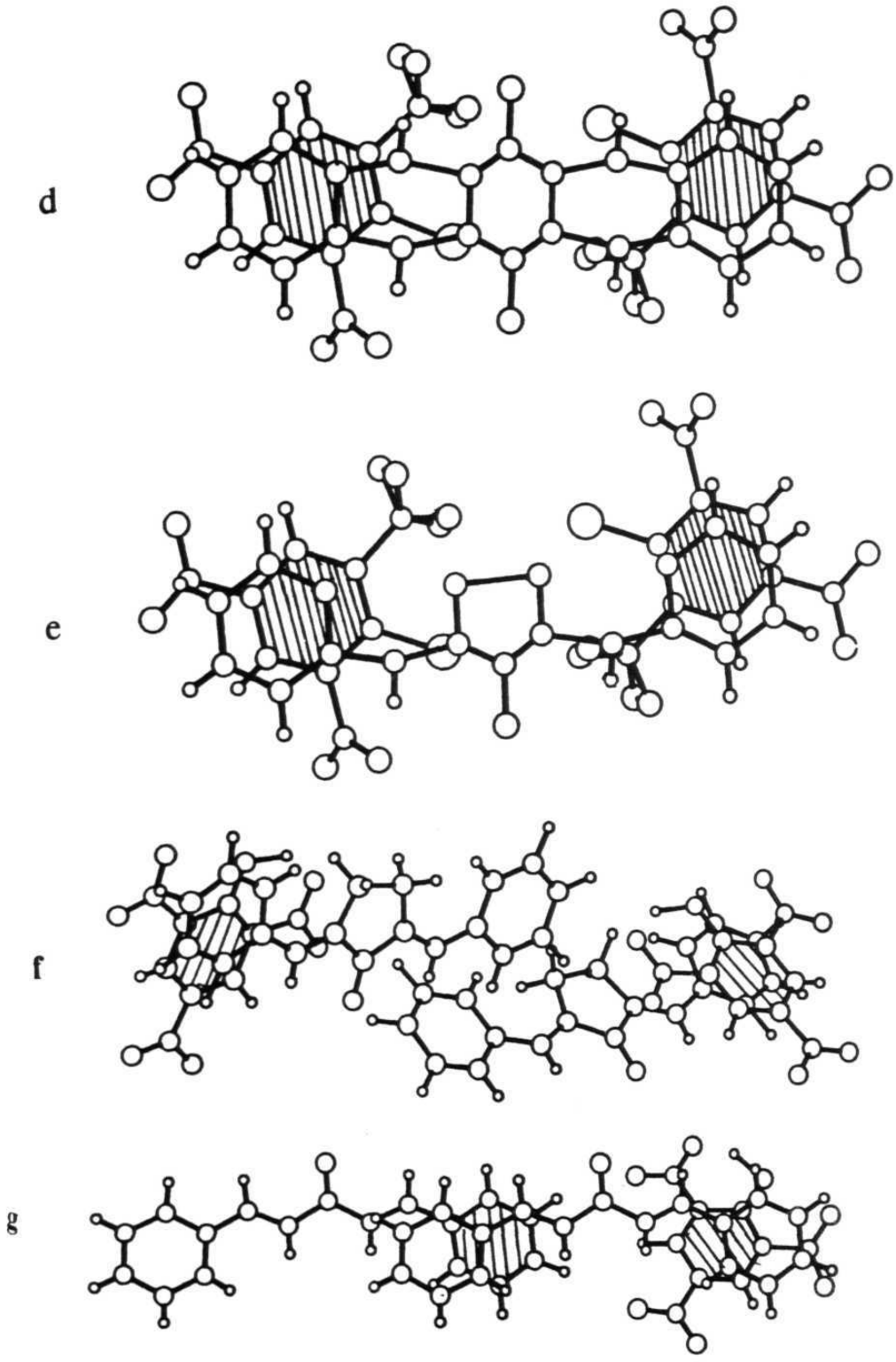

Figure 7. Stacking interactions in complexes **3a**, **3b**, **3c**, **3d**, **3e**, **3f** and **3g** represented as a, b, c, d, e, f and g respectively. The phenyl rings of trinitrobenzene derivatives are shaded for clarity. Note the herringbone interaction in f.

Table 2: Geometrical parameters of π-π interactions in the complexes under study.

Complex	X1X2 (Å)	P1P2 (°)
3a	3.66	3.85
	3.78	4.99
3b	3.85	5.44
	3.81	2.29
3c	3.64	5.87
	3.84	7.29
	3.68	5.59
	3.77	10.06
	3.78	10.02
	3.88	8.38
3d	3.67	2.44
	3.86	2.42
3e	3.85	0.81
	3.69	0.81
3f	4.83	4.73
3g	3.86	10.44
	4.41	6.83

6.2.4 CSD Studies:

The CSD was searched for C-H···O hydrogen bonded interactions III, IV and VIII and O···Cl interactions IV to understand their nature and to ascertain their frequency of occurrence which would indicate their robustness. There are 189, 159, 44 and 18 crystal structures are present for III, IV, VIIIa and VIIIb respectively.

6.2.4.1 Binding features of III, IV, VII and VIII

III is present 205 times in 189 crystal structures. Fig. 8a is the scattergram of C(7)···O(1) versus C(3)···O(5) distances to show the centrosymmetric nature of III. The off-diagonal points are from the structures which have two molecules in the asymmetric unit, in the other words these are formed between symmetry independent molecules. Fig. 8b is the scattergram of C-H···O angle versus C···O distances for III. From this plot it can be seen that many of the C-H···O hydrogen bonds are clustered in the strong hydrogen bonds region i.e. in between the C···O distance of 3.35 to 3.65 Å and C-H···O angle of 155-175^{o}.

There are 173 hits in 159 crystal structures for IV. Fig. 9a is the scattergram of C(9)···O(1) versus C(4)···O(6) and indicates again the centrosymmetric nature of IV. Fig. 9b is the scattergram of C-H···O angle versus C···O distances which are involved in IV. Here too the C-H···O hydrogen bonds are clustered in between C···O distances of 3.25 to 3.55 Å and C-H···O angles of 140 to 160^{o}.

The halogen and O-atom contacts are well studied[15] and especially in the case of iodo and nitro groups O-atom, these interactions have been used in the design of crystal structures.[16] There is a total of 19 crystal structures present for ortho chloro nitro aromatic compounds. To retrieve VII, the bonafide O···Cl interaction has been considered only when the O to Cl distance is in between 2.8 to 4.0 Å. There are a total of 82 hits for

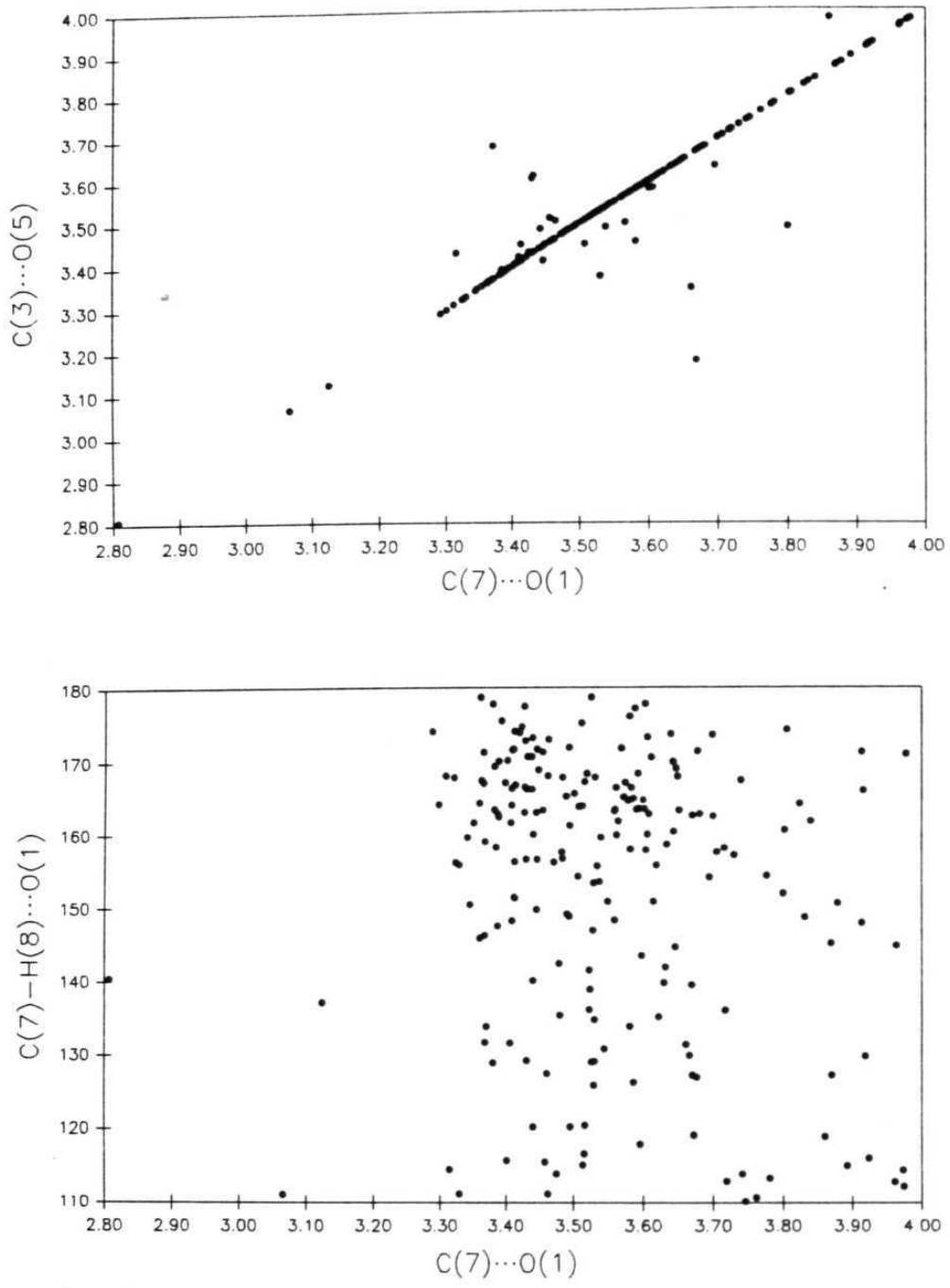

Figure 8. (a) Scatterplot of C···O distances of III to show its centrosymmetric nature (b) Scatterplot of C···O distances versus C-H···O angles in III. Notice that the points are clustered between C···O distances of 3.4 Å to 3.6 Å and C-H···O angles of 155° to 175°.

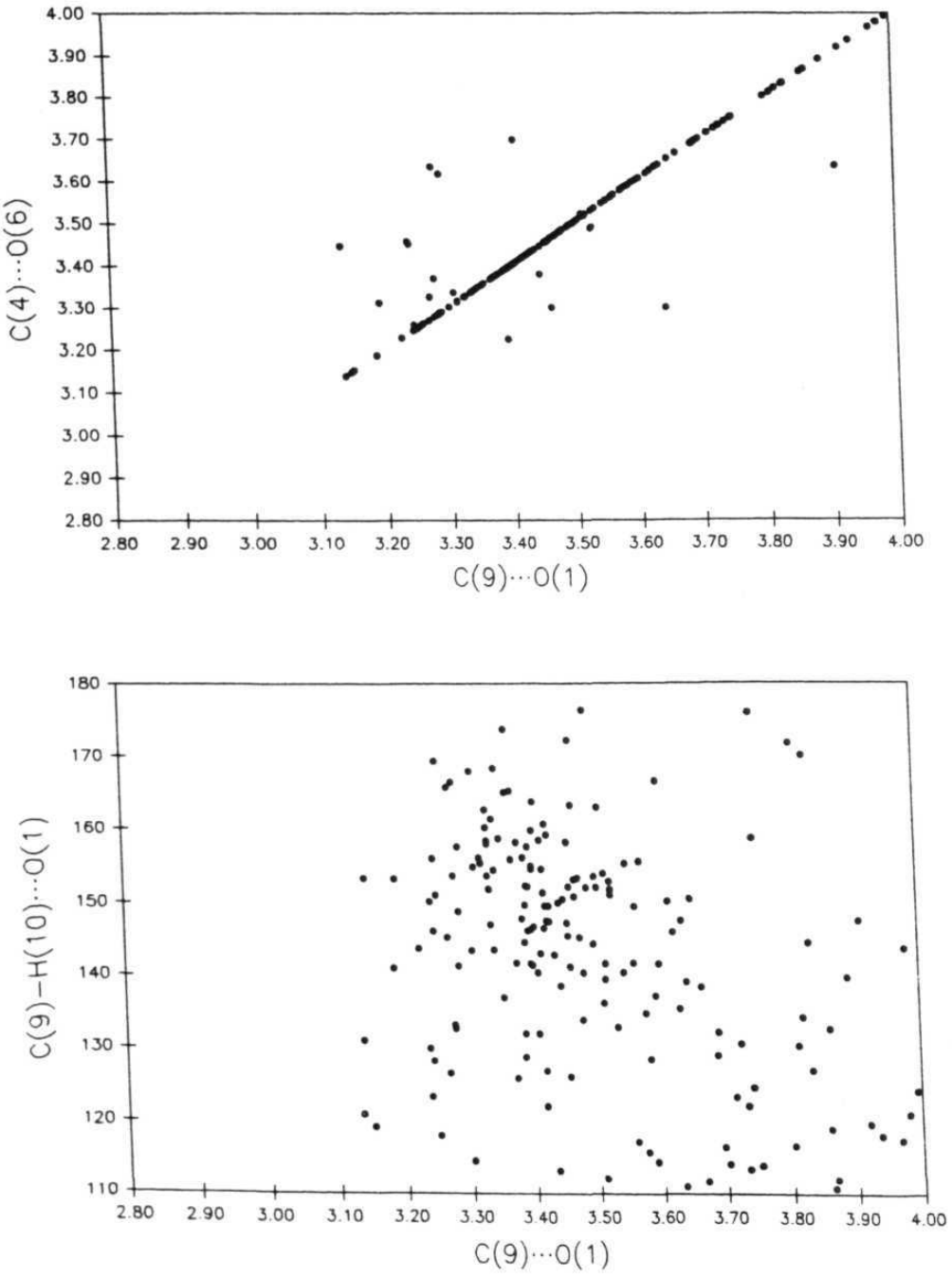

Figure 9 (a) Scatterplot of C···O distances in IV to show the centrosymmetric nature of synthon IV (b) Scatterplot of C···O distances versus C-H···O angles in synthon IV. Notice that the points clustered between C···O distances 3.25 Å to 3.55 Å and C-H···O angles140^{o} to 160^{o}.

VII from 17 crystal structures. Out of these 82 hits, 40 hits corresponds to 2,4,6-trichlorotrinitrobenzene which will be discussed in the next section. The greater number of hits for this structure are due to the presence of three symmetry independent molecules and also to the presence of pattern IX which is formed based on a unsymetrical pattern X. Fig. 10 is the scattergram of Cl(10)···O(1) versus Cl(5)···O(6). From this figure it is clear that the VII can exist either as a symmetrical or as an unsymmetrical pattern.

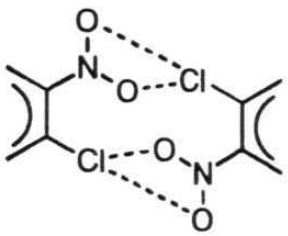

IX

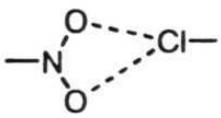

X

The C-H···O hydrogen bonded pattern VIIIa which is observed in complex **3g** is found 47 times in 44 crystal structures and VIIIb was found 18 times in 18 crystal structures. Fig. 11a is the scattergram of C(15)···O(1) versus C(7)···O(9). This plot shows the centrosymmetric nature of VIIIa. Fig. 11b is the scattergram of C···O distances versus C-H···O angles. Open circles are the C-H···O's of VIIIa and filled circles are C-H···O's of VIIIb. The C-H···O hydrogen bonds of VIIIa are clustered between 3.35 to 3.50 Å and C-H···O angles of 145 to 155^{o} and whilst for VIIIb they are clustered between C···O distances of 3.15 to 3.35 Å and

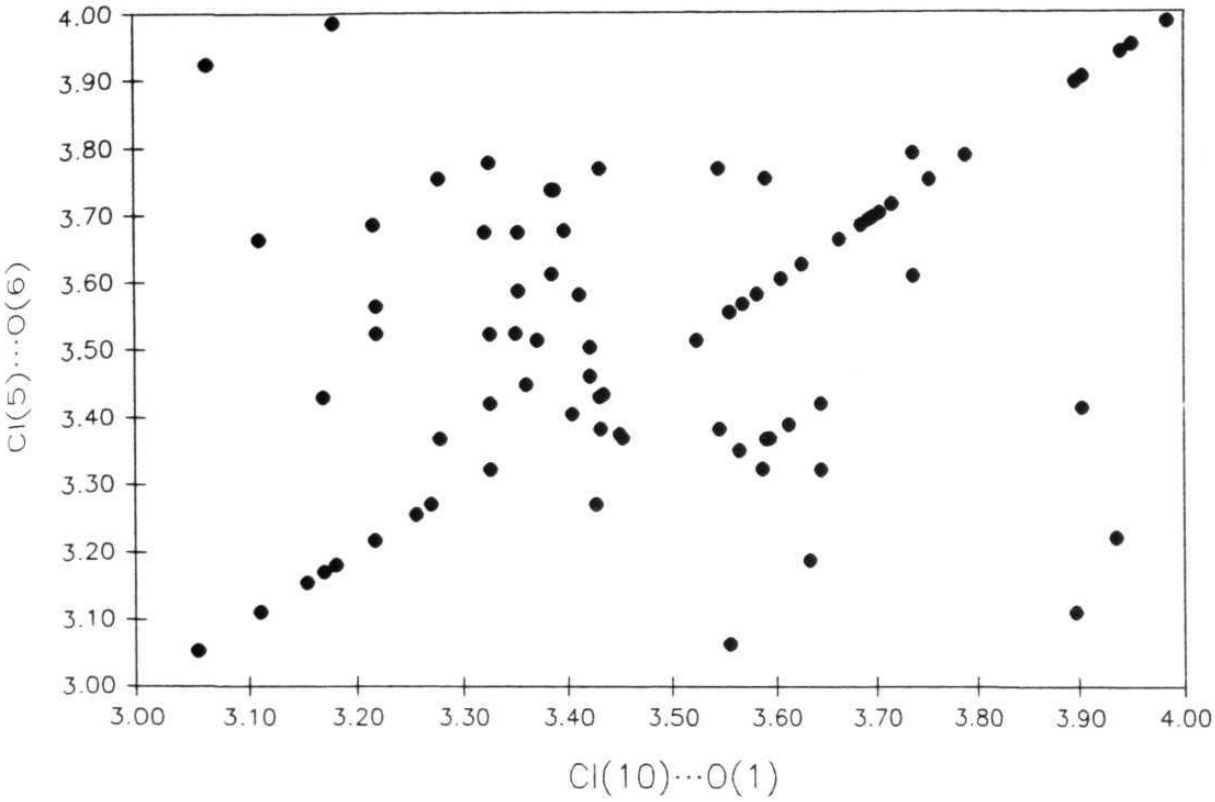

Figure 10. Scatterplot of Cl(10)···O(1) versus Cl(5)···O(6) distances of VII. It may be noted that VII can also exists in a noncentrosymmetric variation in some of the cases.

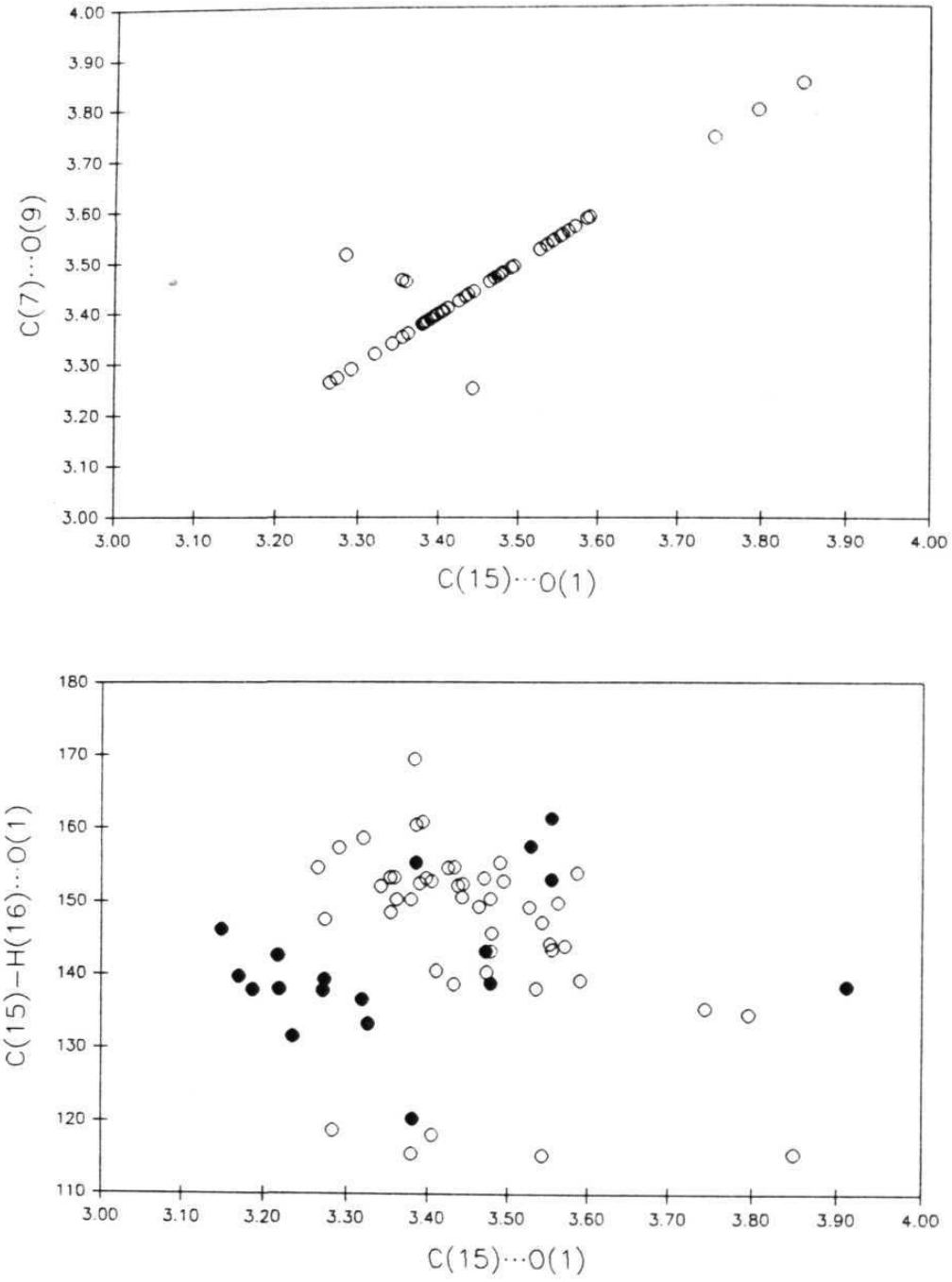

Figure 11. (a) Scatterplot of C(7)···O(9) and C(15)-O(1) distances of VIIIa to show the centrosymmetric nature of VIIIa. (b) Scatterplot of C···O distances versus C-H···O angles in VIIIa and VIIIb. Open circles represents the C-H···O hydrogen bonds of the synthon VIIIa and closed circles represent that of VIIIb.

135 to 145°. These distributions of C···O distances and C-H···O angles indicate that many of the C-H···O's involved in VIIIb are shorter and less linear than the C-H···O bonds in synthon VIIIa. This shows the greater acidic nature of the sp^2 C-H over aromatic C-H. Comparison of this figure with Fig. 8b and 9b, reveals that the C-H···O hydrogen bonds involved in VIII are less linear than those of I and III.

6.2.4.2 III, IV, V and VIII as supramolecular synthons in crystal engineering.

In this section, a few occurrences of III, IV, V and VIII will be discussed to highlight the different aspects these synthons. For this exercise, molecules **4-6** were selected.

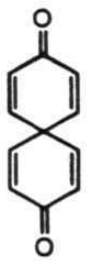

4

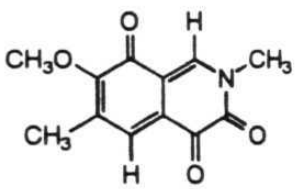

5

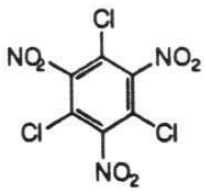

6

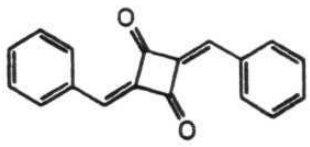

7

Synthon III is the C-H···O variation of the N-H···O hydrogen bonded synthon IX which is formed by cis amides. It is known that the crystal structure of benzoquinone is composed with III to form a sheet structure. Now the crystal structure of **4** where the recognition components which are required to form I are tetrahedrally disposed will be considered.[17] Fig. 12 is the crystal structure of compound **4**. This

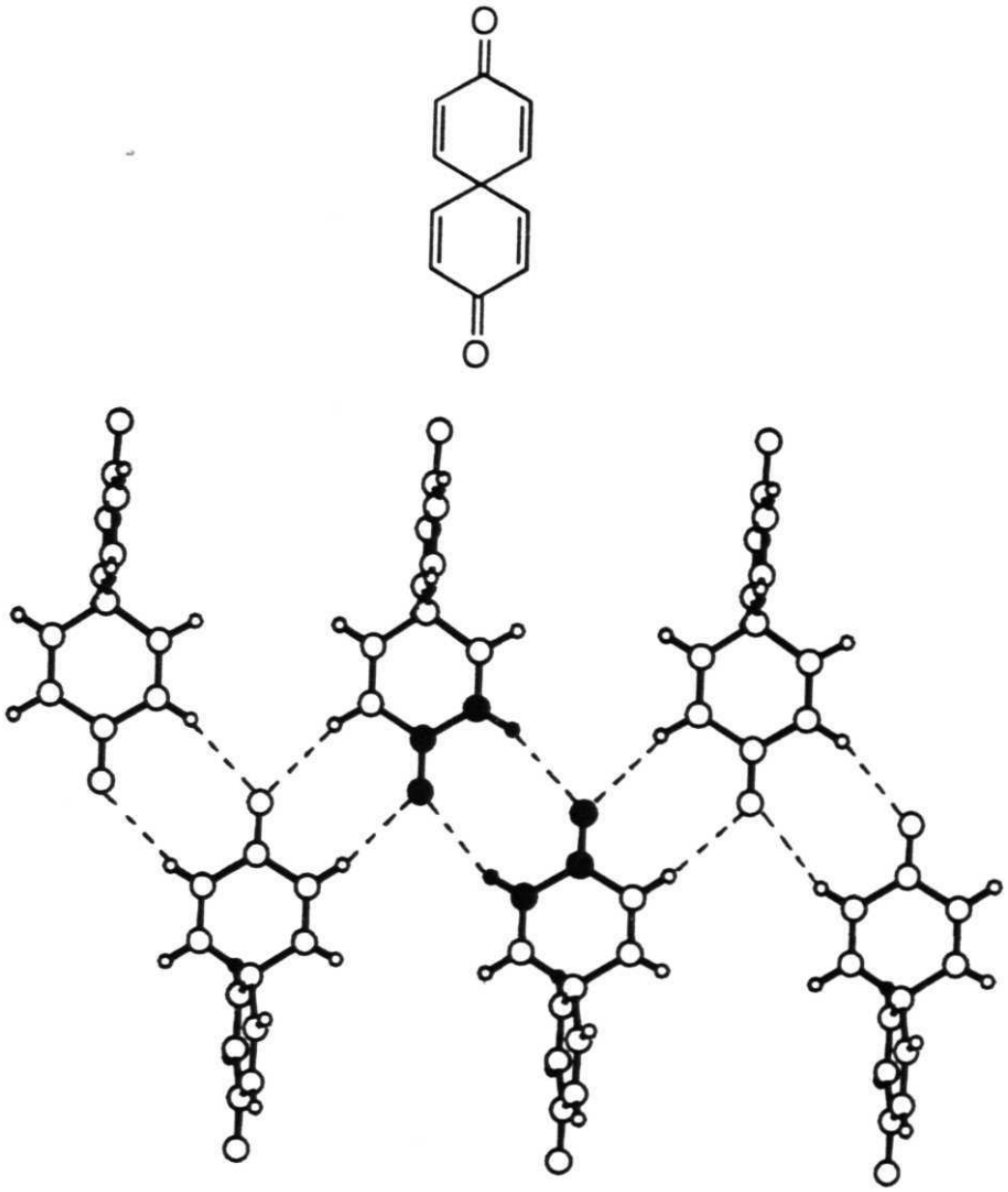

Figure 12. Crystal structure of **4** to show the zigzag chain of molecules joined by C-H···O hydrogen bonded synthon III. In this compound, III is formed between two symmetry independent molecules.

compound forms III and then these molecules are arranged in the zigzag chains similar to those found in secondary amides. The crystal structure of **5** is expected to form a linear chain with IV. Fig. 13 is a crystal structure of **5**. It forms a linear chain with IV as expected.[18]

The crystal structure of **6** (Fig. 14) is of interest as it maintains three fold symmetry with the three nitro groups nearly perpendicular to the plane of the phenyl rings.[19] This arrangement leads to the formation a rosette like structure with VII. The crystal structure of **7** is considered as it contains two molecular components which can lead to form a chain structure through C-H···O hydrogen bonded synthon VIII. Fig. 15 is the crystal structure of **7**.[20] Interestingly in this structure, molecules are linked with VIII to form a linear chain as anticipated. These CSD studies suggest that one can use III, IV, VII and VIII as supramolecular synthons in crystal engineering experiments.

6.3 Conclusions

This work shows that the C-H···O hydrogen bonds can be utilised to design three point supramolecular synthons reliably. The C-H···O hydrogen bonds involved in multi-point synthons are stronger than the other C-H···O hydrogen bonds in the structures. The presence of strong hydrogen bonding functional groups may influence the C-H···O bonded

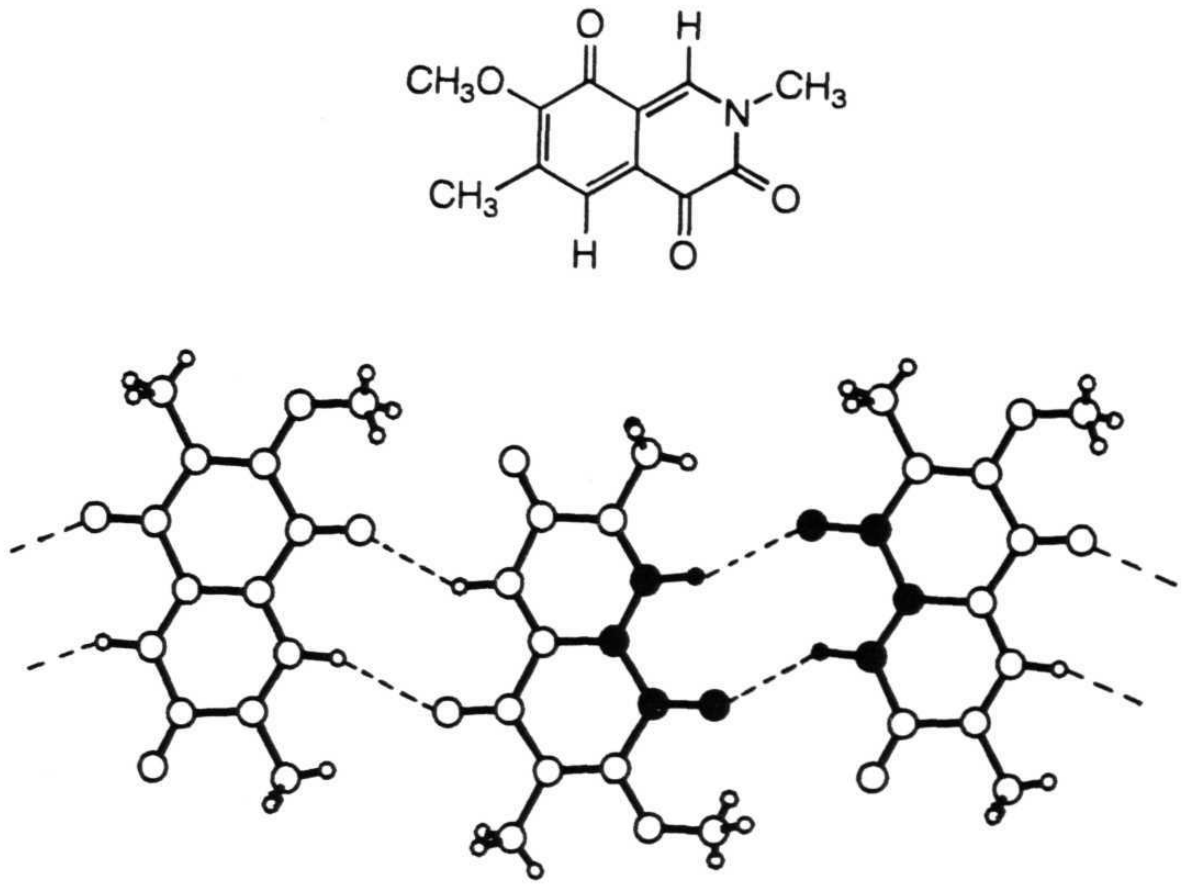

Figure 13. Crystal structure of **5** to show the linear chain of molecules joined by synthon IV

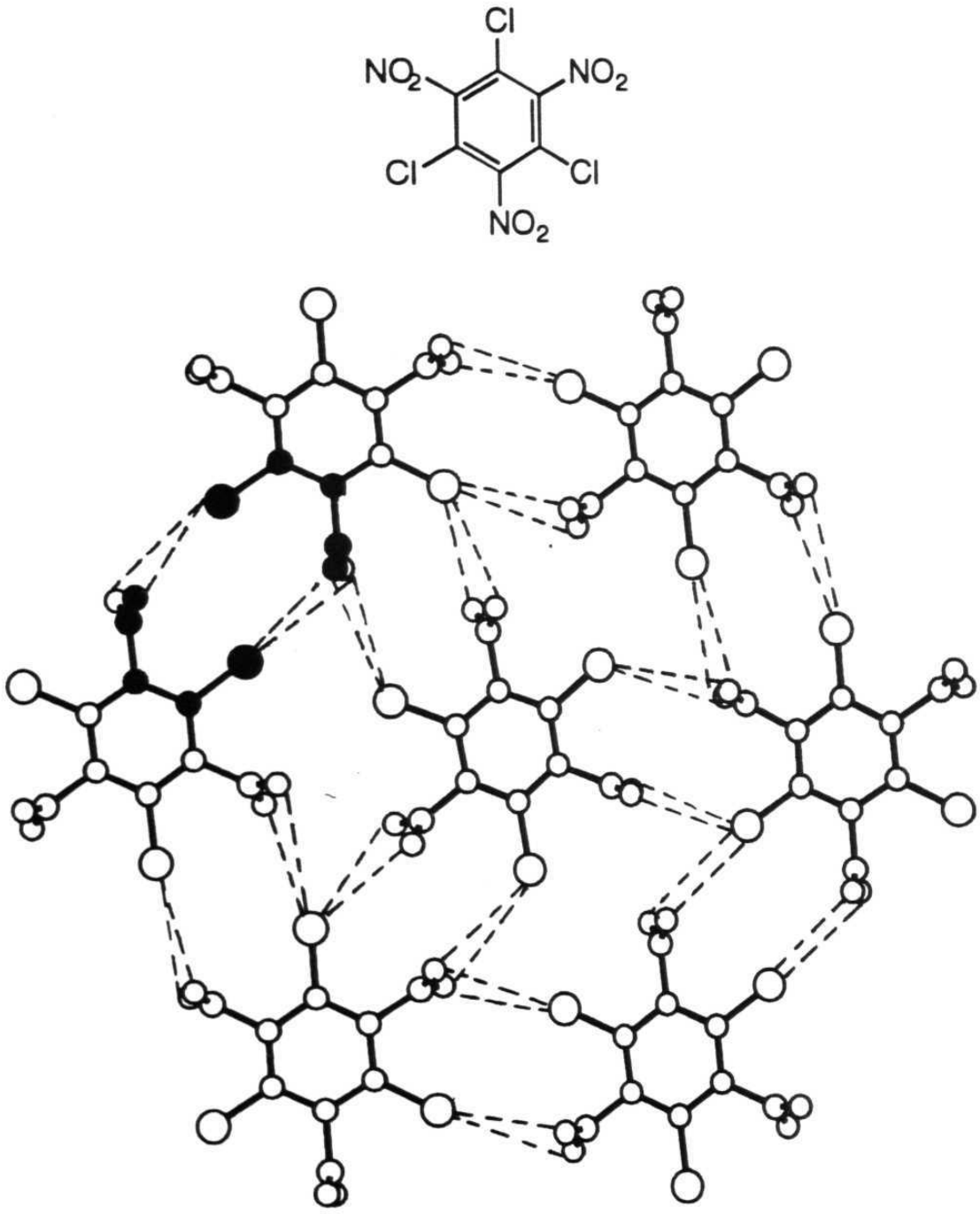

Figure 14. Crystal structure of **6** to show the hexagonal network of molecules linked thorough O···Cl interactions synthon VII.

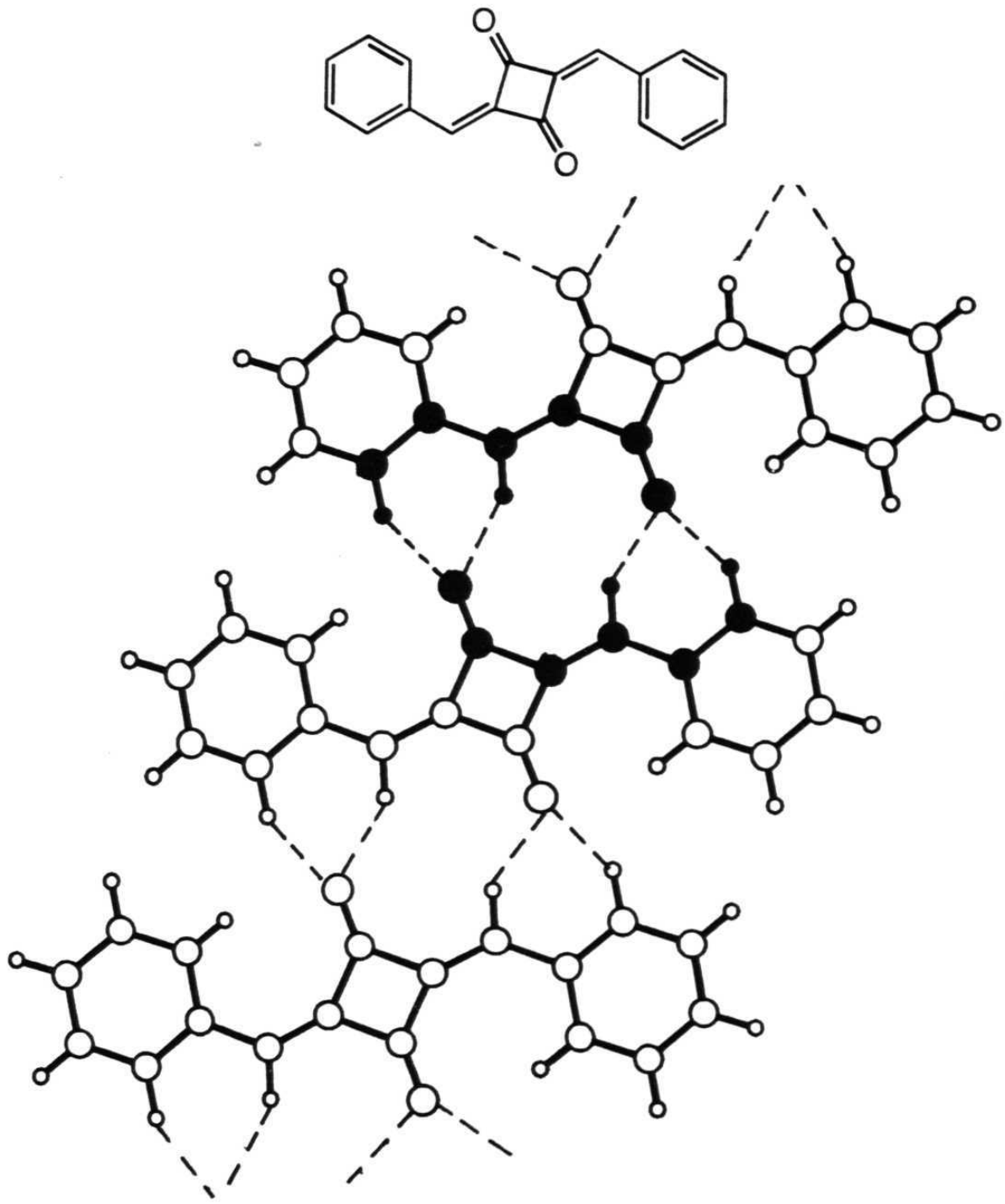

Figure 15. Crystal structure of **7** to show the linear arrangement of molecules linked through C-H···O hydrogen bonded synthon VIIIa.

recognition, but if the strong hydrogen bonds are optimised properly, the recognition through C-H···O hydrogen bonds would be just as effective. This work also shows that the π-π interactions are important in determining the stoicheometry of molecular components and in turn in governing the crystal packing.

6.4 Experimental Section

6.4.1 Material preparation

1,3,5-trinitrobenzene, **2a** was prepared in three steps from 2,4-dinitrotoluene. Nitration of 2,4-dinitrotoluene with fuming HNO_3 and 100% H_2SO_4 gave 2,4,6-trinitrotoluene which was oxidised with $K_2Cr_2O_7$ to give 2,4,6-trinitrobenzoic acid.[21a,21b] This compound was decarboxylated in the presence of NaOH to give compound **2a**.[21c] Picric acid, **2c** was purchased and picryl chloride **2b** was prepared by the reaction of **2c** with $POCl_3$ and N,N-diethylaniline.[22] The dibenzylideneketones were prepared by the condensation reaction of 2 moles of benzaldehyde with 1 mole of the corresponding ketones.[23] Compound **1d** was prepared by the bromination of **1b** at 3,4 positions with NBS/CCl_4 and followed by the debromination with Zn/MeOH.[24] Pentacenedione was prepared by the condensation reaction of 1,4-cyclohexanedione and phthalaldehyde.[25]

6.4.2 Crystals Preparation

Yellow crystals of the 2:1 complex **3a**, **3b** and **3c** were obtained from an equimolar solution of **2a** and **1a**, **1b** and **1c** in 1:1 dichloromethane-hexane respectively. Similarly, yellow crystals of the complexes **3d**, **3e**, **3f** and **3g** were obtained from an equimolar solution of the molecular components in 1:1 chloroform-hexane.

6.4.3 X-ray Crystallographic Studies

Data were collected for all the complexes on an Enraf-Nonius FAST area detector with a rotating anode X-ray source. The structure solution for all the complexes were carried out with the SHELXS86[26] program. Refinements were carried out with the SHELX76 for complexes **3a** and **3b** and for the remaining complexes, SHELXL93 program was used.[27]

Complex **3c** crystallises in the triclinic space group $P\bar{1}$. The structure solution is obtained in the space group P1 as it fails to solve in space group $P\bar{1}$. In complexes **3d** and **3e**, the dibenzylideneketone moiety and one of the nitro groups are disordered. All the non H-atoms were refined anisotropically. All the H-atoms except in complex **3f** were located from difference Fourier maps and refined isotropically in the final stages of the refinement because this is a study of C-H···O hydrogen bonding. The hydrogen atoms of complex **3f** are fixed geometrically and refined through

the riding model. The crystallographic information, tables of coordinates and thermal vibrational parameters for all the complexes are given in Appendix A-5.

6.4.4 CSD Experimental

Data were retrieved from the Cambridge Structural Database (CSD, Version 5.08).[28] Screens -28, 34, 85 and 88 were used to eliminate organometallic entries and unmatched chemical and crystallographic connectivities. Entries with R-factor greater than 0.10 and disordered structures were also excluded. A C-H···O geometry was considered a bonafide hydrogen bond when the C···O distance is less than 4.0 Å and C-H···O angle is between 110^{o} to 180^{o}. Geometrical calculations were performed using QUEST3D-GSTAT, an automatic graphical non bonded search program of the CSD.

6.5 References

1. (a) G.R. Desiraju, *Angew. Chem., Int. Ed. Engl.,* 1995, **34**, 2311. (b) *Perspectives in Supramolecular Chemistry: The Crystal as a Supramolecular Entity*, Vol. 2, Ed. G.R. Desiraju, Wiley, Chichester, **1996**. (c) G.R Desiraju, *Comprehensive Supramolecular Chemistry*, Vol.6, Eds: D.D. MacNicol, F. Toda, R. Bishop, Pergamon, Oxford, **1996**, p. 0000, in the press.

2. (a) J.A.R.P. Sarma and G.R. Desiraju, *Acc. Chem. Res.,* 1986, **19**, 222; (b) G.R. Desiraju, *Acc. Chem. Res.,* 1991, **24**, 290; (c) G.R. Desiraju, *Acc. Chem. Res.,* 1996, **29**, 000 (in press); (d) D.S. Reddy, B.S. Goud, K. Panneerselvam and G.R. Desiraju, *J. Chem. Soc., Chem. Commun.,* 663, 1993; (e) L. Shimoni, H.L. Carrell, J.P. Glusker, M.M. Coombs, *J. Am. Chem. Soc.* 1994, **116**, 8162; (f) D. Braga, F. Grepioni, K. Biradha and G.R. Desiraju , *J. Chem. Soc., Dalton Trans.* 1996, 000 (in press).

3. J.-M. Lehn, *Supramolecular Chemistry*, VCH, Weinheim, 1995. 161-179.

4. (a) T.J. Murray and S.C. Zimmerman, *J. Am. Chem. Soc.,* 1992, **114**, 4010; (b) G. Klebe, in *Structure Correlation, Volume 2.* Eds. H.-B. Bürgi and J.D. Dunitz , VCH, Weinheim, 1994, pp 549-551.

5. A.D. Burrows, C.-W Chan, M.M. Chowdhry and D.M.P. Mingos, *Chem. Soc. Rev.,* 1995, 330.

6. G.M. Whitesides, E.E. Simanek, J.P. Mathias, C.T. Seto, D.N. Chin, M. Mammen and D.M. Gordon, *Acc. Chem. Res.*, 1995, **28**, 37.

7. S.K. Kearsley and G.R. Desiraju, *Proc. Roy. Soc. (London), Ser. A*, 1985, **397**, 157.

8. H. Nagata, Y. In, M. Doi and T. Ishida, *Acta Crystallogr., Sect. B*, 1995, **51**, 1051.

9. V. Agafonov, P. Dubois, F. Moussa, J.M. Cense and S. Toscani, *J. Chem. Soc., Perkin Trans., 2,* 1994, 2007.

10. G.A. Jeffrey and W. Saenger, *Hydrogen Bonding in Biological Structures,* Springer-Verlag, Berlin, 1991, pp. 24.

11. R.S. Rowland, *Amer. Cryst. Assoc. Abstracts*, 1995, **23**, 63 (Abstract 2a.5.B, Montreal Meeting).

12. C.A. Hunter and J.K.M. Sanders, *J. Am. Chem. Soc.,* 1990, **112**, 5525.

13. R. Foster, *Organic Charge-Transfer Complexes*, Academic Press, London, 1969, pp 113.

14. M. Harmata and C.L. Barnes, *J. Am. Chem. Soc.,* 1990, **112**, 5655; (b) M. Harmata, C.L. Barnes, S.R. Karra and S. Elahmad, *J. Am. Chem. Soc.,* 1994, **116**, 8392.

15. J.P.M. Lommerse, A.J. Stone, R. Taylor and F.H. Allen, *J. Am. Chem. Soc.,* 1996, **118**, 3108.

16. (a).V.R.Thalladi, B.S.Goud, V.J.Hoy, F.H.Allen, J.A.K.Howard and G.R.Desiraju, *Chem.Commun.,* 1996, 401; (b) F.H.Allen, B.S.Goud, V.J.Hoy, J.A.K.Howard and G.R.Desiraju, *J.Chem.Soc. Chem.Commun.,* 1994, 2729.

18. D.L. Cullen, B. Hass, D.G. Klunk,T.V. Willoughby, C.N. Morimoto, E.F.M. Junior, G. Farges, A. Dreiding, *Acta Crystallogr., Sect. B*, 1976, **32**, 555.

18. T. Hata, H. Fukumi, S. Sato, K. Aiba and C. Tamura, *Acta. Crystallogr., Sect. B*, 1978, **34**, 2899.

19. F. Gerard, A. Hardy, A. Becuwe, *Acta Crystallogr., Sect. C*, 1993, **49**, 1215.

20. B.M. Gatehouse, *Cryst. Struct. Commun.,* 1982, **11**, 365.

21. (a) H.D. William, H.D. Rosenblatt, W.G.B. Rosenblatt and L.C. Clifford, *J. Chem. Eng. Data,* 1975, **20**, 202. (b)A.I. Vogel, 'A Text-Book of Practical Organic Chemistry' 3rd ed., E.L.B.S., 758, 1975; (c) A.I. Vogel, ibid., 965, 1975

22. E.T. Borrows, J.C. Clayton, B.A. Hems and A.G. Long, *J. Chem. Soc.,* 1949, S190.

23. A.I. Vogel, '*A Text-Book of Practical Organic Chemistry*' 3rd ed., E.L.B.S., 709, 1975.

24. G.R. Desiraju and K.V.R. Kishan, *Ind. J. Chem.*, 1988, **27B**, 953.

25. W. Ried and F. Anthofer, *Angew. Chem.,* 1953, **65**, 601.

26. G.M. Sheldrick, SHELXS86, in *Crystallographic Computing 3;* ed. G.M. Sheldrick, C. Kruger and R. Goddard, Oxford University Press: Oxford, UK, 1985, pp.175-189.

27. (a) G.M. Sheldrick, SHELX76, Program for Crystal Structure Determination, University of Cambridge, England, 1976. (b) G.M. Sheldrick, SHELXL, An Integrated System for Solving, Refining and Displaying Crystal Structures from Diffraction Data, University of Gottingen, Germany, 1993.

28. F.H. Allen, J.E. Davies, J.J. Galloy, O. Johnson, O. Kennard, C.F. Macrae and D.G. Watson, *J. Chem. Inf. Comp. Sci.,* 1991, **31**, 204.

Chapter 7

Correlation of Biological Activity in β-Lactam Antibiotics with Woodward and Cohen Structural Parameters

7.1 Introduction

The importance of the CSD in studies of crystal engineering and structure correlation analysis has been discussed in Chapter 1. Chapters 2-5 have described the utility of the CSD in studies of various types of hydrogen bonds in organometallic crystals. This chapter deals with the CSD analysis of structure-activity relationship of β-lactams. The antibacterial activity of β-lactam compounds is attributed to the formation of a covalent bond between the amide carbonyl group of β-lactams and the active site serine residue of enzymes, which are termed penicillin-binding proteins (PBP). Bicyclic β-lactam antibiotics such as penicillins, cephalosporins, and thienamycins show wide-ranging therapeutic activity and have been in clinical use for the treatment of infectious diseases.[1-4] Their therapeutic efficacy is derived from their ability to disrupt bacterial cell-wall synthesis by inhibiting transpeptidase enzymes which catalyse the cross-linking reaction of D-alanyl peptides on peptidoglycan strands of the growing cell-wall.

The penicillin recognising enzymes such as carboxypeptidases, transpeptidases and β-lactamases have been co-crystallised with antibiotics to study the role of amino acid residues in the formation of the initial non-covalent complex and acyl-enzyme intermediate.[5-8] For example, the crystal structure of the complex of D-Alanyl carboxypeptidase-

transpeptidase from *Streptomyces* R61 and β-lactam shows that binding site sequence is Val-Gly-Ser-Val-Thr-Lys.[5]

The biological activity of β-lactam antibiotics has been correlated with several geometrical parameters such as h, ΣN, r and c. The h and c parameters are represented in Scheme 1. Among these parameters h is well known as the Woodward parameter, that is the distance (height of pyramid) of the N-atom from the plane containing the three adjacent carbon atoms on the bicyclic β-lactam skeleton.[9,10] This parameter is important because it is a measure of amide resonance which can influence the C-N bond strength. If h~0.25-0.50, the strength of the C-N bond is of intermediate value for optimal antibacterial activity. If the h value is less than 0.05Å, the C-N bond is too strong, it will be unreactive and covalent bond formation with the serine residue will not occur. If it is too weak, the antibiotic may be destroyed by reaction with random nucleophiles before it can reach the site of action. The parameters ΣN and r represents the sum of the bond angles at N-atom and C-N bond distance respectively. The parameter is ΣN geometrically related to the h. The parameter r is the C-N bond distance which again depends on the amide bond resonance. Even though ΣN and r are geometrically related to h, they also have been widely used to correlate the biological activity of the β-lactams.[11,12]

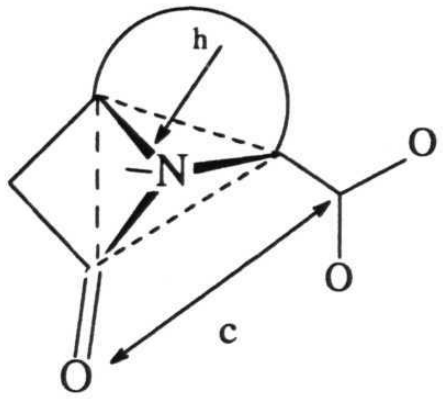

Scheme 1: Representation of Woodward height-of-pyramid parameter h and the Cohen distance parameter c.

The parameter c is independent of the chemistry and geometry of the β-lactam skeleton and was introduced by Cohen.[12] It is defined as the distance between the amide O-atom and C-atom of the carboxylate functional group. Cohen studied conformational changes in the thiazolidine ring of penicillins and its effect on activity. It was shown that a pseudo-equatorial orientation of the acidic carboxyl group, wherein it is nearer to the β-lactam carbonyl O-atom, is decisive in promoting antibiotic activity. A three-dimensional conformational analysis in nine penicillins, cephalosporins and penems showed that the c value lies in the range 3.0-3.9Å for six active structures, as compared to a higher range of 4.1-4.3Å for the three inactive compounds. This value c, is referred to as the Cohen parameter. Thus, Woodward's h parameter ascribes biological activity to the chemical reactivity of the amide bond, whereas Cohen's c parameter lays emphasis on the 3-dimensional conformation of the antibiotic molecule.[13]

There have been numerous attempts in correlating the Woodward parameter, h or the Cohen parameter, c with activity in the search for potent and effective antibiotics. However, all these studies are somewhat limited in their scope and predictability. Firstly, all such studies have used either one or the other of the two independent parameters, h and c. Secondly, the number of examples considered to propose the utility and test the validity of these parameters has always been limited to a small and chemically homogeneous group. In this regard the CSD has been used to analyse the structure activity relationship of β-lactam skeletons.[14,15] The role of small-molecule crystallography and the utility of CSD in elucidating drug-receptor interactions has been well established.[16,17]

In this chapter the following questions will be addressed.

(i) What are the structural features which lead to high activity and potency?

(ii) Why are many molecules with 'favourable' h and c values devoid of antibacterial action?

(iii) Is a molecule inactive because of poor recognition by PBP, or because of inherently low chemical reactivity and possibly a different mechanism of action?

In order to answer these questions the CSD was searched for the β -lactam skeletons **1** and **2** systematically.

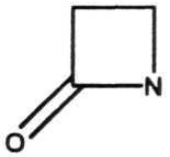

1

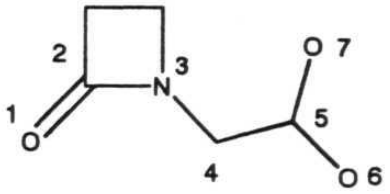

2

7.2 Results and Discussion

There is a total of 150 compounds for fragment **1**. Out of these, 114 compounds contain fragment **2**. The parameters h, ΣN, r and c values of these 114 compounds are given in Appendix A-6.

7.2.1 Histograms of h and c values

Figure 1a and 1b are the histograms of these 114 compounds for h and c values respectively. Figure 1a shows that h values are distributed in the range 0.00-0.60Å and shows three regions of preference. The monocyclic β-lactams (monobactams) are the least populated category with h values in the range 0.05-0.10Å. In compounds with intermediate h-values (0.20-0.25Å), the β-lactam ring is fused to a six-membered ring, for example cephalosporins. The highly populated region with h values between 0.40-0.50 corresponds to the penicillin class of antibiotics. There are very few antibiotics with h between 0.50-0.60Å (highly pyramidal N-atom). This region includes carbapenems and clavulanates. The latter are

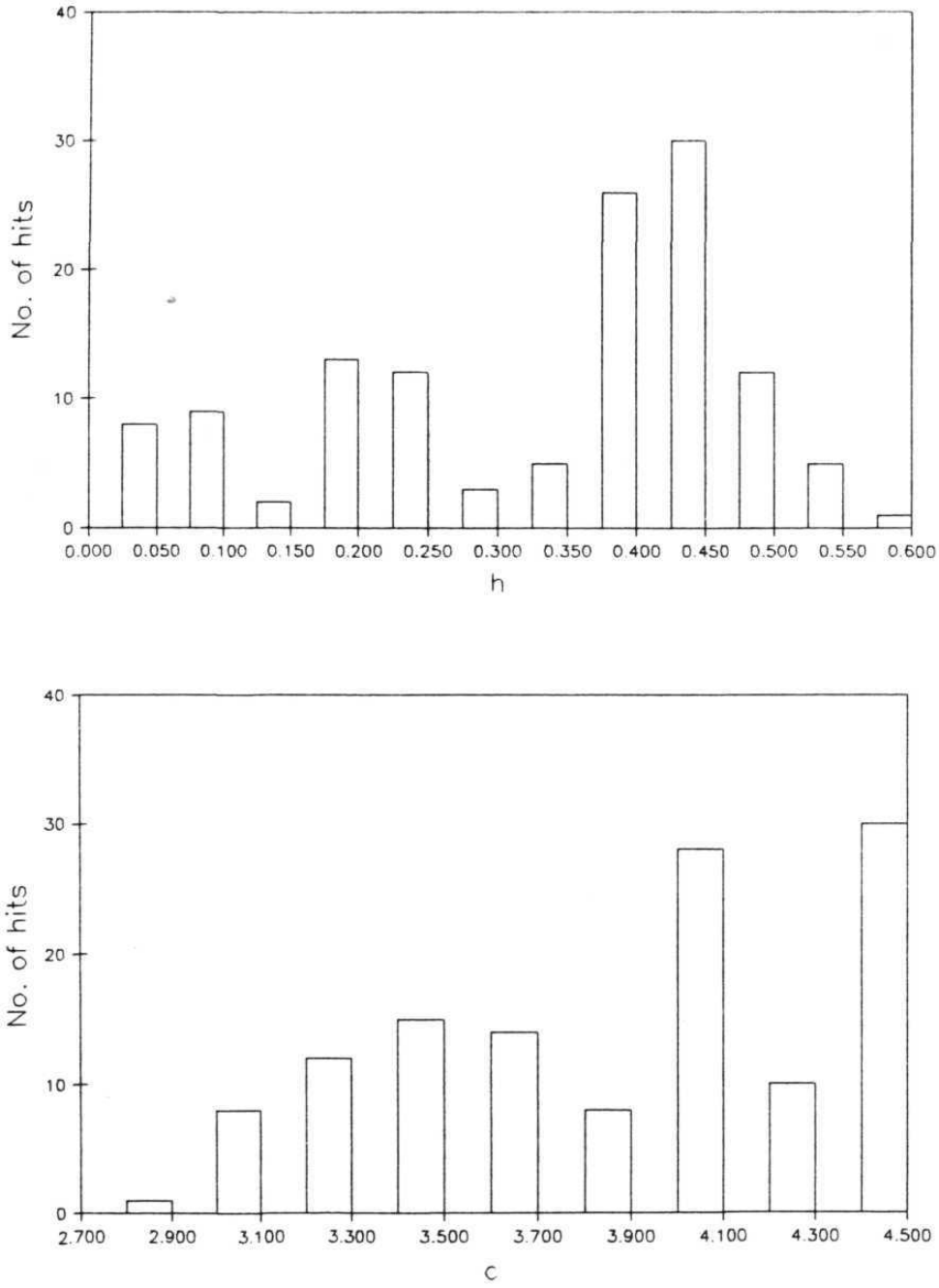

Figure 1. (a) Histogram of the Woodward h-values for the 114 structures in the present study. (b) Histogram of the Cohen c-values for the 114 structures in the present study.

potent β-lactamase inhibitors[18] which are themselves devoid of any antimicrobial activity, but are synergists in combination with β-lactam antibiotics. The populations of these three regions indicates that penicillins have been studied more extensively by crystallographers than cephalosporins and monobactams and the majority of penicillin-like structures in the histogram may well reflect the fact that they are the oldest class of antibacterial agents (pre-1940s). The emergence of cephalosporins (1950s), cephamycins, penems, carbapenems, oxacephems, clavulanates (1970s), and monobactams (1980s) in later years as chemotherapeutic agents[3,4] is reflected in the fewer number of crystal structures for these skeletons in the database.

Examination of Fig 1b reveals that the number of structures with c value between 3.0-3.9Å (active range as defined by Cohen) are less than half of the total structures (114) retrieved. More than 60 structures have c in the range 4.0-4.5Å with local maxima around 4.0 and 4.4Å. While these values correspond to the inactive region as defined by Cohen, many of these compounds are clearly active, such as penicillin G and clavulanic acid. It is likely that this limitation in Cohen's classification arose from the fact that too small a number (nine) of known active and inactive compounds was studied. This highlights, in general, the problem with using limited and specialised data samplings in statistical studies of structure-activity relationships. The ever-increasing size of the CSD,

makes it the method of choice for analysis whenever geometries of small-molecules are sought to be related to chemical or biochemical activity. [19]

7.2.2 Correlation between the geometrical parameters h, ΣN, r and c values:

Figures 2a and 2b are the scattergrams of h versus ΣN and h versus r respectively. Figure 2a shows that the ΣN value increases as h value increases. Conversely, Figure 2b shows that the r value decreases as the h-value increases. These figures reveal the geometrical relationship between h, ΣN and r parameters. In conclusion, all these three parameters are chemically equivalent and conveys the same information. Hence, the present study is confined to only h among these three parameters.

It may be noted that the h parameter is indicative of the chemical changes in the molecule while the c parameter is related to its conformational properties. For example, penicillin and its 3-epimeric carboxylate will have similar h values, but very different c values.[20] These parameters are therefore chemically independent. Hence, the h versus c scatterplot has been examined for the 114 hits (Figure 3). There is a more or less uniform distribution of points in the h range 0.00-0.60Å and the c range 3.0-4.5Å. This scatterplot is uninformative as there is no correlation between these two values.

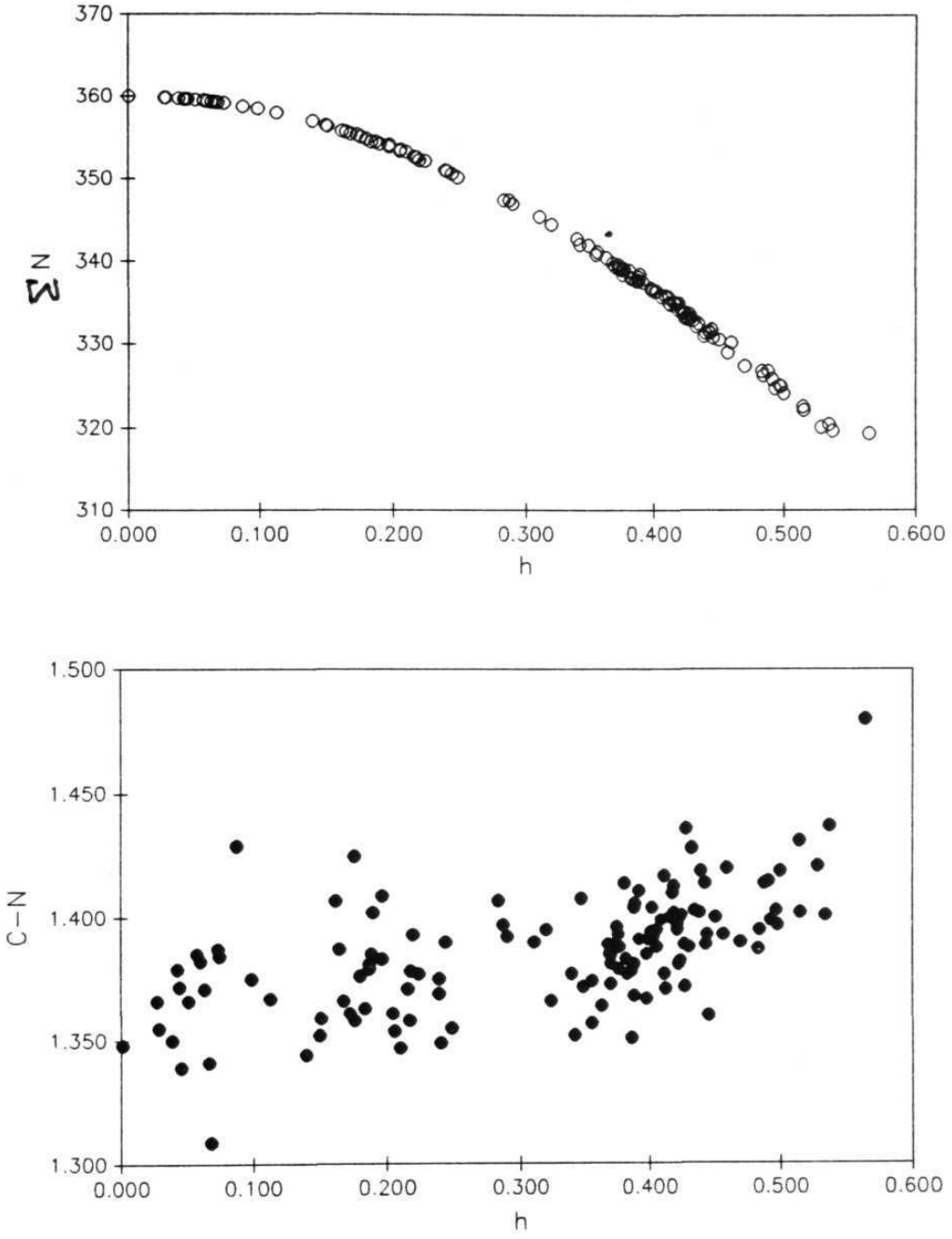

Figure 2.(a) Scatterplot of ΣN versus h (b) Scatterplot of r (C-N distance) versus h for all 114 structures.

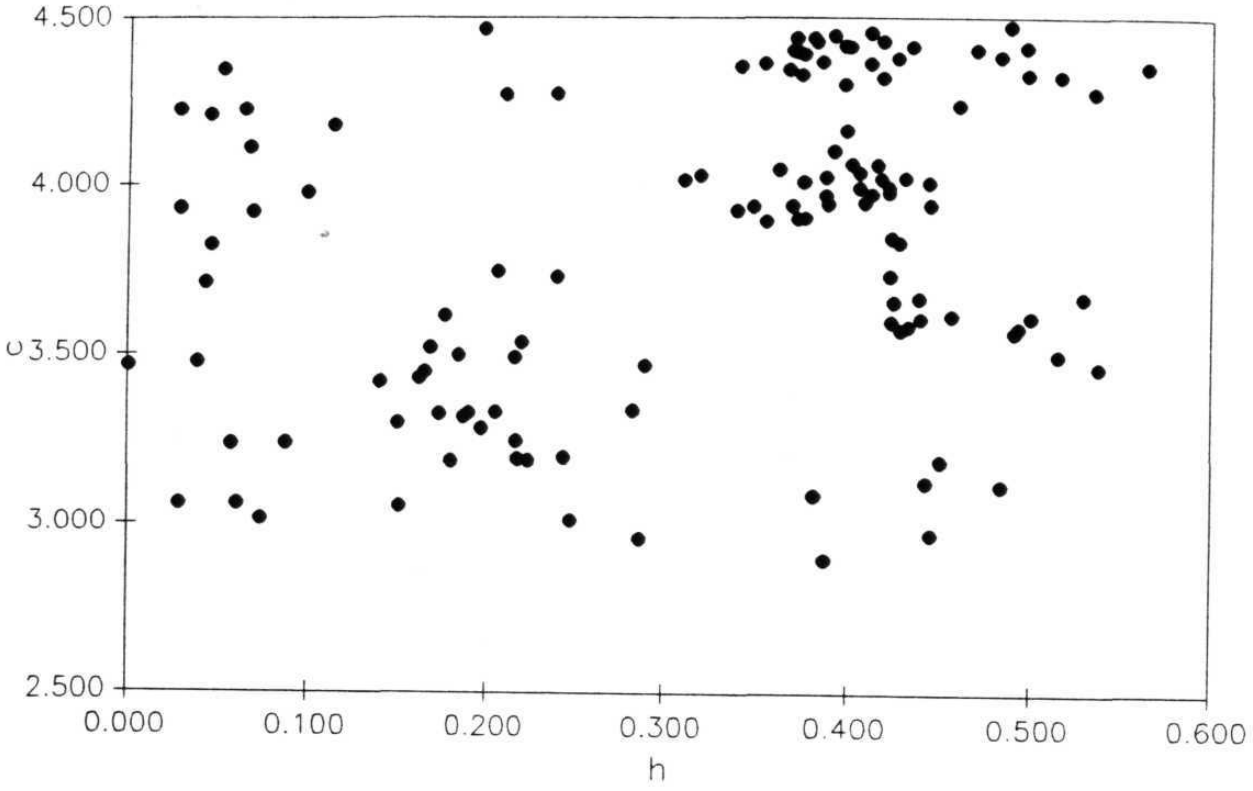

Figure 3. Scatterplot of h *versus* c values for all 114 β-lactams in this study.

At this stage, the active β-lactam skeletons were separated from the 114 structures. As active skeletons, eight bicyclic β-lactam cores - penams, cephems, clavams, penems, carbapenems, oxapenems, carbacephems and oxacephems (Scheme 2) were considered. The identification of these skeletons as active cores was based on a perusal of leading reviews on β-lactam antibiotics[1-4] and the knowledge that each of these groups contains a commercial drug or at least an advanced clinical candidate. A total of 80 hits (out of the original 114) was obtained for these active skeletons and their h-c scatterplot is given in Figure 4a. The h and c values of the remaining skeletons were plotted in Figure 4b. A comparison of Figures 4a and 4b is striking because it shows that the active skeletons (Figure 4a) lie in a limited region of the h-c space, mostly along the diagonal of the scatterplot. While the h-c values in figure 4b lies in off-diagonal which corresponds to the inactive skeletons. Therefore, active compounds are characterised by a combination of either high h (0.35-0.50Å) and high c (3.5-4.5Å) values or by low h (0.15-0.25Å) and low c (3.1-3.6Å) values.

Once the Woodward and Cohen parameters are taken together, a far more rigorous interpretation is obtained about biological activity than is possible by analysis with either parameter alone. This is illustrated by a few representative examples. The CSD refcodes, h and c values of the 3α- and 3β-penams **3** and **4**,[21,22] the Δ^2-cephem **5**,[13] the 4α- and 4β-

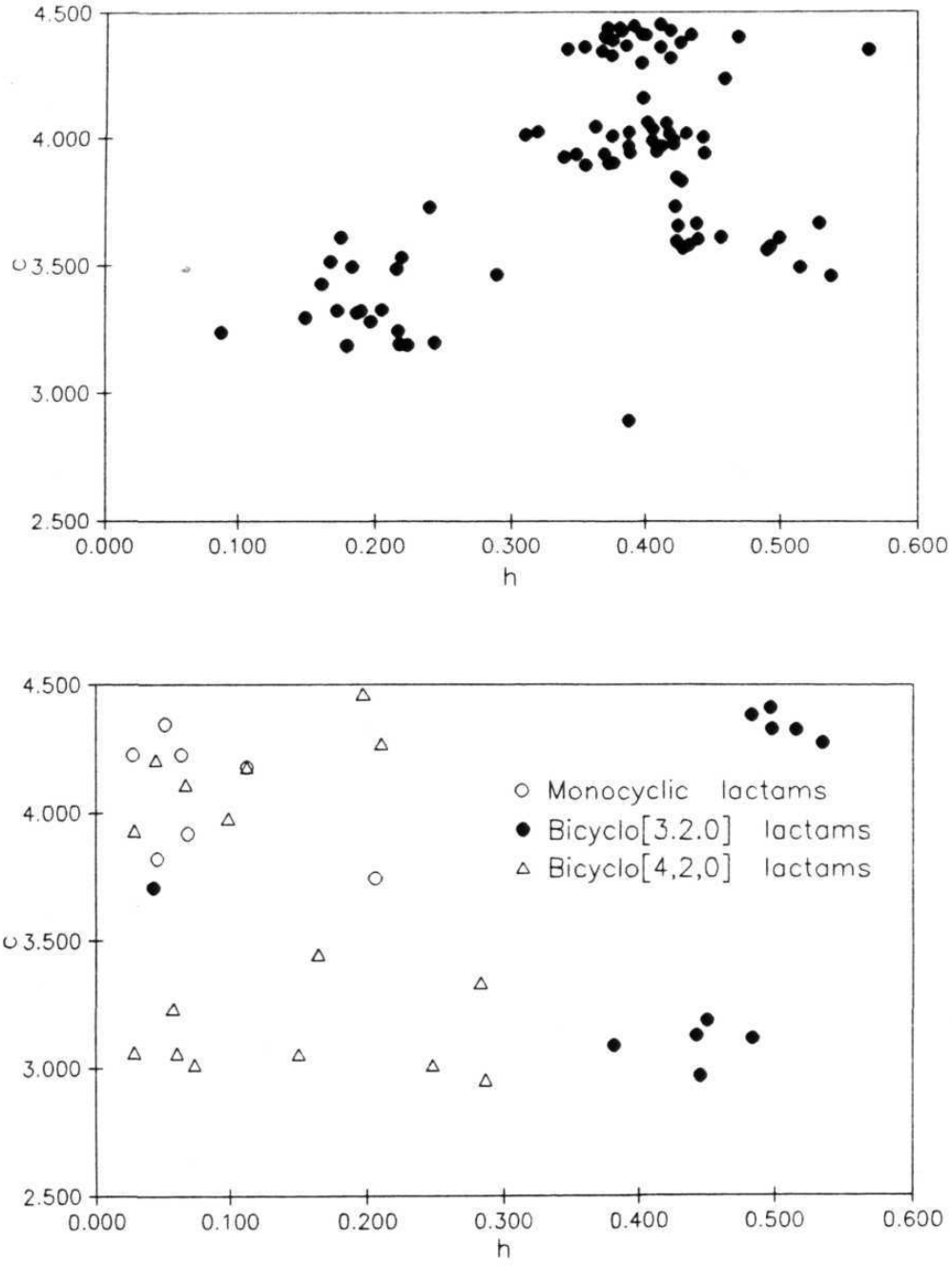

Figure 4. (a) Scatterplot of h *versus* c values for the 80 β-lactams with active skeletons. Note that the points cluster along the diagonal. A few outliers in the high h - moderate c region may be observed. (b) Scatterplot of h *versus* c values for the 30 inactive β-lactams. Notice the wide scatter of points.

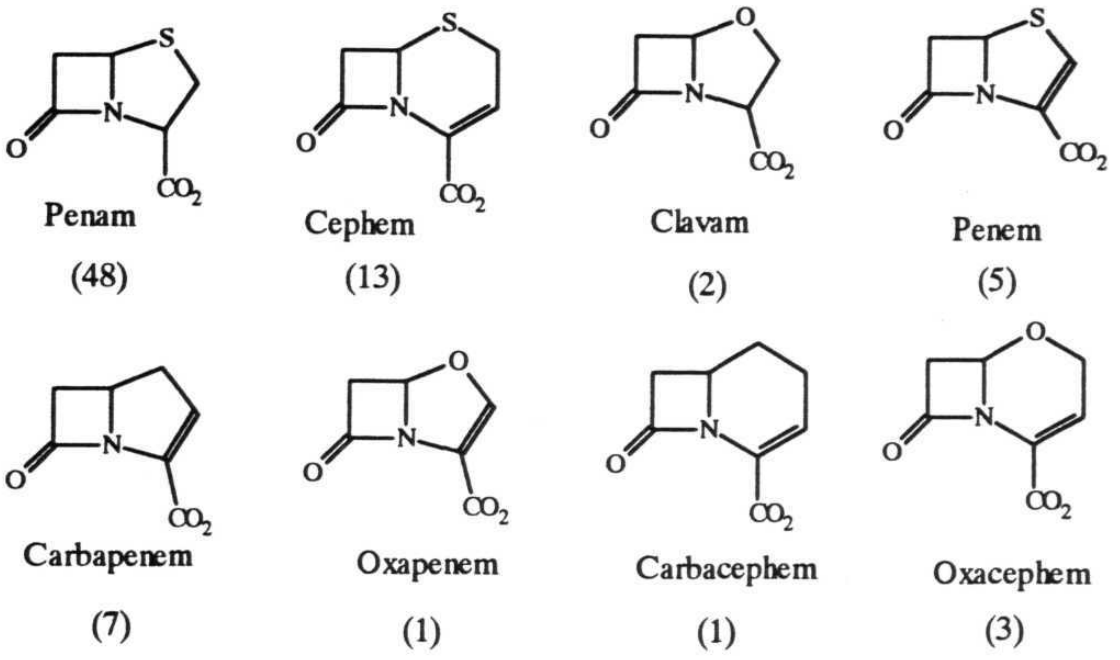

Scheme 2: Active skeletons considered in Figure 4a. The numbers in parenthesis refer to the populations of each group in the plot.

carbacephams **6** and **7**,[23-25] and the Δ^1-carbapenem **8**[26] are shown in Scheme 3. Predictions based on the h parameter alone should lead one to conclude that epimeric penams **3**, **4** should be active because of their reactive amide carbonyl group, while Δ^2-cephem **5** should be predicted to be inactive because of its near-flat shape. In such an analysis, the stereochemistry (α or β orientation) of the $-CO_2H$ group, which contributes significantly to bioactivity (through its intermolecular interactions), is completely ignored. Similarly, predictions based on the Cohen parameter alone could also be equally misleading. Benzylpenicillin, **3** with a c distance of 4.43Å is predicted to be inactive on this count,

whereas it is in actuality one of the earliest-discovered antibiotics. The h-c scatterplot in the present study resolves this ambiguity with the working hypothesis that all active skeletons should have either high h and high c distances or low h and low c distances. That penicillin G, **3** must be a good serine peptidase inhibitor because it falls along the 'active' diagonal is trivially obvious. More importantly, the inactivity of epimeric 3β-penam, **4** is now revealed. Though its h value (0.39Å) is favourable for activity, the *endo* carboxylate group forces a smaller value for the c parameter (2.90Å) and hence this compound is an off-diagonal point in Figure 4. The well well-known inactivity of Δ^2-cephem **5** is further reinforced because not only does it have a very low h but also a very high c distance. It is known that cepham analogues in which the 4-carboxy group is oriented β (*endo* face) are about 8-10 times more active than their 4α (*exo* face) counterparts.[24,27] Accordingly, the more active β-carboxy cephem **7** has low h and low c distances, whereas the inactive 4α-epimer, **6** lies in the off-diagonal region (low h and high c). Finally, Δ^1-carbapenem **8** whose skeleton is more folded than penicillins and penems is found to be completely devoid of antibacterial activity.[26] Here, the two-parameter analysis fails to correctly predict the inactivity of this compound which occurs in the high h - high c region of the 'active' diagonal in Figure 6. While the superiority of simultaneously employing the two independent structural parameters, h and c, for predicting biomolecular properties has

been demonstrated, an inherent limitation of this geometry-based approach is that a predefined structure and conformation of a potential bioactive molecule are necessary but not sufficient conditions for antibacterial activity. There are other factors which are responsible for the 'perfect fit and reactivity' of a substrate in the enzyme pocket.

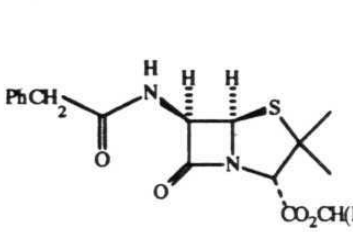

3

h = 0.383

c = 4.427

BENPEN10

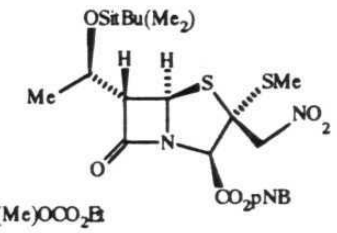

4

h = 0.388

c = 2.896

DIWFOE

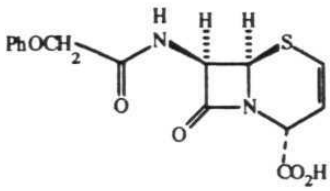

5

h = 0.067

c = 4.110

PODACE

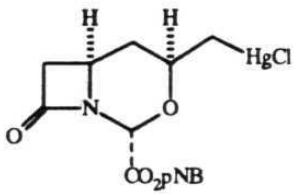

6

h = 0.239

c = 4.272

BOVJEB

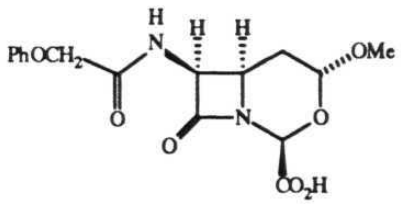

7

h = 0.24

c = 3.024

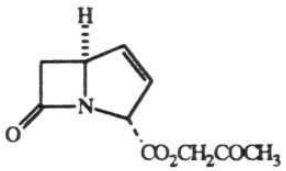

8

h = 0.535

c = 4.276

BALSUC

Scheme 3: Specific compounds in this study with REFCODE, h and c values. For 7, the geometrical parameters have been derived in reference 14.

A closer examination of Figure 4a shows that there are a total of 8 outlier points. Out of these 8 points, 6 points exist in a cluster while the two other exist as isolated points. The h, c values, refcodes and structural formulae of these compounds are shown Scheme 4. Compounds **4** and **9** are isolated points whereas the compounds **10-15** belong to a cluster. (i) The bicyclo[3.2.0] β-lactam **4** synthesised by Hanessian *et al.*[22] is an outlier because the carboxy group is forced into the *endo* orientation by synthetic design. Consequently, c is very small (2.90Å) whereas the h value (0.39Å) is normal for a β-lactam fused to a five-membered ring. (ii) Clavulanate **9** has an unusually high h (0.57Å) because the clavam O-atom inductive effect strongly inhibits amide resonance.[28] (iii) The compounds **10-14** are Δ^2-carbapenems[26,29-32] and **15** is an 1-oxa-Δ^2-penem.[33] These molecules have unusually high h values for bicyclo[3.2.0] β-lactams not only because they are strained by fusion to a five-membered ring but also because amide resonance is inhibited by the enamine N-atom. In other words, these extremely strained molecules are more pyramidal than expected, but the c values are normal.

It may be noted that the gap (h=0.25-0.35Å and c=3.3-3.8Å) in the central portion of the h-c scatterplot (Figure 4a) corresponds to the structural gap between bicyclo[3.2.0] and bicyclo[4.2.0] β-lactams. Changes in molecular geometry between these groups of molecules is so severe that a discrete jump in h values results creating the empty central

region in the scatterplot. To fill this region, compounds like **16** and **17** (Scheme 5) which can show the intermediate pyramidality must be designed by appropriate functional group and/or heteroatom modification, although at present there are no such examples.

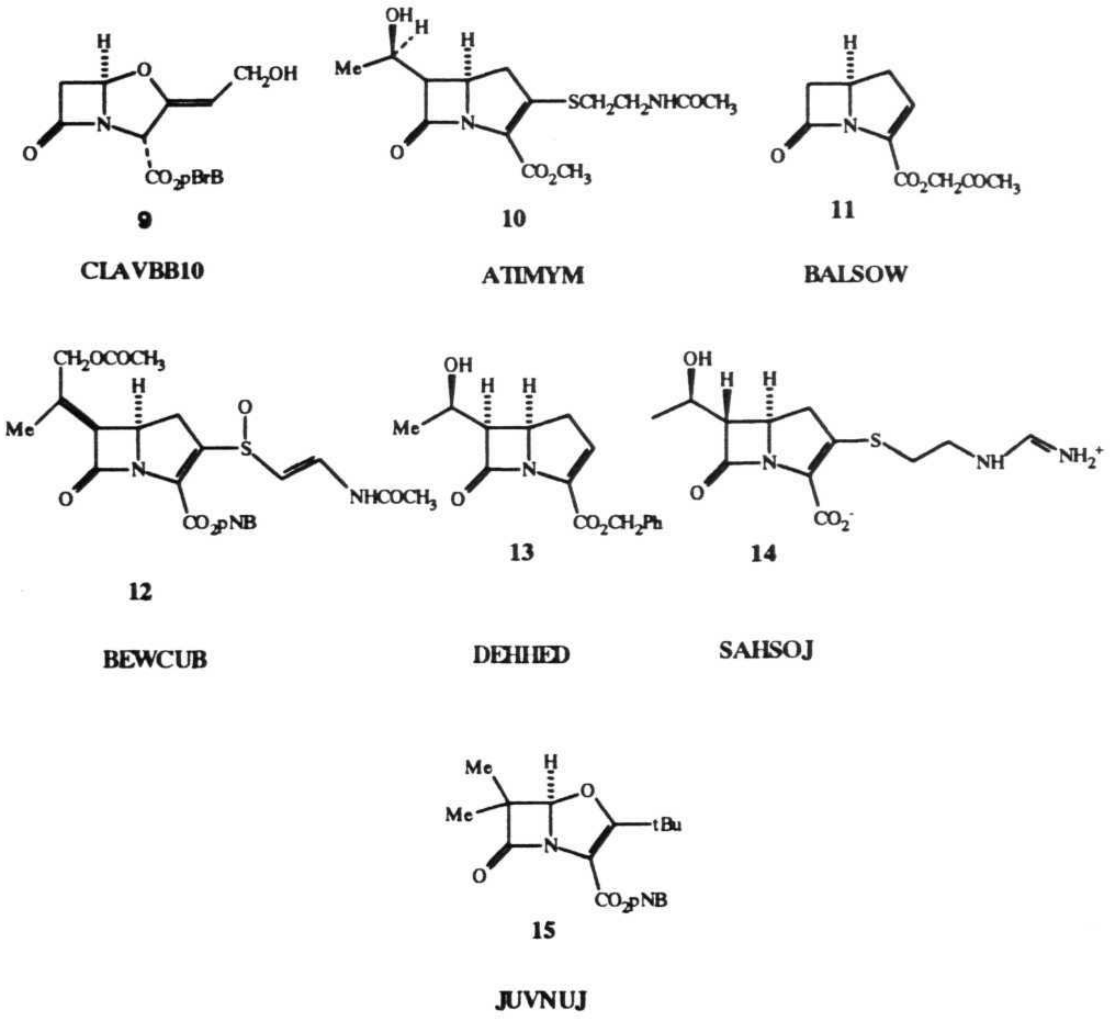

Scheme 4: Structures of outlier compounds in Fig. 4a with REFCODE.

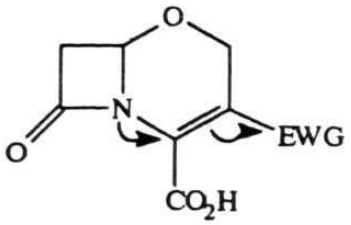

16

h increases

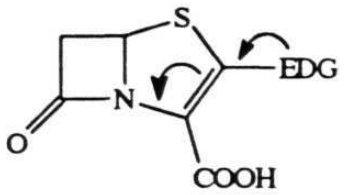

17

h decreases

Scheme 5: Hypothetical molecules with h value in the range 0.25-0.35Å.

The structures in the inactive plot figure 4b (114 original structures minus 80 active structures), can be divided into three categories based on the following skeletons: β-lactams fused to five-membered rings (bicyclo[3.2.0] β-lactams, 12 hits); β-lactams fused to six-membered rings (bicyclo[4.2.0] β-lactams, 12 hits); and monocyclic β-lactams (6 hits). These 30 structures of β-lactams are classified as inactive because these skeletons are not known to be of significant clinical importance. The remaining 4 (**18-21**)[34-37] compounds are found to be miscellaneous structures and the structural formulae and REFCODES of these compounds are given in Scheme 6. The h - c scatterplot of these 30 inactive structures (Figure 4b) shows that less than half the points (13, **8**, **22-33**)[26,38-49] lie along the 'active' diagonal. The chemical formulae and REFCODES of the compounds **22-33** are given in Scheme 7. Many points are scattered all over the plot. The compound **22** has a normal c distance (3.75 Å) and somewhat high h value (0.21 Å) for a mono cyclic β-lactam. This is because the bulky β,β-dimethylacrylic acid substituent on the

nitrogen atom is moved out of the β-lactam ring plane so as to avoid steric crowding with the adjacent ethylsulfinyl residue. Compounds **23-29** are a varied lot of bicyclic β-lactams with no particular commonalty in the nature of the four atom tether or the substitution pattern on the rings. That these seven β-lactams have low h and low c values may be coincidental. In contrast the, the cluster of five bicyclo-β-lactams **8**, **30-33**, have some common structural features, the most obvious being a highly folded bicyclic skeleton with an exo-oriented carboxy group.

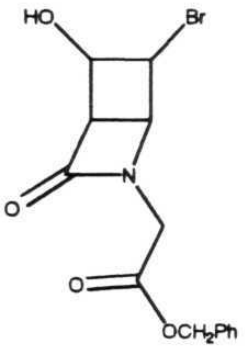

18

BAJXOZ

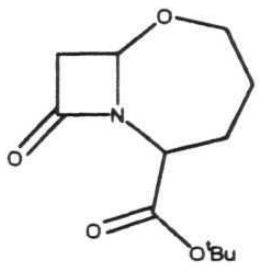

19

CAHDUK

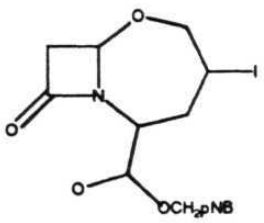

20

FOZKIO

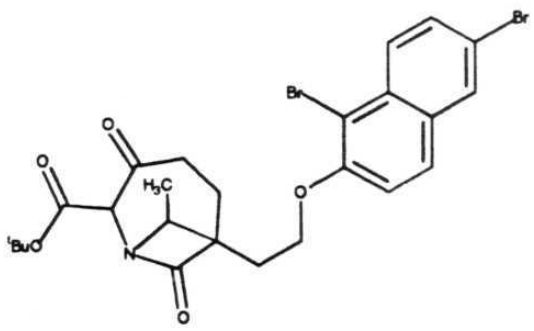

21

KAGPEN

Scheme 6: Miscellaneous compounds in Fig 4b.

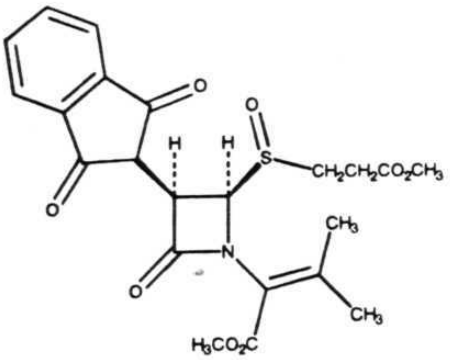

22
BEVCIO

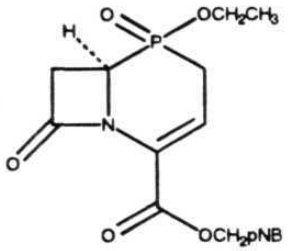

23
CEXJUK

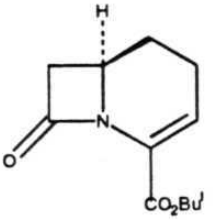

24
COPREE

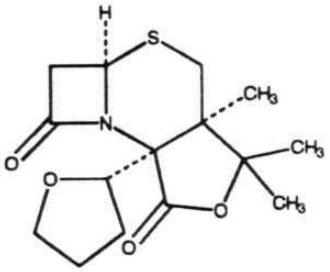

25
DABZEL

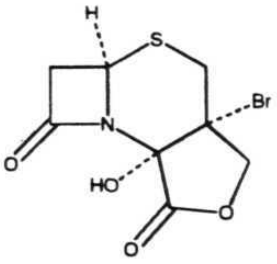

26
DBHCEP

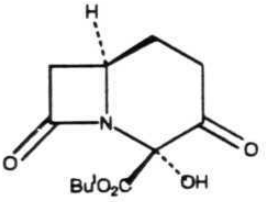

27
JOYFOS

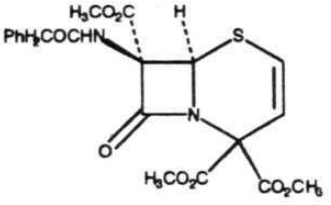

28
PAMXCP

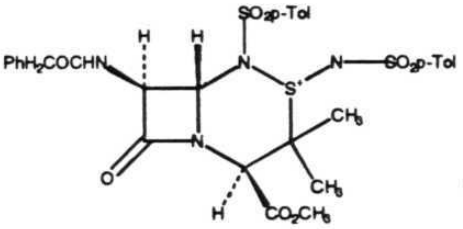

29
PENTOS10

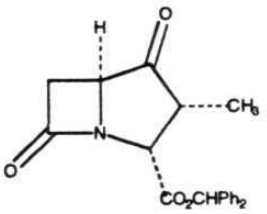

30
BIKKAH

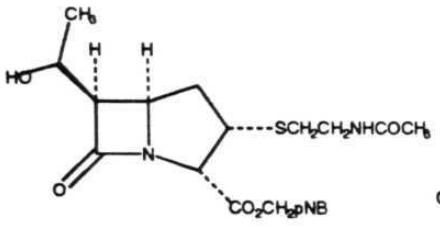

31
CEHKIJ

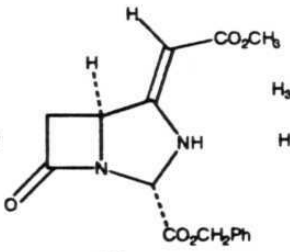

32
DOSCUJ

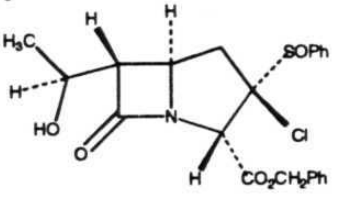

33
JELXED

Scheme 7: Structures of inactive compounds which lying in the active diagonal in Figure 4b.

Figures 4a and 4b are complementary in nature, with active compounds lying along the h-c diagonal and inactive ones in the off-diagonal region, confirms that a simultaneous examination of h and c parameters is crucial in establishing structure-activity relationships in β-lactam antibiotics. These figures reveals why a consideration of either of these parameters in isolation often provides only a poor idea of biological activity. In summary, the correlation between these two independent structural parameters jointly with biological activity is unambiguous and hence the degree of reliability in its use should be far superior.

7.2.3 Model for binding of β-lactams to PBPs

It is known from X-ray crystal structures of carboxypeptidases, transpeptidases and β-lactamases that penicillin-recognising enzymes contain the conserved sequence Ser-X-X-Lys in their active site.[5,50] The importance of non-covalent interactions in facilitating enzyme-substrate recognition is also well-documented.[5-8] In general, it is accepted that there is a three-point binding (Scheme 8) of the enzyme receptor and the β -lactam molecule. Recognition occurs via: (i) the incipient attack by the serine -OH group on the carbonyl group of the lactam; (ii) electrostatic interaction between the lysine NH_3^+ of the enzyme protein and the CO_2^- group at C(3); (iii) hydrogen bonding by the C(6) amide N-H group with a valine carbonyl group (penicillin numbering). For effective binding, these

specific interactions must also be accompanied by a good van der Waals fit of the drug molecule in the receptor pocket.

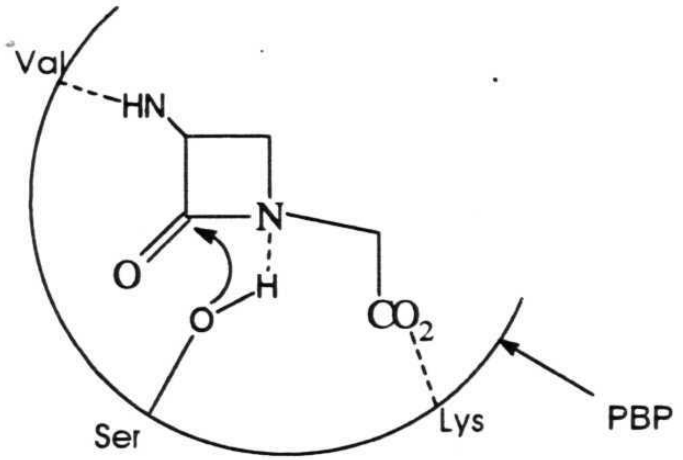

Scheme 8: Three point binding between β-lactam-C-CO_2 fragment and enzyme.

In order to analyse the geometry of these skeletons the superposition plots of β-lactam-C-CO_2 fragment has been examined in active and inactive compounds. Figure 5 is a stereo diagram showing the superposition of the β-lactam-C-CO_2 fragment in 12 active compounds chosen from Figure 4a. Compounds close to the 'active' diagonal are chosen but other than this, the choice was largely random and Figure 4a therefore contains both high h - high c and low h - low c compounds. This plot shows that the lactam carbonyl groups and the carboxylate groups are bunched in their specific regions. So, this depiction is a good pharmacophore model[51] for two-point binding of the β-lactam with the enzyme. It is significant to note that even with the carbonyl and carboxyl

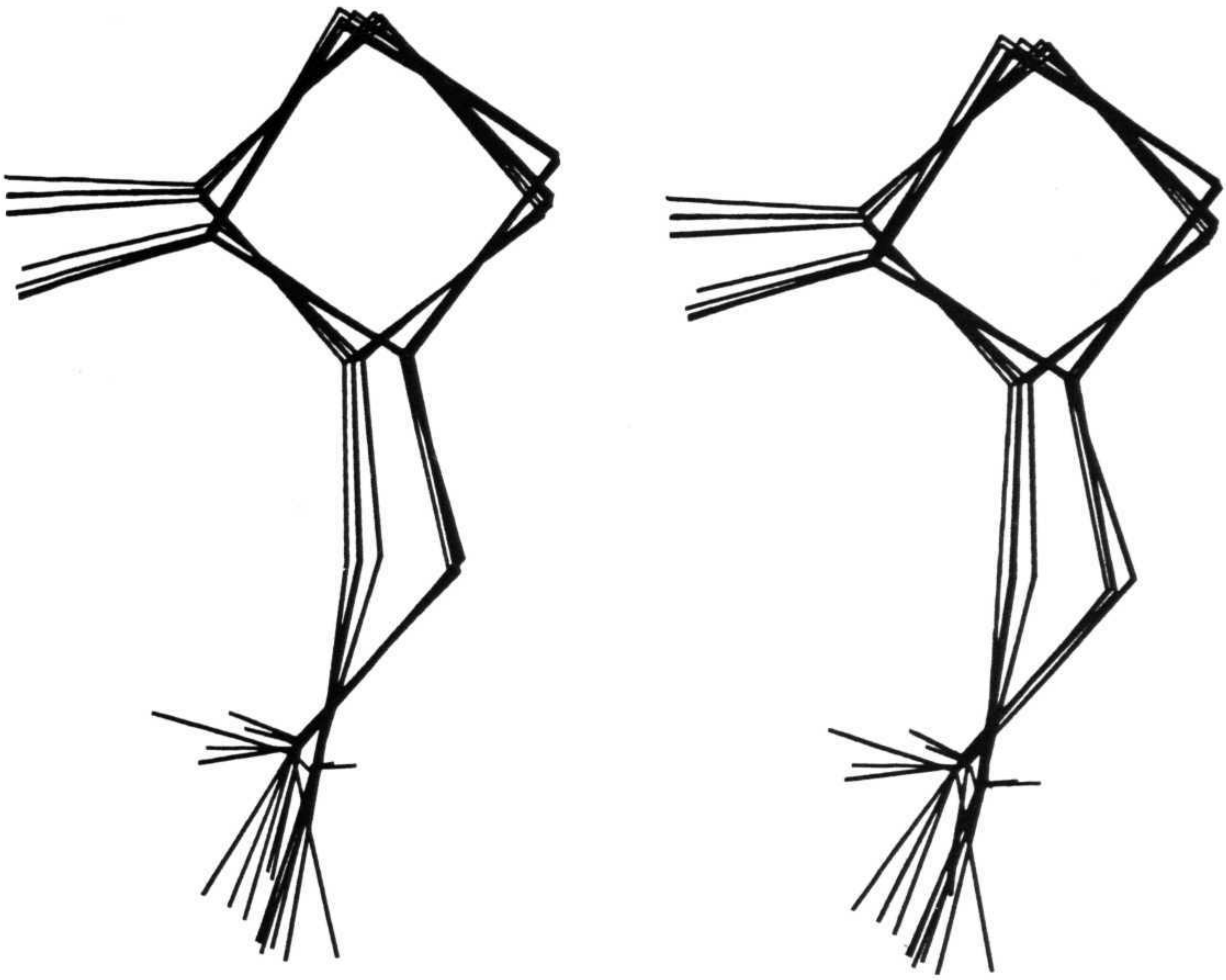

Figure 5. Superposition stereoplot of 12 active structures chosen from Figure 4a. The compounds were chosen as near as possible to the diagonal.

groups thus tethered to the enzyme, there is not much variation in the positioning of the four-membered lactam ring and the connecting -C- linkage in these 12 compounds. Both high h - high c and low h - low c structures are tightly grouped spatially and it is not difficult to visualise that even with the fused 5- or 6-membered ring and attendant substitution filled in, no great spatial variation is expected.

In this regard, the superposition plots of penam, cepham, penem and carbapenem were examined as these skeletons contain more number of structures. The superposition plots of the above skeletons are given in Figure 6. In all these skeletons the bicyclic moieties and carboxylate groups are tightly bunched as expected. However, for penams one can clearly identify the two sets of fragments one with low c and the other with high c. The one which deviates from both the sets is compound **4**. This is because of its very low c value. Similarly, there are 3 structures (Scheme 9, **34-36**) in cephems which stand alone.[52,53] All the penams were examined individually. This examination reveals that the set with high c values contains 21 compounds (22 skeletons) which corresponds to only sulfides and the one with low c values contains 27 compounds (30 skeletons) which corresponds to 7 sulfides, 10 sulfoxides and 10 sulfones. According to Cohen, low c values correspond to the pseudoequatorial conformation (active) and high c values correspond to the pseudoaxial conformation (inactive). This has been debated by others and the

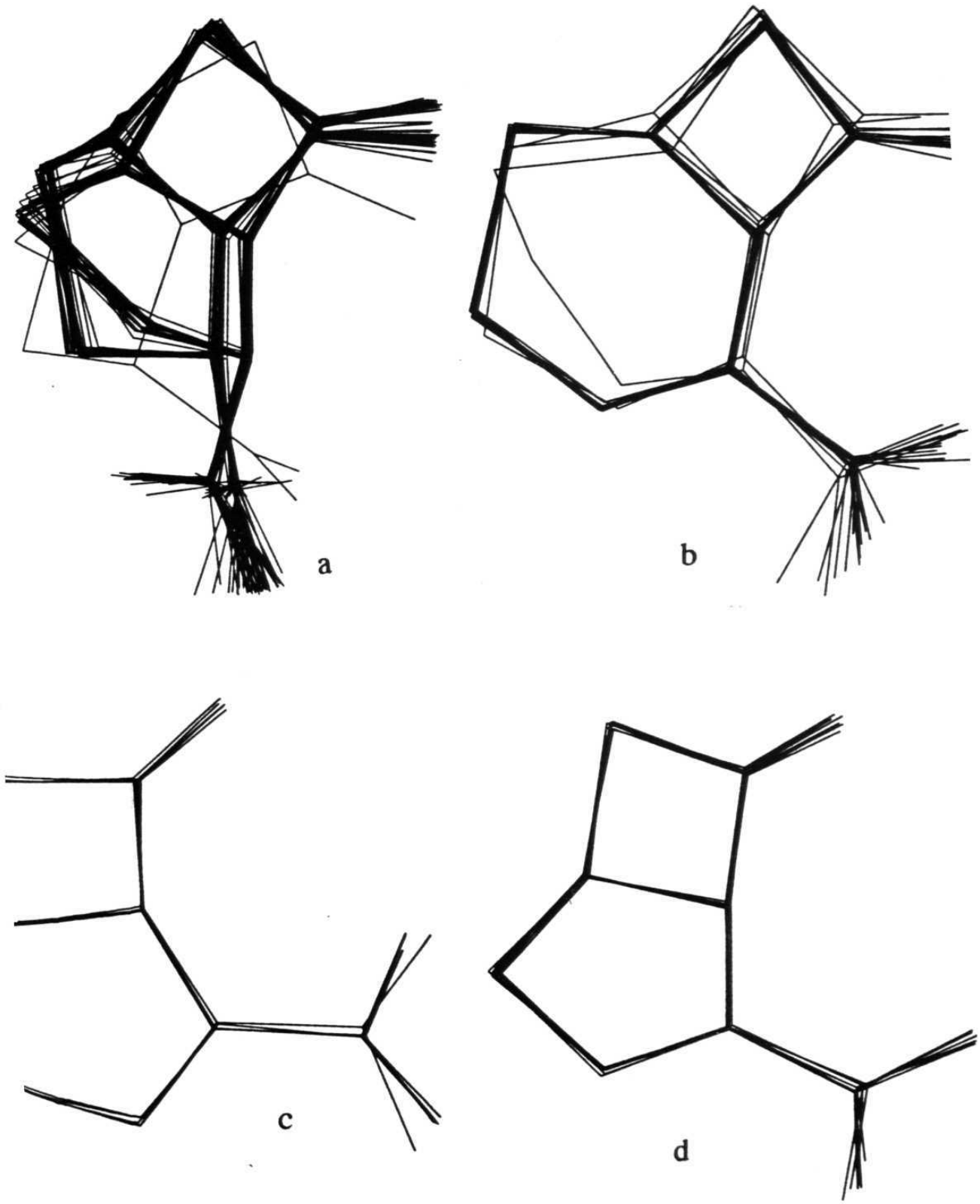

ure 6. Superposition plots of active skeletons (a) Penam, (b) Cephem, Penem and (d) Carbapenem.

pseudoaxial penam carboxylate has also been postulated as the active conformer. Theoretical calculations show that these conformations are in equilibrium with one another and that the pseudoaxial conformation is more stable than the pseudoequatorial conformation by 0.7 kcal.[54] This analysis shows that all sulfides except 7 corresponds to the high c values (>4.2 Å) and all sulfones and sulfoxides corresponds to the low c-values (<4.1 Å). Hence, according to the Cohen parameter, all the sulfones and sulfoxides should be active. To analyse the variation of the c parameter with h parameter in these 52 penam skeletons, the h-c scattergram (Figure 7) was plotted. It may be noted that one can clearly see the two sets of c values and also that there is no correlation between these two parameters.

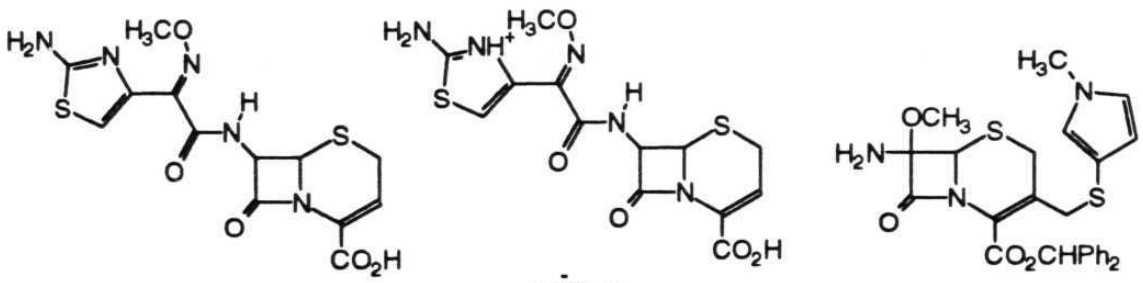

Scheme 9: Structures of cephems which stand alone in the superposition plot 6b.

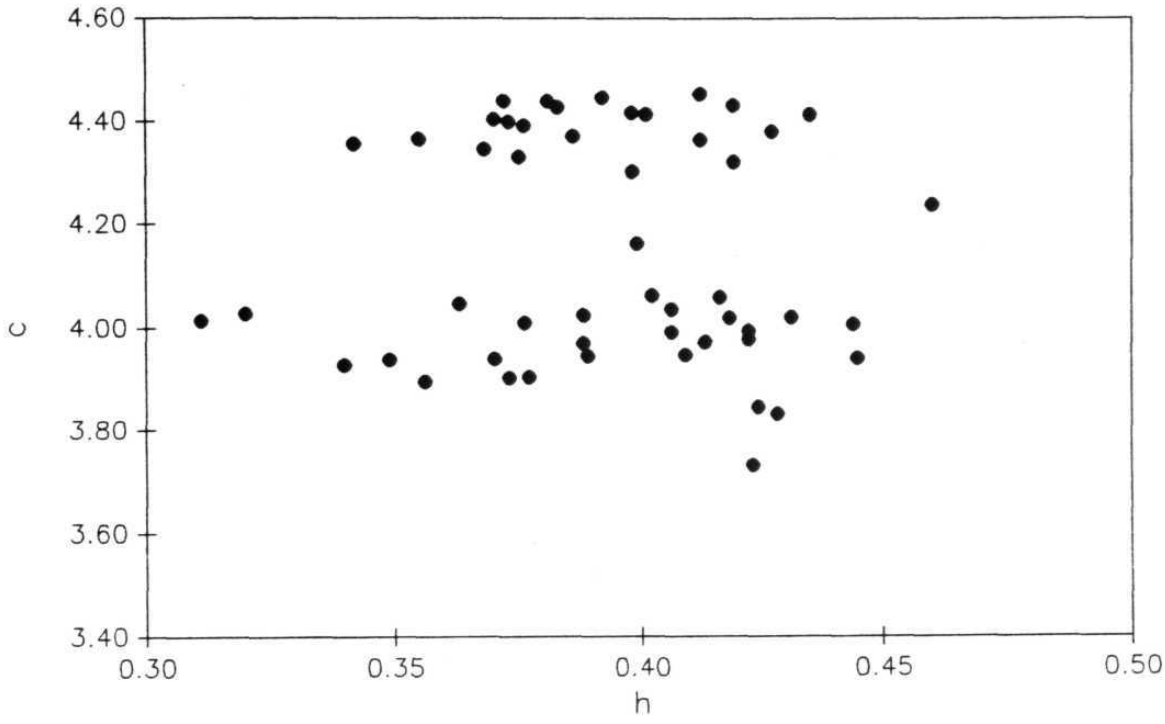

Figure 7. Scatterplot of h versus c values for the 52 penam skeletons. Note the two sets of c values.

Figure 8 is the superposition plot of β-lactam-C-CO_2 fragment in 12 'off-diagonal', inactive compounds selected from Figure 4b. The lactam carbonyl and the carboxylate groups have again been bunched as close as possible (the latter groups perhaps not so effectively as in Figure 5), because this is the prerequisite for binding and eventually, biological activity. However, in the attempt at such a superpositioning, a considerable variation in the positioning of the lactam ring and the -C- linkage is observed. The average lactam ring planes for the low h - high c compounds and the high h - low c compounds are sharply inclined. Further, the positions of the -C- linkage now occur in distinct and widely-distributed spatial regions and it is clear that when the entire molecular structure of the antibiotic is filled in, a considerable spatial variation will result. These figures reveal the importance of 3D-conformation for the activity of β-lactam skeletons.

The importance of these spatial factors has been examined further by considering the torsional angles as they are a better single-parameter descriptors of shape than distances. Accordingly, the torsional angles about non-bonded vectors has been examined to more precisely quantify the shape factors. A number of non-bonded torsional angles were examined and Figure 9 is the histogram of the torsional angle 1-3-4-5. The figure shows that this torsional angle lies in the region 30-160^{o} for the

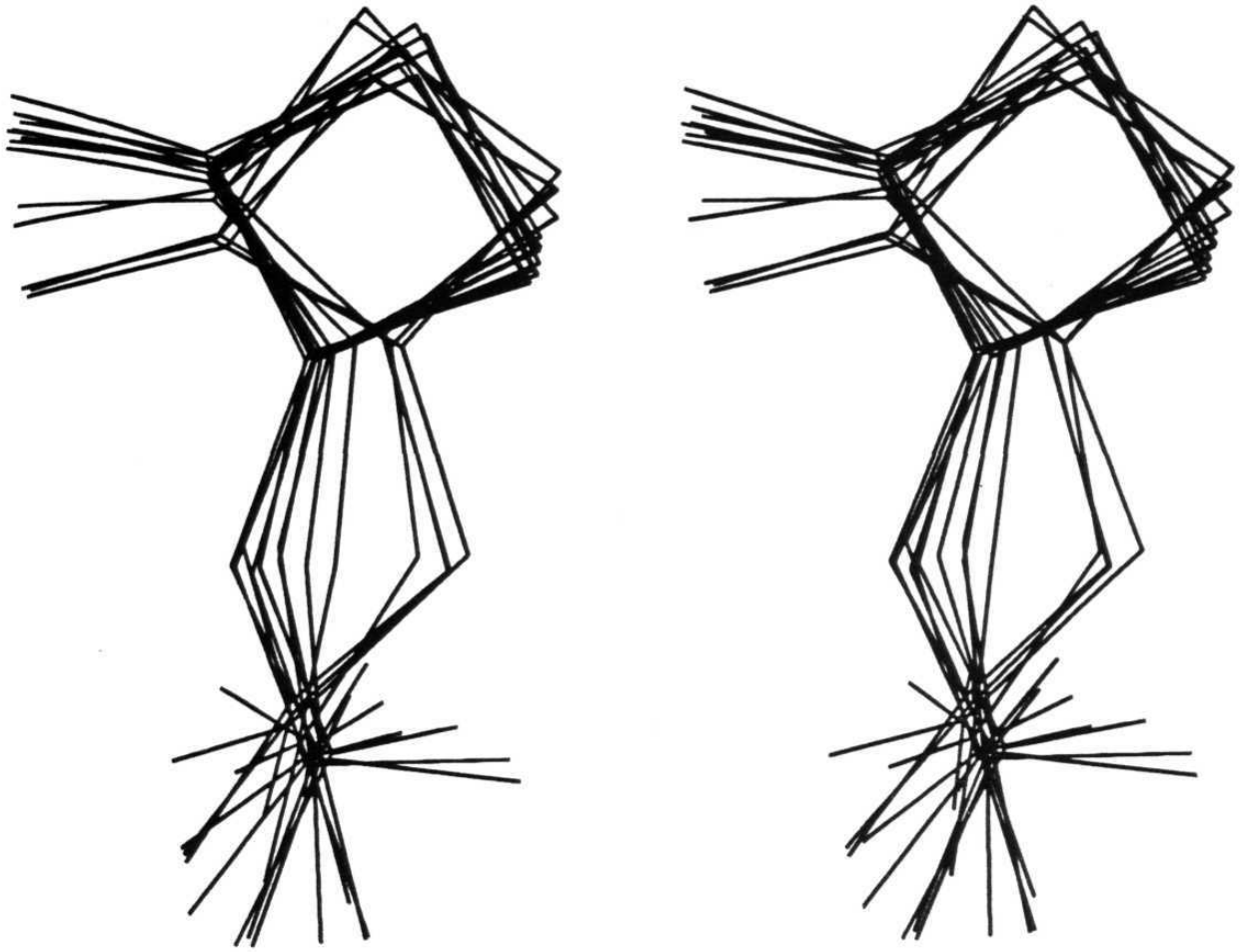

Figure 8. Superposition stereoplot of 12 inactive structures chosen from Figure 4b. The compounds were chosen randomly.

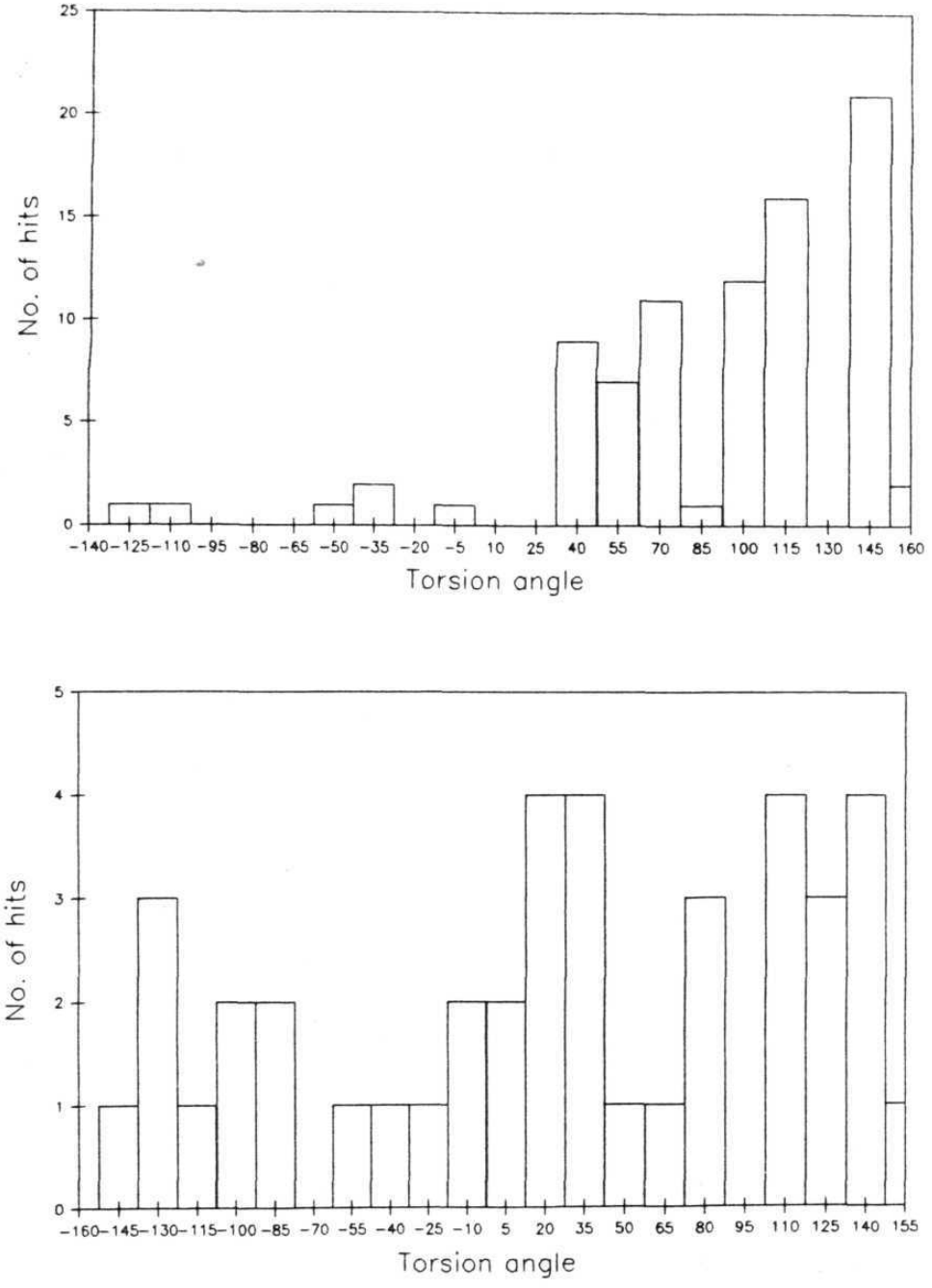

Figure 9. (a) Histogram of the 1-3-4-5 torsional angle values for the 80 active β-lactams. (b) Histogram of the 1-3-4-5 torsional angle values for the remaining 34 structures.

active compounds while the angles for the inactive compounds are scattered in the entire region -160 to +155.

The observations concerning Figures 5, 6, 8 and 9 underscore the fact, recently elaborated by Hahn,[51] that pharmacophore models tend to be geometrically underconstrained, because molecules that fit the model can still be inactive because of additional regions of the molecule that are located in sterically unfavourable locations. In the present context, all β-lactams can be spatially positioned so that the lactam carbonyl group and the carboxylate group can align, to a greater or lesser extent, with relevant complementary regions of the enzyme but an overall fit of the molecule in the receptor cavity is only possible for the high h - high c and low h - low c compounds. These studies reveal that the activity of β-lactam skeletons is dependent on the reactivity of the amide group as well as the ability of antibiotic compounds to reach active site and bind to it. This binding involves the participation of the entire molecule and not just the portion that is undergoing chemical change

7.3 Conclusions

These studies shows that a joint analysis of h and c parameters provides a better, though still empirical, correlation of structure with biological activity. Since the two parameters are independent and their combined consideration leads to better predictions of activity, their

convolution defines a third and more significant parameter. This is shown to be an overall shape factor. Active molecules with high h - high c or low h - low c values are able to adopt nearly similar conformation in the β-lactam-C-carboxylate region while the inactive molecules with high h - low c and low h - high c show much spatial variation. These results indicate that the receptor cavity in penicillin-binding proteins has a well-defined geometry and that shape recognition, without much induced fit,[55] is an important prerequisite for binding of β-lactam antibiotics and subsequent biological activity. The importance of overall shape complementarity between the β-lactam drug and its receptor protein as revealed by the active diagonal on the h-c scatterplot is expected to be a useful guide in the search of newer fourth-generation antibiotics.

7.4 Experimental Section

Data were retrieved from the 1994 update of Version 5.05 of the CSD (109 816 entries) for all the ordered crystal structures with an exact match between chemical and crystallographical connectivity and containing at least one occurrence of the β-lactam fragment **2**. Structures with R-values greater than 0.100 were rejected. Duplicate hits (identified by the same REFCODE) were removed manually by eliminating all but the structure with the lowest R-value in each case. A total of 114 structures was retrieved. Geometrical calculations were performed on the retrieved

data to calculate h, c, r and ΣN using QUEST3D-GSTAT, an automatic graphics search program. The CSD question and summary file are given in Appendix A-6.

7.5 References

1. *Chemistry and Biology of β -Lactam Antibiotics,* eds. R.B. Morrin and M. Gorman, Academic Press, New York, 1982, vol. 1-3.
2. *The Organic Chemistry of β -Lactams,* eds. G.I. Georg, VCH, New York, 1993.
3. W. Dürckheimer, J. Blumbach, R. Lattrell and K.H. Scheunemann, *Angew. Chem. Int. Ed. Engl.*, 1985, **24**, 180.
4. A.G. Brown, *Pure Appl. Chem.*, 1987, **59**, 475.
5. J.A. Kelly, J.R. Knox, P.C. Moews, G.J. Hite, J.B. Bartolone, H. Zhao, B. Joris, J.-M. Frere and J.-M. Ghuysen, *J. Biol. Chem.,* 1985, **260**, 6449.
6. J.A Kelly, J.R. Knox, H. Zhao, J.-M. Frère and J.-M. Ghuysen, *J. Mol. Biol.,* 1989, **209**, 281.
7. J.R. Knox and P.C. Moews, *J. Mol. Biol.,* 1991, **220**, 435.
8. C. Oefner, A. D'Arcy, J.J. Daly, K. Gubernator, R.L. Charnas, I. Heinze, C. Hubschwerlen and F.K. Winkler, *Nature,* 1990, **343**, 284.
9. R.B. Woodward, *Phil. Trans. R. Soc. Lond.,* 1980, **B289**, 239 and references cited therein.

10. D.B. Boyd, in *Chemistry and Biology of β -Lactam Antibiotics,* eds. R.B. Morin, and M. Gorman, Academic Press, New York, 1982, vol. 1, p. 437.

11. R.M. Sweet, and L.F. Dahl, *J. Am. Chem. Soc.,* 1970, **92**, 5489.

12. N.C. Cohen, *J. Med. Chem., 1983,* **26**, 259.

13. D.D. Keith, J. Tengi, P. Rossman, L. Todardo and M. Weigele, *Tetrahedron,* 1983, **39**, 2445.

14. F.H. Allen, J.E. Davies, J.J. Galloy, O. Johnson, O. Kennard, C.F. Macrae, E.M. Mitchel, G.F. Mitchel, J.M. Smith, and D.G. Watson, *J. Chem. Inf. Comput. Sci.,* 1991, **31**, 187.

15. G.R. Desiraju, *Crystal Engineering. The Design of Organic Solids,* Elsevier, Amsterdam, 1989, p. 63.

16. G. Klebe, in *Structure Correlation,* eds. H.-B. Bürgi, and J.D. Dunitz, VCH, Weinheim, 1994, vol 2, p. 544.

17. W.L. Duax, J.F. Griffin and D. Ghosh, in *Structure Correlation,* eds. H.-B. Bürgi and J.D. Dunitz, VCH, Weinheim, 1994, vol 2, p. 605.

18. O.A. Mascaretti, O.A. Roveri, and G.O. Danelon, in *Recent Progress in the Chemical Synthesis of Antibiotics and Related Microbial Products,* eds. G. Lukacs, Springer, Berlin, 1993, vol 2, p 677.

19. R. Taylor and F.H. Allen, in *Structure Correlation,* eds. H.-B. Bürgi and J.D. Dunitz, VCH, Weinheim,1994, vol. 1, p. 111.

20. R. Busson, P.J. Claes and H. Vanderhaeghe, *J. Org. Chem.,* 1976, **41**, 2556.

21. I. Csöregh, and T.-B. Palm, *Acta. Crystallogr.,* 1977, **B33**, 2169.

22. A. Bedeschi, F. Bélanger-Gariépy, S. Hanessian and F. Brisse, *Acta. Crystallogra.,* 1986, **C42**, 442.

23. M.L. Phillips, R. Bonjouklian, N.D. Jones, A.H. Hunt and T.K. Elzey, *Tetrahedron Lett.,* 1983, **24**, 335.

24. J.A. Gleason, T.F. Buckley, K.G. Holden, D.B. Bryan and P. Siler, *J. Am. Chem. Soc.,* 1979, **101**, 4730.

25. N.C. Cohen, P. Colin and G. Lemoine, *Tetrahedron,* 1981, **37**, 1711.

26. H.R. Pfaendler, J. Gosteli, R.B. Woodward and G. Rihs, *J. Am. Chem. Soc.,* 1981, **103**, 4526.

27. C.L. Branch and M.J. Pearson, *J. Chem. Soc., Perkin Trans. 1,* 1986, 1077.

28. A.G. Brown, D.F. Corbett, J. Goodacre, J.B. Harbridge, T.T. Howarth, R.J. Ponsford, I. Stirling and T.J. King, *J. Chem. Soc., Perkin Trans. 1,* 1984, 635.

29. G. Albers-Schönberg, B.H. Arison, O.D. Hensens, J. Hirshfield, K. Hoogsteen, E.A. Kaczka, R.E. Rhodes, J.S. Kahan, F.M. Kahan, R.W. Ratcliffe, E. Walton, L.J. Ruswinkle, R.B. Morin. and B.G. Christensen, *J. Am. Chem. Soc.,* 1978, **100**, 6491.

30. N. Tsuji, K. Nagashima, M. Kobayashi, J. Shoji, T. Kato, Y. Terui, H. Nakai and M.Shiro, *J. Antibiot.,* 1982, **35**, 24.

31. J.H. Bateson, A.M. Quinn, T.C. Smale and R. Southgate, *J. Chem. Soc., Perkin Trans. 1,* 1985, 2219.

32. R.W. Ratcliffe, K.J. Wildonger, L. di. Michele, A.W. Douglas, R. Hajdu, R.T. Goegelman, J.P. Springer and J. Hirshfield, *J. Org. Chem.,* 1989, **54**, 653.

33. H.R. Pfaendler, W. Hendel and U. Nagel, *Z. Naturforsch., Teil B.* 1992, **47**, 1037.

34. W.J. Begley, G. Lowe, A.K. Cheetham and J.M. Newsam, *J. Chem. Soc., Perkin Trans.1*, 1981, 2620.

35. M.D. Bachi, F. Frolow and C. Hoornaert, *J. Org. Chem.,* 1983, **48**, 1841.

36. M. Mori, N. Kanda, Y. Ban, K. Aoe, *J. Chem. Soc., Chem. Comm.,* 1988, 12.

37. R.M. Williams, B.H. Lee, M.M. Miller, O.P. Anderson, *J. Am. Chem. Soc.,* 1989, **111**, 1073.

38. M.D. Bachi, A. Gross, F. Frolow, *J. Org. Chem.,* 1982, **47**, 765.

39. H. Satoh, T. Tsuji, *Tetrahedron Lett.,* 1984, **25**, 1733.

40. C.M. Pant, R.J. Stoodley, A. Whiting, D.J. Williams, *J. Chem. Soc., Chem. Comm.,* 1984, 1289.

41. N.K. Capps, G.M. Davies, P.B. Hitchcock and D.W. Young, *J. Chem. Soc., Chem. Comm.,* 1985, 843.

42. K. Neupert-Laves and M. Dobler, *Cryst. Struct. Commun.,* 1977, **6**, 153.

43. C.M. Gasparski, A. Ghosh and M.J. Miller, *J. Org. Chem.,* 1992, **57**, 3546.

44. E.F. Paulus, *Acta Crystallogr.,* 1977, **B33**, 108.

45. A.F. Cameron, I.R. Cameron, M.M. Campbell and G. Johnson, *Acta Crystallogr.,* 1976, **B32**, 1377.

46. R.L. Rosati, L.V. Kapili, P. Morrissey, J. Bordner and E. Subramanian, *J. Am. Chem. Soc.,* 1982, **104**, 4262.

47. T. Haneishi, M. Nakajima, N. Serizawa, M. Inukai, Y. Takiguchi, M. Arai, S. Satoh, H. Kuwano and C. Tamura, *J. Antibiot.,* 1983, **36**, 1581.

48. C.L. Branch and M.J. Pearson, *J. Chem. Soc., Perkin Trans.1,* 1986, 1077.

49. J.H. Bateson, P.M. Roberts, T.C. Smale and R. Southgate, *J. Chem. Soc., Perkin Trans.1,* 1990, 1541.

50. S. Wolff, *Can. J. Chem.,* 1994, **72**, 1014.

51. M. Hahn, *J. Med. Chem.,* 1995, **38**, 2080.

52. A. Miyamae, S. Koda and Y. Morimoto, *Chem. Pharm. Bull.,* 1986, **34**, 3539.

53. W. Shin and J. Kim, *Acta. Crystalogr.,* 1992, **C48**, 1451.

54. N.V. Joshi, R. Virudachalam and V.S.R. Rao, *Curr. Sci.,* 1978, **47**, 933.

55. Jr., D.E. Koshland, *Angew. Chem. Int. Ed. Engl.,* 1994, **33**, 2375.

Appendices

Appendix A-1

Table 1: Geometrical question for the retrieval N-H...O interactions of type A in primary amides

```
HNORM
T1 *CONN
NFRAG  1
AT1 C 2                          :XY  235  436
AT2 H 1                          :XY  521  333
AT3 N 2 1                        :XY  675  359
AT4 C 2                          :XY  775  448
AT5 O 1                          :XY  821  562
AT6 O 1                          :XY  393  414
AT7 N 2 1                        :XY  179  620
AT8 H 1                          :XY  356  668
BO 2 3 1
BO 3 4 1
BO 4 5 2
BO 1 6 2
BO 1 7 1
BO 7 8 1
GEOM
CONTACT INTER 2 A 6 A 1.4 2.8
DEFINE H...O 2 6
DEFINE N...O 3 6
DEFINE NHOANG 3 2 6
DEFINE COHANG 1 6 2
DEFINE *RFACT
SELECT NHOANG 110 180
HIST H...O
HIST N...O
HIST COHANG
SCAT H...O NHOANG
SCAT N...O NHOANG
SCAT H...O COHANG
C OVERLAP OF CRYSTAL FRAGMENTS PERMITTED
C SEARCH FOR ALL CRYSTAL FRAGMENTS
```

```
NFRAG -99
ENANT NOIN
END
QUEST T1
```

Table 2: Geometrical question for the retrieval N-H...O interactions of type A in secondary amides

```
HNORM
T1 *CONN
NFRAG  1
AT1 O 1
AT2 H 1
AT3 N 3
AT4 C 2
AT5 O 1
AT6 AA 1
BO 2 3 1
BO 3 4 1
BO 4 5 2
BO 3 6 99
GEOM
CONTACT INTER 2 A 1 A 1.4 2.8
DEFINE H...O 2 1
DEFINE N...O 3 1
DEFINE NHOANG 3 2 1
DEFINE *RFACT
SELECT NHOANG 110 180
HIST H...O
SCAT H...O NHOANG
SCAT N...O NHOANG
C OVERLAP OF CRYSTAL FRAGMENTS PERMITTED
C SEARCH FOR ALL CRYSTAL FRAGMENTS
NFRAG -99
ENANT NOIN
END
QUEST T1
```

Appendix A-2

Table 1: CSD query for intermolecular C-H···O interactions for terminal CO ligands (CO-t) in Mn Complexes

```
STOP 10000
SCRE 7 28 -34 35 -55 85 153
HNORM
SAVE 1
T1 *CONN
NFRAG 1
AT1 MN 1
AT2 C 2
AT3 O 1
AT4 H 1
AT5 C 1
BO 1 2 1
BO 2 3 3
BO 4 5 1
GEOM
CONTACT INTER 3 A 4 A 2.0 2.8
DEFINE H...O 3 4
DEFINE C...O 3 5
DEFINE CHOANG 5 4 3
DEFINE COHANG 2 3 4
DEFINE *RFACT
SELECT CHOANG 110 180
C OVERLAP OF CRYSTAL FRAGMENTS PERMITTED
C SEARCH FOR ALL CRYSTAL FRAGMENTS
NFRAG -99
ENANT NOIN
END
QUEST T1
```

Table 2: CSD query for intermolecular C-H···O interactions for bridged CO ligands (CO-t) in Mn Complexes

```
STOP 10000
SCRE 7 28 -34 35 -55 85 153
HNORM
SAVE 1
T1 *CONN
NFRAG 1
AT1 MN 1
AT2 C 3
AT3 O 1
AT4 TR 1
AT5 C 1
AT6 H 1
BO 1 2 1
BO 2 3 2
BO 2 4 1
BO 5 6 1
GEOM
CONTACT INTER 3 A 6 A 2.0 2.8
DEFINE H...O 3 6
DEFINE C...O 3 5
DEFINE CHOANG 3 6 5
DEFINE COHANG 2 3 6
DEFINE *RFACT
SELECT CHOANG 110 180
C OVERLAP OF CRYSTAL FRAGMENTS PERMITTED
C SEARCH FOR ALL CRYSTAL FRAGMENTS
NFRAG -99
ENANT NOIN
END
QUEST T1
```

Table 3: CSD query for intramolecular C-H···O interactions for terminal CO ligands (CO-t) in Mn Complexes

```
STOP 10000
SCRE 7 28 -34 35 -55 85 153
HNORM
SAVE 1
T1 *CONN
NFRAG 1
AT1 MN 1
AT2 C 2
AT3 O 1
AT4 H 1
AT5 C 1
BO 1 2 1
BO 2 3 3
BO 4 5 1
GEOM
CONTACT INTRA 4 999 3 A 4 A 2.0 2.8
DEFINE H...O 3 4
DEFINE C...O 3 5
DEFINE CHOANG 5 4 3
DEFINE COHANG 2 3 4
DEFINE *RFACT
SELECT CHOANG 110 180
C OVERLAP OF CRYSTAL FRAGMENTS PERMITTED
C SEARCH FOR ALL CRYSTAL FRAGMENTS
NFRAG -99
ENANT NOIN
END
QUEST T1
```

Table 4: CSD query for intramolecular C-H···O interactions for bridged CO ligands (CO-t) in Mn Complexes

```
STOP 10000
SCRE 7 28 -34 35 -55 85 153
HNORM
SAVE 1
T1 *CONN
NFRAG 1
AT1 MN 1
AT2 C 3
AT3 O 1
AT4 TR 1
AT5 C 1
AT6 H 1
BO 1 2 1
BO 2 3 2
BO 2 4 1
BO 5 6 1
GEOM
CONTACT INTRA 4 999 3 A 6 A 2.0 2.8
DEFINE H...O 3 6
DEFINE C...O 3 5
DEFINE CHOANG 3 6 5
DEFINE COHANG 2 3 6
DEFINE *RFACT
SELECT CHOANG 110 180
C OVERLAP OF CRYSTAL FRAGMENTS PERMITTED
C SEARCH FOR ALL CRYSTAL FRAGMENTS
NFRAG -99
ENANT NOIN
END
QUEST T1
```

Appendix A-3

Table 1: CSD query for the M-H···O interactions in metal hydrides

```
PRINT 10
SAVE 1
SAVE 3
T1 *CONN
AT1 TR 1
AT2 H 1
AT3 O 1
BO 1 2 99
GEOM
CONTACT INTER 2 A 3 A 1.0 3.2
DEFINE H...O 2 3
DEFINE TR...O 1 3
DEFINE ANGTRHO 1 2 3
HIST H...O
HIST TR...O
HIST ANGTRHO
SCAT H...O ANGTRHO
NFRAG -99
ENANT NOIN
END
PRINT 10
QUEST T1
```

Appendix A-4

Table 1: CSD Quest file for Zr complexes

```
SCRE 5 28 -34 35 85 88
STOP 10000
SAVE 1
T1 *CONN
NFRAG    1
AT1 Ta1
AT2 H 1
AT3 C 1
BO 2 3 1
GEOM
CONTACT INTRA 1 999 2 A 1 A 1.8 2.5
DEFINE C-H 2 3
DEFINE H...ta 1 2
DEFINE C...ta 1 3
DEFINE CHta 3 2 1
DEFINE taCH 1 3 2
C OVERLAP OF CRYSTAL FRAGMENTS PERMITTED
C SEARCH FOR ALL CRYSTAL FRAGMENTS
NFRAG -99
ENANT NOIN
END
QUEST T1
```

Appendix A-5

Table 1: Crystallographic details for complexes **3a**, **3b**, **3c** and **3d**.

Compound	3a	3b	3c	3d
Formula	$C_{20}H_{20}N_6O_{13}$	$C_{31}H_{22}N_6O_{12}$	$C_{84}H_{48}N_{12}O_{26}$	$C_{15.5}H_9ClN_3O_7$
M	660.52	686.56	1641.34	385.71
Crystal system	Monoclinic	Monoclinic	Triclinic	Monoclinic
Space group	$P2_1$	$P2_1/c$	$P\bar{1}$	P21/n
a/Å	7.092(2)	7.493(2)	13.721(3)	7.481(2)
b/Å	27.927(4)	27.384(6)	14.374(4)	15.140(4)
c/Å	7.569(2)	7.491(2)	16.349(7)	14.394(7)
α/°			92.13(2)	
β/°	96.67(2)	92.39(2)	102.67(2)	95.806(10)
γ/°			97.90(2)	
V/Å^3	1488.9(5)	1535.8(6)	3109(2)	1621.9(10)
Temperature/ K	293	293	120	293
Z	2	2	2	4
F(000)	680	708	1688	788
Dc/g cm^{-3}	1.47	1.484	1.754	1.580
λ/Å	0.7107	0.7107	0.7107	0.7107
μ/mm^{-1}	0.76	0.76	0.134	0.283
Crystal size	0.23x0.31x0.30	0.22x0.25x0.33	0.1x0.1x0.2	0.24x0.22x0.35
Radiation	MoKα	MoKα	MoKα	MoKα
θ range /°	1-27.5	1-27.5	2.56-28.69	2.69-25.35
h	-7-7	-7-7	0-11	0-9
k	0-34	0-33	-19-18	0-18
l	0-8	0-8	-21-21	-17-17
Total reflections	2931	3532	11741	2956
Unique relflections	1828	1328	6695	1634
σ-level	3	3	2	2
R1	0.038	0.048	0.049	0.08
wR2	0.041*	0.050*	0.12	0.23
Min. electron density /e Å^{-3}	-0.19	-0.13	-0.404	0.238
Max. electron density /e Å^{-3}	0.13	0.13	1.826	0.282

*R_w values.

Table 2: Crystallographic details for complexes **3e**, **3f**, and **3g**.

Compound	3e	3f	3g
Formula	$C_{15.5}H_9ClN_3O_{6.5}$	$C_{25}H_{10}N_3O_8$	$C_{23}H_{17}N_3O_8$
M	376.71	489.43	463.40
Crystal system	Monoclinic	Orthorhombic	Triclinic
Space group	P21/n	P212121	$P\bar{1}$
a/Å	7.474(1)	5.915(2)	8.979(10)
b/Å	15.287(2)	9.722(6)	11.343(14)
c/Å	14.435(2)	39.097(4)	11.68(2)
α/°			76.63(6)
β/°	96.42(2)		84.39(6)
γ/°			68.84(9)
V/Å^3	1638.9(4)	2248(2)	1079(2)
Temperature/ K	293	293	293
Z	4	4	2
F(000)	768	1016	480
Dc/g cm^{-3}	1.527	1.446	1.426
λ/Å	0.7107	0.7107	0.7107
μ/mm^{-1}	0.276	0.110	0.110
Crystal size	0.26x0.20x0.38	0.20x0.15x0.35	0.15x0.20x0.25
Radiation	MoKα	MoKα	MoKα
θ range /°	2.94-27.30	2.162-28.96	
h	0-9	0-8	0-10
k	0-19	0-13	-11-12
l	-18-18	0-15	-12-13
Total reflections	3571	3171	3062
Unique relflections	2359	1867	1857
σ-level	2	2	2
R1	0.16	0.04	0.05
wR2	0.47	0.12	0.11
Min. electron density /e Å^{-3}	-0.806	-0.204	-0.173
Max. electron density /e Å^{-3}	0.524	0.163	0.195

Table 3. Atomic coordinates (x 10^4) and equivalent isotropic displacement parameters (A^2 x 10^3) for complex **3a**. $U_{(eq)}$ is defined as one third of the trace of the orthogonalized U_{ij} tensor.

Atom	x/a	y/b	z/c	Ueq
Molecule A				
C(1)	3426(5)	1212(1)	5139(6)	54(2)
C(2)	3538(6)	0741(1)	4697(7)	54(3)
C(3)	4257(6)	0431(1)	6010(6)	57(2)
C(4)	4801(6)	0578(2)	7733(7)	62(3)
C(5)	4598(5)	1055(2)	8091(6)	58(3)
C(6)	3960(5)	1387(2)	6819(6)	57(3)
N(1)	5090(6)	1229(2)	9936(6)	82(3)
N(2)	2679(6)	1561(2)	3769(7)	72(3)
N(3)	4488(6)	-0073(1)	5554(7)	78(3)
O(1)	5263(6)	1657(2)	10160(6)	109(3)
O(2)	5232(7)	0930(2)	11080(6)	122(4)
O(3)	5361(6)	-0328(1)	6654(6)	108(3)
O(4)	3772(7)	-0206(1)	4103(7)	114(3)
O(5)	2876(7)	1983(1)	4123(6)	117(3)
O(6)	1885(5)	1410(1)	2395(5)	86(2)
Molecule B				
C(1)	7663(6)	3949(2)	538(7)	58(3)
C(2)	6925(5)	3827(1)	-1163(7)	58(3)
C(3)	6736(5)	3345(2)	-1502(6)	56(3)
C(4)	7206(6)	2997(2)	-261(7)	60(3)
C(5)	7925(6)	3143(2)	1394(6)	57(3)
C(6)	8172(6)	3616(2)	1836(7)	61(3)
N(1)	7913(7)	4465(2)	983(7)	81(3)
N(2)	8454(6)	2779(2)	2786(7)	83(3)
N(3)	5954(6)	3199(2)	-3343(6)	83(3)
O(1)	5766(6)	2772(2)	-3624(5)	102(3)
O(2)	5561(7)	3511(2)	-4420(6)	122(4)
O(3)	8159(7)	2368(2)	2361(7)	127(4)
O(4)	9211(6)	2921(2)	4203(6)	103(3)
O(5)	8799(7)	4556(2)	2440(7)	113(3)
O(6)	7274(7)	4755(1)	-75(7)	113(3)

Table 3 (contd...)

Atom	x/a	y/b	z/c	Ueq
Molecule C				
C(1)	2236(5)	3619(1)	9579(6)	52(2)
C(2)	1771(6)	3294(2)	8245(8)	62(3)
C(3)	1884(6)	2811(2)	8539(9)	74(3)
C(4)	2465(6)	2638(2)	129(8)	78(3)
C(5)	2968(6)	2948(2)	1157(8)	68(3)
C(6)	2853(6)	344(1)	11284(7)	6(2)
C(7)	2123(5)	4135(1)	9334(7)	56(2)
C(8)	1634(6)	4381(2)	7852(7)	6(3)
C(9)	1586(6)	495(1)	7851(6)	62(2)
C(1)	1246(5)	5157(1)	6143(6)	54(2)
C(11)	1365(5)	5629(1)	641(6)	54(2)
C(12)	1133(5)	5936(1)	4471(5)	49(2)
C(13)	1463(6)	6424(1)	4678(7)	57(2)
C(14)	122(6)	6726(1)	3244(7)	65(2)
C(15)	643(6)	6549(2)	1584(7)	67(3)
C(16)	336(6)	667(1)	1343(7)	62(3)
C(17)	577(5)	5758(1)	2778(6)	55(2)
O(1)	1841(5)	513	9272(5)	9(2)

Table 4: Hydrogen coordinates (x 10^3), and isotropic displacement parameters (A^2 x 10^2), for complex **3a**.

Atom	x/a	y/b	z/c	Ueq
Molecule A				
H(2)	312(7)	066(2)	363(8)	9(1)
H(4)	509(6)	032(2)	863(7)	8(1)
H(6)	395(5)	174(1)	717(5)	5(1)
Molecule B				
H(2)	645(6)	405(2)	-222(7)	8(1)
H(4)	710(5)	269(2)	-051(5)	5(1)
H(6)	871(6)	372(2)	306(7)	8(1)
Molecule C				
H(2)	146(5)	337(1)	733(5)	4(1)
H(3)	158(6)	264(2)	757(7)	9(2)
H(4)	255(5)	230(2)	1033(5)	6(1)
H(5)	334(5)	284(1)	1263(6)	6(1)

Table 4 (contd...)

Atom	x/a	y/b	z/c	Ueq
H(6)	319(5)	364(2)	1217(6)	6(1)
H(7)	236(5)	430(1)	1038(6)	5(1)
H(8)	126(5)	426(1)	679(6)	6(1)
H(10)	092(3)	497(1)	502(5)	3(1)
H(11)	175(5)	577(1)	710(6)	7(1)
H(13)	191(5)	653(1)	583(6)	6(1)
H(14)	142(5)	703(1)	338(5)	6(1)
H(15)	042(5)	676(1)	063(5)	6(1)
H(16)	-013(6)	593(2)	008(7)	9(1)
H(17)	033(5)	539(1)	253(5)	6(1)

Table 5. Atomic coordinates (x 10^4) and equivalent isotropic displacement parameters (A^2 x 10^3) for complex **3b**. $U_{(eq)}$ is defined as one third of the trace of the orthogonalized U_{ij} tensor.

Atom	x/a	y/b	z/c	Ueq
Molecule A				
C(1)	-325(4)	1428(2)	1810(4)	63(2)
C(2)	-030(4)	935(1)	1705(4)	64(2)
C(3)	769(3)	712(1)	3165(4)	61(2)
C(4)	1269(4)	959(1)	4699(4)	65(2)
C(5)	954(4)	1453(1)	4717(4)	63(2)
C(6)	156(3)	1701(1)	3293(4)	67(2)
N(1)	-1205(4)	1678(1)	262(4)	87(2)
N(2)	1498(4)	1728(1)	6352(4)	86(2)
N(3)	1116(4)	180(1)	3079(4)	81(2)
O(1)	-1711(4)	1425(1)	-983(1)	117(2)
O(2)	-1395(4)	2114(1)	344(4)	117(2)
O(3)	1354(4)	2164(1)	6300(4)	126(2)
O(4)	2063(4)	1503(1)	7640(4)	117(2)
O(5)	1858(4)	-010(1)	4357(4)	113(2)
O(6)	660(5)	-032(1)	1765(4)	144(3)
Molecule B				
C(1)	5364(29)	-175(7)	1478(31)	60(6)
C(2)	5151(17)	343(5)	1310(5)	57(6)
C(3)	4465(14)	484(4)	-502(18)	63(6)

Table 5 (contd...)

Atom	x/a	y/b	z/c	Ueq
C(4)	4233(35)	1(10)	-1495(33)	70(7)
C(5)	5035(13)	-410(4)	-432(20)	54(7)
C(6)	5515(8)	626(2)	2785(8)	60(4)
C(7)	5326(15)	1152(2)	3074(12)	53(6)
C(8)	6025(24)	1345(5)	4677(13)	59(7)
C(9)	5887(28)	1835(5)	5124(18)	80(8)
C(10)	5235(49)	2140(6)	3818(25)	90(9)
C(11)	4526(16)	1965(3)	2212(15)	79(7)
C(12)	4623(29)	1472(3)	1821(17)	64(7)
C(13)	5236(7)	-868(2)	-658(7)	54(4)
C(14)	4845(17)	-1171(3)	-2212(8)	59(6)
C(15)	5201(24)	-1672(4)	-2100(14)	56(7)
C(16)	4879(47)	-1985(6)	-3515(23)	90(9)
C(17)	4130(29)	-1789(5)	-5061(22)	90(9)
C(18)	3895(26)	-1293(4)	-5332(12)	60(6)
C(19)	4233(14)	-996(4)	-3868(11)	63(6)
O(1)	5943(8)	-407(1)	2701(6)	113(4)

Table 6: Hydrogen coordinates (x 10^3), and isotropic displacement parameters (A^2 x 10^2), for complex **3b**.

Atom	x/a	y/b	z/c	Ueq
Molecule A				
H(2)	-37(3)	751(7)	67(3)	6
H(4)	187(3)	816(7)	567(2)	5
H(6)	-03(3)	2043(8)	338(2)	7
Molecule B				
H(31)	332(7)	66(2)	-48(6)	8
H(32)	536(6)	70(1)	-111(6)	8
H(41)	479(5)	01(1)	-270(5)	6
H(42)	289(5)	-01(1)	-195(5)	6
H(6)	596(6)	43(1)	380(6)	6
H(8)	663(5)	112(1)	562(5)	5
H(9)	594(7)	201(2)	629(7)	10
H(10)	521(7)	247(1)	410(8)	11
H(11)	391(6)	220(2)	141(6)	8
H(12)	424(6)	133(1)	69(5)	8

able 6 (contd...)

tom	x/a	y/b	z/c	Ueq
(13)	576(6)	-102(2)	47(6)	6
(15)	568(5)	-177(2)	-88(4)	6
(16)	533(8)	-232(2)	-337(9)	14
(17)	354(6)	-195(2)	-609(6)	6
(18)	356(6)	-114(2)	-649(4)	5
(19)	407(7)	-66(1)	-409(7)	7

able 7. Atomic coordinates (x 10^4) and equivalent isotropic isplacement parameters (A^2 x 10^3) for complex **3c**. $U_{(eq)}$ is defined as ne third of the trace of the orthogonalized U_{ij} tensor.

Atom	x/a	y/b	z/c	Ueq
lolecule A				
(1)	6911(7)	1911(4)	4105(4)	27(2)
(2)	7860(7)	2415(4)	4338(4)	27(2)
(3)	8356(7)	2645(4)	3711(5)	28(2)
(4)	7929(6)	2381(4)	2858(4)	25(2)
(5)	6992(6)	1844(4)	2682(4)	23(2)
(6)	6456(7)	1603(4)	3288(5)	26(2)
(1)	5521(7)	1183(5)	4552(5)	55(2)
(2)	6730(8)	2007(5)	5471(4)	66(3)
(3)	9806(6)	3293(5)	4683(4)	57(2)
(4)	9700(6)	3578(4)	3371(5)	50(2)
(5)	7003(6)	1732(4)	1271(3)	40(2)
(6)	5704(5)	1009(4)	1662(4)	42(2)
(1)	6333(8)	1684(5)	4760(5)	42(2)
(2)	9366(7)	3213(4)	3932(5)	38(2)
(3)	6531(6)	1504(4)	1803(4)	30(2)
lolecule B				
(1)	8469(6)	3056(4)	-1005(4)	22(2)
(2)	7435(6)	2788(4)	-1232(4)	24(2)
(3)	6967(6)	2828(4)	-2069(4)	23(2)
(4)	7510(7)	3105(4)	-2665(4)	25(2)
(5)	8526(7)	3336(4)	-2399(4)	22(2)
(6)	9034(7)	3335(4)	-1572(4)	24(2)
(1)	9828(5)	3456(4)	112(3)	37(2)
(2)	8474(5)	2649(4)	355(3)	39(2)

Table 7 (contd...)

Atom	x/a	y/b	z/c	Ueq
O(3)	5407(5)	2375(4)	-1784(4)	38(2)
O(4)	5467(6)	2623(5)	-3073(4)	44(2)
O(5)	8639(6)	3736(5)	-3738(4)	47(2)
O(6)	10036(6)	3711(4)	-2817(3)	36(2)
N(1)	8962(6)	3050(4)	-112(4)	28(2)
N(2)	5873(6)	2599(4)	-2330(4)	29(2)
N(3)	9121(7)	3617(4)	-3028(4)	27(2)
Molecule C				
C(1)	-810(7)	-1698(4)	-1371(4)	23(2)
C(2)	-1471(6)	-1958(4)	-861(4)	22(2)
C(3)	-2499(7)	-2189(4)	-1162(4)	24(2)
C(4)	-2876(6)	-2116(4)	-1998(4)	23(2)
C(5)	-2262(6)	-1833(4)	-2547(4)	24(2)
C(6)	-1251(6)	-1654(4)	-2211(4)	22(2)
O(1)	-879(6)	-941(5)	-3373(4)	49(2)
O(2)	255(6)	-1659(4)	-2622(4)	40(2)
O(3)	-194(5)	-1612(4)	340(3)	38(2)
O(4)	-1608(5)	-2410(4)	462(4)	40(2)
O(5)	-4509(5)	-2572(4)	-1853(4)	39(2)
O(6)	-4293(5)	-2288(4)	-3097(4)	40(2)
N(1)	-569(6)	-1398(4)	-2776(4)	29(2)
N(2)	-1054(6)	-1990(4)	49(4)	30(2)
N(3)	-3970(6)	-2337(4)	-2342(4)	27(2)
Molecule D				
C(1)	7512(7)	7173(4)	4145(4)	30(2)
C(2)	8447(7)	7616(5)	4079(5)	33(2)
C(3)	8631(7)	7660(4)	3283(5)	30(2)
C(4)	7940(7)	7267(4)	2571(4)	25(2)
C(5)	7041(6)	6816(4)	2679(4)	22(2)
C(6)	6777(7)	6751(4)	3453(4)	26(2)
O(1)	6402(8)	6822(5)	5009(5)	54(2)
O(2)	7982(7)	7359(5)	5588(3)	59(2)
O(3)	10269(6)	8391(5)	3836(5)	58(2)
O(4)	9722(6)	8308(5)	2479(5)	56(2)
O(5)	6474(5)	6476(3)	1242(3)	37(2)
O(6)	5528(5)	5880(4)	2050(4)	36(2)

Table 7 (contd...)

Atom	x/a	y/b	z/c	Ueq
N(1)	7271(8)	7108(5)	4972(4)	44(3)
N(2)	9612(7)	8163(4)	3194(5)	39(2)
N(3)	6290(6)	6360(4)	1930(4)	27(2)
Molecule E				
O(1)	-1060(5)	100(4)	1233(3)	30(2)
C(1)	-1965(7)	-182(4)	1056(4)	22(2)
C(2)	-2515(6)	-491(4)	1728(4)	21(2)
C(3)	-3565(6)	-1054(4)	1471(4)	24(2)
C(4)	-3807(7)	-1451(4)	560(4)	23(2)
C(5)	-3652(6)	-671(4)	-15(4)	25(2)
C(6)	-2582(6)	-192(4)	171(4)	21(2)
C(7)	-2033(7)	-207(4)	2522(4)	24(2)
C(8)	-2110(7)	244(4)	-385(4)	22(2)
C(9)	-2330(6)	-329(4)	3328(4)	22(2)
C(10)	-3277(7)	-726(4)	3423(4)	25(2)
C(11)	-3487(7)	-817(4)	4213(4)	25(2)
C(12)	-2730(8)	-499(5)	4928(4)	33(2)
C(13)	-1795(8)	-97(5)	4851(4)	34(2)
C(14)	-1587(8)	1(5)	4062(4)	29(2)
C(15)	-2520(6)	363(4)	-1279(4)	22(2)
C(16)	-3546(7)	312(4)	-1651(4)	27(2)
C(17)	-3873(8)	389(5)	-2506(4)	33(2)
C(18)	-3185(7)	540(5)	-3004(4)	31(2)
C(19)	-2162(7)	621(4)	-2655(4)	29(2)
C(20)	-1824(7)	539(4)	-1801(4)	24(2)
Molecule F				
O(1)	8880(5)	4999(4)	1200(3)	36(2)
C(1)	7967(7)	4756(4)	992(4)	23(2)
C(2)	7365(6)	4467(4)	1637(4)	21(2)
C(3)	6315(6)	3939(4)	1338(4)	24(2)
C(4)	6076(7)	3576(4)	424(4)	24(2)
C(5)	6309(6)	4357(4)	-136(4)	22(2)
C(6)	7401(6)	4788(4)	93(4)	21(2)
C(7)	7945(7)	5200(4)	-419(4)	22(2)
C(8)	7839(7)	4728(4)	2439(4)	21(2)

Table 7 (contd...)

Atom	x/a	y/b	z/c	Ueq
C(9)	7497(6)	4639(4)	3232(4)	22(2)
C(11)	7970(7)	4933(4)	4754(4)	27(2)
C(10)	8207(7)	4994(4)	3972(4)	23(2)
C(12)	7017(7)	4519(5)	4811(4)	29(2)
C(13)	6304(7)	4176(5)	4089(4)	26(2)
C(14)	6534(6)	4231(4)	3304(4)	23(2)
C(15)	7641(6)	5373(4)	-1318(4)	22(2)
C(16)	8404(7)	5575(4)	-1755(4)	26(2)
C(17)	8175(8)	5742(5)	-2609(5)	32(2)
C(18)	7178(8)	5690(5)	-3036(4)	32(2)
C(19)	6413(8)	5500(4)	-2615(4)	33(2)
C(20)	6642(7)	5353(4)	-1755(4)	24(2)

Table 8: Hydrogen coordinates (x 10^4), and isotropic displacement parameters (A^2 x 10^3), for complex **3c**.

Atom	x/a	y/b	z/c	Ueq
Molecule A				
H(2)	8185(85)	2629(70)	4924(65)	59(28)
H(4)	8271(68)	2508(55)	2417(51)	22(20)
H(6)	5864(75)	1218(61)	3201(52)	19(22)
Molecule B				
H(2)	7042(73)	2537(61)	-832(56)	36(22)
H(4)	7205(68)	3110(55)	-3234(53)	23(21)
H(6)	9714(71)	3496(50)	-1408(46)	3(17)
Molecule C				
H(1)	-134(70)	-1573(49)	-1144(45)	1(17)
H(3)	-2895(72)	-2429(58)	-812(53)	18(20)
H(5)	-2506(67)	-1729(53)	-3089(49)	38(19)
Molecule D				
H(2)	9059(86)	7920(69)	4565(63)	59(29)
H(4)	8154(71)	7294(59)	2026(54)	21(20)
H(6)	6103(82)	6425(67)	3510(59)	22(25)
Molecule E				
H(7)	-1396(64)	150(49)	2545(41)	0(15)
H(8)	-1382(76)	489(60)	-157(52)	19(21)

Table 8 (contd...)

Atom	x/a	y/b	z/c	Ueq
H(10)	-3786(73)	-1004(56)	2984(54)	24(21)
H(11)	-4182(72)	-1070(57)	4313(49)	28(19)
H(14)	-907(76)	256(60)	3992(51)	38(21)
H(12)	-2862(65)	-535(53)	5448(49)	23(18)
H(13)	-1309(87)	98(74)	5301(67)	35(29)
H(16)	-4042(67)	209(51)	-1345(48)	18(18)
H(17)	-4630(85)	351(64)	-2738(59)	37(24)
H(18)	-3404(74)	590(62)	-3603(53)	28(23)
H(19)	-1633(80)	709(63)	-2948(60)	25(23)
H(20)	-1054(70)	563(49)	-1525(46)	18(17)
H(31)	-3574(64)	-1506(52)	1846(48)	26(18)
H(32)	-4000(50)	-648(63)	1617(52)	28(15)
H(41)	-3352(77)	-1968(64)	499(55)	39(23)
H(42)	-4486(75)	-1714(58)	459(51)	1(20)
H(51)	-4152(77)	-242(64)	46(55)	38(23)
H(52)	-3844(67)	-904(55)	-601(49)	36(19)
Molecule F				
H(7)	8627(73)	5354(53)	-186(49)	19(18)
H(8)	8505(71)	5077(56)	2479(47)	40(18)
H(10)	8890(81)	5271(65)	3861(55)	29(23)
H(11)	8521(77)	5185(63)	5258(58)	61(23)
H(12)	6894(66)	4475(53)	5376(48)	28(18)
H(13)	5640(76)	3899(60)	4115(51)	24(21)
H(14)	5989(70)	3926(55)	2845(50)	18(20)
H(16)	9135(75)	5638(58)	-1455(53)	33(21)
H(17)	8764(75)	5884(59)	-2806(54)	46(22)
H(18)	6982(81)	5857(68)	-3680(63)	15(26)
H(19)	5673(78)	5511(57)	-2930(56)	15(21)
H(20)	6137(68)	5271(51)	-1509(45)	9(17)
H(31)	5838(75)	4358(61)	1417(55)	43(21)
H(32)	6164(72)	3437(62)	1720(55)	36(23)
H(41)	6471(80)	3126(71)	324(60)	41(25)
H(42)	5381(78)	3330(59)	227(53)	17(21)
H(51)	6146(66)	4133(55)	-734(47)	34(19)
H(52)	5842(75)	4836(61)	-109(53)	38(21)

Table 9. Atomic coordinates (x 10^4), and equivalent isotropic displacement parameters (A^2 x 10^3), for complex **3d**. U(eq), is defined as one third of the trace of the orthogonalized Uij tensor.

Atom	x/a	y/b	z/c	Ueq
Molecule A				
Cl(1)	672(2)	8732(1)	9355(1)	99(1)
C(1)	1094(6)	8723(3)	8215(3)	66(1)
C(2)	1661(6)	7964(3)	7808(3)	67(1)
C(3)	1958(6)	7907(3)	6883(3)	66(1)
C(4)	1697(6)	8652(3)	6354(3)	62(1)
C(5)	1162(6)	9434(3)	6704(3)	65(1)
C(6)	871(5)	9470(3)	7637(3)	62(1)
N(1)	1936(8)	7149(3)	8373(4)	98(2)
N(2)	2001(6)	8606(3)	5353(3)	80(1)
N(3)	352(6)	10329(3)	7987(4)	84(1)
O(1)	3163(8)	7142(4)	9010(4)	147(2)
O(2)	887(11)	6577(4)	8231(5)	198(4)
O(3)	2584(6)	7926(3)	5070(3)	108(1)
O(4)	1654(7)	9256(3)	4890(3)	123(2)
O(5)	-625(17)	10777(7)	7443(8)	124(3)
O(51)	933(21)	10975(6)	7641(11)	146(5)
O(6)	-491(17)	10357(7)	8653(8)	124(4)
O(61)	913(16)	10577(8)	8753(8)	128(4)
Molecule B				
C(1)	21(17)	5687(7)	5414(11)	78(4)
C(2)	457(9)	5651(7)	4603(9)	139(4)
C(3)	197(15)	4818(14)	4195(6)	188(7)
C(4)	758(12)	6196(7)	3871(7)	68(2)
C(41)	627(11)	5077(6)	3208(6)	65(2)
C(5)	1281(12)	6375(10)	2886(5)	159(5)
C(6)	1759(13)	7095(8)	2399(9)	148(5)
C(7)	1977(10)	7036(6)	1457(7)	113(3)
C(8)	1636(8)	6249(5)	1018(4)	97(2)
C(9)	1153(7)	5552(4)	1526(5)	92(2)
C(10)	1006(8)	5628(6)	2445(6)	117(3)
O(1)	155(12)	6468(5)	5774(5)	98(2)

Table 10: Hydrogen coordinates (x 10^4), and isotropic displacement parameters (A^2 x 10^3), for complex **3d**.

Atom	x/a	y/b	z/c	Ueq
Molecul A				
H(3)	2194(66)	7384(36)	6682(36)	88(16)
H(5)	949(71)	10008(41)	6284(39)	105(18)
Molecule B				
H(4)	990(116)	6847(70)	4008(65)	80(27)
H(41)	445(109)	4641(58)	2672(62)	67(24)
H(6)	1781(93)	7629(52)	2490(55)	124(29)
H(7)	2176(85)	7455(46)	1269(46)	101(25)
H(8)	1683(77)	6306(39)	279(48)	119(21)
H(9)	1099(68)	4910(40)	1236(37)	97(17)

Table 11. Atomic coordinates (x 10^4) and equivalent isotropic displacement parameters (A^2 x 10^3) for complex **3e**. U(eq) is defined as one third of the trace of the orthogonalized Uij tensor.

Atom	x/a	y/b	z/c	Ueq
Molecule A				
Cl(1)	589(3)	6202(2)	9357(1)	98(1)
C(1)	1057(10)	6222(5)	8202(5)	72(2)
C(2)	1513(10)	7012(4)	7818(5)	72(2)
C(3)	1882(10)	7097(4)	6886(5)	68(2)
C(4)	1656(9)	6354(5)	6337(4)	65(2)
C(5)	1145(8)	5550(4)	6685(5)	62(2)
C(6)	861(9)	5519(4)	7636(4)	64(2)
N(1)	1773(16)	7778(6)	8413(6)	111(3)
N(2)	1934(9)	6426(5)	5354(4)	79(2)
N(3)	441(10)	4623(5)	8004(6)	87(2)
O(1)	3069(16)	7805(6)	9058(6)	157(4)
O(2)	698(18)	8356(7)	8290(8)	184(5)
O(3)	2484(10)	7096(5)	5070(4)	110(2)
O(4)	1571(10)	5767(5)	4866(4)	118(2)
O(51)	1221(21)	4010(7)	7709(13)	115(5)
O(52)	-501(31)	4143(12)	7405(13)	148(6)
O(61)	-719(19)	4599(7)	8583(10)	99(4)
O(62)	1007(25)	4316(10)	8698(11)	122(5)

Table 11 (contd...)

Atom	x/a	y/b	z/c	Ueq
Molecule B				
C(1)	156(19)	10725(11)	4611(12)	67(4)
C(2)	261(25)	10140(17)	4249(9)	178(9)
C(3)	292(16)	9351(7)	4628(12)	139(5)
C(41)	752(18)	9947(8)	3205(8)	66(3)
C(42)	661(20)	8805(10)	3805(10)	76(4)
C(5)	1161(10)	8619(7)	2856(4)	183(9)
C(6)	1654(10)	7898(5)	2355(6)	135(4)
C(7)	1870(9)	7983(4)	1415(6)	114(3)
C(8)	1594(9)	8789(5)	977(4)	103(3)
C(9)	1102(9)	9509(4)	1477(6)	109(3)
C(10)	885(10)	9425(6)	2417(6)	154(7)
O(1)	8(18)	11527(8)	4246(8)	98(3)

Table 12. Hydrogen coordinates (x 10^4), and isotropic displacement parameters (A^2 x 10^3), for **3e**.

Atom	x/a	y/b	z/c	Ueq
Molecule A				
H(3)	2014(95)	7875(52)	6716(52)	93(22)
H(5)	837(124)	5031(66)	6532(62)	86(28)
Molecule B				
H(41)	1195(18)	10483(8)	3028(8)	79
H(42)	447(20)	8244(10)	4017(10)	91
H(6)	1838(14)	7359(6)	2649(8)	162
H(7)	2200(14)	7500(5)	1080(8)	137
H(8)	1739(13)	8845(7)	348(4)	124
H(9)	917(13)	10049(4)	1184(8)	131

Table 13. Atomic coordinates (x 10^4), and equivalent isotropic displacement parameters (A^2 x 10^3), for complex **3f**. U(eq), is defined as one third of the trace of the orthogonalized Uij tensor.

Atom	x/a	y/b	z/c	Ueq
Molecule A				
O(1)	7883(5)	8418(3)	1506(1)	61(1)
O(2)	6610(7)	10311(4)	1085(1)	92(1)
O(3)	3542(7)	11420(4)	1158(1)	85(1)

Table 13 (contd...)

Atom	x/a	y/b	z/c	Ueq
O(4)	-967(6)	10822(4)	2153(1)	99(1)
O(5)	-233(6)	9188(4)	2507(1)	85(1)
O(6)	6197(6)	6451(4)	2385(1)	91(1)
O(7)	8733(6)	6803(4)	2007(1)	88(1)
C(1)	6032(6)	8789(3)	1676(1)	46(1)
C(2)	4519(6)	9827(4)	1569(1)	49(1)
C(3)	2623(7)	10184(4)	1756(1)	54(1)
C(4)	2175(6)	9498(4)	2051(1)	50(1)
C(5)	3551(6)	8456(4)	2169(1)	49(1)
C(6)	5453(5)	8122(3)	1982(1)	47(1)
N(1)	4918(7)	10573(3)	1249(1)	64(1)
N(2)	197(5)	9867(4)	2254(1)	67(1)
N(3)	6895(5)	7029(3)	2133(1)	55(1)
Molecule B				
O(1)	643(4)	8725(3)	895(1)	67(1)
C(1)	2376(5)	8260(4)	767(1)	48(1)
C(2)	3469(5)	8760(4)	450(1)	47(1)
C(3)	5617(7)	7971(5)	390(1)	59(1)
C(4)	5791(6)	6914(4)	686(1)	55(1)
C(5)	3772(6)	7135(4)	914(1)	47(1)
C(6)	3122(6)	6502(4)	1200(1)	50(1)
C(7)	4185(6)	5387(3)	1392(1)	49(1)
C(8)	6276(7)	4802(5)	1310(1)	64(1)
C(9)	7188(8)	3771(5)	1512(1)	72(1)
C(10)	6064(10)	3310(5)	1797(1)	73(1)
C(11)	4016(10)	3869(5)	1883(1)	77(1)
C(12)	3104(8)	4903(4)	1684(1)	62(1)
C(13)	2514(6)	9788(4)	268(1)	49(1)
C(14)	3194(6)	10470(4)	-44(1)	49(1)
C(15)	1781(7)	11484(4)	-177(1)	56(1)
C(16)	2327(8)	12216(5)	-467(1)	67(1)
C(17)	4344(8)	11965(5)	-633(1)	67(1)
C(18)	5769(8)	10956(5)	-512(1)	67(1)
C(19)	5242(7)	10218(5)	-221(1)	61(1)

Table 14. Hydrogen coordinates (x 10^4), and isotropic displacement parameters (A^2 x 10^3), for complex **3f**.

Atom	x/a	y/b	z/c	Ueq
Molecule A				
H(1)	7942(91)	8909(56)	1293(14)	104(16)
H(3)	1448(75)	10960(47)	1671(11)	82(13)
H(5)	3255(60)	7978(36)	2372(9)	46(9)
Molecule B				
H(31)	6995(80)	8645(48)	421(11)	76(12)
H(32)	5451(95)	7481(56)	166(12)	74(17)
H(41)	5780(77)	5943(52)	598(11)	66(13)
H(42)	7207(78)	7098(44)	803(11)	63(12)
H(6)	1769(92)	6777(51)	1288(12)	83(15)
H(8)	7018(89)	5085(51)	1116(13)	85(15)
H(9)	8769(89)	3387(53)	1450(13)	83(15)
H(10)	6714(101)	2625(59)	1959(13)	105(17)
H(11)	3159(99)	3508(59)	2087(15)	117(19)
H(12)	1883(104)	5300(59)	1742(13)	87(17)
H(13)	1301(80)	10068(44)	387(10)	59(12)
H(15)	441(71)	11573(42)	-72(10)	61(11)
H(16)	1228(91)	12856(50)	-525(12)	95(14)
H(17)	4704(76)	12483(47)	-822(11)	72(13)
H(18)	7292(92)	10800(57)	-616(13)	92(16)
H(19)	6249(67)	9497(41)	-154(9)	54(10)

Table 15. Atomic coordinates (x 10^4), and equivalent isotropic displacement parameters (A^2 x 10^3), for complex **3g**. U(eq), is defined as one third of the trace of the orthogonalized Uij tensor.

Atom	x/a	y/b	z/c	U(eq)
Molecule A				
C(1)	1741(4)	8816(3)	8349(2)	49(1)
C(2)	3414(3)	8256(3)	8326(2)	48(1)
C(3)	4241(4)	7667(3)	7440(3)	52(1)
C(4)	3393(4)	7671(3)	6512(2)	53(1)
C(5)	1757(4)	8247(3)	6467(3)	54(1)
C(6)	950(4)	8792(3)	7382(3)	53(1)

Table 15 (contd...)

Atom	x/a	y/b	z/c	Ueq
N(1)	4357(4)	8292(3)	9265(2)	66(1)
N(2)	4259(4)	7014(3)	5577(2)	70(1)
N(3)	-792(4)	9371(3)	7313(3)	82(1)
O(1)	916(3)	9370(2)	9198(2)	73(1)
O(2)	3649(3)	8863(3)	10046(2)	81(1)
O(3)	5788(3)	7759(3)	9239(2)	94(1)
O(4)	5688(4)	6429(3)	5689(2)	95(1)
O(5)	3480(4)	7094(3)	4746(2)	101(1)
O(6)	-1358(4)	9755(4)	6337(3)	137(1)
O(7)	-1566(4)	9392(4)	8216(3)	134(1)
Molecule B				
C(1)	7532(4)	4967(3)	2112(2)	49(1)
C(2)	8862(4)	4425(3)	1442(3)	62(1)
C(3)	10382(5)	3940(4)	1919(4)	82(1)
C(4)	10555(5)	3971(4)	3066(4)	87(1)
C(5)	9267(6)	4496(4)	3727(4)	79(1)
C(6)	7756(5)	5012(3)	3264(3)	61(1)
C(7)	5944(4)	5440(3)	1610(3)	49(1)
C(8)	4569(4)	6014(3)	2109(3)	52(1)
C(9)	3020(4)	6422(3)	1548(3)	53(1)
C(10)	1594(4)	6998(3)	2237(3)	57(1)
C(11)	120(4)	7380(3)	1850(3)	55(1)
C(12)	-1374(3)	7955(3)	2464(3)	48(1)
C(13)	-2822(4)	8282(3)	1909(3)	59(1)
C(14)	-4236(4)	8824(4)	2454(4)	68(1)
C(15)	-4277(4)	9063(4)	3554(4)	69(1)
C(16)	-2868(5)	8756(4)	4105(3)	70(1)
C(17)	-1429(4)	8197(3)	3577(3)	57(1)
O(1)	2922(3)	6300(2)	541(2)	76(1)

Table 16. Hydrogen coordinates (x 10^4), and isotropic displacement parameters (A^2 x 10^3), for complex **3g**.

Atom	x/a	y/b	z/c	U(eq)
Molecule A				
H(1)	1932(59)	9307(45)	9821(40)	144(18)
H(3)	5526(28)	7265(21)	7435(18)	26(6)
H(5)	1267(35)	8230(28)	5818(25)	61(9)
Molecule B				
H(2)	8787(37)	4409(30)	640(28)	68(10)
H(3)	11318(47)	3533(36)	1412(32)	93(13)
H(4)	11668(49)	3602(37)	3348(34)	101(13)
H(5)	9389(48)	4545(39)	4488(35)	106(14)
H(6)	6882(42)	5355(33)	3740(29)	78(12)
H(7)	5950(36)	5303(29)	839(27)	65(9)
H(8)	4582(37)	6112(30)	2862(27)	66(9)
H(10)	1713(42)	7061(34)	3004(30)	85(11)
H(11)	16(45)	7206(37)	1012(33)	100(12)
H(13)	-2730(43)	8082(34)	1076(32)	93(12)
H(14)	-5230(48)	9068(37)	2084(33)	97(13)
H(15)	-5316(41)	9476(32)	3887(28)	72(10)
H(16)	-2917(38)	8892(30)	4786(27)	61(10)
H(17)	-491(33)	8014(26)	3968(23)	45(8)

Table 17: Anisotropic displacement parameters (A^2x10^3) for non-H atoms in complex **3c**. (e.s.d's are in parentheses)

Atom	U_{11}	U_{22}	U_{33}	U_{23}	U_{13}	U_{12}
Molecule A						
C(1)	57(2)	59(2)	46(3)	8(2)	0(2)	-5(2)
C(2)	62(2)	59(3)	40(3)	1(2)	-1(2)	-9(2)
C(3)	63(2)	58(2)	50(3)	2(2)	6(2)	3(2)
C(4)	62(2)	75(3)	47(3)	9(2)	4(2)	7(2)
C(5)	54(2)	78(3)	40(3)	-8(2)	-1(2)	1(2)
C(6)	57(2)	63(2)	52(3)	-3(2)	6(2)	-4(2)
N(1)	82(3)	117(4)	48(3)	-15(3)	4(2)	28(3)
N(2)	82(3)	65(3)	69(3)	17(2)	4(2)	-5(2)
N(3)	98(3)	60(2)	78(3)	-2(2)	13(2)	7(2)
O(1)	120(3)	129(4)	79(3)	-50(3)	4(2)	1(3)
O(2)	144(3)	177(5)	45(3)	4(3)	2(2)	68(3)
O(3)	145(3)	80(2)	99(3)	14(2)	-0(3)	41(2)
O(4)	183(4)	68(2)	90(3)	-23(2)	-12(3)	6(2)
O(5)	191(4)	64(2)	97(4)	20(2)	-17(3)	-20(2)
O(6)	105(2)	93(2)	59(3)	9(2)	-16(2)	7(2)
Molecule B						
C(1)	56(2)	52(2)	66(3)	-5(2)	12(2)	-6(2)
C(2)	58(2)	61(3)	54(3)	-1(2)	9(2)	5(2)
C(3)	50(2)	61(2)	56(3)	-7(2)	9(2)	2(2)
C(4)	61(2)	48(2)	70(4)	-1(2)	14(2)	-0(2)
C(5)	56(2)	64(3)	53(3)	4(2)	4(2)	-6(2)
C(6)	58(2)	73(3)	52(3)	1(2)	2(2)	-10(2)
N(1)	98(3)	64(3)	81(4)	-8(3)	17(3)	-4(2)
N(2)	88(3)	80(3)	81(4)	26(3)	4(2)	-2(2)
N(3)	92(3)	97(4)	58(3)	-15(3)	9(2)	6(2)
O(1)	135(3)	93(3)	80(3)	-38(2)	0(2)	-2(2)
O(2)	192(5)	117(3)	56(3)	2(3)	-23(3)	16(3)
O(3)	178(4)	74(3)	124(4)	35(3)	-14(3)	-18(3)
O(4)	123(3)	124(3)	62(3)	19(2)	-8(2)	-1(2)
O(5)	148(4)	91(3)	101(3)	-32(2)	-4(3)	-29(2)
O(6)	162(4)	61(2)	116(4)	-0(2)	12(3)	11(2)

Table 17 (contd...)

Atom	U_{11}	U_{22}	U_{33}	U_{23}	U_{13}	U_{12}
Molecule C						
C(1)	47(2)	47(2)	62(3)	6(2)	8(2)	-2(1)
C(2)	62(2)	60(2)	65(4)	8(3)	-0(2)	-2(2)
C(3)	78(3)	57(3)	86(4)	-5(3)	1(3)	-5(2)
C(4)	78(3)	45(2)	110(5)	10(3)	10(3)	-1(2)
C(5)	68(3)	59(3)	76(4)	24(3)	5(2)	-1(1)
C(6)	63(2)	58(2)	59(3)	4(2)	9(2)	-1(2)
C(7)	59(2)	51(2)	57(3)	-2(2)	8(2)	-2(2)
C(8)	79(3)	47(2)	54(3)	5(2)	-1(2)	-2(2)
C(9)	87(2)	48(2)	52(3)	-1(2)	7(2)	-6(2)
C(10)	68(2)	49(2)	47(2)	4(2)	-0(2)	0(2)
C(11)	66(2)	50(2)	45(3)	0(2)	3(2)	-1(2)
C(12)	55(2)	41(2)	50(3)	3(2)	3(2)	6(1)
C(13)	64(2)	49(2)	56(3)	-0(2)	0(2)	1(2)
C(14)	81(3)	40(2)	74(4)	7(2)	2(2)	2(2)
C(15)	76(3)	59(2)	66(4)	23(3)	9(2)	15(2)
C(16)	68(2)	63(2)	54(3)	4(2)	4(2)	12(2)
C(17)	62(2)	48(2)	54(3)	1(2)	5(1)	8(1)
O(1)	159(3)	50(2)	59(2)	4(2)	10(2)	1(2)

Table 18: Anisotropic displacement parameters (A^2x10^3) for non-H atoms in complex **3b**. (e.s.d's are in parentheses)

Atom	U_{11}	U_{22}	U_{33}	U_{23}	U_{13}	U_{12}
Molecule A						
C(1)	54(2)	73(2)	63(2)	19(2)	-2(2)	-1(2)
C(2)	57(2)	79(2)	55(2)	2(2)	-3(2)	-6(2)
C(3)	61(2)	64(2)	59(2)	8(2)	3(2)	-1(2)
C(4)	58(2)	81(2)	56(2)	11(2)	-2(2)	8(2)
C(5)	56(2)	70(2)	62(2)	-3(2)	1(2)	3(2)
C(6)	57(2)	64(2)	79(2)	8(2)	4(2)	-0(2)

Table 18 (contd...)

Atom	U_{11}	U_{22}	U_{33}	U_{23}	U_{13}	U_{12}
N(1)	78(2)	98(3)	87(2)	31(2)	-13(2)	-13(2)
N(2)	85(2)	94(3)	80(2)	-18(2)	-3(2)	20(2)
N(3)	90(2)	73(2)	79(2)	7(2)	2(2)	2(2)
O(1)	137(2)	131(2)	84(2)	19(2)	-41(2)	-15(2)
O(2)	125(2)	94(2)	131(2)	44(2)	-31(2)	-1(2)
O(3)	164(3)	91(2)	124(2)	-34(2)	-25(2)	26(2)
O(4)	147(3)	132(2)	71(2)	-16(2)	-26(2)	40(2)
O(5)	139(2)	91(2)	110(2)	15(2)	-19(2)	33(2)
O(6)	245(4)	81(2)	105(2)	-19(2)	-45(2)	10(2)
Molecule B						
C(1)	60(9)	70(7)	57(7)	30(7)	-15(6)	-1(7)
C(2)	78(6)	50(7)	42(7)	27(6)	-12(6)	14(4)
C(3)	97(7)	56(6)	37(5)	-5(6)	-1(5)	6(5)
C(4)	70(8)	70(7)	54(6)	23(9)	-9(6)	-24(8)
C(5)	78(7)	42(6)	43(8)	26(7)	-18(7)	-8(5)
C(6)	81(5)	52(4)	46(4)	6(3)	-6(3)	6(3)
C(7)	65(7)	52(6)	40(7)	3(5)	19(7)	-8(5)
C(8)	66(6)	78(7)	34(7)	10(6)	4(6)	-5(5)
C(9)	110(2)	80(8)	42(8)	-9(8)	18(9)	-30(7)
C(10)	120(8)	57(9)	100(9)	-18(7)	-1(9)	-19(9)
C(11)	10(8)	38(5)	100(8)	8(7)	6(5)	3(5)
C(12)	78(7)	49(8)	68(7)	-5(7)	-7(5)	-9(9)
C(13)	75(4)	49(4)	55(4)	11(4)	-8(3)	3(3)
C(14)	60(5)	62(6)	40(6)	-8(5)	10(6)	-2(4)
C(15)	76(4)	43(8)	49(6)	-1(7)	2(5)	0(6)
C(16)	110(7)	60(8)	90(9)	-6(9)	2(7)	-10(6)
C(17)	90(7)	70(8)	110(9)	-50(9)	-19(9)	8(8)
C(18)	96(7)	51(6)	31(6)	2(5)	7(6)	4(6)
C(19)	79(7)	56(6)	56(7)	3(5)	-4(5)	-8(5)
O(1)	210(6)	59(3)	70(3)	-2(2)	-58(4)	24(3)

Table 19: Anisotropic displacement parameters (A^2x10^3) for non-H atoms in complex **3c**. (e.s.d's are in parentheses)

Atom	U_{11}	U_{22}	U_{33}	U_{23}	U_{13}	U_{12}
Molecule A						
C(1)	32(6)	25(2)	30(3)	5(2)	14(3)	9(3)
C(2)	27(7)	24(3)	31(3)	3(2)	2(3)	13(3)
C(3)	20(6)	22(3)	42(3)	-2(2)	3(3)	6(3)
C(4)	24(6)	22(2)	30(3)	3(2)	8(3)	5(3)
C(5)	26(6)	18(2)	27(3)	1(2)	4(3)	8(3)
C(6)	20(6)	17(3)	43(3)	3(2)	11(3)	3(3)
O(1)	48(7)	59(4)	65(4)	15(3)	30(4)	2(4)
O(2)	12(1)	46(3)	42(3)	1(3)	37(4)	2(4)
O(3)	38(6)	59(4)	60(4)	-4(3)	-17(4)	9(3)
O(4)	36(5)	40(3)	76(4)	-6(3)	24(4)	-3(3)
O(5)	60(6)	36(3)	29(2)	3(2)	16(3)	10(3)
O(6)	31(5)	37(3)	50(3)	-10(2)	-3(3)	2(3)
N(1)	70(8)	27(3)	39(3)	8(2)	29(4)	19(3)
N(2)	26(6)	31(3)	58(4)	-3(3)	8(4)	7(3)
N(3)	36(6)	23(2)	32(3)	-1(2)	4(3)	9(3)
Molecule B						
C(1)	20(6)	26(2)	20(3)	0(2)	4(3)	4(2)
C(2)	28(6)	18(2)	28(3)	-3(2)	10(3)	2(2)
C(3)	14(6)	19(2)	37(3)	-7(2)	10(3)	3(2)
C(4)	26(7)	21(3)	27(3)	-3(2)	4(3)	7(3)
C(5)	20(6)	19(2)	29(3)	-1(2)	10(3)	0(2)
C(6)	17(6)	21(2)	32(3)	0(2)	7(3)	-1(2)
O(1)	24(5)	46(3)	36(2)	1(2)	0(2)	-2(2)
O(2)	33(5)	52(3)	32(3)	12(2)	10(2)	1(3)
O(3)	20(5)	38(3)	56(3)	-2(2)	13(3)	-1(2)
O(4)	30(5)	58(4)	38(3)	-10(2)	-4(3)	8(3)
O(5)	51(6)	66(4)	27(2)	12(2)	12(3)	12(3)
O(6)	28(5)	43(3)	38(3)	-7(2)	17(3)	-9(3)
N(1)	26(6)	30(3)	28(3)	3(2)	4(3)	0(3)
N(2)	22(5)	22(3)	42(3)	-9(2)	6(3)	3(2)
N(3)	29(6)	24(3)	30(3)	1(2)	13(3)	-1(3)
Molecule C						
C(1)	17(6)	21(2)	31(3)	-1(2)	6(3)	2(2)
C(2)	18(6)	22(2)	25(3)	-3(2)	5(3)	0(2)

Table 19 (contd...)

Atom	U_{11}	U_{22}	U_{33}	U_{23}	U_{13}	U_{12}
C(3)	26(6)	19(2)	28(3)	0(2)	12(3)	3(3)
C(4)	17(6)	19(2)	31(3)	-5(2)	6(3)	-1(2)
C(5)	26(6)	24(3)	22(3)	-2(2)	9(3)	3(3)
C(6)	22(6)	19(2)	27(3)	0(2)	8(3)	2(2)
N(1)	33(6)	23(3)	32(3)	-7(2)	14(3)	-2(3)
N(2)	31(5)	32(3)	28(3)	2(2)	5(3)	4(3)
N(3)	23(5)	23(3)	31(3)	-5(2)	5(3)	-1(2)
O(1)	50(6)	61(4)	40(3)	16(3)	20(3)	8(3)
O(2)	33(5)	40(3)	52(3)	-3(2)	24(3)	5(3)
O(3)	26(5)	48(3)	32(3)	-4(2)	-2(2)	-2(3)
O(4)	35(5)	53(3)	31(2)	13(2)	7(2)	6(3)
O(5)	26(5)	41(3)	49(3)	-2(2)	13(3)	-1(2)
O(6)	28(5)	50(3)	38(3)	-1(2)	-2(3)	7(3)
Molecule D						
C(1)	47(7)	24(3)	21(3)	2(2)	5(3)	16(3)
C(2)	36(6)	21(3)	35(3)	-3(2)	-6(3)	7(3)
C(3)	19(6)	26(3)	42(3)	0(2)	2(3)	3(3)
C(4)	21(6)	20(3)	36(3)	5(2)	8(3)	3(3)
C(5)	23(5)	15(2)	25(3)	-1(2)	1(3)	3(2)
C(6)	34(6)	22(2)	27(3)	8(2)	10(3)	10(3)
O(1)	63(7)	63(4)	54(4)	23(3)	35(4)	25(4)
O(2)	94(7)	53(4)	26(2)	-2(2)	3(3)	12(4)
O(3)	46(6)	50(4)	63(4)	-11(3)	-3(4)	-9(3)
O(4)	43(6)	58(3)	65(4)	16(3)	16(3)	-8(3)
O(5)	53(5)	30(2)	24(2)	0(2)	0(3)	4(2)
O(6)	25(5)	29(2)	50(3)	-3(2)	3(3)	-4(2)
N(1)	73(8)	32(3)	31(3)	5(2)	13(4)	21(4)
N(2)	26(6)	33(3)	51(4)	-3(3)	1(3)	0(3)
N(3)	30(5)	22(2)	28(2)	2(2)	1(3)	9(2)
Molecule E						
O(1)	23(5)	41(3)	25(2)	2(2)	7(2)	-2(2)
C(1)	20(6)	23(2)	24(3)	0(2)	5(3)	0(3)
C(2)	21(5)	21(2)	22(3)	0(2)	7(3)	4(2)
C(3)	26(6)	24(3)	20(2)	4(2)	4(3)	-3(3)
C(4)	20(6)	22(3)	25(3)	-4(2)	6(3)	-7(3)
C(5)	25(6)	27(3)	21(2)	-1(2)	7(3)	-3(3)

Table 19 (contd...)

C(6)	18(6)	20(2)	24(3)	-2(2)	8(3)	-1(2)
C(7)	29(6)	20(2)	26(3)	2(2)	10(3)	6(2)
C(8)	23(6)	19(2)	23(3)	-4(2)	8(3)	-3(3)
C(9)	24(6)	16(2)	26(3)	2(2)	7(3)	5(2)
C(10)	26(6)	25(3)	25(3)	2(2)	7(3)	10(3)
C(11)	27(6)	27(3)	26(3)	2(2)	12(3)	7(3)
C(12)	57(7)	26(3)	22(3)	3(2)	17(3)	12(3)
C(13)	52(7)	26(3)	20(3)	-2(2)	3(3)	2(3)
C(14)	37(7)	21(3)	27(3)	2(2)	4(3)	2(3)
C(15)	31(6)	14(2)	21(3)	-2(2)	8(3)	-1(2)
C(16)	29(6)	23(2)	31(3)	4(2)	12(3)	3(3)
C(17)	40(7)	25(3)	29(3)	3(2)	1(3)	4(3)
C(18)	46(6)	22(3)	25(3)	2(2)	12(3)	5(3)
C(19)	33(7)	29(3)	28(3)	2(2)	14(3)	1(3)
C(20)	22(6)	22(3)	24(3)	-6(2)	5(3)	-3(2)
Molecule F						
O(1)	24(5)	55(3)	24(2)	3(2)	2(2)	-9(3)
C(1)	18(6)	27(3)	23(3)	0(2)	6(3)	-1(3)
C(2)	22(6)	17(2)	24(3)	2(2)	5(3)	-1(2)
C(3)	23(6)	26(3)	24(3)	1(2)	10(3)	2(3)
C(4)	24(6)	23(3)	27(3)	-3(2)	9(3)	0(3)
C(5)	20(6)	24(3)	19(2)	-3(2)	1(2)	1(3)
C(6)	18(6)	22(3)	22(3)	-2(2)	3(3)	-1(2)
C(7)	15(6)	23(3)	27(3)	-1(2)	5(3)	0(3)
C(8)	18(6)	21(2)	22(3)	2(2)	3(3)	-1(3)
C(9)	30(5)	17(2)	19(3)	1(2)	3(2)	8(2)
C(11)	34(6)	21(3)	24(3)	-3(2)	-1(3)	4(3)
C(10)	28(6)	22(2)	19(3)	-1(2)	6(3)	3(3)
C(12)	42(6)	26(3)	19(3)	0(2)	6(3)	9(3)
C(13)	25(6)	24(3)	28(3)	-6(2)	8(3)	2(3)
C(14)	26(6)	23(2)	20(2)	1(2)	3(2)	5(2)
C(15)	28(6)	13(2)	24(3)	-1(2)	7(3)	-2(2)
C(16)	25(6)	24(3)	27(3)	-2(2)	7(3)	-1(3)
C(17)	41(8)	26(3)	35(3)	2(2)	24(4)	3(3)
C(18)	47(7)	24(3)	25(3)	0(2)	12(3)	0(3)
C(19)	43(7)	22(3)	31(3)	4(2)	-1(3)	6(3)
C(20)	22(6)	23(2)	28(3)	3(2)	9(3)	1(2)

Table 20: Anisotropic displacement parameters (A^2x10^3) for non-H atoms in complex **3d**. (e.s.d's are in parentheses)

Atom	U_{11}	U_{22}	U_{33}	U_{23}	U_{13}	U_{12}
Molecule A						
Cl(1)	103(1)	138(2)	61(1)	-6(1)	29(1)	-4(1)
C(1)	66(3)	75(3)	58(3)	-9(2)	18(2)	-6(2)
C(2)	80(3)	64(3)	58(2)	5(2)	15(2)	-9(2)
C(3)	75(3)	57(3)	66(3)	-7(2)	14(2)	-8(2)
C(4)	66(2)	67(3)	53(2)	-3(2)	7(2)	-14(2)
C(5)	61(2)	65(3)	69(3)	0(2)	9(2)	-7(2)
C(6)	59(2)	63(3)	67(3)	-12(2)	9(2)	-8(2)
N(1)	136(4)	75(3)	85(3)	18(3)	24(3)	-13(3)
N(2)	92(3)	92(3)	59(2)	-2(2)	14(2)	-16(2)
N(3)	84(3)	75(3)	95(3)	-18(3)	13(3)	3(2)
O(1)	161(5)	142(5)	133(5)	61(4)	-5(4)	-1(4)
O(2)	300(9)	105(4)	175(6)	51(4)	-51(6)	-81(5)
O(3)	150(4)	111(3)	70(2)	-21(2)	38(2)	-8(3)
O(4)	177(4)	122(4)	74(3)	28(3)	33(3)	19(3)
O(5)	161(9)	64(5)	144(9)	-8(5)	1(8)	13(7)
O(51)	202(12)	58(5)	191(13)	-17(6)	85(11)	-14(7)
O(6)	151(9)	101(6)	131(8)	-43(6)	65(8)	1(7)
O(61)	127(8)	132(9)	125(8)	-73(7)	6(7)	14(7)
Molecule B						
C(1)	84(7)	54(6)	90(10)	-33(6)	-23(7)	-18(5)
C(2)	92(4)	151(7)	187(8)	119(7)	71(5)	38(4)
C(3)	141(8)	350(20)	67(5)	-51(9)	-13(5)	139(11)
C(4)	67(5)	67(6)	70(6)	-4(5)	12(4)	-9(4)
C(41)	65(5)	76(6)	54(5)	1(4)	12(4)	-11(4)
C(5)	131(7)	278(15)	70(5)	30(6)	20(4)	124(9)
C(6)	125(6)	155(9)	151(10)	-70(8)	-52(6)	61(6)
C(7)	96(4)	107(6)	135(7)	38(6)	-4(4)	-6(4)
C(8)	85(4)	139(6)	70(3)	24(4)	20(3)	22(4)
C(9)	78(3)	93(4)	109(5)	19(4)	25(3)	5(3)
C(10)	81(4)	167(7)	111(5)	76(5)	50(4)	42(4)
O(1)	149(7)	76(5)	72(5)	-6(4)	36(4)	-27(5)

Table 21. Anisotropic displacement parameters (A^2x10^3) for non-H atoms in complex **3e**. (e.s.d's are in parentheses)

Atom	U_{11}	U_{22}	U_{33}	U_{23}	U_{13}	U_{12}
Molecule A						
Cl(1)	107(2)	128(2)	63(1)	1(1)	26(1)	-6(1)
C(1)	83(5)	72(4)	65(4)	3(3)	24(3)	-13(3)
C(2)	91(5)	58(4)	71(4)	-5(3)	27(3)	-2(3)
C(3)	86(5)	54(4)	66(4)	1(3)	13(3)	-2(3)
C(4)	71(4)	72(4)	55(3)	-3(3)	21(3)	11(3)
C(5)	59(4)	53(4)	72(4)	-2(3)	1(3)	3(3)
C(6)	71(4)	59(4)	65(3)	11(3)	15(3)	17(3)
N(1)	16(1)	85(6)	95(6)	-36(5)	55(6)	-16(5)
N(2)	93(5)	88(4)	56(3)	1(3)	4(3)	13(3)
N(3)	92(5)	69(4)	101(5)	7(4)	15(4)	-9(4)
O(1)	21(1)	136(7)	119(7)	-50(6)	11(6)	-31(6)
O(2)	28(1)	110(7)	159(9)	-55(6)	-2(8)	38(8)
O(3)	16(1)	98(4)	74(3)	24(3)	31(4)	4(4)
O(4)	15(1)	125(5)	78(4)	-26(4)	22(4)	-21(4)
O(51)	13(1)	42(5)	18(1)	13(7)	40(10)	28(6)
O(52)	21(2)	105(12)	12(1)	6(10)	-1(1)	13(13)
O(61)	12(1)	71(7)	117(9)	18(6)	46(8)	-7(6)
O(62)	17(2)	93(9)	10(1)	47(8)	-6(9)	-8(9)
Molecule B						
C(1)	55(7)	70(9)	79(10)	23(7)	19(7)	18(6)
C(2)	18(2)	243(21)	97(9)	47(12)	-28(9)	-13(2)
C(3)	13(1)	71(6)	23(2)	-56(7)	93(10)	-16(5)
C(41)	78(8)	63(7)	56(6)	11(5)	1(6)	4(6)
C(42)	74(9)	76(9)	74(8)	1(7)	-6(7)	3(7)
C(5)	16(1)	315(24)	73(6)	-3(1)	17(6)	-16(2)
C(6)	13(1)	168(12)	104(8)	7(8)	-18(7)	-55(8)
C(7)	94(7)	124(9)	126(8)	-41(7)	20(6)	-6(5)
C(8)	11(1)	131(9)	73(5)	-12(6)	25(4)	-15(6)
C(9)	74(5)	104(7)	156(9)	-22(6)	40(5)	-1(4)
C(10)	10(1)	22(2)	15(1)	-11(1)	77(8)	-79(9)
O(1)	14(1)	82(8)	71(6)	-10(6)	23(6)	12(6)

Table 22. Anisotropic displacement parameters (A^2x10^3) for non-H atoms in complex **3f**. (e.s.d's are in parentheses)

Atom	U_{11}	U_{22}	U_{33}	U_{23}	U_{13}	U_{12}
Molecule A						
O(1)	55(1)	72(2)	56(2)	4(1)	11(1)	5(1)
O(2)	105(3)	95(2)	78(2)	29(2)	31(2)	15(2)
O(3)	95(2)	80(2)	80(2)	25(2)	-16(2)	8(2)
O(4)	68(2)	104(3)	124(3)	2(2)	3(2)	38(2)
O(5)	71(2)	88(2)	97(2)	-7(2)	34(2)	-3(2)
O(6)	84(2)	97(2)	92(2)	49(2)	14(2)	24(2)
O(7)	74(2)	105(3)	86(2)	16(2)	18(2)	44(2)
C(1)	47(2)	46(2)	45(2)	-4(2)	-5(1)	-4(1)
C(2)	50(2)	48(2)	48(2)	0(2)	-8(2)	-7(1)
C(3)	53(2)	45(2)	63(2)	-2(2)	-14(2)	-1(2)
C(4)	42(2)	51(2)	58(2)	-8(2)	-2(2)	-2(1)
C(5)	47(2)	52(2)	47(2)	-3(2)	2(2)	-3(1)
C(6)	45(2)	46(2)	50(2)	-2(2)	-7(1)	3(1)
N(1)	82(2)	57(2)	54(2)	10(2)	-11(2)	-3(2)
N(2)	46(2)	71(2)	85(3)	-11(2)	1(2)	5(2)
N(3)	54(2)	54(2)	58(2)	0(2)	-4(2)	6(1)
Molecule B						
O(1)	55(1)	76(2)	69(2)	15(2)	18(1)	17(1)
C(1)	40(2)	56(2)	50(2)	-7(2)	4(1)	1(1)
C(2)	43(2)	53(2)	46(2)	-2(2)	4(1)	0(1)
C(3)	53(2)	67(2)	55(2)	4(2)	10(2)	13(2)
C(4)	48(2)	58(2)	58(2)	2(2)	7(2)	9(2)
C(5)	45(2)	45(2)	50(2)	-6(2)	2(1)	2(1)
C(6)	47(2)	50(2)	52(2)	-3(2)	1(2)	2(1)
C(7)	51(2)	48(2)	49(2)	-5(2)	-1(2)	5(2)
C(8)	61(2)	65(2)	66(3)	4(2)	1(2)	11(2)
C(9)	67(3)	70(3)	81(3)	-2(2)	-1(2)	24(2)
C(10)	92(3)	65(2)	63(3)	1(2)	-7(3)	20(2)
C(11)	100(3)	73(3)	59(3)	13(2)	13(3)	17(3)
C(12)	66(2)	63(2)	58(2)	1(2)	12(2)	8(2)
C(13)	41(2)	56(2)	51(2)	-7(2)	5(1)	1(1)
C(14)	46(2)	50(2)	51(2)	-8(2)	0(2)	-1(1)
C(15)	52(2)	63(2)	54(2)	0(2)	1(2)	3(2)
C(16)	70(2)	76(3)	54(2)	8(2)	-4(2)	1(2)

Table 22 (contd...)

Atom	U_{11}	U_{22}	U_{33}	U_{23}	U_{13}	U_{12}
C(17)	75(3)	82(3)	43(2)	4(2)	2(2)	-9(2)
C(18)	61(2)	86(3)	55(2)	-2(2)	12(2)	-6(2)
C(19)	56(2)	67(2)	58(2)	-1(2)	6(2)	6(2)

Table 23. Anisotropic displacement parameters (A^2x10^3) for non-H atoms in complex **3g**. (e.s.d's are in parentheses)

Atom	U_{11}	U_{22}	U_{33}	U_{23}	U_{13}	U_{12}
Molecule A						
C(1)	57(2)	45(2)	43(2)	-14(1)	7(1)	-13(2)
C(2)	58(2)	53(2)	33(1)	-8(1)	-5(1)	-20(2)
C(3)	57(2)	51(2)	48(2)	-12(2)	3(1)	-21(2)
C(4)	70(2)	53(2)	40(2)	-16(1)	10(2)	-26(2)
C(5)	66(2)	59(2)	45(2)	-14(2)	-6(2)	-27(2)
C(6)	47(2)	52(2)	55(2)	-12(2)	-2(1)	-13(2)
N(1)	78(2)	74(2)	48(2)	-14(2)	-5(2)	-29(2)
N(2)	93(2)	80(2)	52(2)	-28(2)	20(2)	-45(2)
N(3)	60(2)	83(2)	100(3)	-26(2)	-11(2)	-14(2)
O(1)	78(2)	74(2)	59(1)	-30(1)	12(1)	-10(1)
O(2)	104(2)	91(2)	54(1)	-33(1)	-10(1)	-27(2)
O(3)	64(2)	132(3)	84(2)	-30(2)	-18(1)	-25(2)
O(4)	89(2)	104(2)	85(2)	-43(2)	33(2)	-22(2)
O(5)	130(3)	140(3)	62(2)	-53(2)	17(2)	-69(2)
O(6)	82(2)	177(4)	126(3)	-10(2)	-49(2)	-17(2)
O(7)	61(2)	192(4)	136(3)	-62(3)	19(2)	-18(2)
Molecule B						
C(1)	55(2)	45(2)	49(2)	-12(1)	-3(1)	-18(1)
C(2)	57(2)	65(2)	62(2)	-12(2)	0(2)	-20(2)
C(3)	55(2)	80(3)	107(3)	-15(2)	-1(2)	-22(2)
C(4)	64(3)	86(3)	113(4)	-3(3)	-32(3)	-31(2)
C(5)	87(3)	76(3)	83(3)	-9(2)	-31(2)	-35(2)
C(6)	72(2)	59(2)	60(2)	-14(2)	-8(2)	-28(2)
C(7)	57(2)	47(2)	44(2)	-13(1)	-2(1)	-17(2)
C(8)	56(2)	56(2)	40(2)	-17(2)	-1(2)	-12(2)
C(9)	58(2)	56(2)	47(2)	-20(2)	2(1)	-17(2)
C(10)	60(2)	61(2)	49(2)	-18(2)	-1(2)	-17(2)
C(11)	55(2)	57(2)	56(2)	-21(2)	-3(2)	-18(2)

Table 23 (contd...)

Atom	U_{11}	U_{22}	U_{33}	U_{23}	U_{13}	U_{12}
C(12)	52(2)	40(2)	54(2)	-10(1)	-3(1)	-17(1)
C(13)	57(2)	57(2)	70(2)	-21(2)	-9(2)	-20(2)
C(14)	50(2)	66(2)	91(3)	-20(2)	-6(2)	-19(2)
C(15)	52(2)	65(2)	86(3)	-17(2)	12(2)	-20(2)
C(16)	73(3)	81(3)	56(2)	-24(2)	11(2)	-26(2)
C(17)	55(2)	64(2)	54(2)	-12(2)	-5(2)	-23(2)
O(1)	69(2)	102(2)	60(1)	-41(1)	-5(1)	-17(1)

Appendix A-6

Table 1. Geometrical Question for the retrieval and the calculations of h, r ΣN and c of β-lactams

```
SCRE -28 35 88 153
T1 *CONN
NFRAG  1
AT1 N 3
AT2 C 2
AT3 C 3
AT4 O 1
AT5 O 1
AT6 C 2
AT7 C 2
AT8 C 3
AT9 O 1
BO 1 2
BO 1 6
BO 1 8
BO 2 3
BO 3 4 99
BO 3 5 99
BO 6 7
BO 7 8
BO 8 9 2
GEOM
SETUP P1 2 6 8
DEFINE DIS1 P1 1
DEFINE DIS2 9 3
DEFINE CO 8 9
DEFINE CN 8 1
DEFINE TOR1 8 1 2 3
TRANSFORM ABSDIS = ABS DIS1
TRANSFORM ABSTOR = ABS TOR1
SCAT CO CN
HIST ABSDIS
HIST DIS2
```

```
SCAT ABSDIS DIS2
SCAT ABSTOR DIS2
SCAT ABSDIS ABSTOR
SCAT ABSDIS CN
SCAT ABSDIS CO
C OVERLAP OF CRYSTAL FRAGMENTS PERMITTED
C SEARCH FOR ALL CRYSTAL FRAGMENTS
NFRAG -99
SYMCHK ON
C REJECTION OF SYMMETRY EQUIVALENT CRYSTAL
C FRAGMENTS IS ON
ENANT NOIN
ENANT NOIN
END
QUEST T1
```

Table 2: List of 126 hits from the 114 b-lactams in this study giving relevant geometrical parameters.

	Refcode	h	c	C=O	C-N	∑N
1	ACPENC10	0.440	3.607	1.204	1.419	331.5
2	AMOXCT10	0.388	3.971	1.192	1.368	337.8
3	ATIMYM	0.491	3.568	1.217	1.415	325.9
4	BACMEC10	0.424	3.847	1.190	1.382	334.0
5	BAFVOT	0.377	3.904	1.201	1.388	339.2
6	BAFVUZ	0.373	3.902	1.196	1.389	339.6
7	BAJXOZ	0.140	3.419	1.219	1.344	356.9
8	BALSOW	0.500	3.613	1.194	1.419	324.2
9	BALSUC	0.535	4.276	1.210	1.401	320.5
10	BEBBUF	0.428	3.833	1.198	1.372	333.8
11	BENPEN10	0.383	4.427	1.206	1.377	338.2
12	BEVCIO	0.206	3.746	1.196	1.354	353.5
13	BEWCUB	0.538	3.464	1.196	1.437	319.7
14	BEZSUU	0.184	3.497	1.209	1.363	354.5
15	BEZSUU	0.168	3.519	1.201	1.366	355.3
16	BIBGIC	0.349	3.938	1.195	1.372	342.0
17	BIKKAH	0.497	4.412	1.205	1.403	325.1

18	BIXHOF	0.052	4.346	1.203	1.366	359.6
19	BOVFOH	0.113	4.178	1.207	1.367	357.9
20	BOVJEB	0.239	4.272	1.201	1.375	351.0
21	BPENCE10	0.398	4.417	1.201	1.367	336.7
22	BUYGOR	0.099	3.978	1.194	1.375	358.5
23	CAHDUK	0.039	3.478	1.223	1.350	359.8
24	CARCED	0.402	4.063	1.191	1.404	336.5
25	CEBZOY	0.064	4.226	1.200	1.371	359.3
26	CEHKIJ	0.498	4.330	1.188	1.397	325.0
27	CEHXES01	0.205	3.328	1.206	1.361	353.3
28	CEPHAP	0.224	3.189	1.211	1.377	352.1
29	CEPHHM10	0.244	3.198	1.214	1.390	350.6
30	CETHNA	0.150	3.296	1.206	1.352	356.4
31	CETHNA	0.088	3.238	1.154	1.429	358.8
32	CETVIG	0.470	4.404	1.208	1.390	327.4
33	CEXJUK	0.165	3.448	1.204	1.387	355.6
34	CIJLEM	0.240	3.729	1.219	1.349	350.9
35	CLAVBB10	0.565	4.354	1.192	1.480	319.4
36	CMIPEN	0.392	4.446	1.184	1.391	337.5
37	COPREE	0.283	3.335	1.191	1.407	347.4
38	CUJPOM	0.427	4.381	1.194	1.389	333.1
39	CUWZUP	0.376	4.391	1.207	1.379	338.5
40	DABZEL	0.061	3.059	1.209	1.382	359.4
41	DAXKOC	0.340	3.928	1.177	1.377	342.9
42	DBHCEP	0.074	3.016	1.208	1.387	359.1
43	DCLOXL	0.412	4.365	1.188	1.417	335.7
44	DCLOXL	0.412	4.454	1.197	1.377	335.0
45	DEHHED	0.493	3.580	1.199	1.399	325.0
46	DEHHON	0.046	3.825	1.208	1.339	360.0
47	DEHHON	0.069	3.921	1.214	1.309	359.2
48	DIWFOE	0.388	2.896	1.183	1.404	338.2
49	DOHZOP	0.342	4.356	1.214	1.352	342.1
50	DOHZUV	0.355	4.364	1.199	1.357	340.9
51	DOJLUJ	0.356	3.895	1.180	1.374	341.3
52	DOJMAQ	0.363	4.048	1.193	1.364	340.6
53	DOSCUJ	0.516	4.326	1.195	1.402	322.2
54	DUFJUJ	0.370	3.940	1.183	1.373	339.5
55	DUKSUX	0.320	4.028	1.193	1.395	344.5

56	DUKTAE	0.409	3.949	1.179	1.399	335.9
57	DUKVUA	0.370	4.403	1.199	1.384	339.4
58	FAHRAH	0.435	4.414	1.208	1.403	332.6
59	FAJMAE	0.162	3.429	1.210	1.407	355.7
60	FAJMEI	0.216	3.490	1.208	1.371	352.6
61	FECPAE	0.386	4.370	1.202	1.378	337.7
62	FECPEI	0.406	3.993	1.201	1.395	335.9
63	FOLMIC	0.398	4.302	1.190	1.385	336.9
64	FOLMIC	0.460	4.239	1.188	1.420	330.3
65	FOPLIF	0.413	3.974	1.207	1.371	334.9
66	FOWFEC	0.197	4.465	1.208	1.409	354.1
67	FOZKIO	0.001	3.467	1.214	1.348	360.0
68	FUFBEN	0.290	3.467	1.192	1.392	347.0
69	FUWVIC	0.376	4.010	1.197	1.393	339.3
70	FUWVOI	0.187	3.316	1.199	1.381	354.5
71	GARPUK	0.416	4.061	1.188	1.400	335.1
72	GEBRUA	0.372	4.438	1.193	1.387	339.7
73	GEXHUM	0.423	3.733	1.184	1.381	334.1
74	IPENSX	0.406	4.037	1.192	1.388	335.8
75	IZCEPL	0.176	3.614	1.161	1.425	355.0
76	JANDOR	0.439	3.668	1.201	1.402	331.0
77	JEJGEK	0.433	3.585	1.184	1.428	332.3
78	JELXED	0.483	4.384	1.195	1.387	326.8
79	JELXIH	0.382	3.088	1.199	1.383	338.1
80	JELXIH	0.446	2.970	1.225	1.360	330.9
81	JIMZAG	0.422	3.979	1.204	1.395	334.1
82	JIMZAG	0.431	4.022	1.199	1.388	333.0
83	JOSVUI	0.217	3.244	1.215	1.358	352.5
84	JOSWAP	0.218	3.192	1.194	1.378	352.6
85	JOTLAF	0.401	4.413	1.193	1.394	336.4
86	JOTLEJ	0.422	3.995	1.192	1.397	334.2
87	JOYFOS	0.151	3.054	1.207	1.359	356.4
88	JUVNUJ	0.529	3.671	1.197	1.421	320.2
89	KAGPEN	0.488	4.472	1.200	1.414	326.8
90	KECGII	0.389	3.945	1.172	1.406	338.6
91	KEHGAF	0.045	4.208	1.197	1.372	359.7
92	KOFNIC	0.418	4.021	1.185	1.410	334.9
93	KOFNIC	0.388	4.025	1.188	1.381	337.8

94 MBAPEN	0.368	4.346	1.205	1.389	339.9
95 MCMXCM	0.197	3.280	1.193	1.383	353.8
96 METHIC	0.444	4.008	1.196	1.389	331.5
97 MOACPM	0.220	3.536	1.201	1.393	352.2
98 MOSNCO	0.419	4.431	1.190	1.413	335.1
99 MPIXPS	0.381	4.438	1.211	1.414	339.0
100 NBPENC	0.424	3.598	1.196	1.400	333.3
101 NBPEPC	0.419	4.322	1.192	1.402	334.2
102 PACWUL	0.248	3.011	1.211	1.355	350.1
103 PACWUL	0.287	2.956	1.223	1.397	347.5
104 PAMXCP	0.029	3.061	1.197	1.355	359.9
105 PAMXCP	0.029	3.932	1.197	1.355	359.9
106 PEJJUJ	0.484	3.116	1.200	1.395	326.3
107 PEJKEU	0.392	4.100	1.173	1.411	337.6
108 PENTOS10	0.058	3.235	1.197	1.385	359.5
109 PIPCIL	0.445	3.943	1.181	1.393	331.9
110 PODACE	0.067	4.110	1.223	1.341	359.3
111 PRPENG	0.399	4.162	1.200	1.391	336.6
112 SAHSOJ	0.515	3.499	1.172	1.431	322.6
113 SAWHED	0.425	3.658	1.196	1.401	333.4
114 SILSUB	0.443	3.126	1.183	1.414	331.6
115 SILSUB	0.451	3.188	1.204	1.400	330.6
116 SISTUJ	0.210	4.271	1.226	1.347	353.2
117 SITKIP	0.429	3.574	1.164	1.436	333.2
118 SIYHOX	0.043	3.710	1.186	1.379	359.7
119 TZACOL	0.190	3.325	1.181	1.402	354.2
120 TZACOL	0.180	3.186	1.211	1.376	354.8
121 VENWIU	0.173	3.324	1.198	1.361	355.3
122 VUCJEI	0.457	3.617	1.208	1.393	329.1
123 VUKHUE	0.375	4.331	1.194	1.396	339.1
124 VUKJAM	0.373	4.398	1.194	1.387	339.3
125 VUKJIU	0.311	4.015	1.196	1.390	345.4
126 WASNUZ	0.028	4.226	1.211	1.366	359.9

List of Publications

1. **Kumar Biradha**, C.V.K. Sharma, K. Panneerselvam, L. Shimoni, H.L. Carrel, D.E. Zacharias and G.R. Desiraju, "Solid State Supramolecular Assembly via C-H···O Hydrogen Bonds: Crystal Structures of the Complexes of 1,3,5-Trinitrobenzene with Dibenzylideneacetone and 2,5-Dibenzylidene-cyclopentanone", *J. Chem. Soc., Chem. Commun.*, 1993, 1473-1475.

2. D. Braga, F. Grepioni, **Kumar Biradha**, V.R. Pedireddi, G.R. Desiraju, "Hydrogen Bonding in Organometallic Crystals. 2. C-H···O Hydrogen Bonds in Bridged and Terminal First-Row Metal Carbonyls", *J. Am. Chem. Soc.*, 1995, **117**, 3156-3166.

3. **Kumar Biradha**, R.E. Edwards, G.J. Foulds, W.T. Robinson, G.R. Desiraju,"(4-Dimethylaminopyridine)$_5$ (Benzoic Acid)$_3$ $(H_2O)_{10}$ - A Two - Dimensional Clathrate Hydrate" *J. Chem. Soc., Chem. commun.*, 1995, 1705-1707.

4. **Kumar Biradha**, G.R. Desiraju, D. Braga and F. Grepioni, "Hydrogen Bonding in Organometallic Crystals. Part 3. Transition Metal Complexes Containing Amido Groups" *Organometallics*, 1996, **15**, 1284-1295.

5. A. Nangia, **Kumar Biradha** and G.R. Desiraju, "Correlation of Biological Activity in β-Lactam Antibiotics with Woodward and Cohen Structural Parameters - A Cambridge Database Study" *J. Chem. Soc., Perkin Trans., 2*, 1996, 943-953.

6. D. Braga, F. Grepioni, E. Tedesco, **Kumar Biradha** and G.R. Desiraju, "Hydrogen Bonding in Organometallic Crystals: Part 4. M-H···O Hydrogen Bonding Interactions" *Organometallics*, 1996, **15**, 2692.

7. D. Braga, F. Grepioni, **Kumar Biradha** and G.R. Desiraju, "Agostic Interactions in Organometallic Compounds. A Cambridge Structural Database Study" *J. Chem. Soc., Dalton Trans,* 1996, 000 (in press).

8. **Kumar Biradha**, G.R. Desiraju, H.L. Carrell and A.K. Katz, "2,6-Dibenzoyl-hydroquinone" *Acta Cryst.* 1996, **C52**, 000 (in press).